General Disclaimer

One or more of the Following Statements may affect this Document

- This document has been reproduced from the best copy furnished by the organizational source. It is being released in the interest of making available as much information as possible.

- This document may contain data, which exceeds the sheet parameters. It was furnished in this condition by the organizational source and is the best copy available.

- This document may contain tone-on-tone or color graphs, charts and/or pictures, which have been reproduced in black and white.

- This document is paginated as submitted by the original source.

- Portions of this document are not fully legible due to the historical nature of some of the material. However, it is the best reproduction available from the original submission.

NASA CR- 152611

FEASIBILITY AND SYSTEMS DEFINITION STUDY FOR MICROWAVE MULTI-APPLICATION PAYLOAD (MMAP)

GE Report No. 77SDS4220
CONTRACT NO. NAS-5-23734

Prepared by

General Electric Company
Valley Forge Space Division
Box 8555
Philadelphia, Pa. 19101

SEPTEMBER 1977

Prepared for

GODDARD SPACE FLIGHT CENTER
National Aeronautics and Space Administration
Communication and Navigation Division
Greenbelt, Maryland 20771

FINAL REPORT

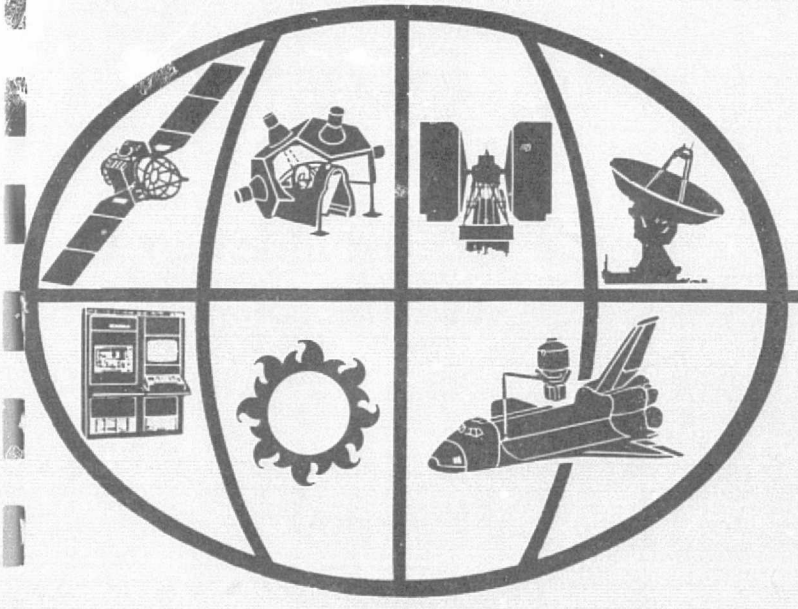

space division

GENERAL ELECTRIC

TECHNICAL REPORT STANDARD TITLE PAGE

1. Report No.	2. Government Accession No.	3. Recipient's Catalog No.

4. Title and Subtitle
Feasibility and Systems Definition Study for Microwave Multi-Application Payload (MMAP)

5. Report Date
September 1977

6. Performing Organization Code

7. Author(s)
J. B. Horton, C. C. Allen, M. J. Massaro, J. L. Zemany, J. W. Murrell, R. W. Stanhouse, G. P. Condon, R. F. Stone, J. Swana, M. Afifi, R. Milton

8. Performing Organization Report No.
77SDS4220

9. Performing Organization Name and Address
General Electric Company
Valley Forge Space Center
P. O. Box 8555
Philadelphia, Pa. 19101

10. Work Unit No.

11. Contract or Grant No.
NAS-5-23734

12. Sponsoring Agency Name and Address
National Aeronautics & Space Administration
Goddard Space Flight Center
Greenbelt, Md. 20771
John J. Woodruff

13. Type of Report and Period Covered
Final Report September 1976-September 1977

14. Sponsoring Agency Code
952

15. Supplementary Notes

16. Abstract

This report covers work completed on three Shuttle/Spacelab experiments: Adaptive Multibeam Phased Array Antenna (AMPA) Experiment, Electromagnetic Environment Experiment (EEE) and Millimeter Wave Communications Experiment (MWCE). Definition of these experiments proceeded in parallel. Work on the AMPA experiment was completed. Results included the definition of operating modes, sequence of operation, radii of operation about several ground stations, signal format, foot prints of typical orbits and preliminary definition of ground and user terminals. Definition of the MOD I EEE (121.5 to 2700 MHz) was completed; this work included conceptual hardware designs, Spacelab interfaces, data handling methods, experiment testing and verification, and EMC studies. The MWCE-MOD I has been defined conceptually for a steerable high gain antenna. Work was completed on a fixed antenna conceptual design called MWCE-MOD II. Work on the EEE-MOD II (121.5 MHz-43 GHz) conceptual design and system block diagram diagram has been completed.

17. Key Words (Selected by Author(s))	18. Distribution Statement
Shuttle, Spacelab, Microwave, Payloads, Antennas, Receivers, Ground Terminals, Communications	

19. Security Classif. (of this report)	20. Security Classif. (of this page)	21. No. of Pages	22. Price*
Unclassified	Unclassified		

*For sale by the Clearinghouse for Federal Scientific and Technical Information, Springfield, Virginia 22151.

TABLE OF CONTENTS

TABLE OF CONTENTS (Cont'd)

LIST OF ILLUSTRATIONS

LIST OF ILLUSTRATIONS (Cont'd)

LIST OF TABLES

PREFACE

The objective of this study is to provide NASA with a Feasibility and Systems Definition Study for Shuttle/Spacelab Microwave Multi-Applications Payload Experiment (MMAP). This study includes the selection and definition of the system design approach for certain key experiments, and includes the study of equipment requirements, and Shuttle interfaces for each of these experiments. Cost effective design is a major objective of the study. Work included the definition of the Adaptive Multi-beam Phased Array (AMPA) Experiment, the Electromagnetic Environment Experiment (EEE), and the Millimeter Wave Communications Experiment (MWCE). Work on the AMPA Experiment definition included user and ground terminal definition, and data reduction requirements. Definition of the MOD I EEE (121.5-2700 MHz) and MOD II (2.7-43 GHz) was completed. Work during the final contract period primarily included effort on the EEE MOD II. Task studies completed and submitted as separate contract items (CI's) are as follows:

CI 7	Ground Handling and Test Operations Plan
CI 8	Payload Specialist Functions Plan
CI 9	Mission Operations Plan
CI 10	Data Handling Plan
CI 12	List of Critical and Long Lead Items
CI 16	Reliability and Quality Assurance Criteria (Reliability vs. Cost)
CI 17	Electromagnetic Compatibility Test Plan

The authors gratefully acknowledge the contributions of S. Durrani (AMPA), L. Ippolito (MWCE), R. E. Taylor (EEE), and J. Woodruff (MMAP) for their many contributions and suggestions in defining the MMAP experiments.

GLOSSARY

AMPA	Adaptive Multibeam Phased Array Experiment
ARE	Antenna Range Experiment
ATTN	RF Attenuator
BPF	Bandpass Filter
BPF/DIP	Band Pass Filter and Diplexer Combination
BPF/MUX	Band Pass Filter and Multiplexer Combination
bps	Bits per Second
BW	Bandwidth, Refers to Frequency
CMD	Command
CONUS	Continental United States
CRT	Cathode Ray Tube
CSSR	Cooperative Surveillance Spacelab Radar Experiment
CTRL	Control
DCMB	Data Collection With Multi-Beam Experiment
DEMOD	Signal Demodulator
DEMUX	Demultiplexer
DIP	Frequency Diplexer
DN/CNVR	Down Converter
EE	Electromagnetic (interference) Environment
EEE	Electromagnetic Environment Experiment
EIRP	Effective Isotropic Radiated Power
EMC	Electromagnetic Compatibility
F	Frequency
FCC	Federal Communications Commission
Forward Link	Data Link from OCC to Deployed Satellite or Sensor System
GPS	NAVSTAR/GPS Experiment
H	Orbit Height
HDDT	High Density Digital Tape
HPBW	Half Power Beam Width
ID	Identification
I/F	Attitude/Position Location Interferometer
I/O	Input to and/or Output from a Computer
IP	Input
IPD	Information Processing Division
IRAC	Interdepartment Radio Advisory Committee (U.S. Government)
ITU	International Telecommunications Union
K	Kilo-one Thousand
Kbps	Kilo-bits per Second
KM	Kilometers
LHCP	Left Hand Circular Polarization
LNA	Low Noise Amplifier
LNA/DIP	Low Noise Amplifier and Diplexer Combination
LO	Local Oscillator Signal
LOGP	Log Periodic RF Feed

M	Mega - One Million
Mbps	Mega-bits per Second
METRAD	Meterological Radar
MMAP	Microwave Multi-Application Payload
MUX	Multiplexer
MWCE	Millimeter Wave Communications Experiment
OCC	Operations Control Center, A Ground Facility for Mission Control
OSP	Orbiting Standards Platform
PLI	Position Location Interferometer
POCC	Payload Operations Control Center
POLC	Polarization Control
PS	Payload Specialist
RCVR	Receiver
Record	An Entry in a Data File
Reverse Link	Data Link from a Deployed Satellite or Sensor to OCC
RF	Radio Frequency
RFI	Radio Frequency Interference
RHCP	Right Hand Circular Polarization
S&R	Search and Rescue
SMS R/M	Soil Moisture and Salinity Radiometer Experiment
SSR	Surface Spectrum Radar Experiment
STAT(S)	Statistic(s)
STDN	Spaceflight Tracking and Data Network
T&C	Telemetry and Control
TBD	To Be Determined
TCS	Technical Consultation Services
TDRS	Tracking and Data Relay Satellite
TDRSS	Tracking and Data Relay Satellite System
TLM	Telemetry
TT&C	Telemetry, Tracking and Control
WARC	World Administrative Radio Conference (ITU)
WBR	Wide Band Receiver
XMT	Transmitter

SECTION 1

INTRODUCTION

The National Aeronautics and Space Administration (NASA) initiated this study to define a number of Shuttle/Spacelab experiments which are common in technology and which will further the technology goals of NASA in the communication and navigation fields. These experiments all fall within the scope of microwave technology and are grouped to form the Microwave Multi-Application Payload (MMAP) experiments. The experiments are:

1. Electromagnetic Environment Experiment (EEE)
2. Adaptive Multibeam Phased Array Antenna (AMPA) Experiment
3. Millimeter Wave Communications Experiment (MWCE)
4. Orbiting Standards Platform (OSP)
5. Antenna Range Experiment (ARE)
6. Cooperative Surveillance Spacelab Radar (CSSR) Experiment
7. Data Collection with Multibeam (DCMB) Experiment
8. NAVSTAR GPS Experiment (GPS)

During this study, most of the effort was directed toward the EEE, AMPA, and MWCE experiments. These experiments have been partially defined in previous studies [1,2,3] and material from these studies has been utilized in this study. This study was directed toward definition of experiment instrumentation such as antennas, receivers, data processing equipment, Shuttle interfaces and, if required, instrument pointing systems. Other areas of investigation included Ground Handling and Test Operation, Mission Operations plans, Data Handling Plan, Payload Specialist functions, R&QA criteria, an EMC test plan, and a listing of critical and long lead items. This final report covers work done during the contract period, September 1976 through September 1977.

1.1 EXPERIMENT OBJECTIVES

The objective of this study is to provide NASA with a Feasibility and Systems Definition Study for candidate Shuttle/Spacelab Microwave Multi-Applications Payload Experiments. The study includes the selection and definition of the system design approach for certain key experiments, and includes the study of equipment requirements, Shuttle interfaces and ground equipment.

1.2 STUDY APPROACH

The basic approach to defining the individual MMAP experiments is to apply cost effective design to each experiment. Equipment such as antennas, transmitters, receivers, power supplies, control systems and thermal/mechanical systems is expected to be mostly pallet-mounted and unique for each experiment. Data processing equipment, control and display equipment, recorders (if required) and Shuttle interface equipment will be located in the Spacelab Module or Igloo and the Aft Flight Deck (AFD) area. The approach used in this study is to define each experiment for the best cost compromise between experiment-unique equipment and Shuttle/Spacelab equipment available to all experiments, such as the Command and Data Management Subsystem (CDMS).

Several factors have resulted in changes in the initial experiment definition. These include the role that the Payload Specialist will have in the experiment, the accessibility of the TDRSS real-time data link to the experiment, the amount of operating time an experiment will have, the viewing angle of the experiment antennas, and availability of the Spacelab Module. These factors have not necessarily changed the design-to-cost approach, but have affected the overall philosophy of experiment operation and data management.

Functional definition of each experiment was carried out to show feasibility of design, and mechanical interfaces with the Shuttle. For the MMAP, all experiments have antennas and associated equipment such as receivers, transmitters, power supplies, etc. Design of the equipment must include field-of-view of the antenna and space to accommodate the associated equipment. Therefore, location of the equipment on the Shuttle is a principal design factor for each experiment. Similarly, other Shuttle-related environmental factors, e.g.,

electromagnetic compatibility (EMC), are considered in the feasibility study.

Ground support equipment, as required, is included with each experiment. This includes test equipment for the instrument, and user ground terminal equipment for experiment operation. Where practical, existing NASA equipment is used for these ground operations.

The overall study approach follows the primary cost effective design approach by using experiment-unique equipment, optimizing operation of this equipment by careful selection of its location in the Shuttle, allowing for maximum operating time when practical, and using existing equipment on the Shuttle and at ground locations whenever practical. This approach should provide the most reliable design and minimum practical cost for each experiment.

SECTION 2

EXPERIMENT ORBITAL DEFINITION

This section includes work completed to date on orbital parameter considerations of three MMAP experiments: AMPA, EEE and MWCE. Each of these experiments was studied, not only to determine the feasibility of the instrument design, but to assure satisfactory experiment operation and compatibility of the experiment with the Shuttle [4,5] mission. In performing the operational studies, a 400 km, 57° inclination orbit was assumed. Details of these orbits are included in this section.

A typical orbit profile for the MMAP studies was performed in a previous study to establish operating times for an experiment and to obtain the maximum geographical coverage possible on a typical 7-day Shuttle mission during the 1981-82 time frame.[1] During this time period the Shuttle will be launched from the Eastern Test Range (ETR), Cape Canaveral, Florida, and the maximum orbit inclination being 57°. Results of this study are included here for reference.

To obtain reasonable operation parameters, certain mission guidelines were established. For example, a 7-day orbiter mission is in reality a 6-day mission for EEE, since 1/2 day is needed for orbiter check-out, equipment power-up and experiment check-out, and 1/2 day is needed for orbiter landing preparation. A circular orbit is assumed and orbit altitude is assumed 400 km. Knowing that the launch will be from the ETR, the basic mission parameters for the study can be established as follows:

1. Mission Duration: 6 days
2. Orbit Inclination: 57°
3. Altitude: 400 km
4. Orbit Shape: Circular
5. Insertion Point: ETR (28.5°N, 80.5°W)

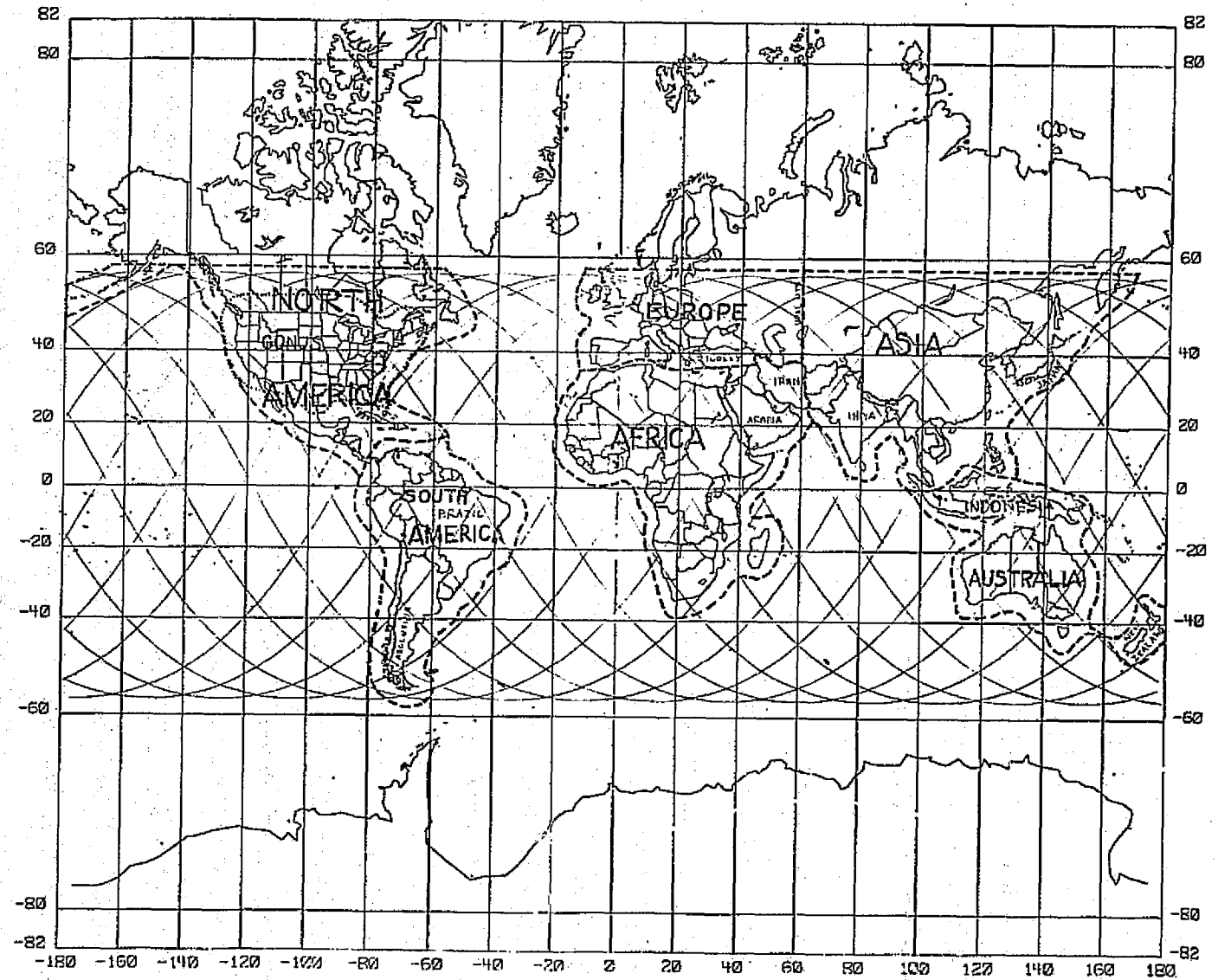

Figure 2-1. Typical EEE Region of Interest/First Day Orbit Traces

The above parameters define a mission profile that covers an area symmetrical about the equator and bounded by $\pm 57^{o}$ latitude. Figure 2-1 shows the typical first-day traces of an orbiter inserted in orbit at the ETR and exhibiting these parameters. Characteristics of the profile are:

1. Exact 3 day repeat orbit
2. Orbit period 92.65 minutes (15.54 revolutions/day)
3. Orbits per 6 day missions: 93.34
4. Distance between adjacent orbits 7.8^{o} = 470.4 nm = 871 km (ref. Equator)
5. Orbits over CONUS: 21 per 3 day cycle = 42

Figure 2-1 shows a representative orbit pattern for the first day of a mission. During the second and third days the orbit traces move progressively eastward to fill the area between the traces shown, providing two additional traces between each trace shown in Figure 2-1. The resulting grid over the CONUS is shown in Figure 2-2. This grid and similar grids over the other regions of interest was used to determine fly-over times and EEE operating periods.

Table 2-1 shows typical viewing time for each of the regions outlined in Figure 2-1. Note that the total viewing time for all six geographical regions is 58.93 hours for the entire 6-day mission. Extending this analysis to the CONUS only (Table 2-2), the viewing time is about 50 minutes per day and only 5.15 hours total. Some fly-over times are extremely short, e.g., Nos. 5 and 35 orbits, and no fly-over occurs for orbits Nos. 20 and 66.

The distribution of the CONUS observations times can be seen in Figure 2-3. Shown are the times of orbit coverages for the six days (from Table 2-2 data) plotted on a 24-hour basis starting with the indicated T_0 time reference. Note that all operating times are in nearly the same block of hours each day, thus a six-day mission would not provide for viewing during both daylight and night hours. An early daylight Shuttle launch would be preferred for EEE to obtain viewing during daylight hours, since the major electromagnetic radiation activity occurs during those hours. To cover both day and night on the same mission, a longer mission period is required or orbit parameters must be altered, e.g., change of altitude, orbit inclination and launch site.

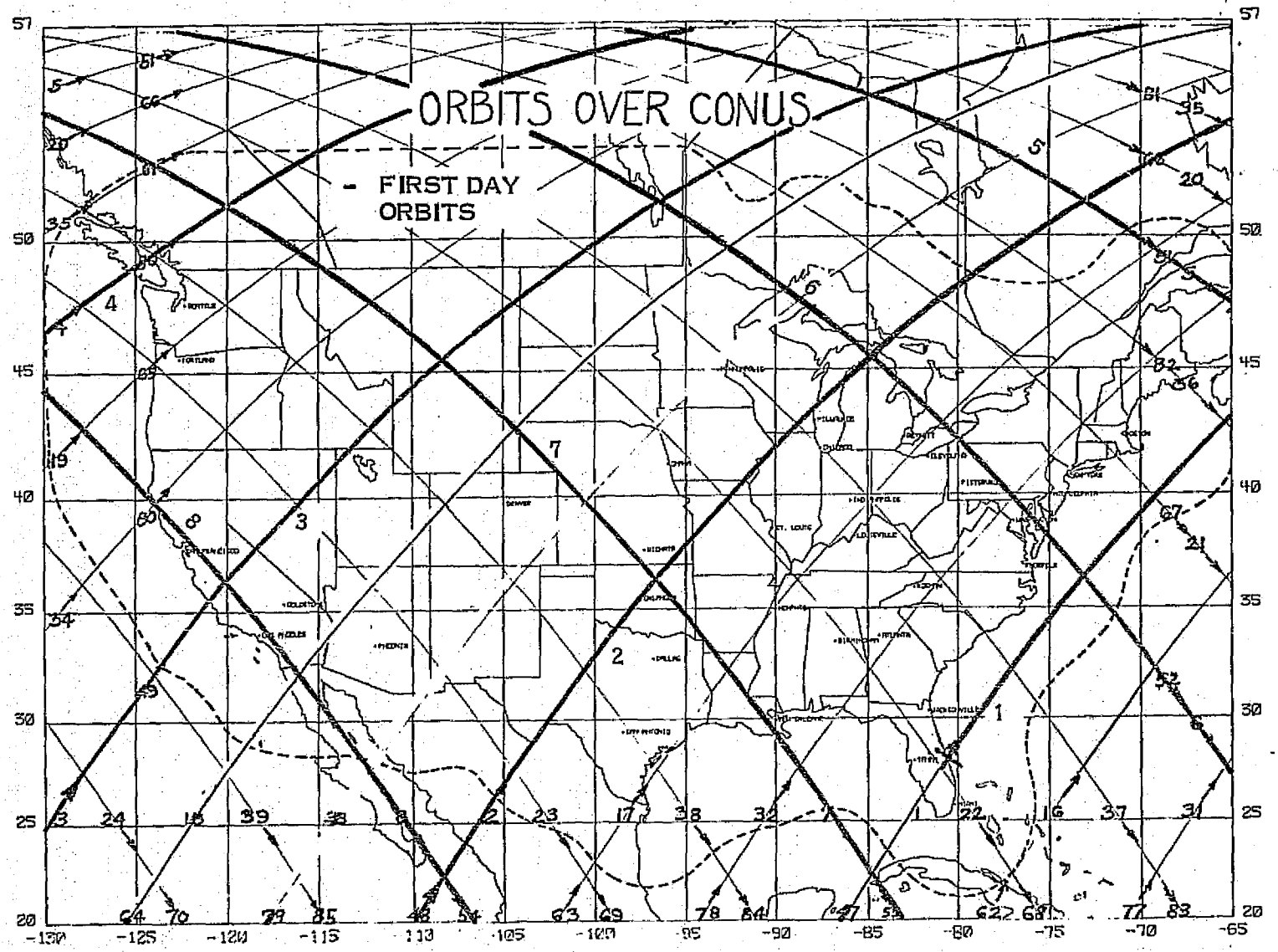

Figure 2-2. CONUS Orbit Pattern (6-Day Mission)

Table 2-1. Estimated Viewing Times* for Global Areas

Areas	Time - 6 Day Mission
CONUS - also included in North America time	5.15 Hours
North America - Includes, Canada, Central America, and Caribbean area as well as CONUS	11.87
South America - As shown	7.12
Europe	7.21
Africa	11.00
Asia	15.44
Australia	6.29
Six-Day Total	58.93 Hours

*Includes one minute operation at each end of each orbit outside applicable boundary or shoreline (See Figure 2-1)

Table 2-2. Operating Time Over CONUS* (Minutes)

Day 1		Day 2		Day 3		Day 4		Day 5		Day 6	
Orbit	Time	Orbit	Time	Orbit	Time	Orbit	Time	Orbit	Time	Orbit	Time
1	7.5	17	9.75	32	4.98	48	8.4	64	8.82	79	8.15
2	8.4	18	8.82	33	8.15	49	7.7	65	4.75	80	6.65
3	7.7	19	4.75	34	6.65	50	2.65	66	x	81	.50
4	2.65	20	x	35	.50	51	1.85	67	6.35	82	3.05
5	1.85	21	6.35	36	3.05	52	7.75	68	11.35	83	8.5
6	7.75	22	11.35	37	8.5	53	9.75	69	8.4	84	9.8
7	9.75	23	8.4	38	9.8	54	5.3				
8	5.3										
										93	7.5
		32	3.0	47	7.5	63	9.75	78	7.98	94	8.4
Total	50.90		52.42		49.13		53.15		50.65		52.55
Six Day Total: 308.80 Minutes 5.15 Hours											

*Assumes one additional minute of operation at each end of orbit path over the U.S. beyond the border/coastline crossings (See Figure 2-2)

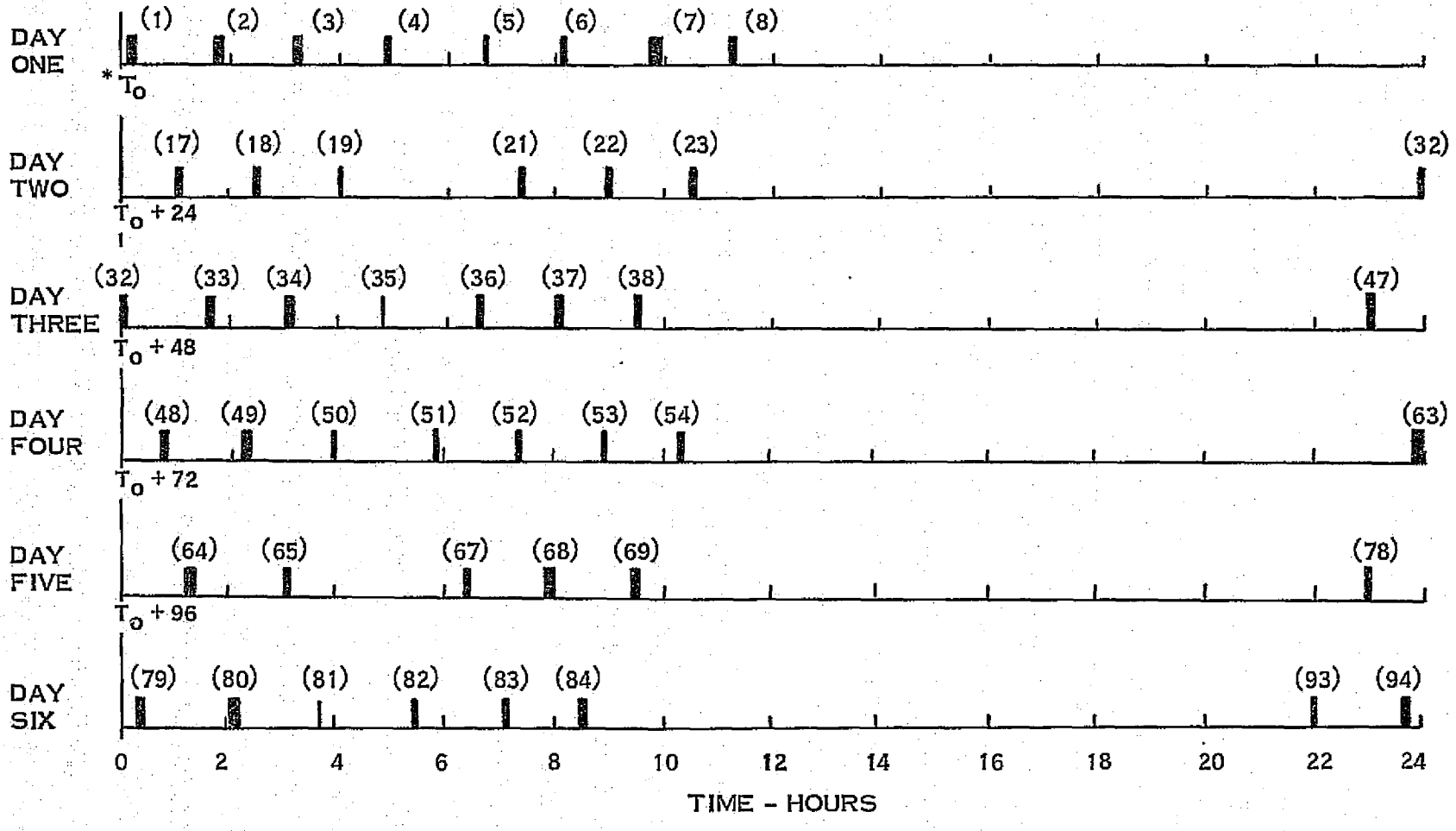

*T_o REFERENCE IS ORBIT NO. 1 CROSSING OF EQUATOR, ASCENDING ORBIT, 57° INCLINATION

( ) = ORBIT NUMBER

Figure 2-3. Operating Times Over CONUS for Six Day Mission

2.2 ADDITIONAL EQUAL AREA PROJECTION PROFILES

The orbital data previously generated and described in Subsection 2.1 required many manual and semi-automated calculations in addition to a number of computer runs to define ground sites, contact times, and antenna elevation radius of contact zones. The analysis was primarily performed on a Mercator projection of the Continental U.S., which inherently portrays distances, orbital tracks and geographical areas in a non-linear scale. This necessitated a complex approach to preliminary analysis efforts. The resultant efforts revealed a need for portraying the orbital ground track and geographical parameters in a format compatible with constant scale factors for velocities and distances.

The constant scale approach would have reduced the initial feasibility analysis to a mechanical layout of constant-radius circles for determining contact zones, scaled measurements for distances and velocities, and prescaled antenna/sensor footprint patterns applicable to all latitudes depicted on the plot. Of course, this assumes a constant look angle of the orbiting platform from nadir. This approach would also lend itself to multiple analysis iterations, without plot regeneration, for studies requiring common orbital parameters. This requirement has already been identified through conversations with the EEE P.I.

To accommodate these requirements, GE has expanded its computerized plot generation capability to include an Albers equal area projection commonly used for geographic presentations in area maps and world/area Atlases. This plot represents global sections with sufficient accuracy for wide area analysis without the non-linearity problem of Mercator projections. Each of the following Figures 2-4 to 2-10 for each mission day indicates the orbital inclination and altitude, provides scaling factors for distance and ground-track time. The figures also identify the orbital number, orbital direction, and ground track start-time relative to an arbitrary time for launch.

FIG. 2-4 MISSION DAY 1.0

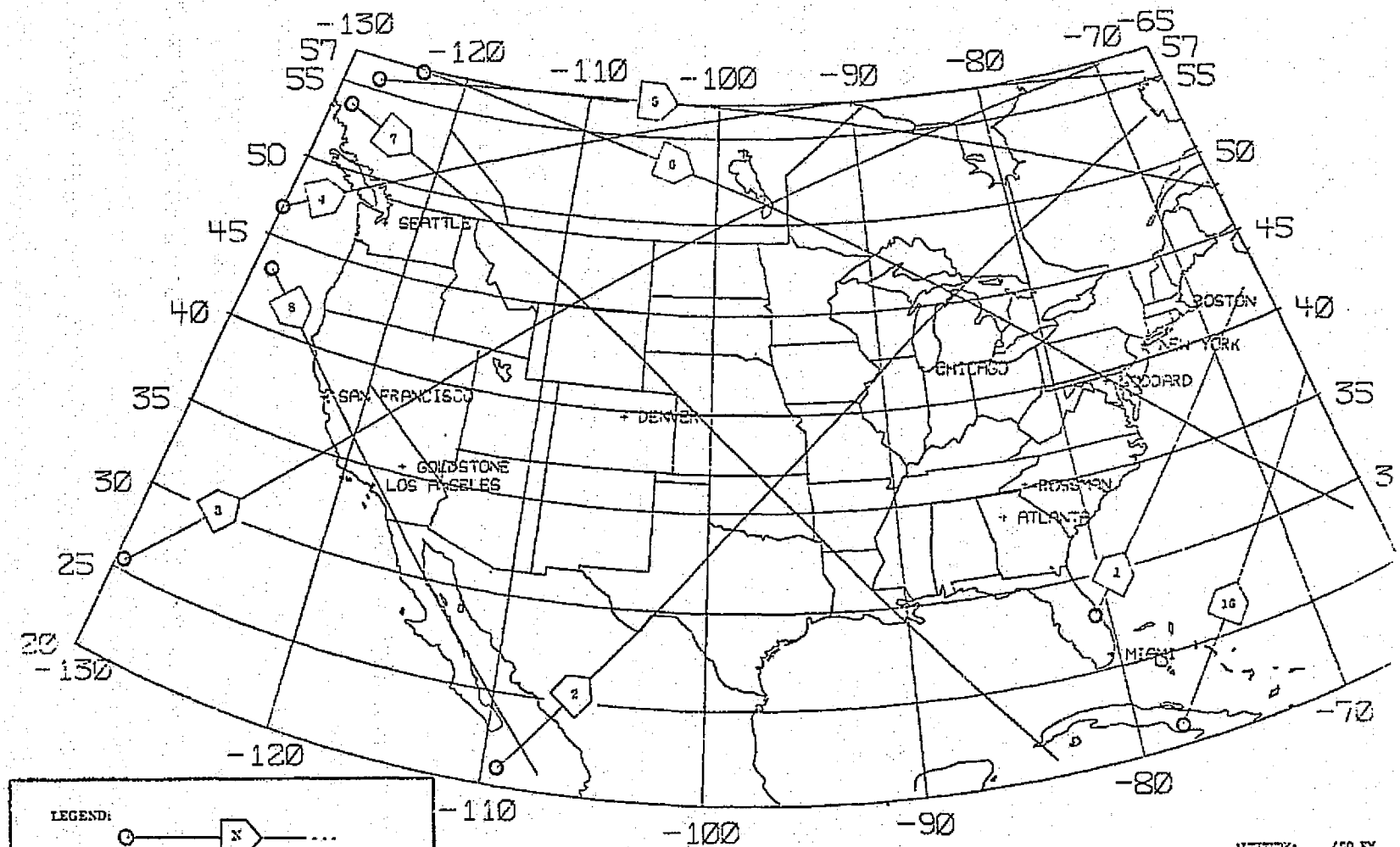

LEGEND:

Start of referenced ground track (see below)

N — Direction and orbit number

Orbit	Time from Launch	Orbit	Time from Launch
1	00.0 MIN	6	7 HRS 58.5 MIN
2	1 HRS 10.5 MIN	7	9 HRS 34.0 MIN
3	3 HRS 05.5 MIN	8	11 HRS 11.5 MIN
4	4 HRS 44.5 MIN	16	23 HRS 06.0 MIN
5	6 HRS 22.0 MIN		

SCALE:

0 100 300 500 700 900 Nautical Miles

0 100 300 600 700 900 Statute Miles

0 100 300 600 700 900 Kilometers

0 1 3 5 Minutes (ground track time)

ALTITUDE: 450 KM
INCLINATION: 57°

GENERAL ELECTRIC
SPACELAB PROGRAM OPERATIONS

ALBERS EQUAL AREA PROJECTION

FIG. 2-5. MISSION DAY 2.0

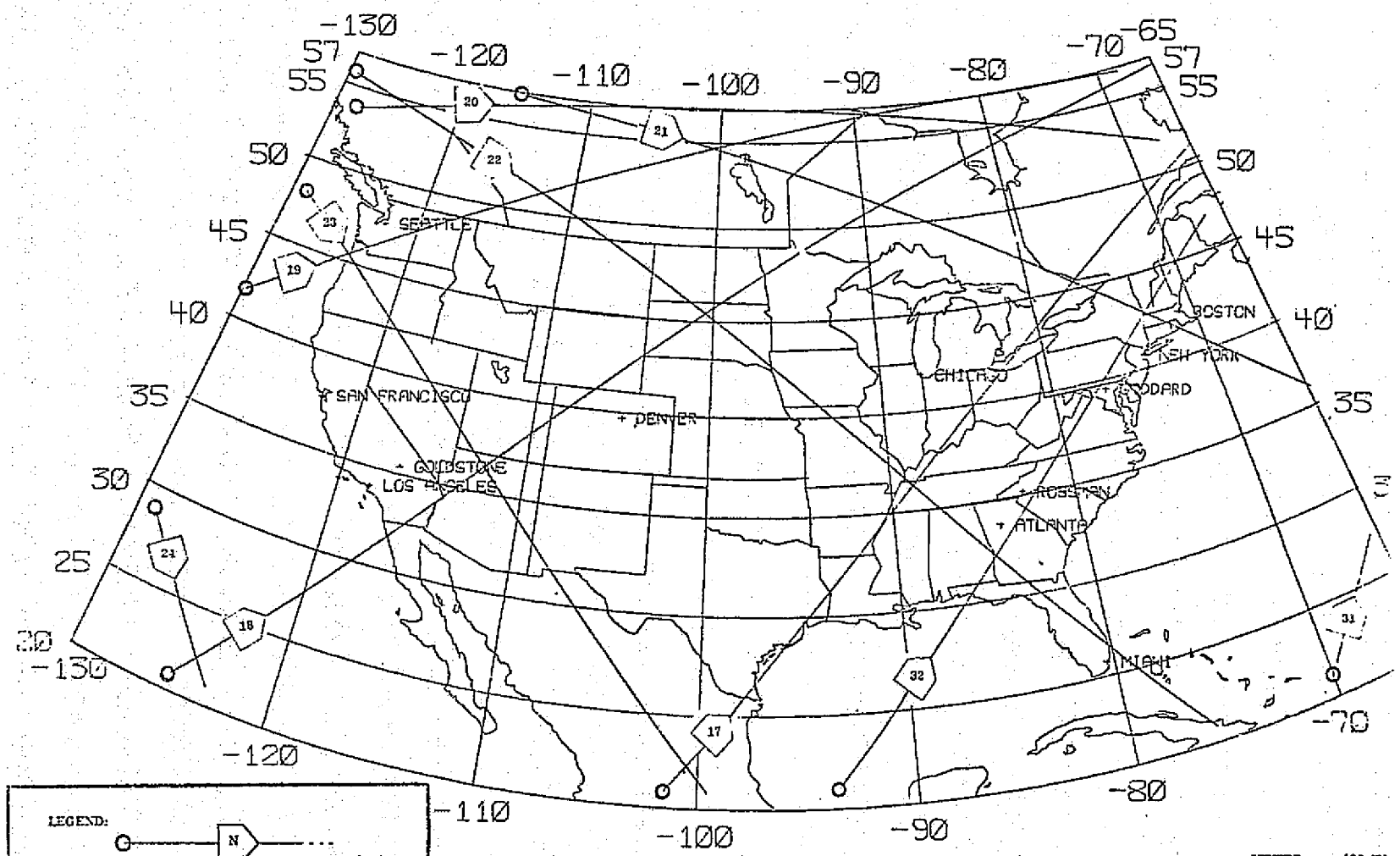

LEGEND:

Start of referenced ground track (see below) — N — Direction and orbit number

Orbit	Time from Launch	Orbit	Time from Launch
17	1 DAY 0 HRS 28.5 MIN	22	1 DAY 8 HRS 40.5 MIN
18	1 DAY 2 HRS 11.0 MIN	23	1 DAY 10 HRS 17.5 MIN
19	1 DAY 3 HRS 50.5 MIN	24	1 DAY 11 HRS 57.0 MIN
20	1 DAY 5 HRS 28.5 MIN	31	1 DAY 22 HRS 14.0 MIN
21	1 DAY 7 HRS 06.5 MIN	32	1 DAY 23 HRS 46.5 MIN

SCALE:

0 100 300 500 700 900 Nautical Miles

0 100 300 500 700 900 Statute Miles

0 100 300 500 700 900 Kilometers

0 1 3 5 Minutes (ground track time)

ALTITUDE: 400 KM
INCLINATION: 57°

GENERAL ELECTRIC
SPACELAB PROGRAM OPERATIONS

ALBERS EQUAL AREA PROJECTION

FIG. 2-6 MISSION DAY 3.0

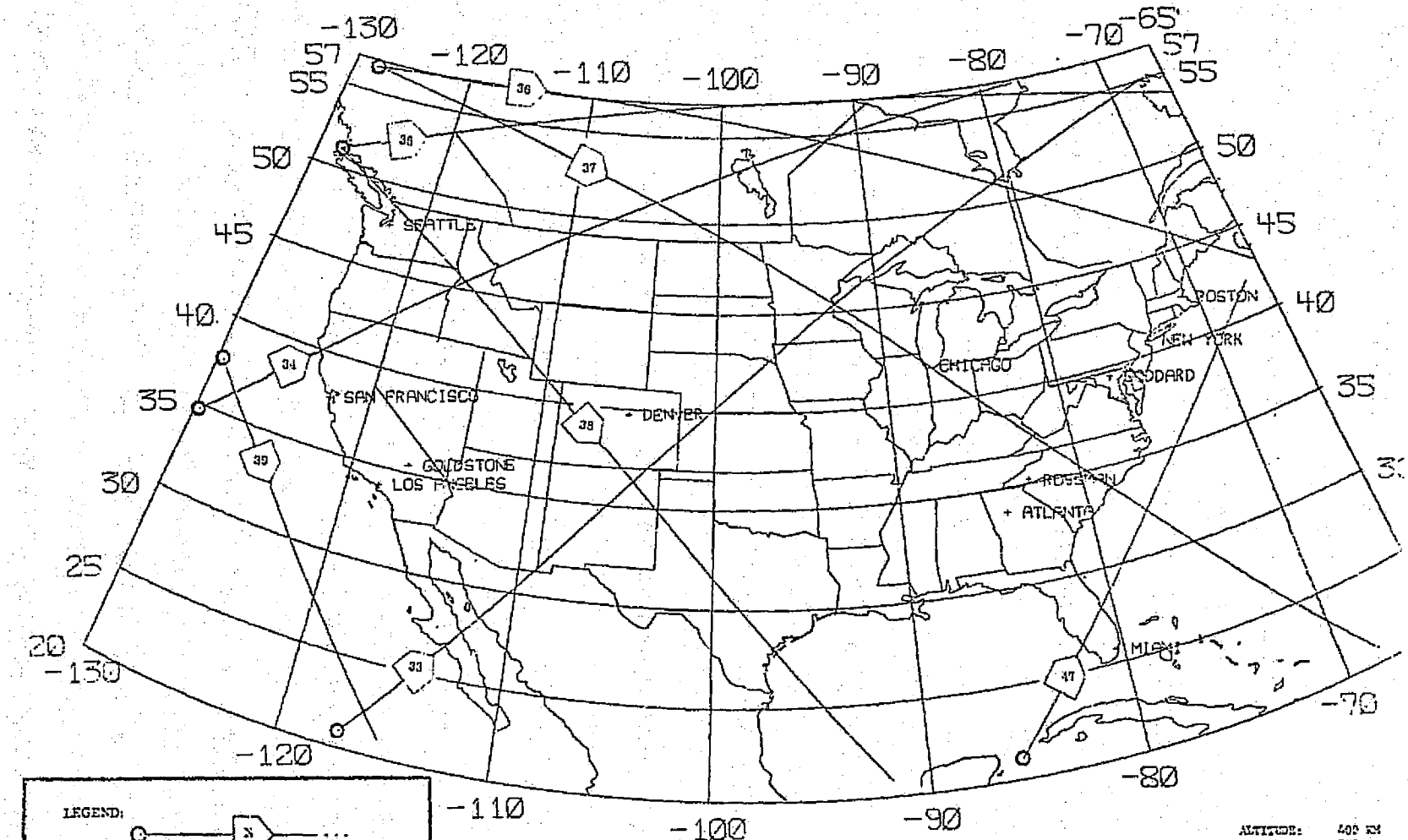

LEGEND:

Start of referenced ground track (see below)

N ... Direction and orbit number

Orbit	Time from Launch	Orbit	Time from Launch
33	2 DAY 1 HRS 19.0 MIN	38	2 DAY 9 HRS 24.0 MIN
34	2 DAY 2 HRS 56.0 MIN	39	2 DAY 11 HRS 02.0 MIN
35	2 DAY 4 HRS 35.0 MIN	47	2 DAY 22 HRS 54.5 MIN
36	2 DAY 6 HRS 11.5 MIN		
37	2 DAY 7 HRS 47.5 MIN		

SCALE:

0 100 300 500 700 900 Nautical Miles

0 100 300 500 700 900 Statute Miles

0 100 300 500 700 900 Kilometers

0 1 3 5 Minutes (ground track time)

ALTITUDE: 400 KM
INCLINATION: 57°

GENERAL ELECTRIC
SPACELAB PROGRAM OPERATIONS

ALBERS EQUAL AREA PROJECTION

FIG. 2-7. MISSION DAY 4.0

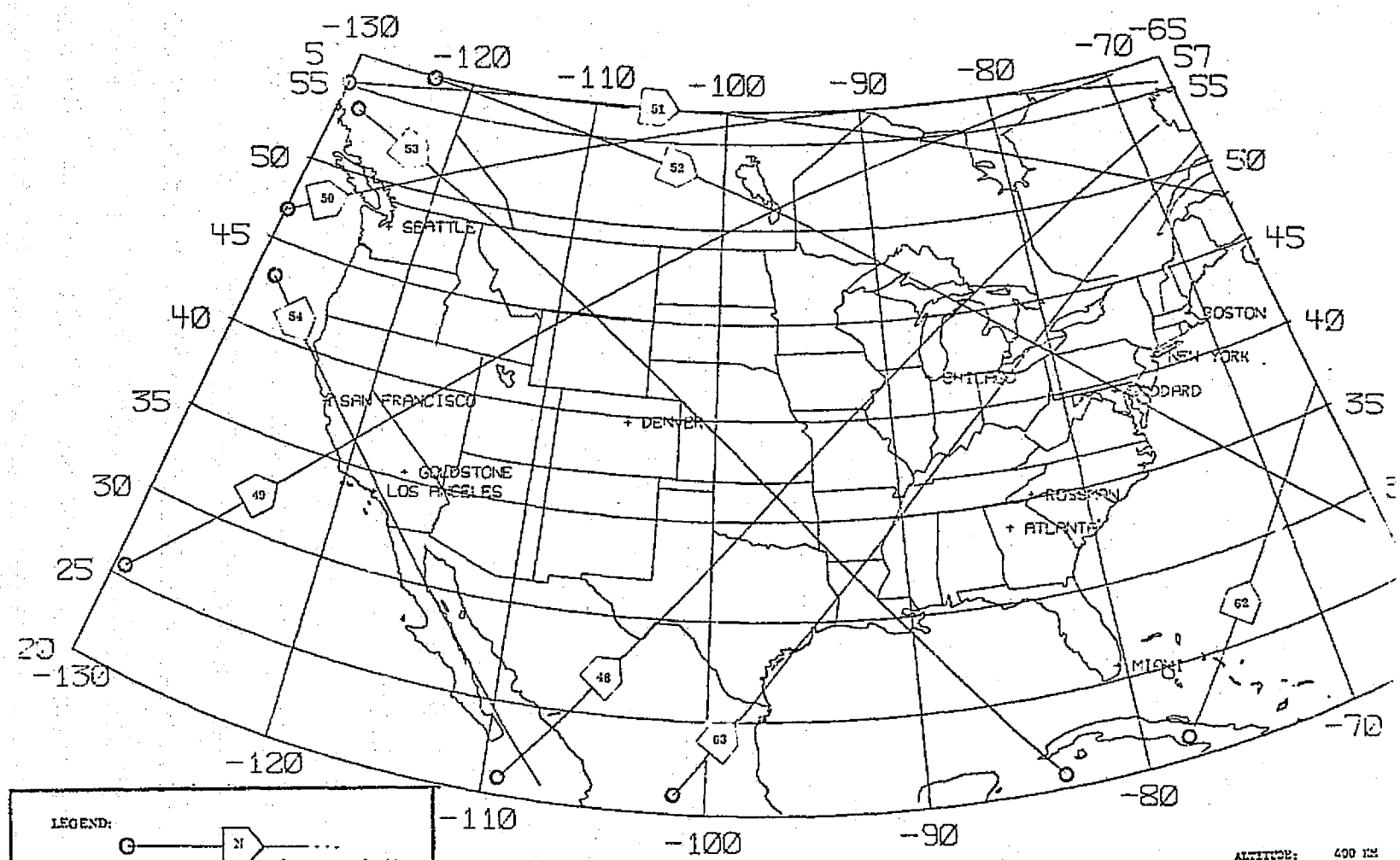

LEGEND:

Start of referenced ground track (see below)

Direction and orbit number

Orbit	Time from Launch	Orbit	Time from Launch
48	3 DAY 0 HRS 27.0 MIN	53	3 DAY 8 HRS 30.5 MIN
49	3 DAY 2 HRS 01.0 MIN	54	3 DAY 10 HRS 08.0 MIN
50	3 DAY 3 HRS 41.0 MIN	62	3 DAY 22 HRS 02.5 MIN
51	3 DAY 5 HRS 18.0 MIN	63	3 DAY 23 HRS 35.0 MIN
52	3 DAY 6 HRS 55.0 MIN		

SCALE:

0 100 300 500 700 900 Nautical Miles

0 100 300 500 700 900 Statute Miles

0 100 300 500 700 900 Kilometers

0 1 3 5 Minutes (ground track time)

ALTITUDE: 400 NM
INCLINATION: 57°

GENERAL ELECTRIC
SPACELAB PROGRAM OPERATIONS

ALBERS EQUAL AREA PROJECTION

FIG. 2-8. MISSION DAY 5.0

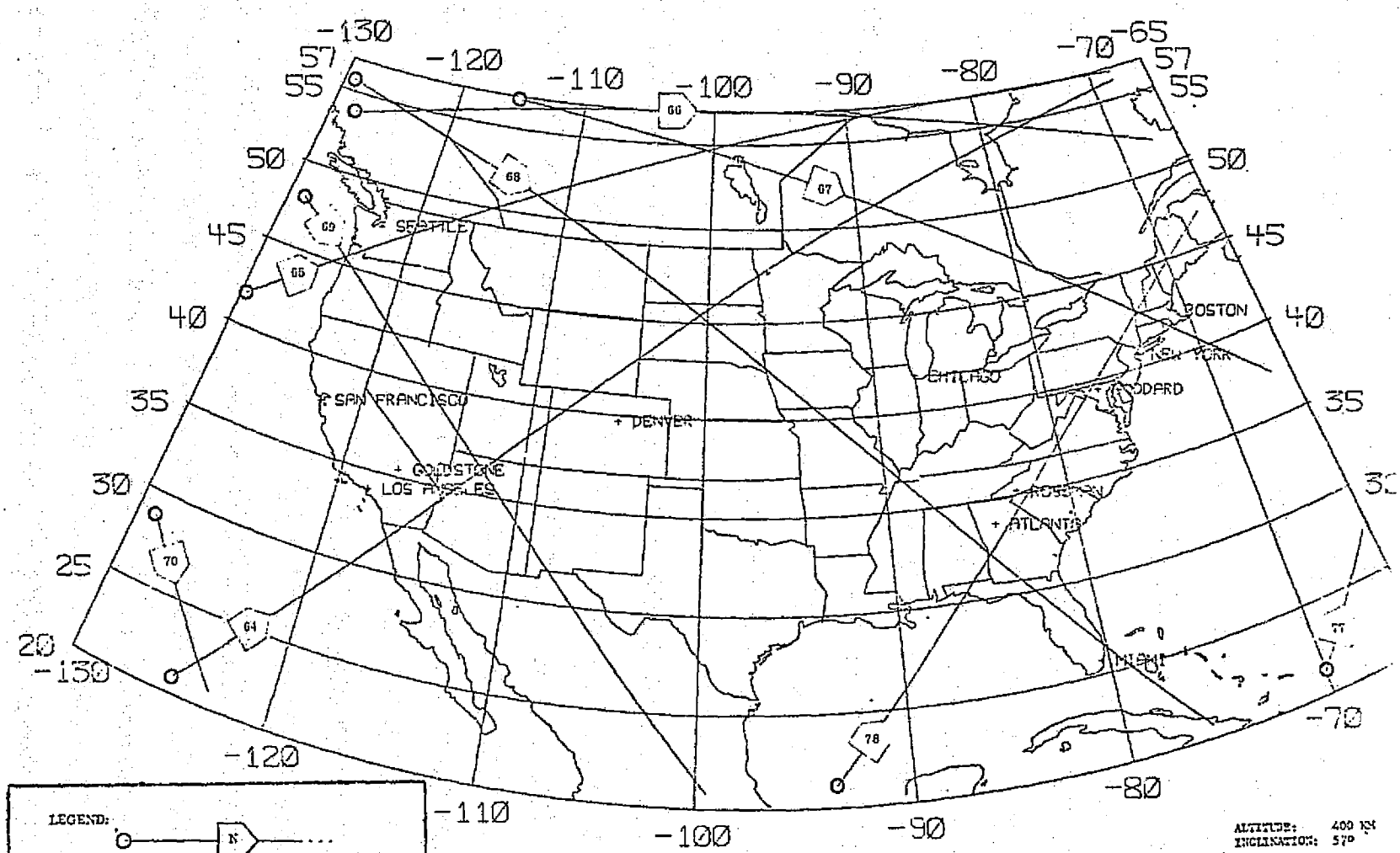

LEGEND:

Start of referenced ground track (see below)

N — Direction and orbit number

Orbit	Time from Launch	Orbit	Time from Launch
64	4 DAY 1 HRS 07.5 MIN	69	4 DAY 9 HRS 14.0 MIN
65	4 DAY 2 HRS 47.0 MIN	70	4 DAY 10 HRS 53.5 MIN
66	4 DAY 4 HRS 25.0 MIN	77	4 DAY 21 HRS 10.5 MIN
67	4 DAY 6 HRS 03.0 MIN	78	4 DAY 22 HRS 43.0 MIN
68	4 DAY 7 HRS 37.0 MIN		

SCALE:

0 100 300 500 700 900 Nautical Miles

0 100 300 500 700 900 Statute Miles

0 100 300 500 700 900 Kilometers

0 1 3 5 Minutes (ground track time)

ALTITUDE: 400 NM
INCLINATION: 57°

GENERAL ELECTRIC - SPACELAB PROGRAM OPERATIONS

ALBERS EQUAL AREA PROJECTION

FIG. 2-9. MISSION DAY 6.0

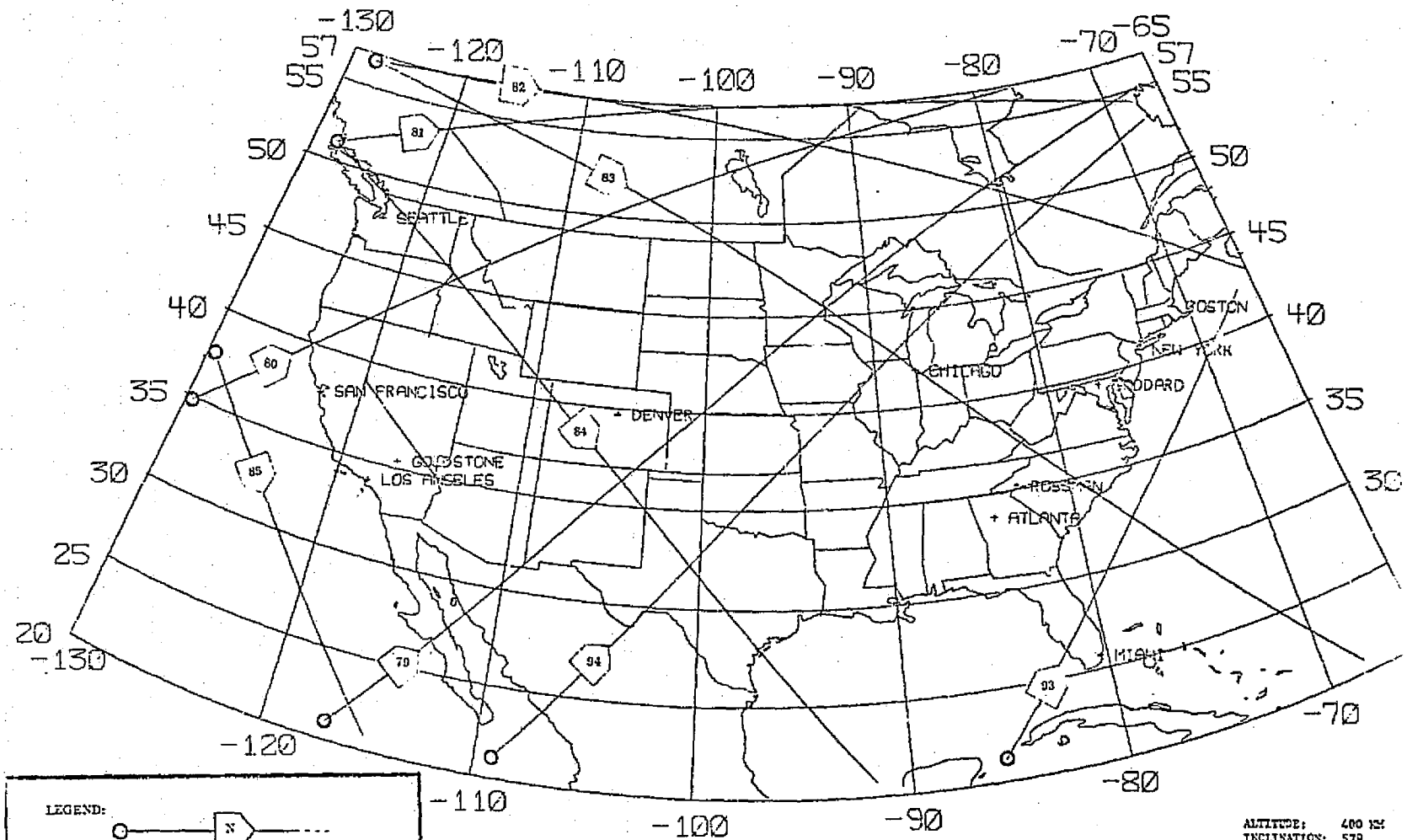

LEGEND:

Start of referenced ground track (see below)

N

Direction and orbit number

Orbit	Time from Launch	Orbit	Time from Launch
79	5 DAY 0 HRS 15.5 MIN	84	5 DAY 8 HRS 20.5 MIN
80	5 DAY 1 HRS 52.5 MIN	85	5 DAY 9 HRS 58.5 MIN
81	5 DAY 3 HRS 31.5 MIN	93	5 DAY 21 HRS 51.0 MIN
82	5 DAY 5 HRS 08.0 MIN	94	5 DAY 23 HRS 23.5 MIN
83	5 DAY 6 HRS 44.0 MIN		

SCALE:

0 100 300 500 700 900 Nautical Miles

0 100 300 500 700 900 Statute Miles

0 100 300 500 700 900 Kilometers

0 1 3 5 Minutes (ground track time)

ALTITUDE: 400 NM
INCLINATION: 57°

GENERAL ELECTRIC
SPACELAB PROGRAM OPERATIONS

ALBERS EQUAL AREA PROJECTION

FIG. 2-10. MISSION DAY 7.0

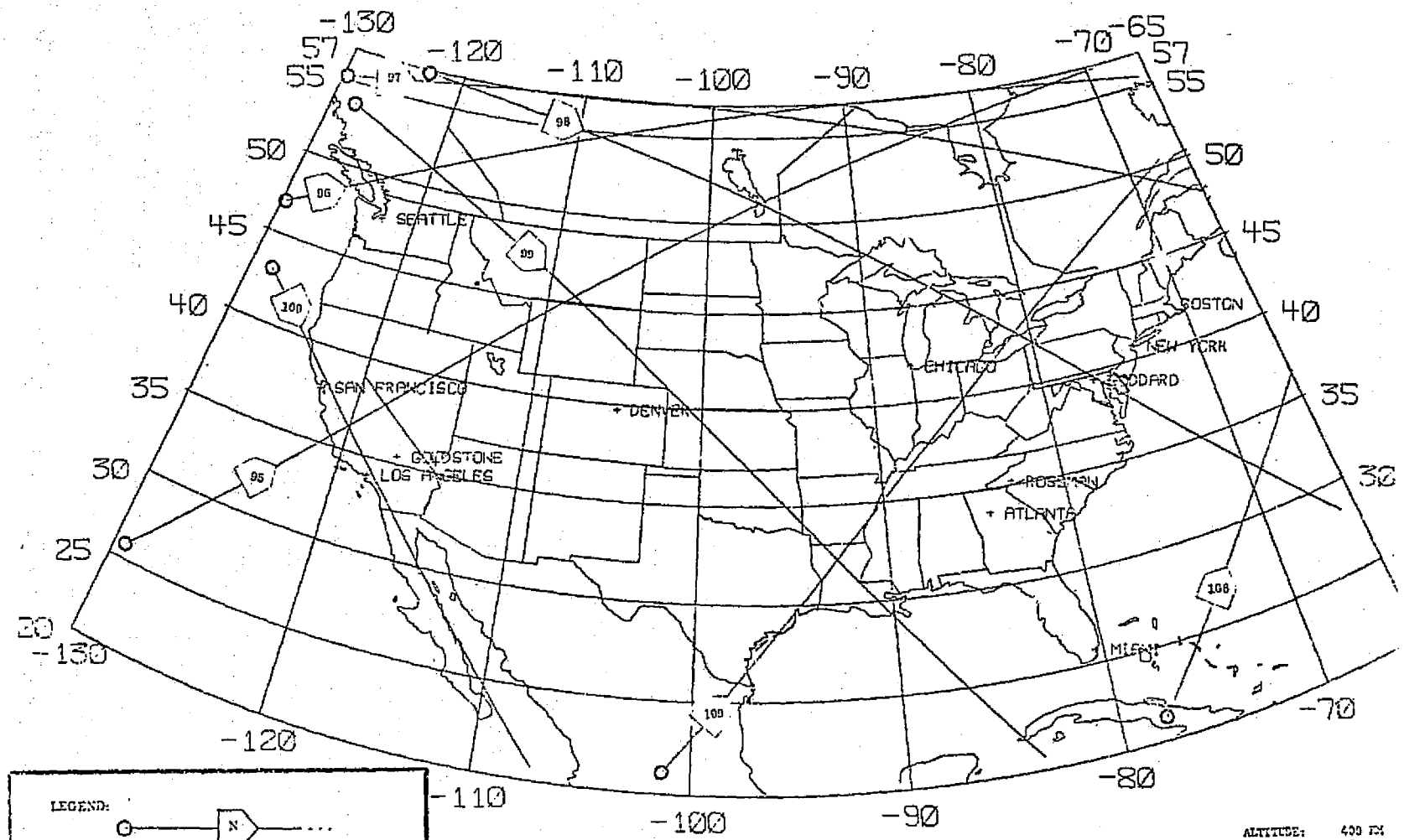

LEGEND:

Start of referenced ground track (see below)

N ... Direction and orbit number

Orbit	Time from Launch	Orbit	Time from Launch
95	6 DAY 0 HRS 57.5 MIN	100	6 DAY 9 HRS 04.5 MIN
96	6 DAY 2 HRS 37.5 MIN	109	6 DAY 20 HRS 59.0 MIN
97	6 DAY 4 HRS 14.5 MIN	109	6 DAY 22 HRS 31.5 MIN
[illegible]	6 DAY 5 HRS 51.5 MIN		
99	6 DAY 7 HRS 27.0 MIN		

SCALE:

0 100 300 500 700 900 Nautical Miles

0 100 300 500 700 900 Statute Miles

0 100 300 500 700 900 Kilometers

0 1 3 5 Minutes (ground track time)

ALTITUDE: 400 KM
INCLINATION: 57°

GENERAL ELECTRIC
SPACELAB PROGRAM OPERATIONS

ALBERS EQUAL AREA PROJECTION

SECTION 3

ADAPTIVE MULTIBEAM PHASED ARRAY (AMPA) EXPERIMENT

Definition of the AMPA experiment is being conducted in four study phases. These are:

1. AMPA Experiment Definition. This is the basic definition phase and covers the conduct of the experiment; defining the equipment needed at the Spacelab, ground and user terminals; specifying the parameters to be observed and the method of recording them; and definition of the Spacelab to TDRS link with respect to data transmission and format.

2. User-Terminal Preliminary Design. This phase covers identification of the user-terminal requirements; preliminary design of the basic user-terminal equipment; and specification of calibration beacons.

3. Ground Control-Terminal Preliminary Design. This phase covers identification of the ground control-terminal requirements; and preliminary design of the basic ground control-terminal equipment.

4 Data Reduction Requirements. This phase covers identifying the data reduction requirements during flight and after flight; and specifying the format, amount, and method of data reduction and analysis.

Effort during the first interim report period was concentrated primarily on the experiment definition, with some preliminary effort applied to user terminal definition in order to establish the user-terminal parameters assumed for communications link calculations. All four phases have now been completed and are covered in this interim report.

The AMPA Experiment Definition is reported in Section 3.1 and covers several related areas: discussion of the AMPA Experiment concepts with definition of the operational modes and sequence of operations for each; the AMPA radii of operation for typical orbits and operating times; the AMPA footprints on earth; the AMPA system parameters, operating conditions, and link calculations; the AMPA Experiment equipment; the AMPA Experiment parameters; the AMPA signal structure; and the AMPA data link via TDRS.

The User-Terminal Preliminary Design is reported in Section 3.2; the Ground Control Terminal Preliminary Design is reported in Section 3.3; and the Data Reduction Requirements are reported in Section 3.4.

3.1 AMPA EXPERIMENT DEFINITION

3.1.1 AMPA EXPERIMENT CONCEPT AND PURPOSE

The basic concept of the AMPA Experiment is the use on a spacecraft of independently steerable high-gain agile beams that can be formed adaptively on those low power users that signal a valid address or user code. Simultaneously, undesired interfering signals that are not properly coded will be adaptively rejected. By providing high EIRP on the spacecraft portion of the overall communications system and rejecting interference, the Adaptive Multibeam Phased Array (AMPA) system enables many small user applications to be met, such as low-power point-to-point communications between small users, data collection from widely distributed low power sources, emergency aid to users in distress, search and rescue operations, hospital/medical data relay, etc. The basic AMPA L-band Communications Experiment configuration is illustrated in Figure 3-1, which was generated during the AMPA Phase A Feasibility Study.[2]

The general purpose of the AMPA Experiment on Spacelab is to provide a test bed for demonstrating and verifying the feasibility of adaptively establishing such a two-way (duplex) communications link at L-band between typical low-power user terminals via a low orbiting spacecraft. Ultimately, such a system could be used as a free flyer or at synchronous geostationary orbit and tailored to specific applications. The heart of the AMPA Experiment is the Adaptive Multibeam Phased Array, which as presently envisioned would have only two adaptively formed transmit/receive beams. Two beams are sufficient to conduct the experiment and minimize the AMPA equipment costs. The use of two beams is not limiting, however, and the experimental results will be directly applicable to expanded AMPA systems for applications requiring 6, 8, 12 or more simultaneous, independently steerable, adaptively formed beams. Such an expanded AMPA system would use the same phased array radiating elements, microwave distribution networks, and RF amplifiers as the two-beam array, but would have additional adaptive beamforming circuits and transponders for the added channels.

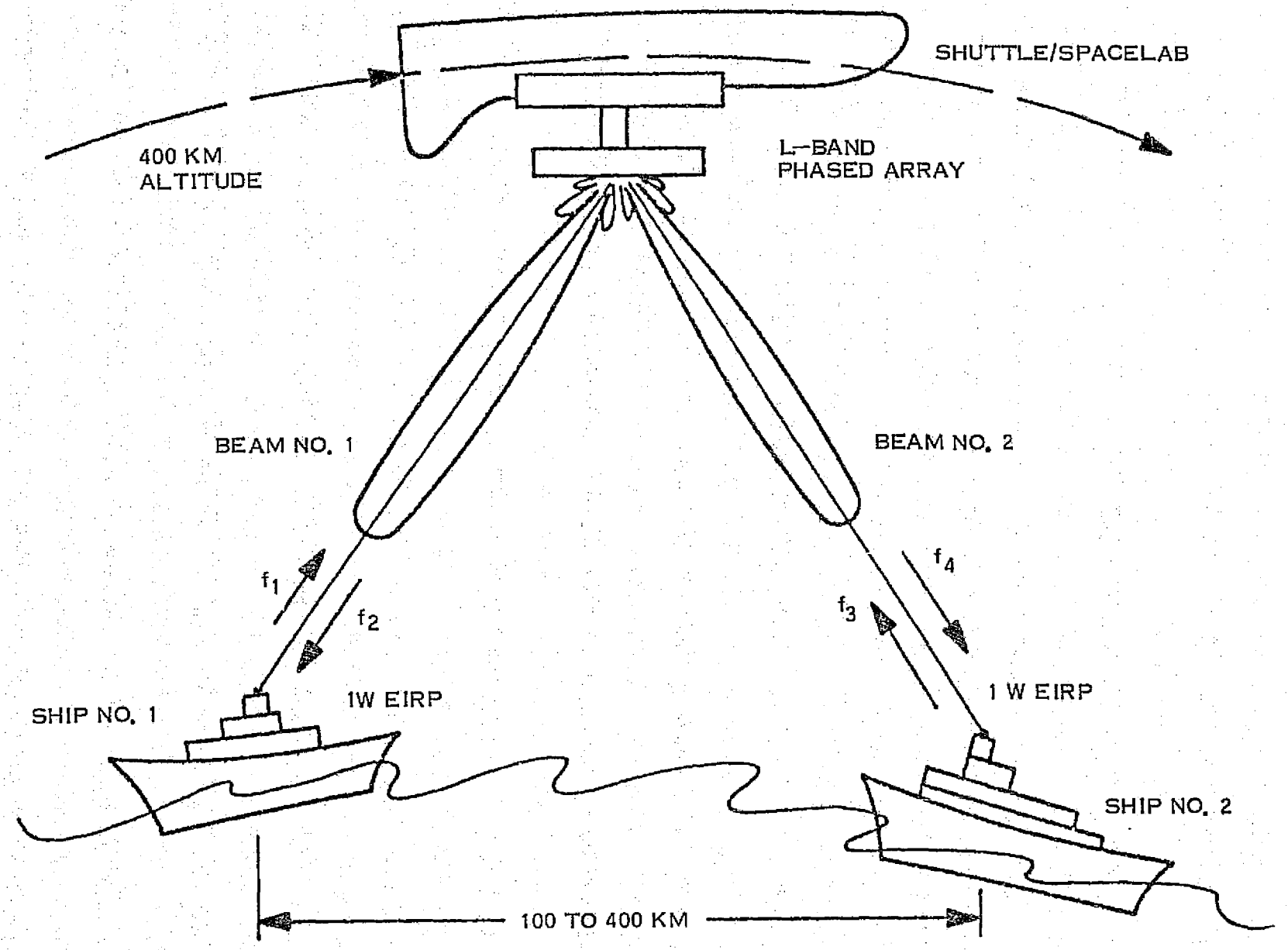

Figure 3-1. AMPA L-band Communications Experiment Configuration

3.1.2 AMPA EXPERIMENT OPERATIONAL CONCEPTS

Two major operational concepts have been considered for the AMPA Experiment. The first uses fully-adaptive beamforming and interference rejection, as described briefly in paragraph 3.1, and is by far the most versatile and effective operational use of the AMPA system, since it fully utilizes the inherent AMPA capabilities.

The second operational concept for the AMPA Experiment uses a programmed search or commanded beam steering to acquire and track each valid user with a beam, and only uses the adaptive circuitry to reject interference. This operation of the AMPA system is less versatile than the first since it requires some prior knowledge of the user locations in order to function efficiently. An undue amount of time could be used up in the search mode without such a priori information.

It is assumed here, therefore, that the AMPA equipment is capable of fully-adaptive operation for both beamforming and interference rejection. It is also assumed, however, that the adaptive beamforming mode of operation can be switched to a programmed search or commanded beam steering mode of operation for operational flexibility. Both operational concepts can thus be employed for the AMPA Experiment.

3.1.2.1 Fully-Adaptive AMPA Experiment Operational Modes

Four fully-adaptive operational modes are currently envisaged for the AMPA Experiment. These are listed below:

1. User/User Operation (paired AMPA Beams)/Duplex Comm Link without interference
2. User/User Operation (paired AMPA Beams)/Duplex Comm Link with interference
3. User/Spacelab Operation (independent AMPA Beams)/Duplex Comm Link
4. User/Spacelab Operation (independent AMPA Beams)/One-Way Comm Link

Adaptive operation in all four modes would consist of:

1. Acquisition of valid User
2. Beamforming on User
3. Tracking of User
4. Retrodirected transmit beam
5. Interference rejection

For all four full-adaptive modes, it is assumed that each user terminal has a unique identification code and frequency, that each user terminal has hemispheric coverage antennas, and that the normal to the AMPA on Spacelab is pointed along the nadir.

The first mode in the above list is a basic operational mode for the AMPA system and is that pictured in Figure 3-1 for duplex communications between two user terminals. For this mode, the AMPA system would adaptively form two receive beams and two corresponding transmit beams to establish a duplex communications link between two co-operating shipboard or mobile terminals within the coverage area. The data relayed via the AMPA antenna system would be recorded on board the Spacelab or be relayed to ground in order to evaluate the received and relayed signal quality. The signals received by each user terminal would also be recorded for evaluation. Other key measurement parameters to be recorded for evaluation are the user acquisition time, the tracking accuracy, the signal-to-noise (S/N) ratio at Spacelab and at the user terminals, and the Doppler compensation achieved at Spacelab.

The second mode is a variation of the first, in which interference of a controlled type and level is present from a third user terminal whose signal does not have a valid user code. The purpose of this mode is to permit evaluation of the AMPA adaptive interference rejection in a systematic manner for various levels and types of interfering signals. The data recorded would be the same as that for the first mode plus measures of the interference rejection/cancellation under the different controlled conditions and the degree to which signal-to-noise plus interference, S/(N+1), is maximized for the desired transmission.

The third mode listed is likewise a variation of the first in which a duplex communications link is established adaptively between a single user terminal and the AMPA system, which is used as a Spacelab terminal in this mode rather than as a relay. Controlled interference could be introduced with this mode, as was described for the second mode, to permit further evaluation of the AMPA adaptive interference rejection capability.

The fourth mode is similar to the third except that the single beam is used for receive only in a one-way communications link. This mode could be used for such experiments as data collection from buoys and platforms having suitable beacon terminals or search and rescue operations with a suitable distress beacon terminal.

Both the third and fourth modes could be used also as special check-out modes for each beam of the AMPA system to evaluate its technical performance as an instrument, as compared to its operational performance. In such a checkout mode, antenna performance parameters such as acquisition time, S/N at Spacelab, Doppler compensation achieved, and angle tracking would be recorded for analysis.

A typical sequence of operation for the AMPA Experiment operated in its User/User dual-beam duplex communications link mode is as follows:

1. Shuttle/Spacelab flies into radius of operation of User Terminal
2. Adaptive Loops Acquire User Identification Signal and Form Beam No. 1
3. AMPA sends Verification Signal to User
4. Shuttle/Spacelab flies into Radius of Operation of 2nd User Terminal, Acquires, Forms Beam No. 2, and Verifies Contact to both Users.
5. AMPA Relays Data Transmission between Users simultaneously, sequentially, or responsively during contact.
6. Adaptive Loops Track Users and Reject Interference
7. AMPA Alerts Users when Contact Termination is imminent.
8. Sequence Repeats for Next User as Shuttle/Spacelab enters its Radius of Operation.

3.1.2.2 Programmed AMPA Experiment Operation

The programmed search or commanded beam steering mode is an alternative mode of operation for AMPA to fully-adaptive signal acquisition, beamforming, and tracking. Prescribed search patterns can be generated for special purposes with this mode, while the adaptive array circuitry only provides interference rejection. This is a desirable feature to provide for the AMPA system, since it permits either adaptive beamforming or commanded beam steering for greater operational versatility.

Programmed operational modes for the AMPA Experiment would be similar to the four listed in paragraph 3.1.2.1 for fully-adaptive AMPA operation. User terminal locations would have to be known priori to use these modes for duplex communication links, however, and this would limit their utility. It is more likely that the programmed operational modes would be found useful in search operations for user terminals that do not have the identification codes required for adaptive beamforming operation of the AMPA system.

3.1.3 AMPA COVERAGE AREA/RADIUS OF OPERATION

A study was made of AMPA radii of operation for typical Shuttle/Spacelab earth orbits to determine the geographic area coverage obtained and the typical times of operation. Calculations were made for a 5^{o} ground-station elevation angle, which represents the lowest practical ground-station elevation angle, and also for a 23^{o} ground-station elevation angle, which corresponds to a 60^{o} scan angle of the AMPA from the normal to the array face. A 400 km orbit altitude is assumed with a nadir-pointing beam at 0^{o} scan. A scan angle of 60^{o} represents the practical limit usually used for phased-array scan angles. Since the AMPA is adaptive, however, and can self-compensate to some extent for the detrimental effects of mutual coupling etc. at large scan angles, it should be possible to scan beyond 60^{o} somewhat and thus achieve greater coverage area and operating time. The AMPA scan angle only increases to 69.6^{o} for a 5^{o} ground-station elevation angle and the 400 km orbit altitude, but the corresponding increase in coverage area is large because of the earth curvature, and total operating time is increased 5 to 7 times.

Typical operating areas over the CONUS (Continental United States) are shown in Figure 3-2 for ground stations located at NASA/GSFC, Rosman, NASA/Lewis, and Goldstone. NASA sites were selected for more convenient experiment planning and operation. The lighter contour line about each location is for a 23^{o} ground-station elevation angle, while the heavy contour line is for a 5^{o} elevation angle. For general information, a horizon contour line is also included for the Goldstone location and corresponds to an AMPA scan angle of 70.2^{o}. The Shuttle/Spacelab orbits shown are for a 400 km. orbit altitude at an inclination angle of 57^{o}, which results in a series of orbits that progress from east to west (see orbit numbers) and repeat every 3 days.

For the User/Spacelab single-beam modes of AMPA system operation with a ground station (the third and fourth modes discussed in paragraph 3.1.2.1), each radius-of-operation contour defines the area of coverage under the specified conditions. Any orbit passing through this area will permit a User/Spacelab single-beam communications link to be established with the ground station during the time the Shuttle/Spacelab is within the area. While the radii-of-operation contour lines are slightly egg-shaped on a Mercator projection, they are true circles about the ground-station locations. Arc radius is indicated in Figure 3-2 for three contours about Goldstone.

AMPA User/Spacelab operating times are given in Table 3-1 for the 23^{o} elevation-angle contours about NASA/Goddard, Lewis, and Rosman and for the 5^{o} elevation-angle contour about Rosman. The table gives the daily number of orbits through each coverage area and the total contact time per day, as well as the total six-day contact time. A comparison of the two sets of figures for Rosman shows that the average time per orbit with a 5^{o} elevation angle is roughly twice that for the 23^{o} elevation angle and that the average number of orbits per day is more than doubled, thus the total contact time is nearly 5 times as great. The total 6-day experiment operational time would be 680 minutes for four stations and 1020 minutes with 6 stations.

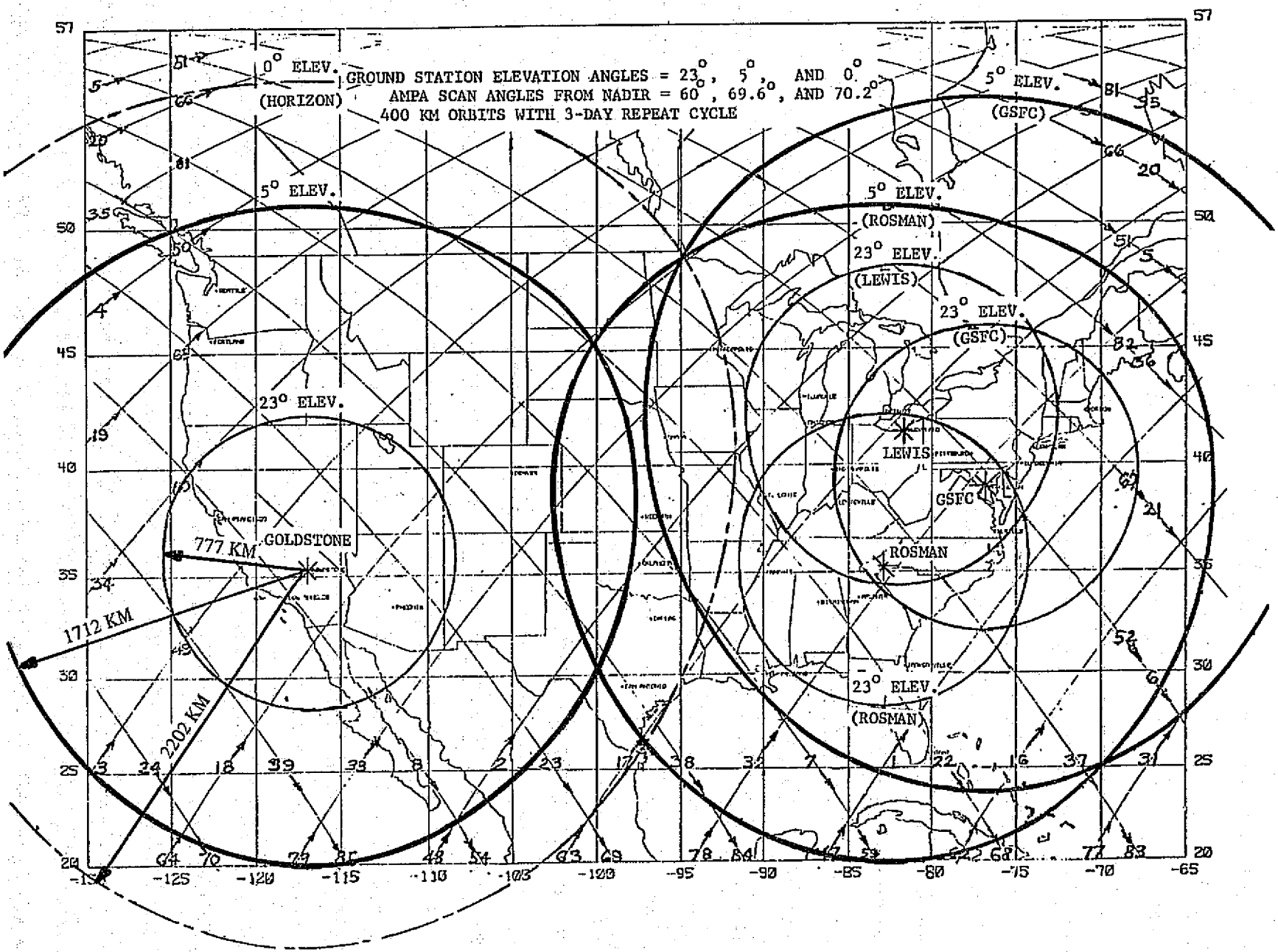

Figure 3-2. Typical Operating Areas Over CONUS

Table 3-1. Typical AMPA User/Spacelab Operating Times for 5° and 23° Ground Station Elevation Angles

(TIME IN MINUTES; # = NO. OF ORBITS)

STATION	DAY 1		DAY 2		DAY 3		DAY 4		DAY 5		DAY 6		6 DAY TOTAL TIME	AVE. TIME PER ORBIT	AVE. NO. OF ORBITS/DAY
	#	MIN.	#	MIN.	#	MIN.	#	MIN.	#	MIN.	#	MIN.			
GSFC (23°)	2	6.6	3	8.8	2	5.8	2	6.2	2	6.2	1	2.8	36.4	3.03	2.00
LEWIS (23°)	2	6.1	3	9.0	1	3.3	3	9.7	2	5.4	1	3.3	36.8	3.07	2.00
ROSMAN (23°)	2	3.5	3	9.8	2	5.5	2	4.5	2	6.8	1	3.5	33.6	2.80	2.00
ROSMAN (5°)	4	28.5	6	36.6	5	27.1	5	34.2	4	23.3	4	19.1	169.2	6.04	4.67

For the User/User dual-beam modes of AMPA system operation with a pair of ground stations (the first and second modes discussed in paragraph 3.1.2.1), the area common to two overlapping radius-of-operation contour lines defines the User/User region of operation for the two ground stations under the specified conditions. Any orbit passing through this region will permit a dual-beam communications link to be established between the two ground stations during the time the Shuttle/Spacelab is within the region.

Referring to Figure 3-2, it is seen that very little contact time would be available between Goldstone and Rosman even with 5^{o} ground-station elevation angles. For Rosman and Goddard, however, as well as for Rosman and Lewis and for Goddard and Lewis, there is a relatively large region of operation with 23^{o} ground-station elevation angles and an even larger region with 5^{o} elevation angles. For Goddard, Rosman, and Lewis, a part of their coverage areas is common to all three ground stations and defines a potential region in which three-beam operation could be performed or in which a User/User two-beam communications link could be established between two of the three stations while controlled interference was transmitted from the third (i.e., the second mode discussed in paragraph 3.1.2.1).

In order to obtain greater total operating time for the AMPA Experiment with the User/User mode of operation, more ground stations could be provided. Typical operating areas over the CONUS are shown in Figure 3-3 for ground stations located at Goldstone, White Sands, Johnson Space Center, St. Louis, Rosman, and Goddard. For clarity, the radius-of-operation contour lines are shown only for the 23^{o} ground-station elevation angle; however, much larger regions of operation can be visualized with the overlapping contours for 5^{o} elevation angles.

AMPA User/User operating times are given in Table 3-2 for the adjacent station pairs (Goldstone/White Sands, White Sands/Johnson, Johnson/St. Louis, St. Louis/Rosman, and Rosman/Goddard) for the 23^{o} ground-station elevation angle. Also included in the table are the User/User operating times for the Rosman/Goddard station pair for a 5^{o} elevation angle, as obtained from Figure 3-2. Comparison of the two sets of figures for the Rosman/Goddard station pair shows that the average time per orbit with a 5^{o} elevation angle is over three times that for the 23^{o} elevation angle and that the average number of orbits per day

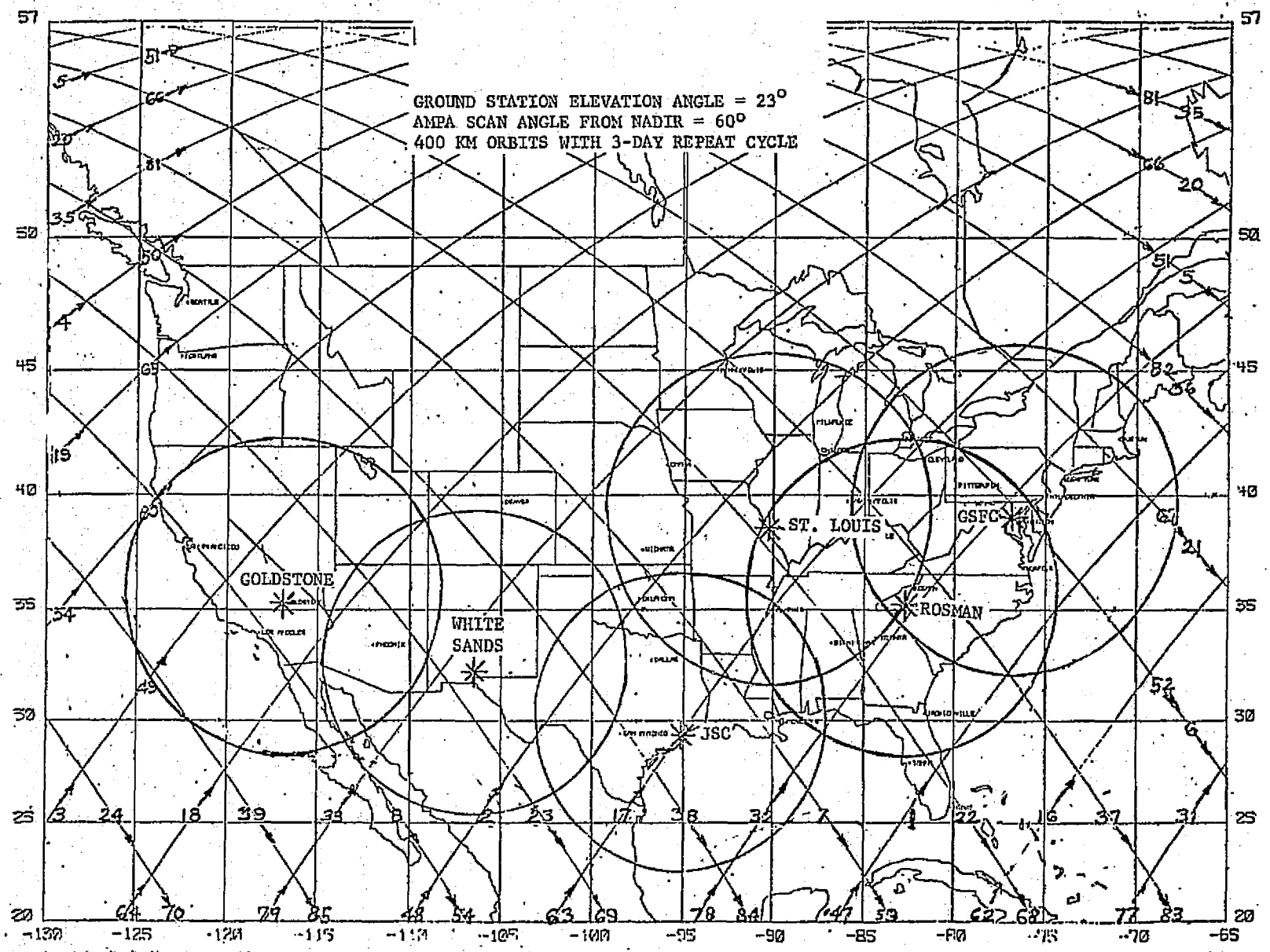

Figure 3-3. Typical Operating Areas Over CONUS

Table 3-2. Typical AMPA User/User Operating Times for 5° and 23° Ground Station Elevation Angle

(TIME IN MINUTES; # = NO. OF ORBITS)

STATION PAIR	DAY 1		DAY 2		DAY 3		DAY 4		DAY 5		DAY 6		6 DAY TOTAL TIME	AVE. TIME PER ORBIT	AVE. NO. OF ORBITS/DAY
	#	MIN.	#	MIN.	#	MIN.	#	MIN.	#	MIN.	#	MIN.			
GOLDSTONE/ WHITE SANDS (23°)	0	-	2	3.2	0	-	0	-	2	3.2	0	-	6.4	1.60	0.67
WHITE SANDS/ JSC (23°)	1	1.7	0	-	1	1.2	1	1.7	0	-	1	1.2	5.8	1.45	0.67
JSC/ ST. LOUIS (23°)	2	2.0	1	1.1	0	-	3	3.1	0	-	0	-	6.2	1.03	1.00
ST. LOUIS/ ROSMAN (23°)	0	-	2	4.6	1	1.6	1	2.8	1	1.8	1	1.6	12.4	2.07	1.00
ROSMAN/ GSFC (23°)	2	2.5	2	3.2	2	3.8	2	2.6	1	2.1	1	2.8	17.0	1.70	1.67
ROSMAN/ GSFC (5°)	4	20.5	5	29.4	4	20.6	5	25.0	3	18.7	3	14.4	128.6	5.36	4.00

is more than doubled, thus the total time for User/User operation is over 7 times as great. The total 6-day experiment operational time for the User/User mode would then be 640 minutes for the five pairs of stations.

3.1.4 AMPA FOOTPRINT ON EARTH

The footprint of the AMPA beams on earth was studied to determine the combined effects of beam broadening with angle of scan from nadir and increased space attenuation with greater slant range. For a 2 meter by 2 meter array aperture, the -3 dB beamwidth at 0^{o} scan is about 7.5^{o} at 1500 MHz. The beamwidth increases in the plane of scan inversely as the cosine of the scan angle, to a first approximation. At a 60^{o} scan angle, therefore, the -3 dB beamwidth is about 15^{o} in the plane of scan, which places the -3 dB angles at about 52.5^{o} and 67.5^{o}. Because of the rapidly increasing space attenuation with increasing scan angle in this region, the relative -3 dB levels on earth occur at angles that are somewhat smaller than given above and the 0 dB reference level also occurs at a smaller angle than the scan angle.

Footprints of the AMPA -3 dB contours on earth are shown in Figure 3-4 for scan or viewing angles of 0^{o}, 15^{o}, 30^{o}, 45^{o}, and 60^{o} from nadir. The footprints are plotted against radial arc length on earth from nadir, and the central earth angle from nadir is also indicated for reference. Shown dotted for comparison are the -3 dB beamwidth contours without space attenuation (path loss) for the 45^{o} and 60^{o} scan angles. For any point on an orbit within an AMPA single-beam coverage area or dual-beam region of operation, the footprint on the earth about the ground-station location can be obtained by interpolation from Figure 3-4 and placed on the operating area maps shown in Figures 3-2 and 3-3.

3.1.5 AMPA PARAMETERS, OPERATING CONDITIONS, AND LINK CALCULATIONS

A set of assumed parameters and operating conditions was established for the AMPA system in order to permit link calculations to be made for the AMPA Experiment operation. These assumed operating conditions are shown in Table 3-3 for the AMPA antenna system and in Table 3-4 for the User Terminals (ground stations that will be used to simulate small user terminals). The variation in AMPA receive and transmit gain was assumed to vary as the

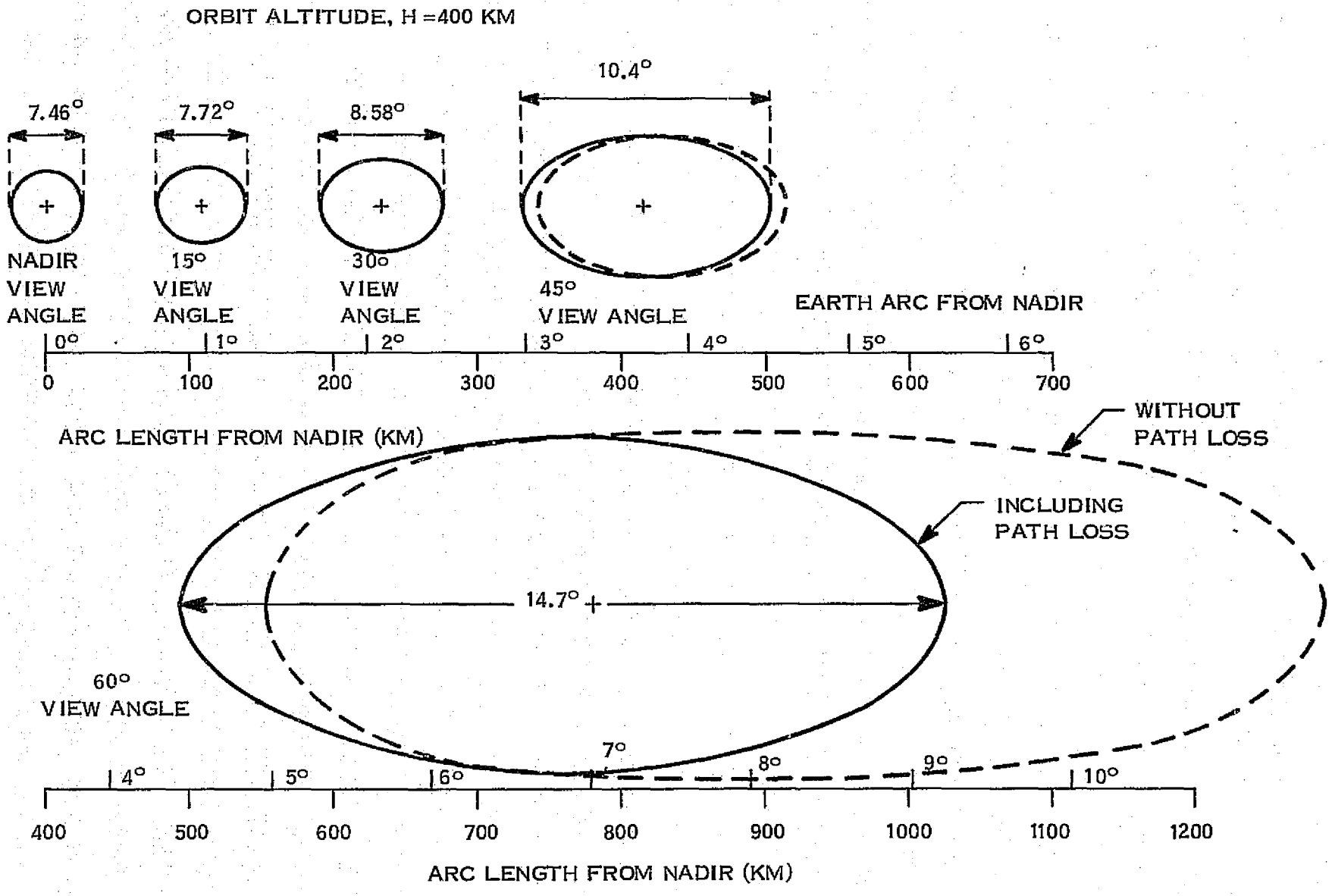

Figure 3-4. Footprint of AMPA -3 dB Contour on Earth for Several View/Scan Angles from Nadir

cosine of the scan angle. The full array gain is assumed for transmit, and the radiated power per beam takes into account the beam-splitting loss incurred with simultaneous independent beams. The system noise temperature assumes a receiver noise figure of 5 dB (627^{o}K) plus 83^{o}K for circuit losses and a 290^{o}K antenna/ground temperature.

Table 3-3. AMPA Experiment Parameters and Operating Conditions

AMPA Antenna System
• Number of Radiating Elements = 32
• Field of View = $\pm 70^{o}$
• Gain (Beams Formed) = 19.2 dB/Beam at 0^{o} Scan
• Radiated Power = 6.6 Watts/Beam (8.2 dBW)
• System Noise Temperature = 1000^{o}K*
• Transmit Frequency = 1.54 GHz
• Receive Frequency = 1.64 GHz
• RF Bandwidth = 7.5 MHz (3 Bands of 2.5 MHz)
• Comm Signal Bandwidth = 50 KHz
• Pilot Signal Bandwidth = 1 KHz

*Note: $T_S = T_A + T_R$

Table 3-4. AMPA Experiment Parameters and Operating Conditions

User Terminals
• Antenna Coverage = Hemispheric
• Radiated Power = 1 Watt EIRP Above 23^{o} Elevation Angle (5 Watts EIRP for 5^{o} Elevation Angle)
• System Noise Temperature = 860^{o}K*
• Transmit Frequency = 1.64 GHz
• Receive Frequency = 1.54 GHz

*Note: $T_S = T_A + T_R$

Link calculations were made for the AMPA communications channel and for the adaptive beamforming channel. The carrier-to-noise ratio (C/N) for the communications channel was calculated for the uplink from a ground station to Spacelab, for the downlink from Spacelab to a ground station, and for the total dual-beam link between two ground stations having the same elevation angle to Spacelab. The results are shown plotted against AMPA view/scan angle in Figure 3-5 with the corresponding ground-station elevation angles also indicated. The available C/N margins above a 10 dB minimum are also indicated. It is seen that the assumed operating conditions are adequate out to an AMPA view/scan angle of 62^{o}, and that an additional 7 dB of ground station power (5 Watts EIRP) would permit operation out to 69.6^{o}, which corresponds to a 5^{o} ground-station elevation angle.

The carrier-to-noise ratio for the adaptive beamforming channel was calculated only for the uplink, since the corresponding transmit beam is retro-directed by an algorithm that uses the adapted radiating-element weights of the receive beam. The results are shown plotted against AMPA view/scan angle in Figure 3-6. It is seen that the assumed operating conditions are adequate in this case out to an AMPA view/scan angle of over 66^{o}, thus the adaptive beamforming channel is not the limiting link in the AMPA Experiment.

3.1.6 AMPA EXPERIMENT EQUIPMENT

The AMPA Experiment requires equipment on Spacelab, at user terminals, at the ground control terminal, and at the data processing facility. The equipment required on Spacelab has received the most attention to date. Preliminary designs of the User Terminal and of the Ground Control Terminal are covered in paragraphs 3.2 and 3.3, while special equipment needed for data reduction is covered in paragraph 3.4.

A block diagram of the AMPA L-band antenna system on Spacelab is shown in Figure 3-7. Part of the AMPA antenna system equipment is located on a Spacelab pallet and the rest is inside the Spacelab module, as indicated by the dashed line on the block diagram. When the adaptive loops are at the array as shown here, the pallet equipment consists primarily of the L-band radiating element modules, the adaptive beamforming network and control, and

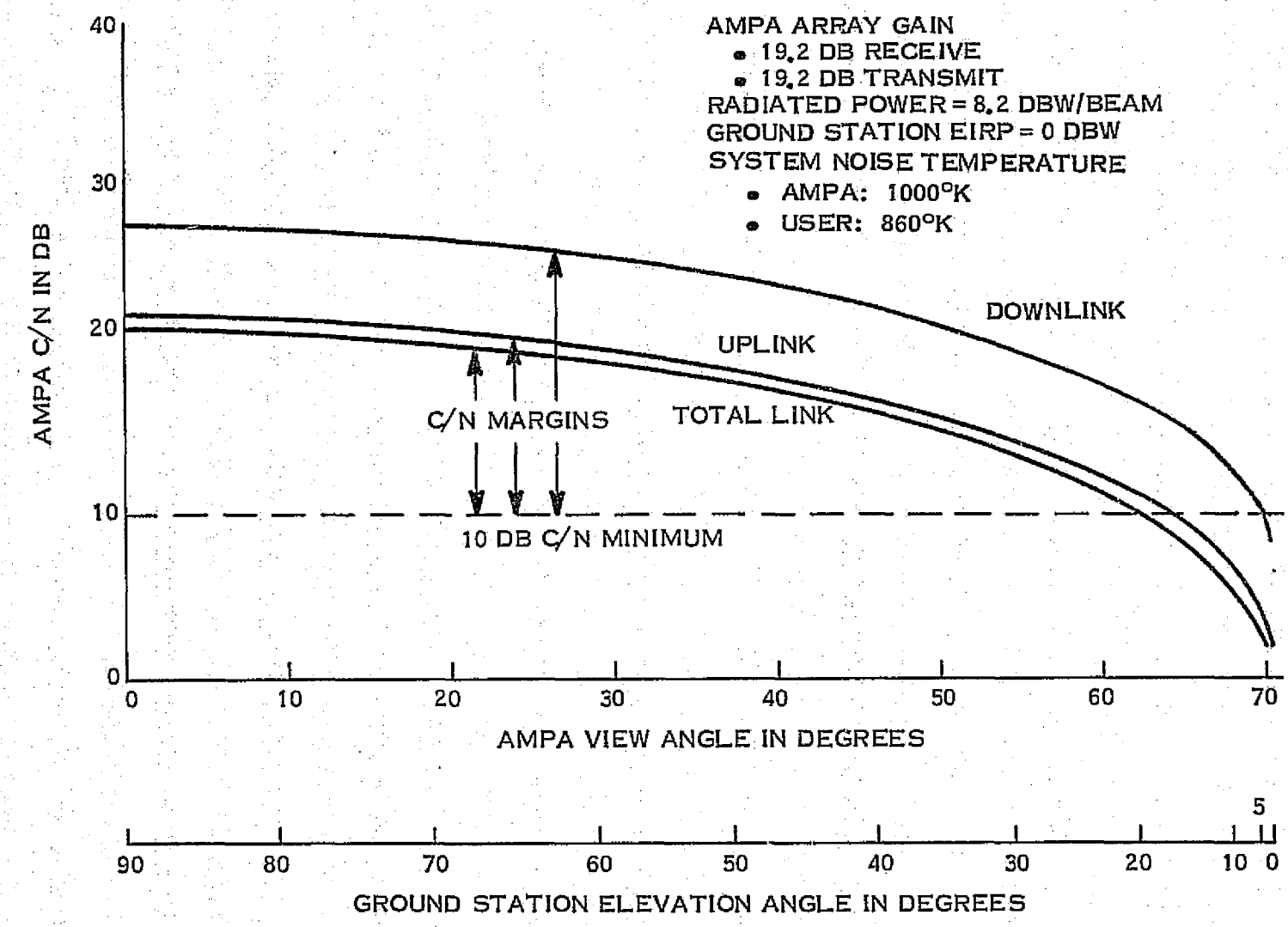

Figure 3-5. AMPA Carrier-to-Noise Ratio for 50 KHz Communication Channel

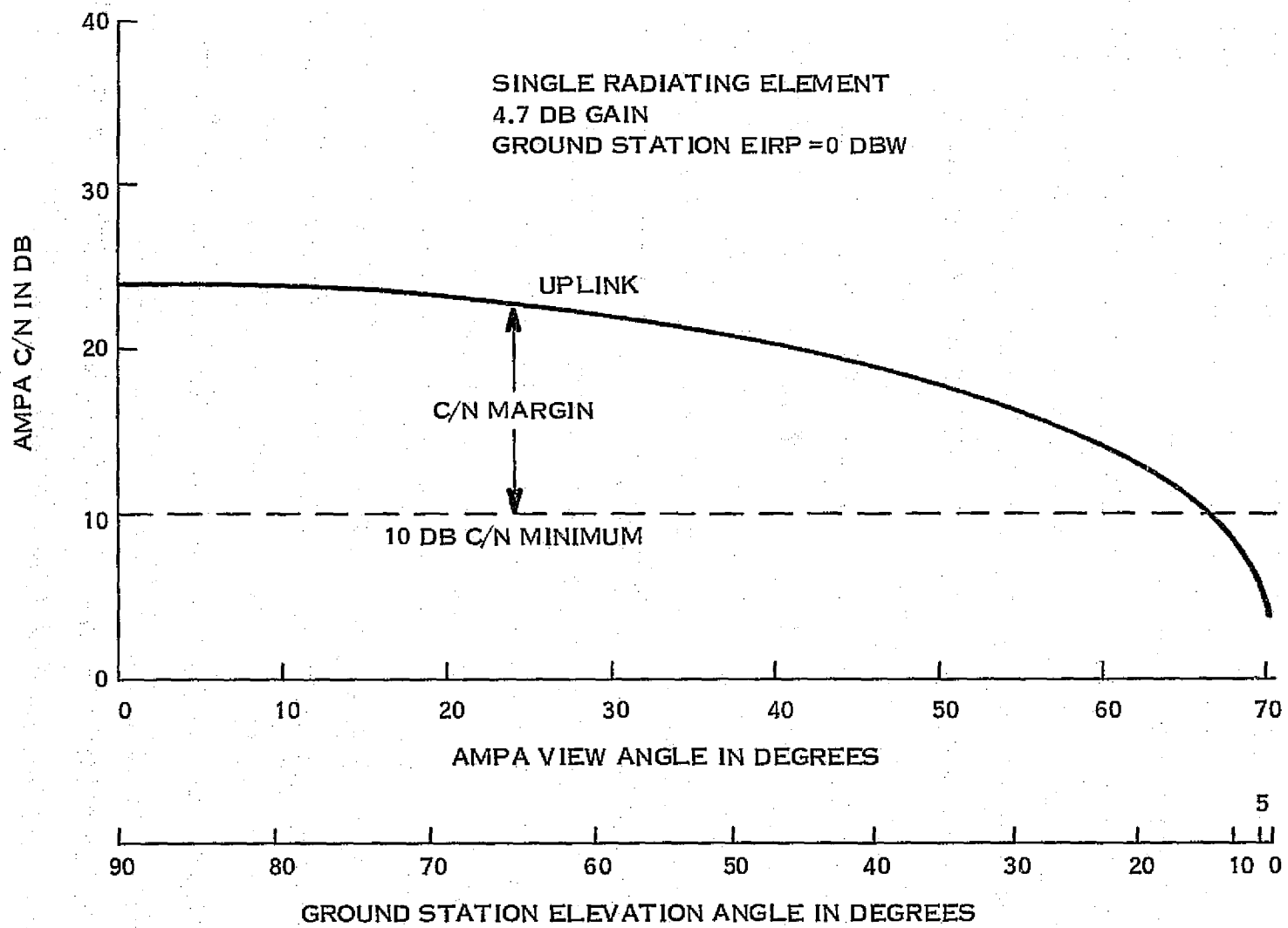

Figure 3-6. AMPA Carrier-to-Noise Ratio for 1 KHz Adaptive Beamforming Channel

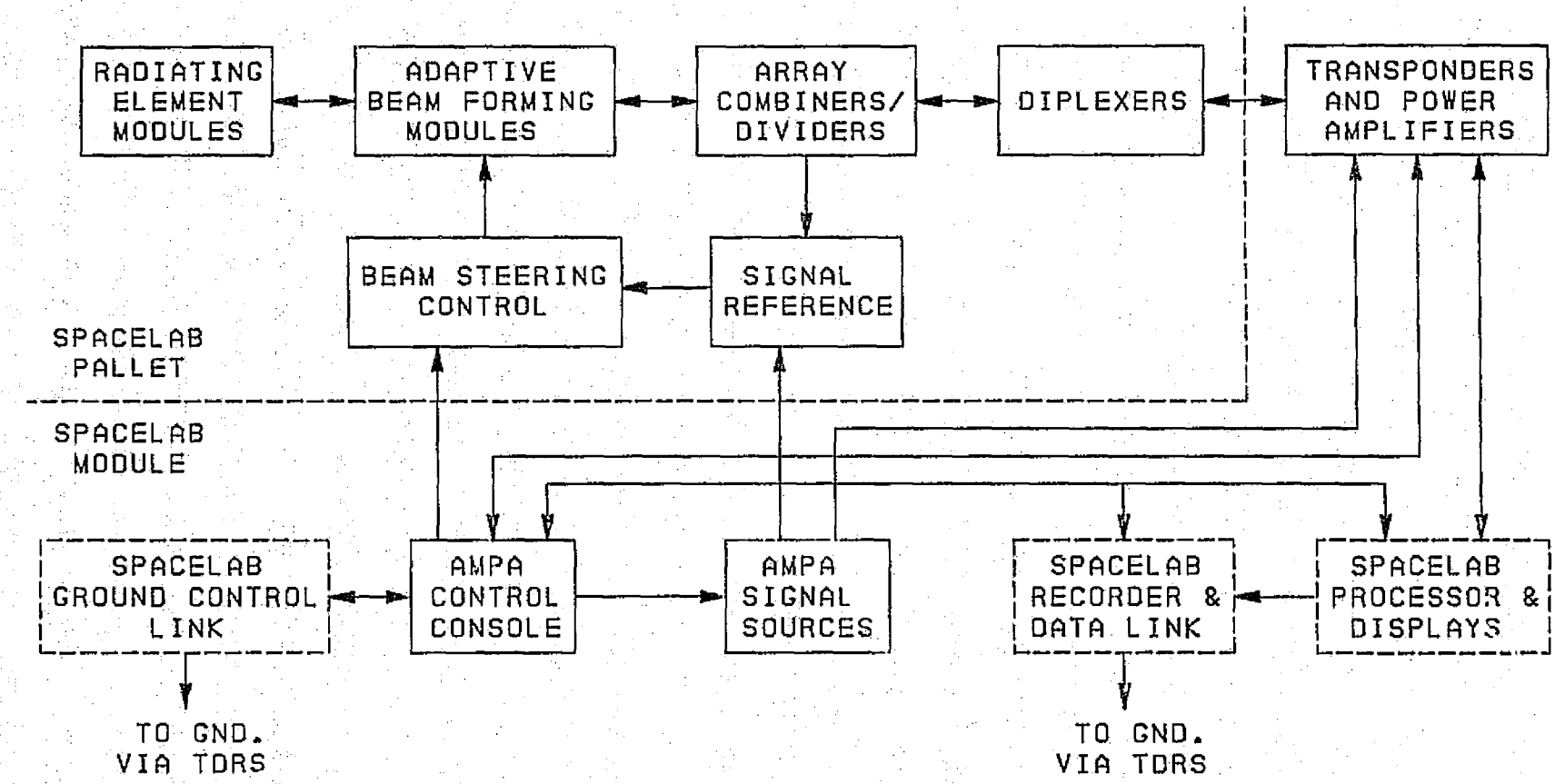

Figure 3-7. AMPA L-Band Antenna System Block Diagram

the diplexers. Equipment inside the Spacelab module consists of the beam-level receivers and transmitters, the AMPA signal sources, and the AMPA control console. As an alternative, the receivers, transmitters, and signal sources could also be located on the pallet, with only the AMPA control console in the Spacelab module. Alternatively, the adaptive circuitry could be placed inside the module, in which case only the radiating element modules would be on the pallet. Interfaces with Spacelab equipment are also indicated in the AMPA antenna system block diagram for on-board data recording, processing, and display, for a data link to ground via TDRS, and for a control link to ground via TDRS.

Figure 3-8 shows one configuration of the L-band AMPA Experiment pallet equipment mounted on a standard Spacelab pallet. Alternative configurations are being considered to permit this equipment to occupy only one half of a pallet.

3.1.7 AMPA EXPERIMENT PARAMETERS

The principal parameters to be observed during the AMPA Experiment include all those necessary to evaluate the overall AMPA system performance. These fall into two categories:

1. Parameters which are required in order to determine the AMPA functional operation.
2. Parameters which are needed to evaluate signal quality and communications link performance.

Some of these parameters will be available for continuous display on board the Shuttle/Spacelab for monitoring purposes. All will be relayed from Shuttle via TDRS to the AMPA Ground Control Center at NASA/JSC, and to the IPD data processing center at NASA/GSFC for detailed post-flight data reduction. Basic parameters will also be relayed to NASA/JSC for display/monitoring, recording, and relay to NASA/GSFC for AMPA Experiment monitoring, data recording, and short term (day-to-day) data processing.

Most of the operating parameters will be monitored and recorded continuously, while some parameters can be sampled periodically. In order to reconstruct real-time operating conditions during post-flight data reduction and analysis, experiment operating time in GMT and Shuttle/Spacelab ephemeris data will be recorded at least at 0.1 second intervals

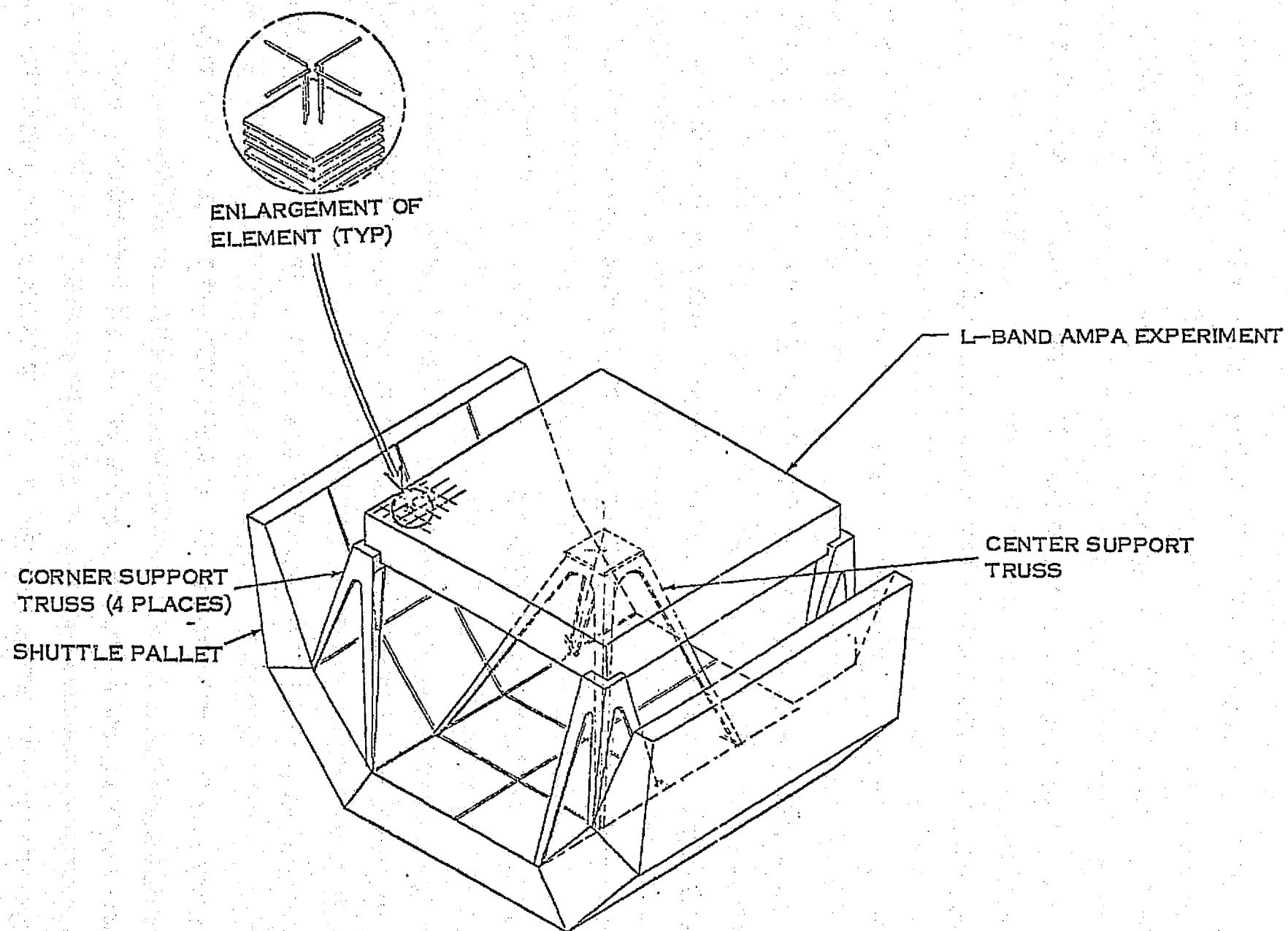

Figure 3-8. L-band AMPA Experiment Pallet Complement

during actual AMPA operation (i.e., just prior to, during, and just after contact in any AMPA operational mode with User terminals).

One of the key measurement parameters of the AMPA antenna system is the acquisition time. This is the time taken to form a beam on a User Terminal with full phased array gain after the User first enters the AMPA field of view. This will be determined by monitoring and recording the S/N (signal-to-noise ratio) in an adaptive beamforming loop and in the main communications data channel. The start of User signal acquisition is determined by the time at which the S/N in the adaptive loop crosses a reference threshold of say 10dB, and the completion of User signal acquisition is determined by the time at which the S/N in the main data channel rises above a corresponding threshold.

Once acquisition is completed, the AMPA antenna system must track the User Terminal and must also compensate for Doppler shift during the Shuttle/Spacelab pass. In order to evaluate the AMPA tracking accuracy, the adapted radiating element weights for all 32 elements will be sampled and recorded periodically for later reconstruction of the wavefront during data processing and comparison with the actual User Terminal direction obtained from the corresponding ephemeris data. The frequency of the signal received in each main data channel will be sampled and recorded periodically after the LO phase-lock circuitry in the receiver, in order to evaluate the Doppler compensation attained at Spacelab during post-flight data processing.

Data received from User Terminals, data relayed via the AMPA antenna system to a second User Terminal, and transmissions from AMPA to a User Terminal will be displayed on board Spacelab and also relayed to ground via the TDRS data link in order to evaluate the received and relayed signal quality. These data will be monitored both on board Spacelab and at the Ground Control Terminal for near real-time evaluation. They will also undergo post-flight data processing and analysis for a more extensive evaluation of signal quality and communications link performance.

An especially important part of the communications data monitoring, recording, and evaluation is that done in the presence of controlled interference from a third cooperating ground station. The signal from this interfering station would not have a valid user identification code, as would the other two User Terminals in the User/User operational mode. The interfering station would have a programmed format of controlled levels of interference and several different types of modulation, as well as intervals of no transmission in between the various steps. The S/N of the communications data channel will be continuously monitored and recorded in order to determine (1) the response time of the adaptive loops for interference rejection and (2) the degree of interfering signal rejection achieved (i.e., cancellation ratio) for the various interfering signal levels and types of modulation.

Signals transmitted by the User Terminals and received from Shuttle/Spacelab via AMPA will be recorded also at the User locations, together with time reference signals corresponding to those recorded on Spacelab. The tapes from these recordings will be used in conjunction with the data relayed from Spacelab for complete AMPA Experiment evaluation during post-flight data processing and analysis.

3.1.8 AMPA SIGNAL STRUCTURE

The signal transmitted from an AMPA User Terminal will consist of (1) a narrow-band coded pilot signal and (2) a communications signal. The pilot signal is used by the AMPA for adaptive signal acquisition, beamforming, and tracking of valid User Terminals (i.e., those having a correct identification code). Any signal that does not have such a coded pilot will be rejected by AMPA by adaptively forming a null in the direction of such a signal.

The AMPA pilot signal transmitted by each User Terminal will have a unique User identification code. The pilot signal bandwidth will be 1 kHz, and the modulation will be PCM/BPSK. The pilot signal will also be used for telemetry and transmission control between the User and Spacelab. Several different signal formats could be used for the composite pilot signal. In a relatively noise-free environment, a simple 8-bit word that is repeated four or five times to form a four or five word group could be used with a 75 to 80 percent time interval between code groups. The interval between code groups would be used to send User telemetry/mon-

itor signals, such as S/N and verification of AMPA signal reception, and to initiate data transmission by AMPA. While simple in principle, this format introduces some difficulties in the temporal code filter design for the adaptive loops.

A better format for the AMPA pilot signal is a continuously repeated PN code sequence of moderate duration that is continuously received by a bipolarized temporal correlation detector. Once this code becomes synchronized, it permits the pilot signal to operate the adaptive loops for signal acquisition, beamforming, and tracking. A suitable code might have 31 bits ($2^5 - 1$) and a duration of about 20 msec. The telemetry and transmission control data would be biphase modulated on this PN code stream at a slow rate corresponding to the code duration.

The AMPA communications signal will have a bandwidth of 50 kHz. The modulation will be selectable between either PCM/BPSK or FM. Because of the limited contact time (about five minutes) for each transmission in any of the AMPA operational modes (User/Spacelab or User/User, either duplex or one-way), pre-recorded test tapes will be used for the data transmissions. These tapes will provide a sequence of 30-second test segments for transmission. Each test segment will provide a different type of data in order to maximize the amount and type of data transmission that can be evaluated on each Shuttle/Spacelab pass by a User Terminal. The types of data modulation that will be evaluated include voice, slowed video (i.e., telefax), and digital data.

Special data transmissions will be permitted by providing for override of the programmed test tapes by ground control, User Terminal command, or on-board control by the Payload Specialist.

3.1.9 AMPA DATA LINK VIA TDRS

The data link between Spacelab and TDRS for the relay of AMPA telemetry and communications data to the AMPA Ground Control Terminal at NASA/JSC and the AMPA Experiment Control at NASA/GSFC will use the Ku-band data link on TDRS. This will insure adequate chan-

nel capacity for full evaluation of both the AMPA functional operation and the signal transmission quality and communications link performance.

The Ku-band data link will have a capacity of over 6 MBps. The two AMPA duplex communications channels will use up to 100 kBps for full data transmission. While the various operating parameters are sampled at a fairly slow rate, a large number of simultaneous data points are required for full evaluation of AMPA functional operation. These consist of the 32 adaptive complex weights, signal-to-noise ratio, frequency, etc. If these telemetry data are sent in serial bit streams, the total telemetry data rate will not exceed about 250 kBps. The total Spacelab to TDRS data link will thus require a maximum of 350 to 400 kBps. These data should be sent in real-time as they are acquired in order to provide near real-time monitoring (i.e., quick-look data display) at the Payload Operations Control Center (POCC), and to achieve maximum effectiveness of AMPA Experiment Control at NASA/GSFC. These data link requirements are summarized in Table 3-5.

Table 3-5. AMPA Experiment Data Link Requirements

1. Duplex Communication Link:	100 kBps
- 2 User/Spacelab Links, or User/User via AMPA Link	
- BW = 50 kHz/Channel	
- Data Rate = 25 kBps/Channel	
- Max. Data = 4 x 25 = 100 kBps	
2. Adaptive Complex Weights:	205 kBps
- 32 Elements x 2 Beams = 64 Wts.	
- 2 Words/Wt. x 16-Bit Words = 2048 Bits/Sample Set	
- 2048 x 100 Samples/Sec = 204.8 kBps	
3. Signal-to-Noise and Frequency:	13 kBps
- S/N and f for 2 Communication Channels	
- S/N for 2 Adaptive Loops	
- 2 Doppler Compensated Tx Freqs.	
- 8 Values x 16 Bits x 100 Samples/Sec. = 12.8 kBps	
4. GMT and Ephemeris Data	16 kBps
- Time	
- Latitude, Longitude, and Orbit Height	
- 3 Velocity Components	
- 3 Orientation Components	
- 10 Values x 16 Bits x 100 Samples/Sec = 16 kBps	
5. Monitor/Status Data:	2 kBps
- 250 Monitor Voltages	
- 250 Values x 8 Bits x 1 Sample/Sec = 2 kBps	
6. Experiment Reserve Data Capacity:	64 kBps
Total AMPA Experiment Data Link Requirements	400 kBps

3.2 AMPA USER-TERMINAL PRELIMINARY DESIGN

This section covers identification of the AMPA User-Terminal requirements, preliminary design concepts for the basic User-Terminal equipment, and specification of the calibration beacons. Earlier in the program, some preliminary User-Terminal parameters were assumed to permit link calculations and overall systems analysis to be conducted. Those initial parameters were given in Table 3-4 of paragraph 3.1.5.

3.2.1 AMPA USER-TERMINAL REQUIREMENTS

The User Terminals for the AMPA Experiment are required to operate in a duplex mode with a nominal transmit frequency of 1.64 GHz and a nominal receive frequency of 1.54 GHz. The actual frequency difference is 101.5 MHz. For maximum AMPA operating times in both the User/Spacelab and User/User modes, the User Terminals are required to operate down to a 5^{o} elevation angle above the ground. The User-Terminal antenna must thus provide nearly hemispheric overhead coverage from the zenith down to a 5^{o} elevation angle. The User Terminals are required to transmit and receive left-hand circular polarization (LHCP).

The transmit EIRP must be at least 5 Watts (7 dBW) at 5^{o} elevation angle, as discussed in paragraph 3.1.5, but only needs to be 1 Watt (0 dBW) at 23^{o} elevation angle and 0.10 Watt (-10 dBW) at 90^{o} elevation angle. The radiated transmitter power required to achieve these values of EIRP depends greatly on the User-Terminal antenna gain as a function of elevation angle. If the radiated power were uniformly distributed over the hemisphere at a 5 Watt EIRP level, for example, the total power radiated would be only 2.5 Watts.

The gain of practical ground-terminal antennas generally is greater overhead and falls off at low elevation angles, thus, more User-Terminal transmitter power is needed to achieve the required 5 Watts EIRP at 5^{o}. As an upper limit, for instance, an antenna with a $\cos^{2}\theta$ power pattern that is rotationally symmetric about the zenith would require 110 Watts radiated power to achieve 5 Watts EIRP at 5^{o} elevation angle (85^{o} from the zenith) and would thus be a poor choice for the User-Terminal antenna. A better choice would be a turnstile type of antenna which has higher gain at low elevation angles and also provides overhead coverage. Severe

ground multipath effects can occur with such an antenna, however, unless care is taken to minimize gain at angles toward the ground.

The User-Terminal antenna is therefore required to have moderate gain from the zenith to 30^{o} elevation angle, greatest gain at low elevation angles, and negligible ground illumination. Assuming an antenna gain of 3 dB from 0^{o} to 30^{o} elevation and 0 dB from 30^{o} to 90^{o} would require a radiated power of 1.5 Watts to meet the EIRP requirements. Allowing 3 dB for polarization loss and 2.2 dB for antenna feed network and diplexer losses, the required User-Terminal transmitter power is 5 Watts.

The User-Terminal system noise temperature must be less than 860^{o}K. If the antenna noise temperature is 150^{o}K and the circuit losses are 1.1 dB (83^{o}K), the noise figure of the User-Terminal receiver must not exceed 5 dB (627^{o}K).

The AMPA User Terminals must be able to operate with either FM or PCM/BPSK communications signals, as discussed in paragraph 3.1.8. The bandwidth of the communications channel will be 50 kHz. Pre-recorded test tapes will be used for the data transmissions from the User Terminals to Spacelab.

In addition, each AMPA User Terminal must transmit a narrow-band coded pilot signal which provides a unique identification code. The pilot signal will have a 1 kHz bandwidth with PCM/BPSK modulation. It will be used for operation of the AMPA adaptive beam processors and also for telemetry and transmission control between the User and Spacelab.

As auxiliary equipment for the AMPA Experiment, each User Terminal will require a tape recorder for recording all signals transmitted and received during the AMPA operation. These tapes will be used together with the Spacelab data relayed and recorded for post-flight data reduction and analysis.

These User-Terminal requirements are summarized in Table 3-6.

Table 3-6. Summary of AMPA User-Terminal Requirements

Basic Requirements		
Antenna Coverage	=	Hemispheric
Receive G/T	=	-29 dB/°K Min.
Radiated Power	=	5 Watts EIRP above 5° Elevation Angle
Transmit Frequency	=	1642.5 to 1645 MHz
Receive Frequency	=	1541 to 1543.5 MHz
Polarization	=	LHCP Transmit and Receive
Typical User-Terminal Requirements		
Antenna Gain	=	> 3 dB from 5° to 30° Elevation Angle > 0 dB from 30° to 90° Elevation Angle < -3 dB below 0° Elevation Angle
Axial Ratio	=	10 dB or Less over 5° to 90° Elevation Angle
RF Bandwidth	=	2.5 MHz for both Transmit and Receive
Radiated Power	=	5 Watts EIRP from 5° to 30° Elevation Angle 1 Watt EIRP from 30° to 90° Elevation Angle
Transmitter Power	=	5 Watts
Feed Network and Diplexer Losses	=	2.2 dB Max.
System Noise Temperature	=	860°K Max.
Data Channel Carrier Separation	=	50 kHz
Data Modulation	=	FM and PCM/BPSK
Data Inputs	=	Microphone and Tape
Pilot Channel Bandwidth	=	1 kHz
Pilot Modulation	=	PCM/BPSK
Pilot Inputs	=	PN Identification Code, Telemetry Data, and Transmission Control
Auxiliary Equipment	=	Tape Player for Pre-Recorded Tapes, Tape Recorder (Multi-Track)

3.2.2 AMPA USER-TERMINAL DESIGN CONCEPTS

In order to provide User Terminals for the AMPA Experiment that will be highly reliable operational equipment and yet will have a low cost, the design approach selected is to modify commercial mobile radio equipment to meet the AMPA User-Terminal requirements. A commercial equipment suitable for this purpose is the General Electric MASTR ® Executive II Mobile Radio. This mobile radio transmits in the 806 to 825 MHz band and receives in the 851 to 870 MHz band. It is crystal controlled with a stability of ± 0.0002 percent (2Hz per MHz). It operates in a simplex mode (push to talk) and uses the crystal controlled exciter as the local oscillator (LO) on receive. Simplified block diagrams of the transmitter and the receiver are given in Figures 3-9 and 3-10, respectively.

The GE MASTR ® Executive II Mobile Radio can be furnished with four different transmit frequencies as standard equipment. These are selectable by a panel knob which switches in different ICOM (Integrated Circuit Oscillator Module) boards. Each modified mobile radio unit could thus be used at four different AMPA User sites on different channel frequencies.

An AMPA User Terminal would combine two GE MASTR ® Executive II Mobile Radios for duplex operation with one modified for use as the transmitter and the other modified for use as the receiver. A power amplifier doubler stage would be added to the unit that is used for the transmitter. To transmit at 1644 MHz, for example, the ICOM used in the transmit mobile radio unit would be selected for a normal transmit frequency of 822 MHz. The modified transmitter output would be fed through a high isolation diplexer to the hemispheric coverage User-Terminal antenna. These modifications are shown in Figure 3-11.

Additional modifications required for the transmit part of the AMPA User Terminal are provisions for pre-recorded tape input, the coded pilot signal, and PCM/BPSK modulation as an alternate to FM. The coded pilot signal and PCM/BPSK modulation are shown applied to the L-band power amplifier in the block diagram to simplify the modification, but these could be

® Registered Trademark

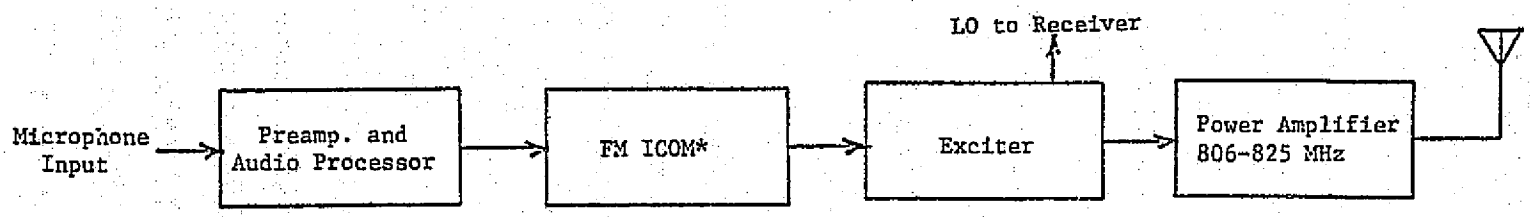

* ICOM = Integrated Circuit Oscillator Module (X tal Freq. = Tx Freq./48)

Figure 3-9. Simplified Transmitter Block Diagram of GE MASTR ® Executive II

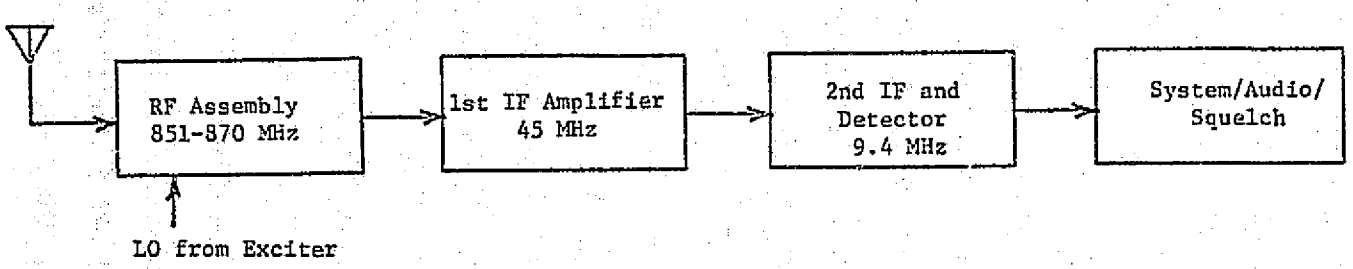

Figure 3-10. Simplified Receiver Block Diagram of GE MASTR ® Executive II

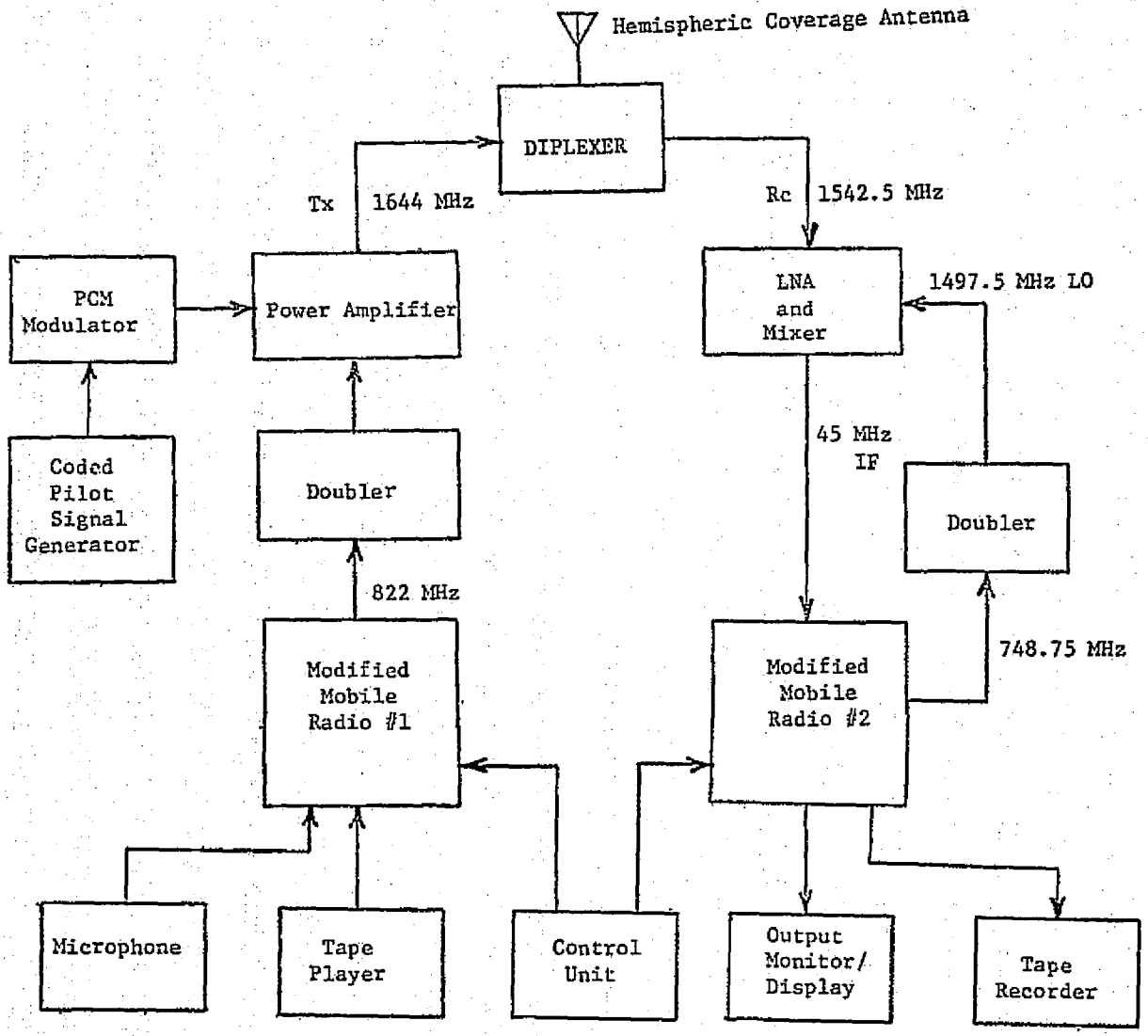

Figure 3-11. AMPA User-Terminal Block Diagram Showing Typical Operating Frequencies

introduced at a lower level in the mobile radio unit with further internal modification.

The mobile radio unit used for the AMPA User-Terminal receiver would be modified by the addition of a low noise amplifier (LNA) and mixer operating at L band. In order to use the existing 45 MHz IF amplifier of the second mobile radio unit, a local oscillator frequency of 1497.5 MHz would be required for a received signal at 1542.5 MHz (to continue the example started above for transmit). This can be provided by doubling a 748.75 MHz LO signal from the second mobile radio unit, which can be obtained by using a special out-of-band ICOM and modifying the tuning of the frequency multiplier chain slightly.

Additional modifications required for the receive part of the AMPA User Terminal are provisions for an audible or visual display monitor and for recording all signals received during AMPA operation. A control unit is also required for selecting the operating modes and controlling the AMPA User-Terminal operation.

3.2.3 AMPA CALIBRATION BEACONS

Calibration beacons for the AMPA Experiment will be located at two or possibly three of the User-Terminal sites. For economy and experiment flexibility, it is planned that these beacons will be specially equipped versions of standard User Terminals.

Several purposes will be served by the calibration beacons. For overall AMPA system evaluation, they will provide: (1) standard reference level signals; (2) standard reference modulations; and (3) master pilot-signal identification codes. For those AMPA Experiment modes of operation that require a controlled source of uncoded interference, they will provide: (1) controlled levels of interference; and (2) several types of modulation (such as AM, FM, PCM, CW tone, and PN spectrum).

The block diagram for an AMPA Calibration Beacon would be similar to that shown in Figure 3-11 for the AMPA User Terminal, but it would include additional means for setting transmitter power levels, modulation types and levels, and pilot codes. Transmitted power level could be controlled by a calibrated attenuator that is either designed into the transmit doubler

stage or integrated into the transmit mobile radio during modification. The actual transmitted power level could be monitored by an output power meter coupled to the transmit power amplifier. Similarly, the modulation level, types of modulation, and master pilot codes would be controlled by additional modifications to the basic User-Terminal design.

3.3 AMPA GROUND CONTROL-TERMINAL PRELIMINARY DESIGN

Consideration of this design phase is limited to the AMPA control link as illustrated in Figure 3-12. Control signals from the POCC (Payload Operations Control Center) at JSC to White Sands will be either through land lines or leased satellite facilities from a domestic satellite carrier. These control signals will then be sent via the TDRS (Tracking and Data Relay Satellite) to the CDMS in the Shuttle using the Ku-band link. This link and the AMPA data requirements are discussed in more detail under the next Subsection 3.4.

All of the command and control operations are handled by the POCC and the associated AMPA Experiment Control Center. Control of the experiment will be digital using a keyboard and display in conjunction with experiment-unique software. A voice link between the Principal Investigator (PI) and Payload Specialist (PS) will also be used and will aid in experiment coordination and control.

3.4 AMPA DATA REDUCTION REQUIREMENTS

The AMPA Experiment data fall into two basic categories: (1) primary data required to evaluate the AMPA overall system performance; and (2) operational data concerned with the AMPA Experiment operation. The AMPA Experiment parameters to be determined for evaluating overall system performance were discussed in paragraph 3.1.7, and the AMPA Experiment data link requirements were given in Table 3-5. All AMPA Experiment data are sent from Spacelab to ground in a digital data stream via the High Rate Multiplexer (HRM) and the TDRS Ku-band link. These data are then transmitted by land line or leased domestic satellite links to the AMPA Ground Control Terminal at NASA/Johnson Space Center and to the Information Processing Division (IPD) at NASA/Goddard Space Flight Center for recording and post-flight data processing. These two areas of AMPA Experiment control and data handling are indicated in Figure 3-13.

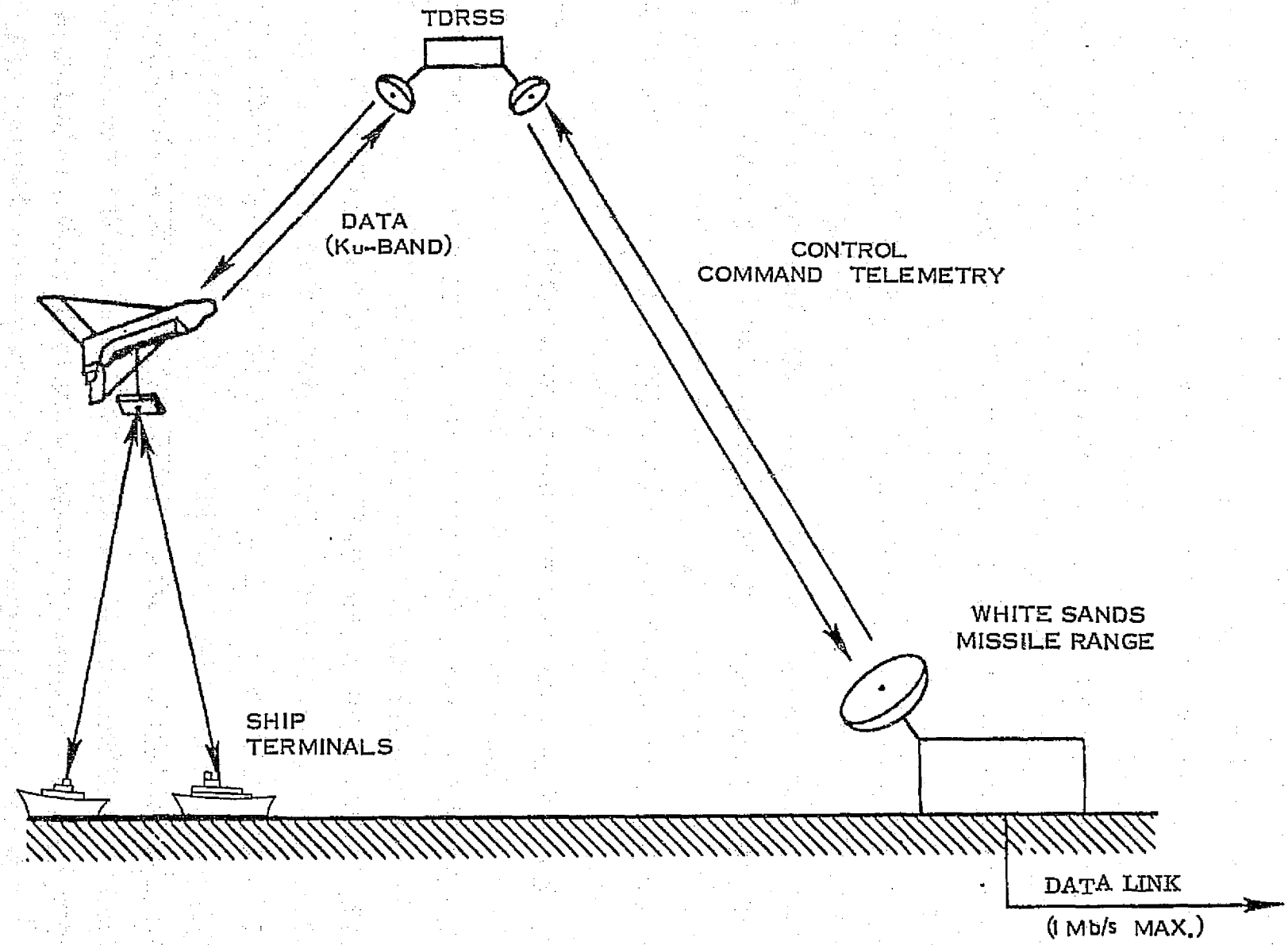

Figure 3-12. AMPA Control and Data Link

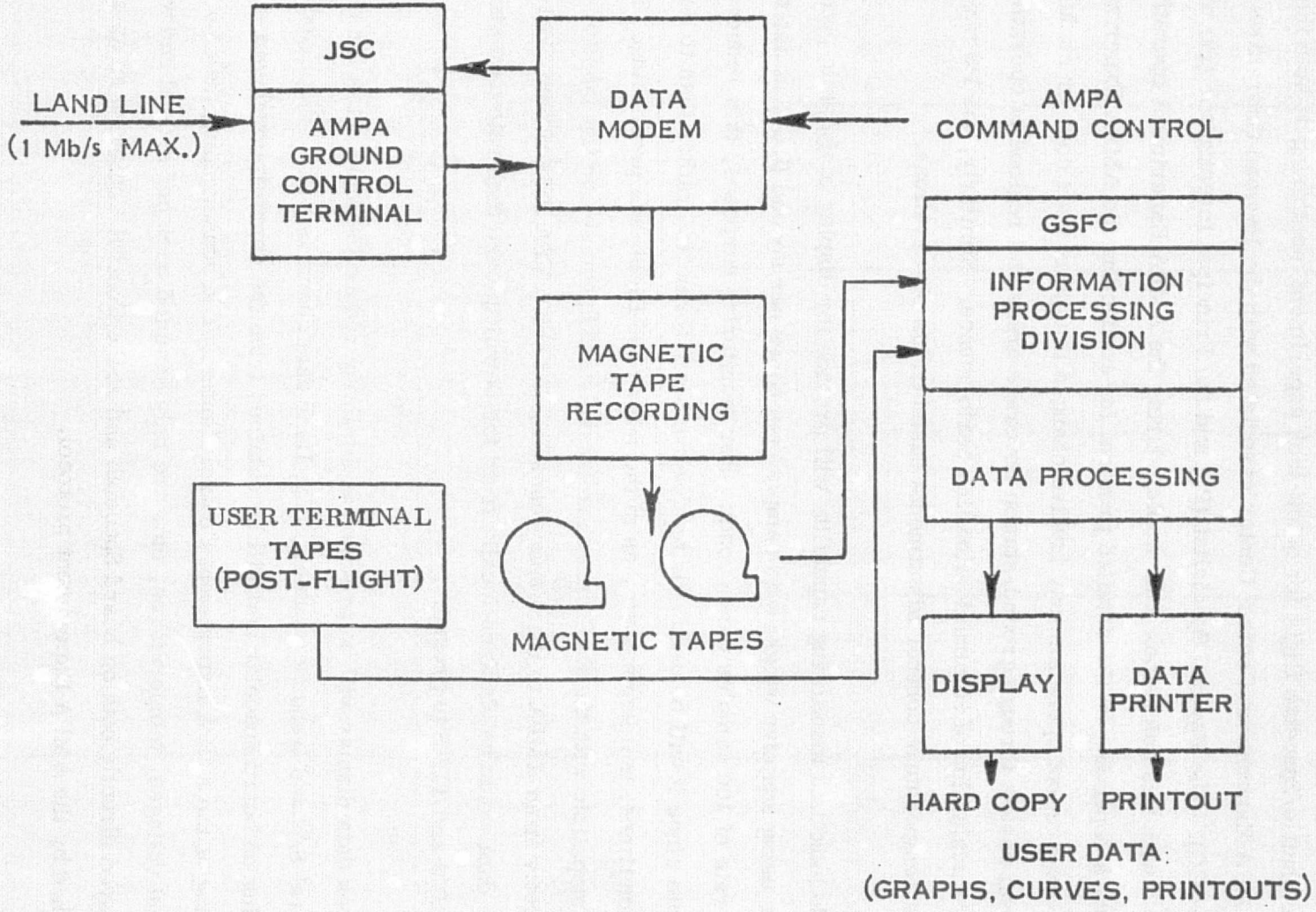

Figure 3-13. AMPA Experiment Control and Data Handling

Some of the AMPA Experiment data will be processed and displayed in near real-time during the Shuttle/Spacelab flight for quick-look experiment monitoring at both the Spacelab and the AMPA Experiment Control Center associated with the Payload Operations Control Center (POCC). The Payload Specialist (PS) and the Principal Investigator (PI) will both be involved with this quick-look data display during the AMPA Experiment operation in various ways depending on the detailed protocol for conducting the AMPA Experiment. For example, experiment operation may involve changes in type of user code or modulation during orbit passes through ground-station coverage areas and regions of operation, based on the PI's evaluation of communication link performance. Similarly, the PS may make voltage or temperature control adjustments based on his observations.

The quick-look data monitoring capability will provide for display of dynamic pattern formation using adaptive weight data sampled ten times per second (i.e., at one tenth of its full data rate of 100 samples per second). For monitoring purposes, this reduced data rate is adequate since it will be used only to observe beam formation rather than to determine acquisition times, null depths, etc. as in the later post-flight data processing. The reduced rate is compatible with the RAU data capacity on board Spacelab, so the monitor data can be sent directly from AMPA to the display console. At the AMPA Experiment Control Center, the same data would be obtained locally from the demultiplexed high rate data stream sent via the HRM and TDRS to ground.

Quick-look data display will be provided at similarly reduced sample rates for monitoring the several S/N and frequency values. The User data channels will be displayed directly for monitoring on board Spacelab and will be obtained from the demultiplexed data stream for monitoring at the AMPA Experiment Control Center. The housekeeping data for monitoring equipment voltages, temperatures, etc. are only sampled once per second and will thus be displayed directly both on board Spacelab and at the Control Center on an as-needed basis established by the AMPA Experiment protocol.

Post-flight data reduction at the IPD will use the full AMPA Experiment data relayed via the HRM and TDRS. It will also make use of the User Terminal tapes, as indicated in

Figure 3-13. Time sequence patterns will be generated for each beam from the adaptive weights in order to analyze various performance parameters related to beam formation, beam shape, sidelobe levels, null depths, etc. The quality of these parameters will be evaluated for the various operating conditions, and the beam and null formation response times will be determined by correlating the patterns with the S/N data as discussed in paragraph 3.1.7. The beam tracking accuracy will be evaluated, and the interference cancellation ratios for the different levels and types of modulation will be determined. The transmitted, received, and relayed communications signal quality will also be evaluated during post-flight data processing by comparison of the several data sources.

Software programs developed for system test of the AMPA equipment should be useful for performing some of these analyses and evaluations of the AMPA Experiment operation and system performance.

Further information on the AMPA data requirements and data system implementation is given in the Data Handling Plan, Contract Item 10.

3.5 ADDITIONAL AMPA MATERIAL GENERATED

Payload Data Sheets (Level A and B Data) for the AMPA Experiment were revised on November 5, 1976 and submitted to NASA/GSFC.

Viewgraphs were prepared for the AMPA Experiment Concept Review held at NASA/GSFC on February 2, 1977. A presentation on the AMPA Experiment configuration was given at the review.

Final Task Report, Contract Item 7, dated May 31, 1977 was prepared. This covers the AMPA Experiment Ground Handling and Test Operations in considerable detail.

Final Task Report, Contract Item 10, dated July 14, 1977 was prepared. Section 1 covers the AMPA Experiment Data Handling Plan in detail.

SECTION 4

ELECTROMAGNETIC ENVIRONMENT EXPERIMENT (EEE)

Definition of the EEE was conducted in three phases: MOD I design (121.5 to 2700 MHz), MOD II design (2.7 to 43 GHz) plus the MOD I frequencies, and preparation of a listing of terrestrial emitters or a Frequency Utilization Study for the bands being scanned.

The MOD I EEE definition work included several aspects of the experiment, but was concentrated in the following areas:

1. EEE Operation and Sensitivity
2. Payload Configuration
3. Operational Environment and Data Management
4. Instrument Tests During Development

4.1 EEE OPERATION AND SENSITIVITY

The Electromagnetic Environment Experiment is designed to monitor radio frequency interference emitters located on the earth. Figure 4-1 shows the EEE concept and the major functional parts of the experiment. The Shuttle/Spacelab segment is composed of the antennas, the receiver, associated Command & Data Management Subsystem (CDMS) equipment such as displays, data entry, and interface equipment to control the experiment and transmit data to the ground station. The TDRSS is the principal means of transmitting real-time data to the Payload Operations Control Center (POCC) at JSC. Final processing of data and distribution of information to Users will be accomplished at GSFC's Data Processing Facility.

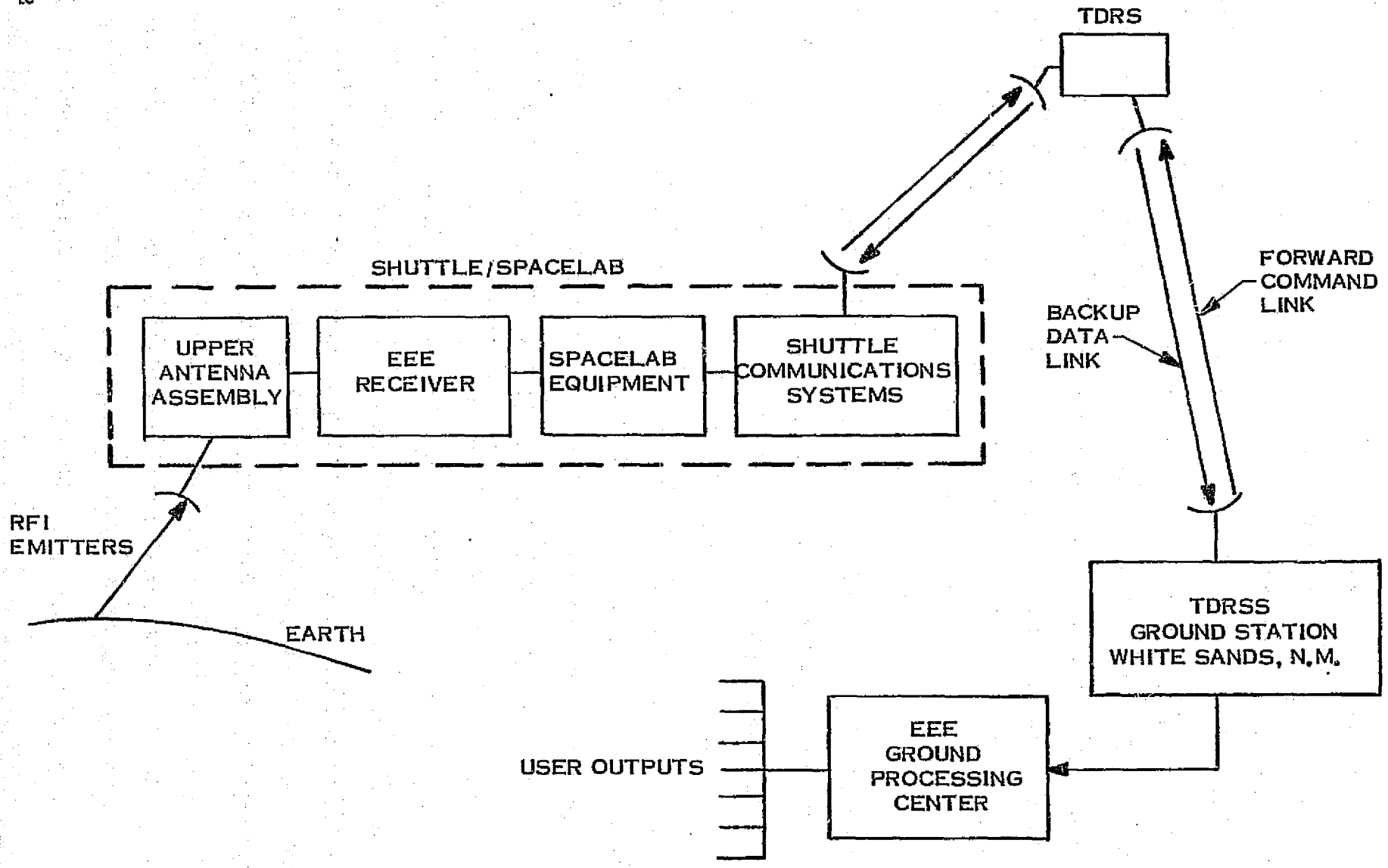

Figure 4-1. EEE Functional System

Control of the EEE will be by three different modes: via ground command, by programmed automatic procedures, or by manual control by the Payload Specialist. Figure 4-2 shows the principal functions of the EEE and the Spacelab equipment involved in operation of the on-board equipment. Control via command from the ground station will be routed through the TDRSS by means of the CDMS. Similarly, status of the equipment will be sent to the ground station through TDRSS, and to the POCC at JSC.

The Spacelab computer and Payload Specialist are directly involved in the programmed/automatic control mode. This mode will be controlled almost totally by the special EEE software maintained in the Spacelab computer. The Payload Specialist will be involved in this mode, but probably only to activate the mode and to monitor the operation of the experiment on the Spacelab displays.

The manual control mode is provided as a back-up mode and specifically for operation of the experiment by the Payload Specialist. A keyboard is provided at the AFD's Payload Station for command inputs and status monitoring. The CDMS data display is used for monitoring of incoming data and equipment checkout.

Operation of the EEE is centered about two main functional parameters, the frequency bands of interest and the receiver sensitivity to earth-emitter electromagnetic signals. Figure 4-3 shows the RF frequency bands and their usage to be covered in the design of EEE. The frequency range of 121.5 to 2700 MHz shown above the dotted line is the range to be covered in EEE-MOD I. A possible expanded EEE design, the MOD II, will cover the MOD-I range up to approximately 43 GHz.

Sensitivity of the EEE-MOD I is shown in Figure 4-4. The RF frequency bands are grouped according to the proposed antenna designs listed. Receiver bandwidths are typical minimum and maximum bandwidths expected to be used. Sensitivity is given as Effective Isotropic Radiated Power (EIRP) from the earth. Note that the sensitivity varies

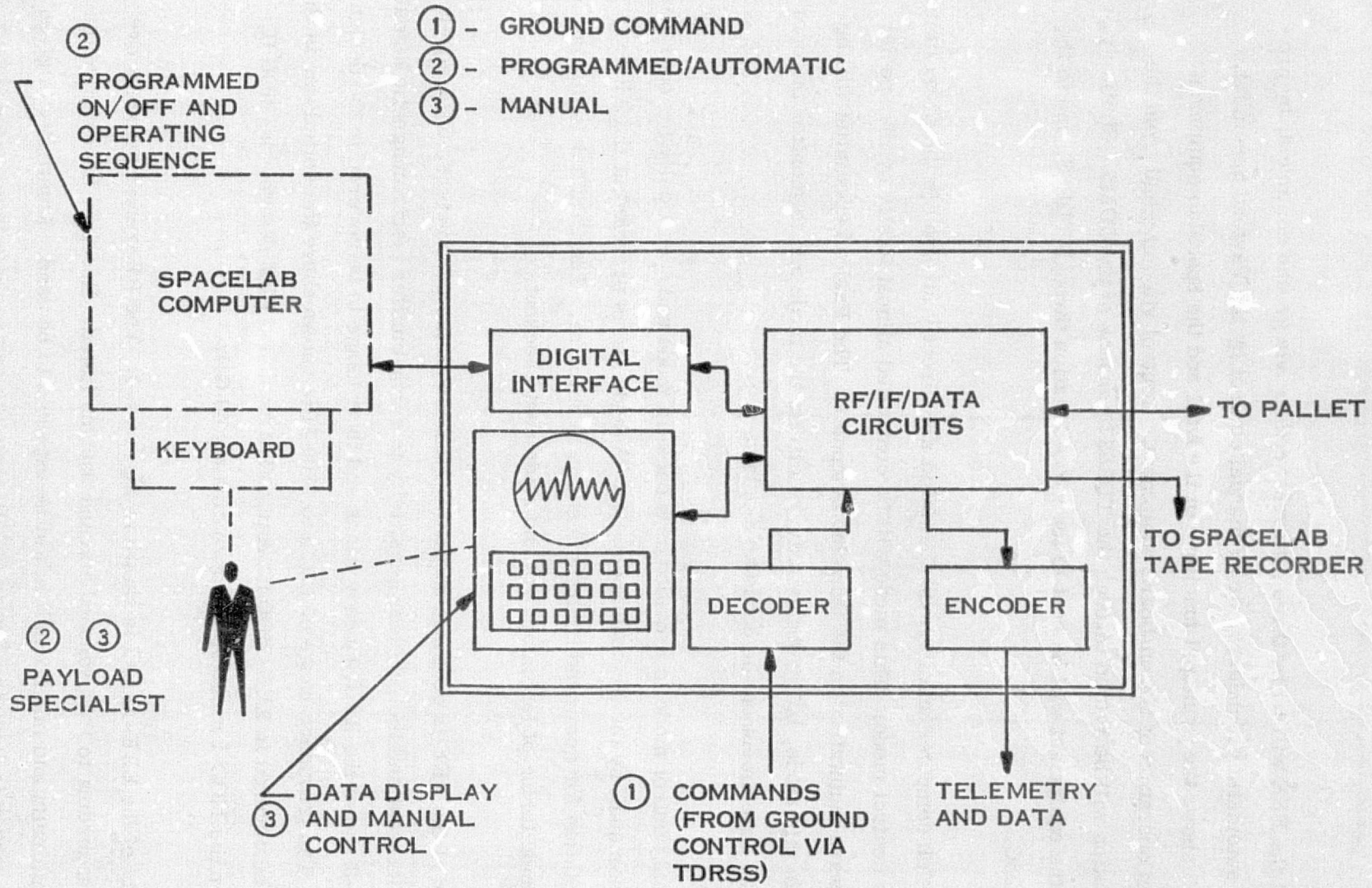

Figure 4-2. EEE Receiver Operation Modes

Band Number	Planned Mission Bands	Spectrum Bandwidth	Use
1	121.475-121.525 MHz	50 kHz	Emergency Distress, Search and Rescue (121.5 MHz)
2	242.975-243.025 MHz	50 kHz	Emergency Distress, Search and Rescue (243.0 MHz)
3	150-174 MHz	24 MHz	Land Mobile, Radio Astronomy
4a 4b	399.9-410.0 MHz 406.00-406.10 MHz	10.1 MHz 100 kHz	NASA Space Operation, Data Collection & Radio Astronomy Search and Rescue (406.05 MHz)
5	450.0-470.0 MHz	20 MHz	NASA Meteor. Sat. Data Collection, Land Mobile
6	806-947.0 MHz	141	Land Mobile, Public Service Satellite
7	1215-1300 MHz	85	MMAP SSR Experiment, NASA SEASAT SAR (1275±9.5 MHz)
8	1350-1450 MHz	100	MMAP SMS R/M Experiment, Radio Astronomy (H Line) (1400-1427 MHz)
9	1636.5-1670 MHz	33.5	Maritime/Aeronautical Mobile Sat., Radio Astronomy OH Line
10	2040-2110 MHz	70	NASA Earth to Sat. Data/Telecommand/Ranging
11	2200-2300 MHz	100	NASA Sat. Data Relay (TDRSS S-Band)
12	2655-2690 MHz	35	Fixed Sat. (Earth to Space)
13	2690-2700 MHz	10	Intern. Protected Exclusive Radio Astronomy
14	4200-4400 MHz	200	Passive Microwave Sensor (Sea-Surface Temperature)
15	4950-5000 MHz	50	Radio Astronomy (exclusive)
16	5250-5350 MHz	100	Space Research, Radio Location
17	5725-5925 MHz	200	Fixed Sat. (Earth to Space)
18	5925-6425 MHz	500	NASA Sat. (Earth to Space)
19	6475-6725 MHz	250	NASA Sat: Nimbus G SMMR
20	7900-7975 MHz	75	Fixed Sat. (Earth to Space)
21	9.50-10.05 GHz	55	MMAP SSR Experiment
22	10.6-10.7 GHz	0.1 GHz	Radio Astronomy (Exclusive)
23	10.95-11.2 GHz	0.25	Fixed Sat. (Earth to Space)
24	12.5-12.75 GHz	0.25	Fixed Sat. (Earth to Space)
25	13.1-15.7 GHz	2.6	NASA Fixed Sat. (Earth to Space) - Seasat Wind Field Scatterometer, Short Pulse Altimeter, ATS-6 MMW Experiment, TDRSS Ku-Band
26	17.0-24.0 GHz	7	ATS-6 MMW experiment, Nimbus - F SCAM Radiometer, Nimbus-5 (ESMR), Nimbus-G SMMR, and Radio Astronomy (H_2O vapor line), MMAP A&O R/M (18 GHz)
27	27.5-35.2 GHz	7.7	Fixed Sat., Space Research and Radio Astronomy (31.3-31.5 GHz, 33.0-33.4 GHz). Nimbus-5 NEMS (31.4 GHz), Nimbus-F SCAM (31.65 GHz), MMAP MMWC (29.7-30.2 GHz)
28	35.2-43 GHz	7.8	NASA Sat: Nimbus-F ESMR (37 GHz), Nimbus G SMMR (37 GHz), MMAP A&O R/M (36 GHz)
29	50-65 GHz	15	Space Research, Passive Microwave Sensor (future)

ACRONYM DEFINITIONS:

SSR	Surface Spectrum Radar
SMS R/M	Soil Moisture and Salinity Radiometer
SEASAT SAR	Seasat (Spacecraft) Synthetic Aperture Radar
SMMR	Scanning Multichannel Microwave Radiometer
SCANS	Scanning Microwave Spectrometer
ESMR	Electrically Scanning Microwave Radiometer
A & O R/M	Atmospheric and Oceanographic Imaging Radiometer
MMWC	Millimeter Wave Communications
NEMS	Nimbus E Microwave Spectrometer

Figure 4-3. Radio Frequency Bands for the EEE

Band	Frequency Band[1] (MHz)	Antenna	Beamwidth (degrees)	Gain (dB)	Efficiency (%)	Free Space Loss[2] (dB)	System Temp.[3] (K)	RCVR Bandwidth	Sensitivity[4] Min. Detectable EIRP (dBW)	In-Orbit Power-Flux Density[2] (dBW/m^2)
1	121.5	Log Periodic (1.4 dia x 1.8 ht)	70	8	40	128	900	±25 kHz	-19	-142
2	243.0	↓	70	8	40	134	900	±25 kHz	-13	-136
3	150-174		70	8	40	131	900	20 kHz 1 MHz	-20 -3	-143 -126
4, 5	399.9-470.0	UHF Array (1.0 x 1.3 m)	43	13	70	137	900	20 kHz 100 kHz 1 MHz	-19 -12 -2	-142 -135 -125
6-13	806-2700	0.7 m Parabolic	37-11	11-22	40	143 to 153	1200	20 kHz 1 MHz	-10 +7	-133 -116
6-13	806-2700	Conical Helix (0.17 dia x 0.17 m)	70	6	-	145 to 155	1200	20 kHz	-3 to +7	-126 to -116

[1] Calculations except beamwidth are at mid-band frequency.

[2] Altitude of 400 km referenced to nadir; altitude of 70° beamwidth referenced to beamedge.

[3] System Noise Temperature $T_S = T_R + T_A$, where T_R = Receiver noise temperature and $T_A = 290°$ = effective antenna noise temperature.

[4] Includes 10 dB Signal to Noise Ratio, Antenna Gain at HPBW. EIRP is referenced to Earth's surface.

Figure 4-4. EEE Sensitivity Analysis Summary for EEE MOD I

from -22 to +7 dBw, depending on the frequency band and bandwidth selected. In-orbit, power-flux density gives the expected power density incident on the antenna. These values can be used to evaluate the effects of Shuttle generated RF interference signals on the EEE sensitivity.

The type of signals expected to be received by the EEE is shown in Figure 4-5 from Reference 6. These data are typical and are representative of one form of user outputs. Typical user data outputs will be generated in graphs, charts and tabular form, examples* of which are:

EEE Scanning Receiver:

- EIRP vs. Frequency
- % Channel Occupancy vs. Frequency
- Channel Occupancy Tabular Ranking
- Power-Flux Density (In Orbit)

EEE S&R Fixed-Tuned Receivers:
(121.5 , 243.0 & 406.05 MHz)

- Antenna-Noise Temperature Meas.
- Receiver IF Measurement
- AM Detector Measurement

4.2 PAYLOAD CONFIGURATION

The equipment located on the Shuttle represents the basic EEE payload configuration. Figure 4-6a shows the block diagram for the antennas, receiver and Spacelab interface equipment. This particular design shows four basic antennas:

1. UHF Array (1.0 x 1.3m)
2. Parabolic Dish (0.7m)
3. Conical Helix (0.17m Dia x 0.17m Height)
4. Log Periodic (1.2m Dia x 1.8m Height)

Signal level control and receiver protection are provided by the attenuator and limiter shown at the receiver input. The bandpass filter (BPF) provides band integrity and protection from out of band jamming. Signal downconversion is provided by the series of low noise amplifiers (LNA) and downconverters. Signals are conducted from the pallet

*Examples suggested by R.E. Taylor.

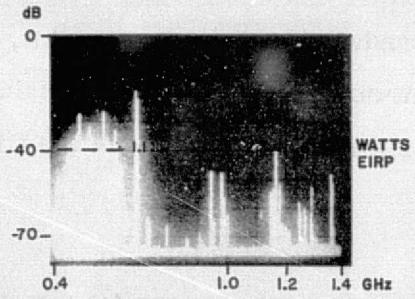

(a) Chicago, Morning, May 1, 1975
Time: 081741 (Start Run)

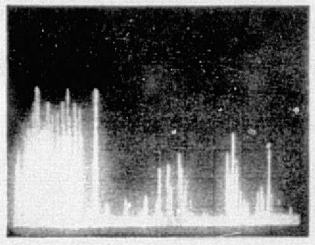

(b) Chicago, Morning, May 1, 1975*
Time: 081842 (4 Mile Point)

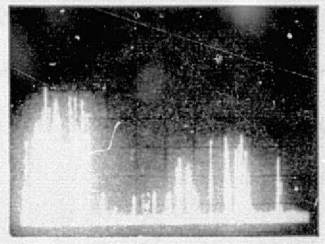

(c) Chicago, Morning, May 1, 1975*
Time: 082009 (10 Mile Point)

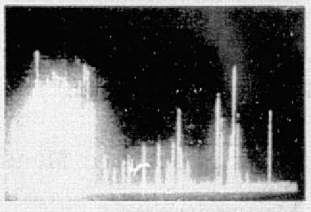

(d) Chicago, Night, May 1, 1975*
Time: 223035 (Start Run)

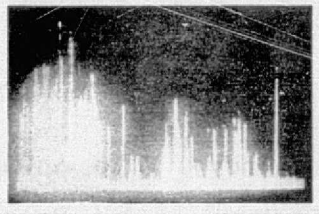

(e) Chicago, Night, May 1, 1975*
Time: 223746 (Run Midpoint)

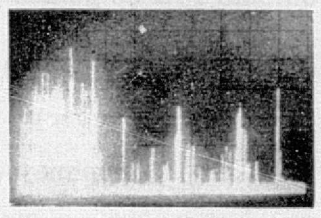

(f) Chicago, Night, May 1, 1975*
Time: 224427 (End of Run)

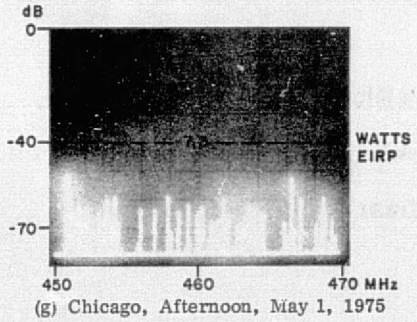

(g) Chicago, Afternoon, May 1, 1975
Time: 150111 (Start Run)

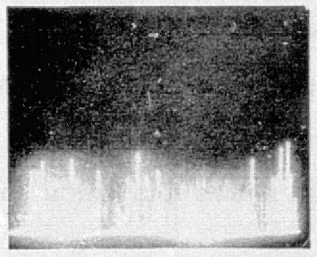

(h) Chicago, Afternoon, May 1, 1975**
Time: 150234 (6 Mile Point)

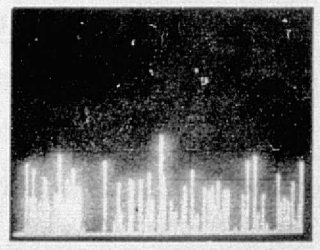

(i) Chicago, Afternoon, May 1, 1975**
Time: 150406 (10 Mile Point)

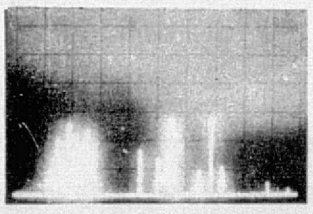

(j) Chicago, Night, May 1, 1975**
Time: 230120 (Start Run)

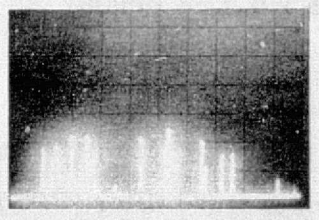

(k) Chicago, Night, May 1, 1975**
Time: 230251 (5 Mile Point)

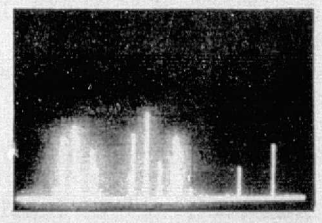

(l) Chicago, Night, May 1, 1975**
Time: 230422 (10 Mile Point)

Figure 11. Chicago (Morning-Nighttime) -0.4 to 1.4 GHz and 450 to 470 MHz
Scale: *Same as (a) Altitude: 10,500 ft Analyzer Bandwidth: Antenna: NADIR
**Same as (g) Aircraft Heading: North Fig. 11a to 11f -30kHz
Fig. 11g to 11l -10kHz

Figure 4-5. Typical EIRP versus Frequency Data Display

equipment to the Module/Aft Flight Deck equipment by coaxial cables. The IF signal frequencies are typical frequencies, but are consistent with keeping the IF signals low; i.e., no greater than 500 MHz, to avoid high signal loss. Figure 4-6(b) shows typical Spacelab equipment needed to route the detected signals to the TDRSS downlink, and the EEE displays. The equipment shown in Figure 4-6(b) represents the operational modes shown in Figure 4-2.

Layout of the EEE pallet mounted equipment is shown in Figure 4-7. The antennas shown are those depicted in Figure 4-4, and are representative of antennas needed to cover the EEE bands. In this design,space is left for additional antennas for bands above 2700 MHz, which will then just fill the area across one pallet.

RF electronics are located below the antenna platform. Figure 4-8 shows the vertical locations of the components and clearance angles for each antenna. Note that the center-of-gravity (CG) range for the vertical profile is below the top of the pallet. Figure 4-9 shows the pallet equipment mounted in the Shuttle bay. Similarly, Figure 4-10 shows the Aft Flight Deck area and the panel configuration for all experiments. Figure 4-11 shows the estimated weight, size and power required for the EEE payload equipment.

Location of the pallet equipment in the Shuttle bay could affect the antenna patterns if the Shuttle blocks a portion of the pattern. Figure 4-12 shows two locations which would offer almost no pattern distortion by the Shuttle. These positions represent the closest that the equipment can be located to the ends of the bay. A nominal blockage of the widebeam antenna patterns caused by the Shuttle's tail will not significantly affect performance of the EEE.

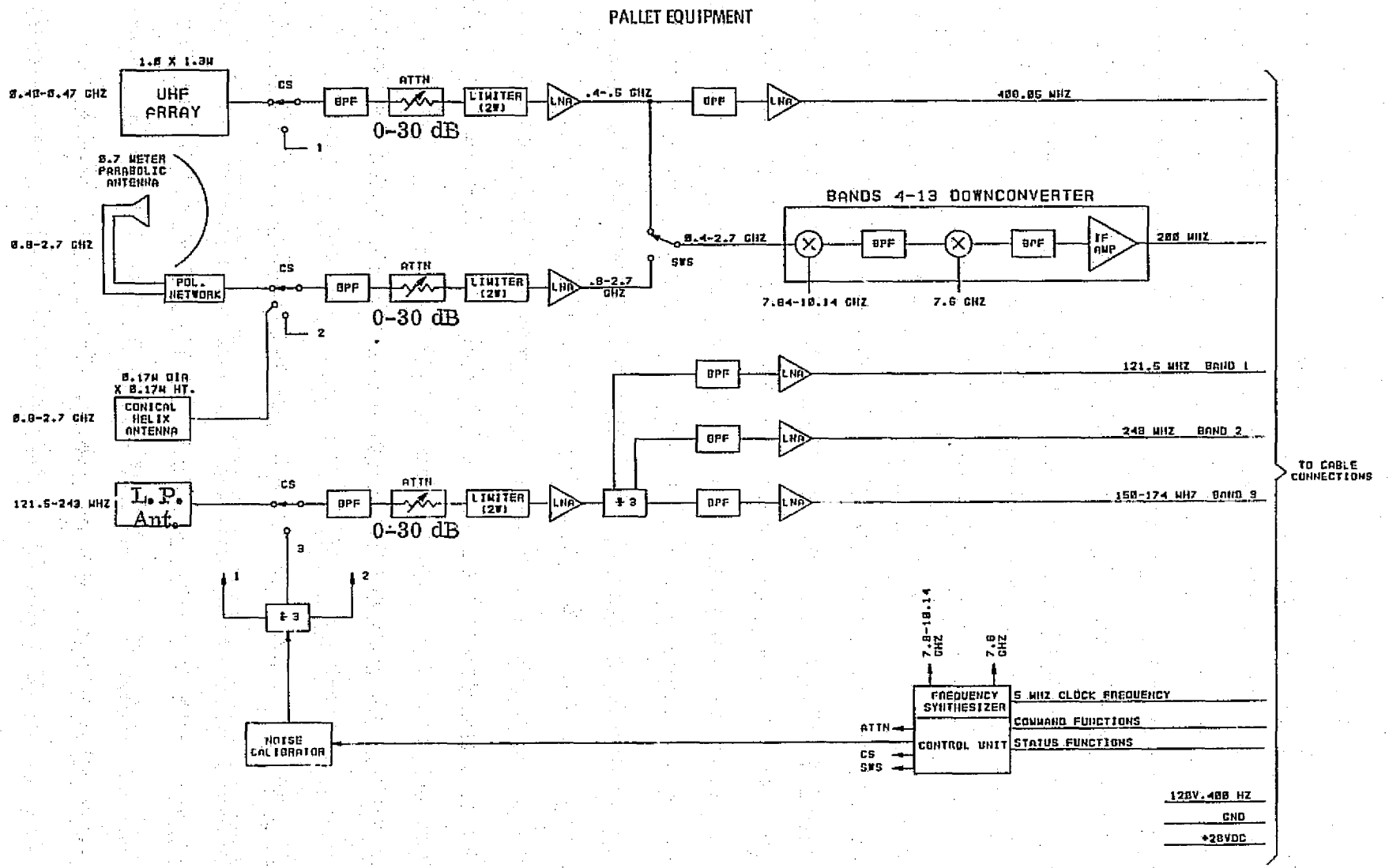

Figure 4-6a. EEE-MOD I System Block Diagram

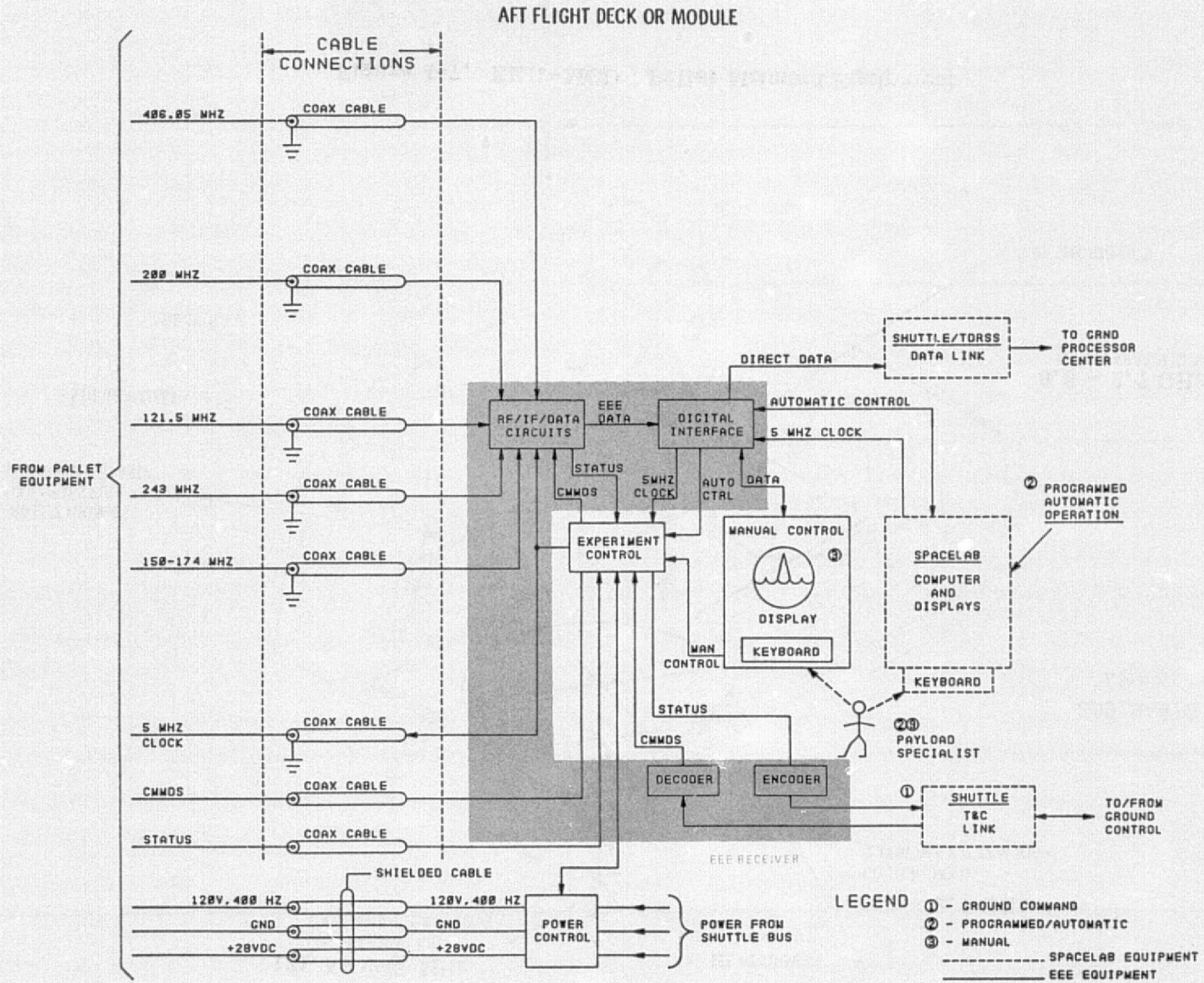

Figure 4-6(b). EEE-MOD I System Block Diagram

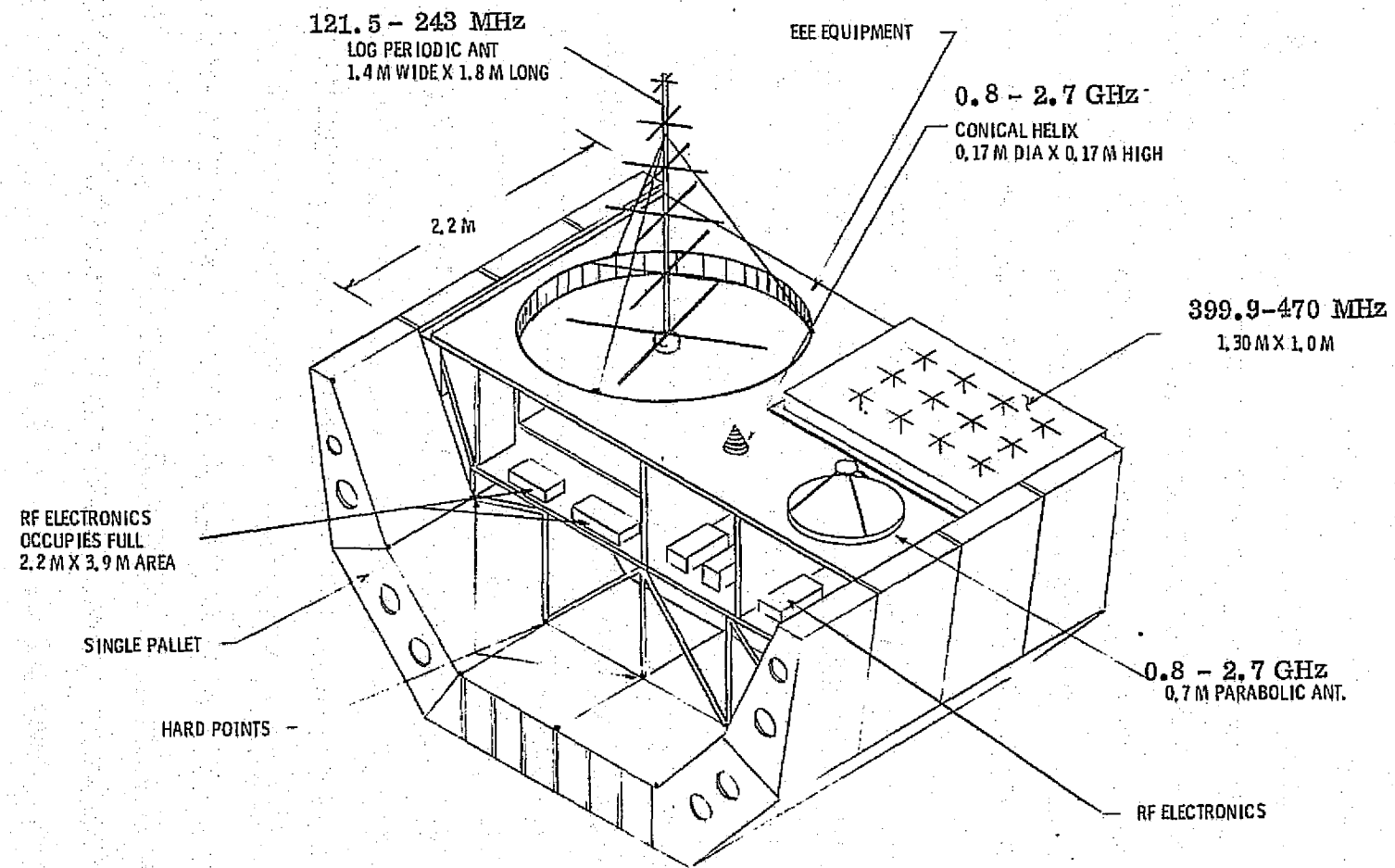

Figure 4-7. EEE-MOD I Pallet Mounted Equipment

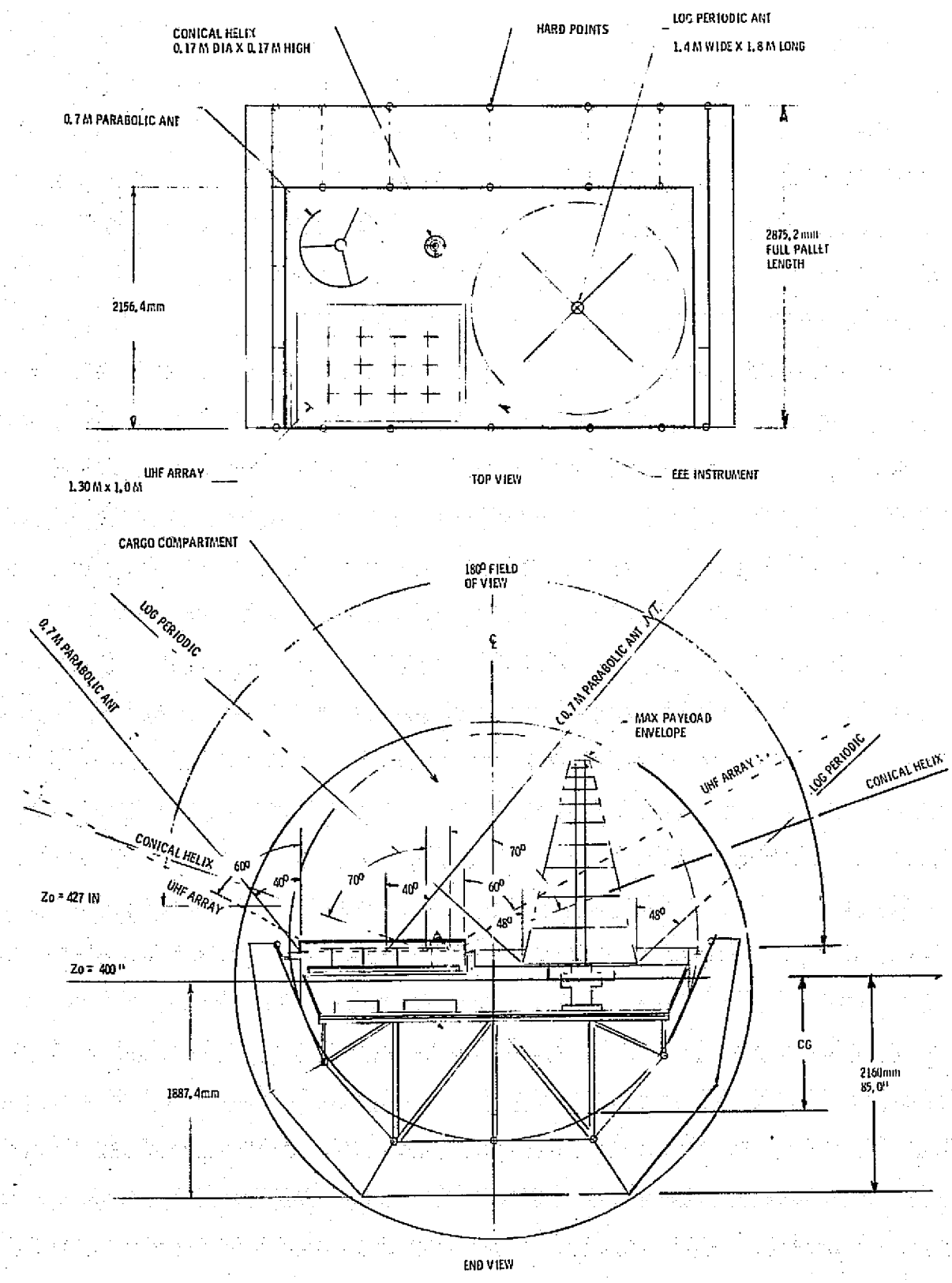

Figure 4-8. EEE Pallet Layout and Antenna Field of View

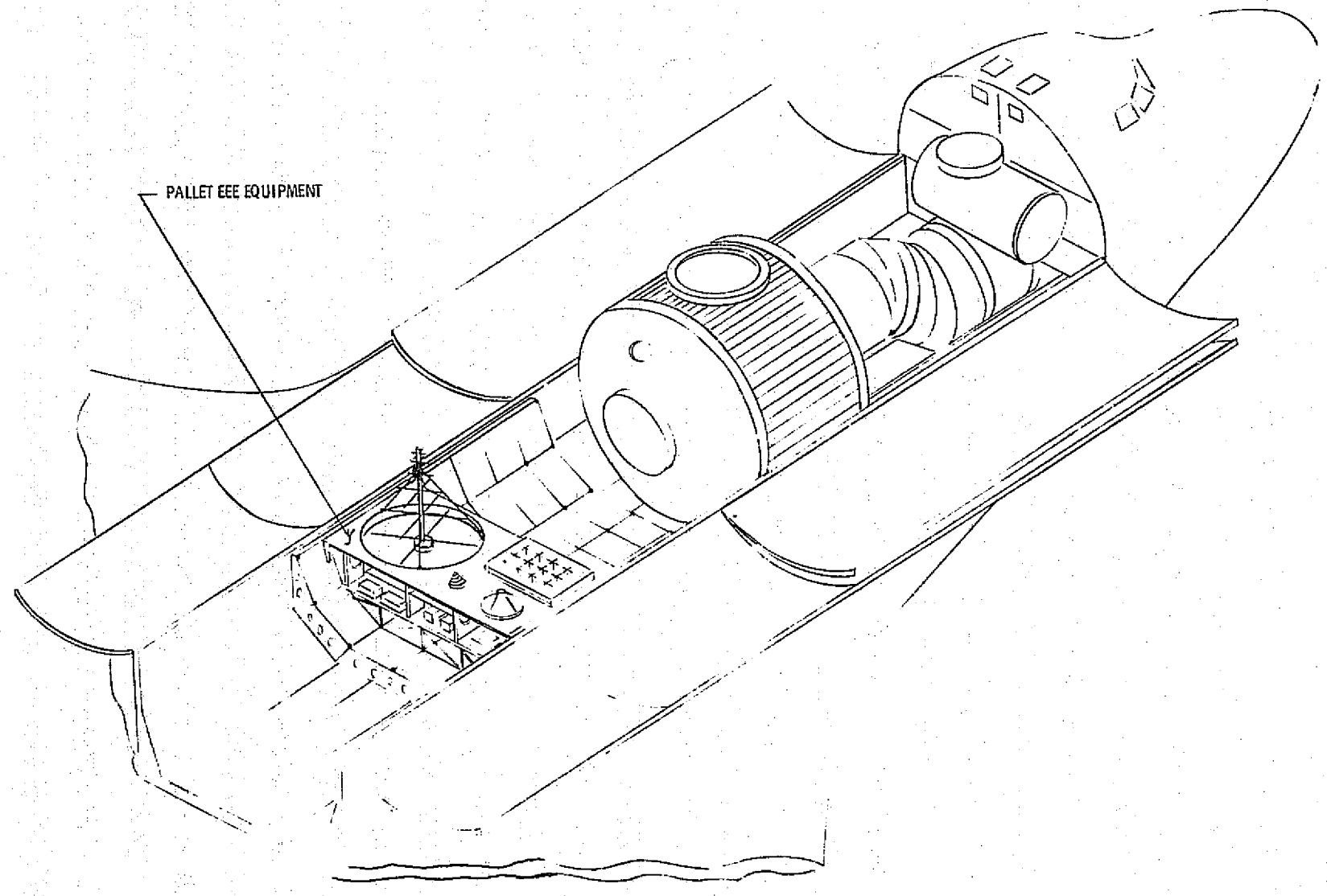

Figure 4-9. EEE - MOD I Spacelab Flight Configuration

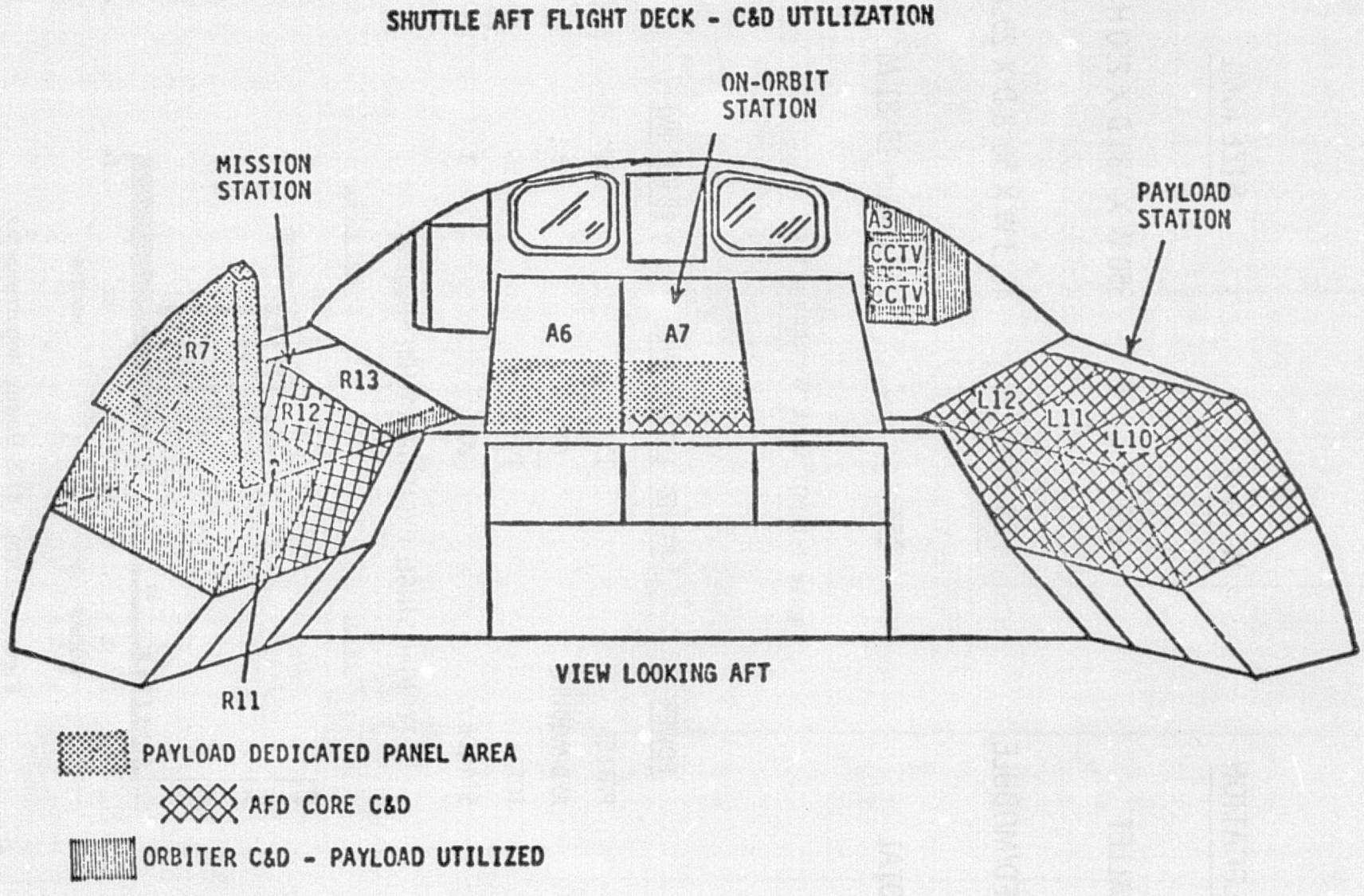

Figure 4-10. Aft Flight Deck Panel Configuration

LOCATION	WT (kg)	SIZE (CM)
PALLET	128	350 W X 180 D X 250 H
AFD/MODULE	28	48.3 W X 50.8 D X 25.4 H
TOTAL	156	VOLUME = 15.81 M^3

Figure 4-11(a). EEE Weight and Size

POWER	400 HZ, 120 VAC (W)	28 VDC (W)
PALLET	150	25
AFD/MODULE	40	5
TOTAL	190	30
STANDBY	20	3

TYPICAL SINGLE CYCLE OPERATION SEQUENCE

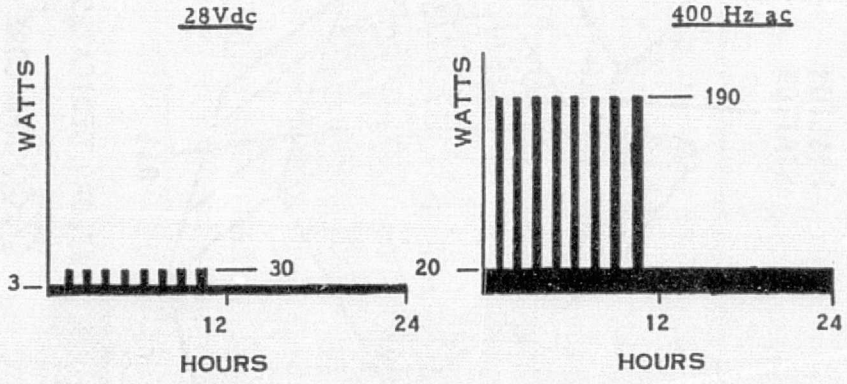

Figure 4-11(b). EEE Power Requirements

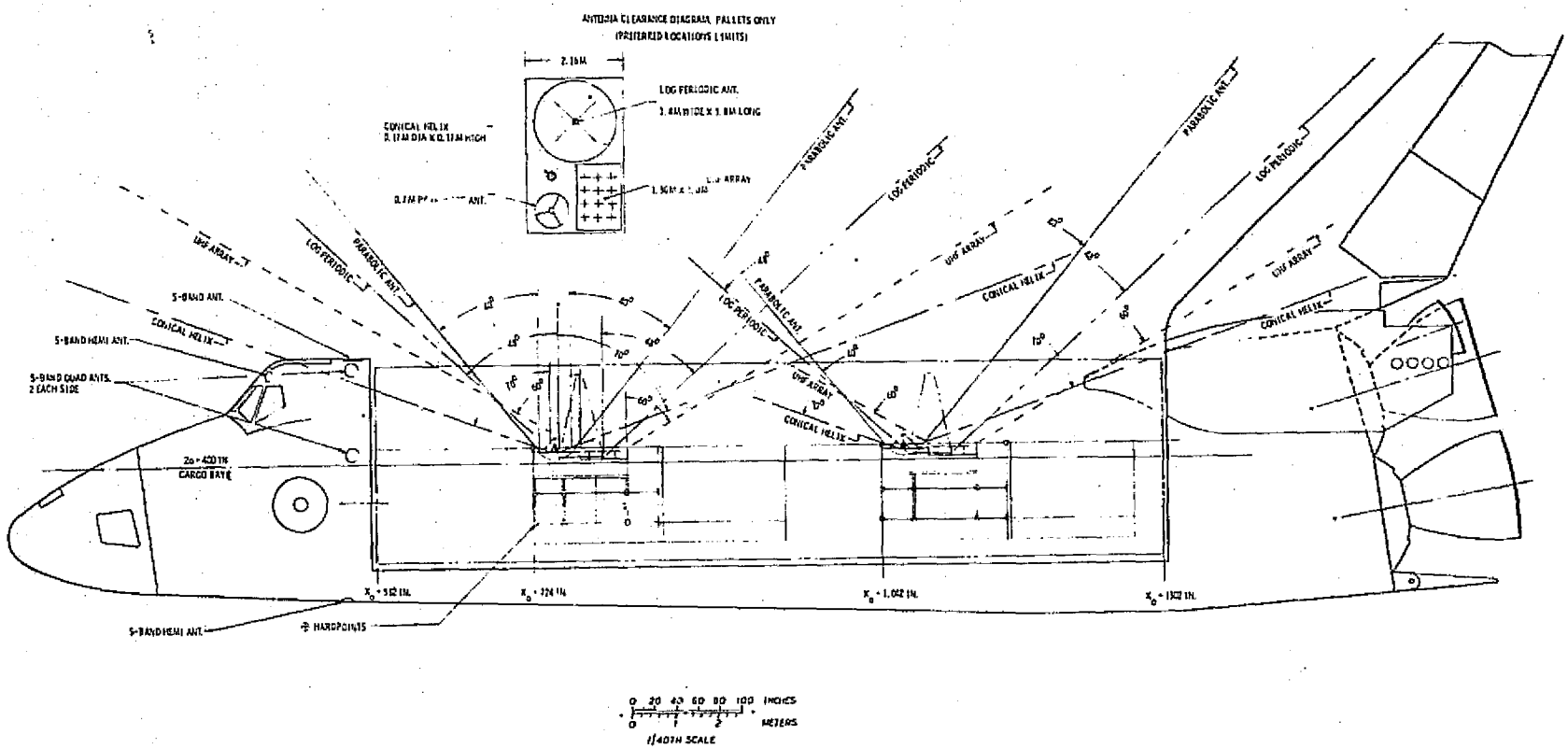

Figure 4-12. Antenna Clearance Diagram, Pallets Only

4.3 OPERATIONAL ENVIRONMENT AND DATA MANAGEMENT

Figure 4-6(b) shows the functional interfaces for the EEE, and the conceptional approach to the experiment control and operation. Further definition of the interfaces and environment was carried out to determine the physical and RFI (radio frequency interference) environment the equipment will be exposed to, and to define a data management scheme. This work has included a study of the expected environment related to the Shuttle[5], interfaces with the Spacelab on-board systems[4], and a proposed method of managing the EEE data. Experiment control is intimately involved in data management and experiment operation and is included here to show involvement of the Payload Specialist and ground control personnel.

4.3.1 EEE ENVIRONMENT CONSIDERATIONS

After a study of the Shuttle bay payload environment conditions and the types of equipment that could be used on EEE, a set of physical operating parameters was formulated. These parameters include temperature, humidity, acoustic limits, acceleration, radiation and RFI susceptibility. These parameters and the expected limits are shown in Figure 4-13.

In general, the limits for temperature and humidity shown in Figure 4-13 are those normally expected for military equipment and weatherized commercial equipment. Acoustic and acceleration limits are those required for Shuttle launch and landing, but are reasonable for microwave equipment, also. However, it is not expected that the EEE equipment will survive a crash landing, except to stay in contact with the pallet.

PARAMETERS	LIMITS	
	AFD MODULE	PALLET
TEMPERATURE		
TYPE CONTROL	AIR	PASSIVE (COATING,ETC.)
OPERATING	0 TO 50°C	-65 TO 65°C
(PREFERRED)	(25)	(25)
NON-OPERATING	-65 TO 65	-65 TO 65
HUMIDITY		
OPERATING	40 TO 60%	40 TO 60% (TEST)
NON-OPERATING	0 TO 100	0 TO 100
ACOUSTIC LIMITS		
NON-OPERATING	145 dB	145 dB
ACCELERATION		
NON-OPERATING	5.0 G	5.0 G
OPERATING	1×10^{-2}	1×10^{-2}
RADIATION (NUCLEAR)	NOT A PROBLEM	
RFI SUSCEPTIBILITY		
ELECTROMAGNETIC	EMC ANALYSIS	
GENERATED RFI	NOT A PROBLEM	

{ DERIVED FROM JSC-07700, VOL. XIV

Figure 4-13. EEE Environment Considerations
(Ref: Spacelab Accommodation Handbook)

Nuclear radiation is not expected to be a problem to the EEE, since the flights are short and no equipment is susceptible to normal nuclear environment experienced during a low orbit Shuttle flight. RFI susceptibility is a different type of problem, however, and must be dealt with in depth. The generated RFI from the EEE will be very low, since the EEE is primarily a receiver.

The RFI susceptibility problem was studied to determine the effect the Shuttle bay RFI will have on principal EEE operating parameters such as sensitivity. Figure 4-14 shows the RFI specification limits imposed by the Shuttle payload requirements[4] and the expected EEE sensitivity levels for each frequency band. An additional RFI level that could be caused by digital logic radiation is shown at the bottom of the graph.

The major significance of Figure 4-14 is that the EEE sensitivity levels are far below the Shuttle cargo bay specification limits. Figure 4-15 shows the range of isolation needed to allow EEE to operate at its maximum sensitivity levels. The significance of the levels shown in Figure 4-15 is very apparent when it is realized that the typical

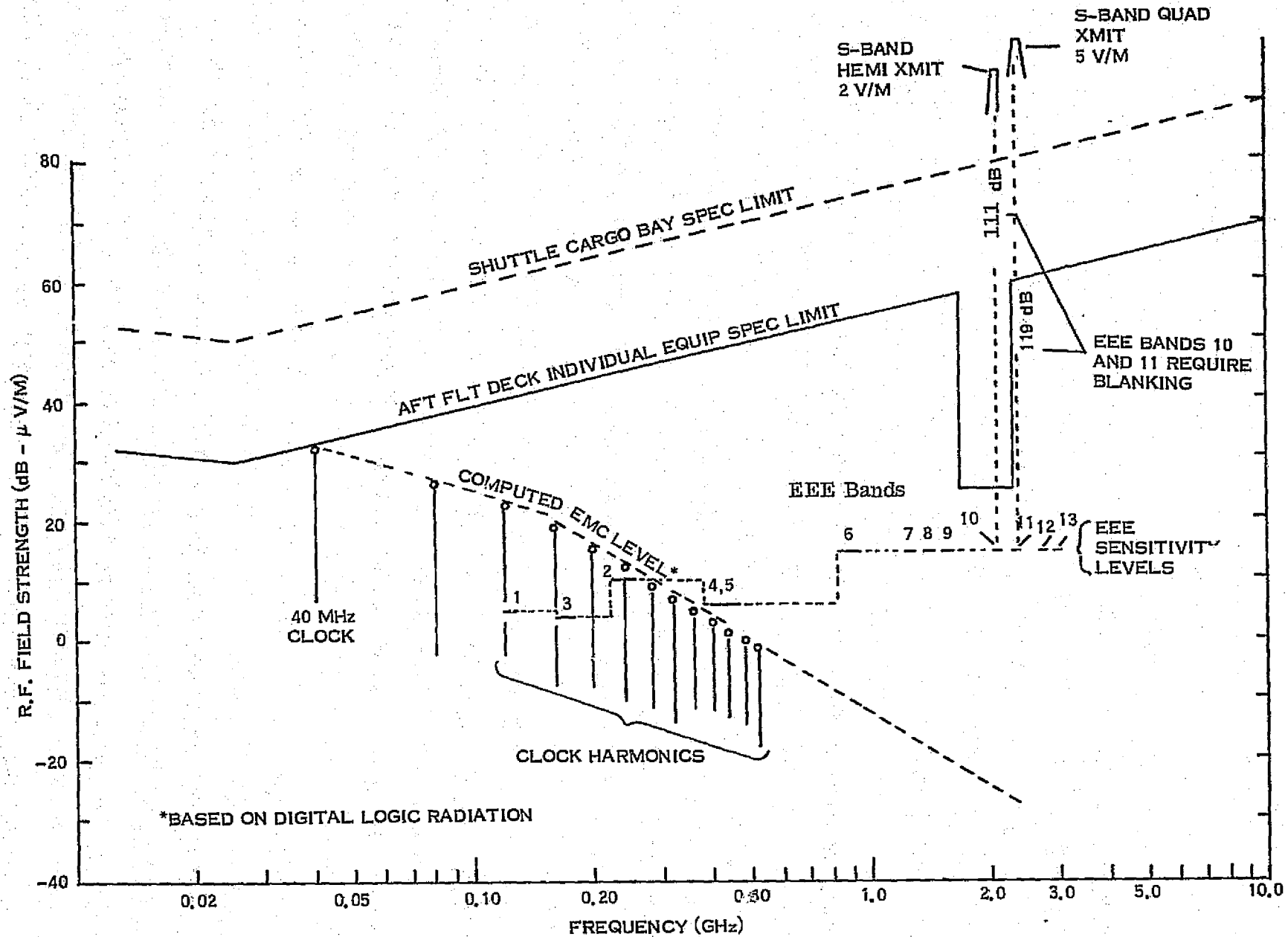

Figure 4-14. Shuttle Bay Electromagnetic Compatibility Environment (Other On-Board Experiments Excluded)

SOURCE OF RADIATION (dB – μV/M)

EEE BANDS	FREQUENCY MHz	SHUTTLE LIMIT dB	EQUIPMENT LIMIT dB	DIGITAL LOGIC* (1 M DISTANCE)
1	121.5	57	37	21 dB
2	243.0	55	35	5 dB
3	150–174	60	40	18 dB
4	399.9–410	64	44	0 dB
5	450–470	64	44	0 dB
6	806–947	59	39	–15 dB
7	1220–1285	62	42	–20 + dB
8	1350–1450	63	43	–20 + dB
9	1636.5–1670	64	44	–20 + dB
10	2040–2110	106 dB BLANKING REQ. – S-BAND HEMI		
	OTHER	10 dB	10	–20 dB +
11	2200–2300	119 dB BLANKING REQ. – S-BAND QUAD		
	OTHER	10 dB	10	–20 dB +
12	2655–2690	67	47	–20 dB +
13	2690–2700	67	47	–20 dB +

*DIGITAL LOGIC RADIATION

RADIATED ENVELOPE OF 40 MHz, 5 VOLT CLOCK SIGNAL

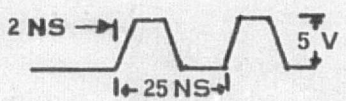

BASED ON
- TWISTED SHIELDED PAIR – ≈ 50 dB ATTENUATION
- PATH LOSS = 50 dB 1ST METER OF SPACING

Figure 4-15. Shuttle Bay to EEE EMC Isolation Required

isolation provided by a receiver antenna (back radiation) is on the order of 20-25 dB. For the Shuttle limit and individual equipment limit, the EEE sensitivity will be affected greatly, raising the detection levels of the receiver. For a normal digital logic level, however, the receiver should be able to operate without loss of sensitivity.

In addition to the random noise levels specified by the Shuttle specifications, individual Shuttle communications transmitters will cause receiver saturation and will be blocked from the receiver by filters.

It should be noted that this study does not take into account the RFI generated by other experiments. At this time, other experiments have not been specified. However, when serious interference is expected from another experiment, time sharing of operation time must be arranged.

4.3.2 EEE DATA MANAGEMENT AND MONITORING

Management of the EEE involves both data management and control of the experiment from detection of signals to user outputs. Organization of received data is also a principal factor in all phases of data management and control. Work completed on this aspect of EEE includes a preliminary estimate of received data, a proposed arrangement of the data format and a method by which these data can be controlled by any one of the three proposed operation modes.

Figure 4-16 shows the expected data rates needed to manage and operate the EEE. Receiver data is estimated to be 85 kbps and will be buffered and formed into a serial bit-stream. These data are from bands 3-13 of the receiver (see Figures 4-3 and 4-6). The search and rescue (S&R) bands will not be frequency scanned, and will be monitored using analog detection. These channels are to be monitored and recorded as separate channels. Typical user data outputs are given on pages 4-7. All data will be recorded on magnetic tape on the ground at the POCC.

TYPES OF DATA	DATA RATE
FREQUENCY-SCANNING RECEIVER OUTPUT	DIGITAL: 85 kbps TYPICAL ANALOG. 150 KHZ (3 S&R CHANNELS) (182 kbps AFTER DIGITIZING)
ON-BOARD DATA STORAGE	(NONE)
COMMAND	0.25 bps TYPICAL
TELEMETRY (EQUIP. STATUS)	430 bps TYPICAL
EPHEMERIS DATA	
DAY TIME LONGITUDE LATITUDE ALTITUDE SHUTTLE ATTITUDE	SHUTTLE SUPPLIED (REF: AIRBORNE DIGITAL DATA ACQUISITION SYSTEM-ADDAS)

Figure 4-16. EEE Data Management and Control

Experiment control via TDRSS will be by command and telemetry. Estimated command link capacity is 0.25 bps. Equipment status should require no more than 430 kbps for telemetry and monitoring.

Ephemeris information to be supplied with the receiver data will provide information needed to reduce the detected receiver data to user formats. Examples of ephemeris data are: calendar day, time of day, Shuttle position (longitude and latitude), Shuttle altitude, Shuttle attitude (reference to radii), and other experiment operational inputs such as reference signals.

Figure 4-17 shows a proposed arrangement of detected receiver data. This scheme could apply to other experiments as well as EEE and contains initial identification of the experiment and the type of data being recorded. For the EEE, band number, band resolution and frequency will provide the parameters to define sensitivity. Information about the attenuator setting at the receiver input is being supplied with the band number. Using the minimum cell size of 20 kHz, a five-filter bank is proposed for MOD I EEE. This allows for 0.1 MHz frequency steps by the receiver. All bands are to be serially stepped; e.g., in the normal mode, starting at band 2, each band will be searched for power output until band 13 is completed, and the scan repeats. Alternate modes can be set up by preprogramming a manual control, allowing specific bands to be searched. S&R bands are to remain open and sampled periodically, without frequency scanning.

The proposed control monitoring method for EEE is shown in Figure 4-18. Provision is made for monitoring data, test information and equipment status at the EEE receiver on the Shuttle, at the Spacelab display panel, by the Experiment Operator at NASA JSC. Data will be monitored near-real time, with displays of the type shown in Figure 4-5.

Additional information on data handling is given in the task report, CI 10.

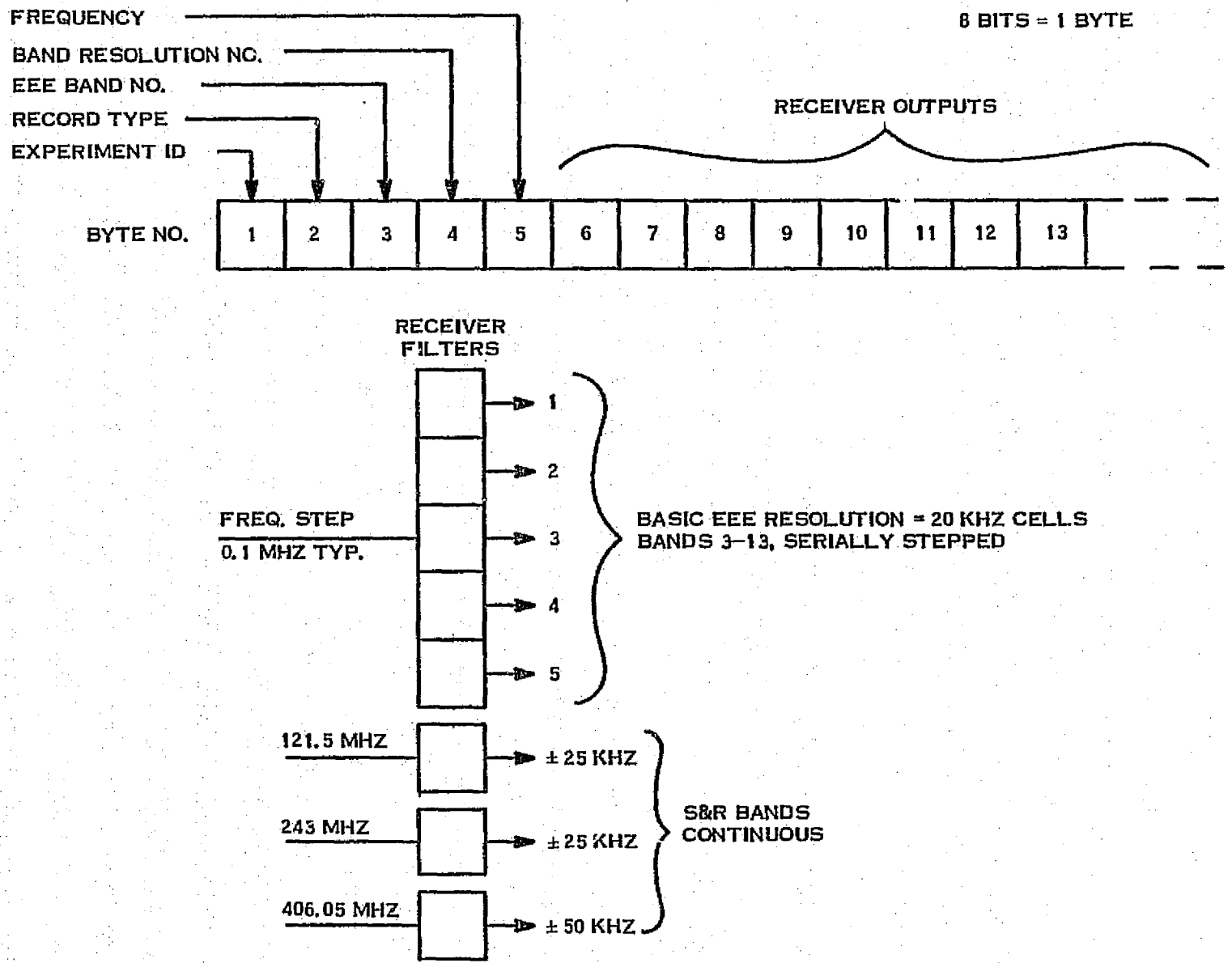

Figure 4-17. EEE Receiver Data Management

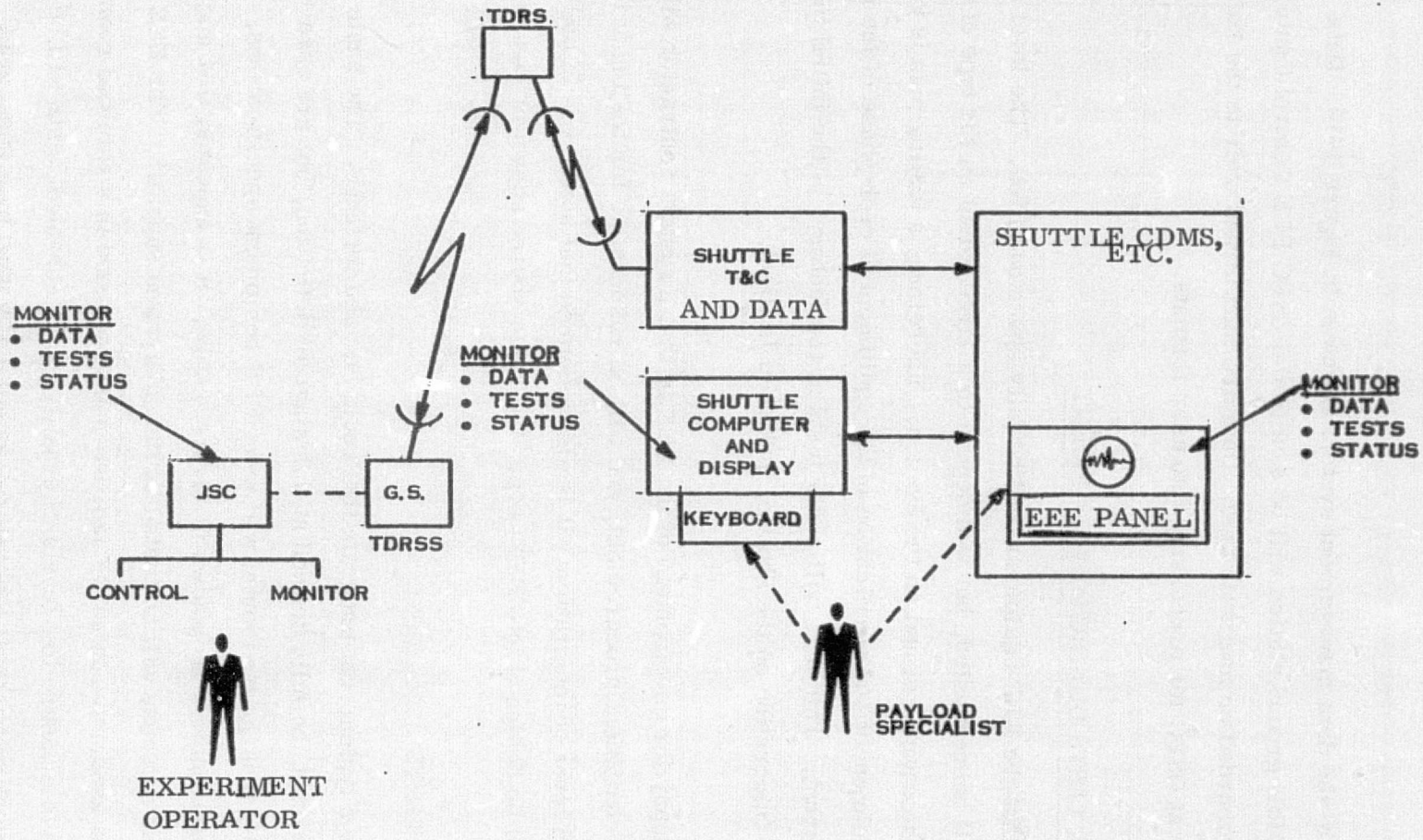

Figure 4-18. Receiver Control and Monitoring

Further definition of the data management system is shown in Figure 4-19. Data received by the TDRSS ground station will be sent to the GSFC EEE Control Center via Houston, and recorded on magnetic tape. Data are then turned over to the Data Processing Center at GSFC for processing into user formats.

4.4 INSTRUMENT TESTS DURING DEVELOPMENT

It is not expected that the EEE equipment will be fully space qualified. The level of qualification is still being studied, but will depend to a large extent on the type of testing to be done on the equipment and on the system. Therefore, a testing plan is key to defining the development and verification of the equipment at each phase of the EEE equipment development. This plan will cover tests at the factory, at the initial integration stage, and integration on the Shuttle, and when in flight.

The overall philosophy for development of the EEE is that a system contractor will manage the initial equipment procurement, and will be responsible for testing at the factory and at each level of integration. It is also assumed that some type of built-in test equipment will be designed into EEE; e.g., the noise source shown in Figure 4-6(a).

4.4.1 FACTORY TESTS

Figure 4-20 shows a typical test program that could be used for EEE. The basic acceptance tests cannot be fully defined at this stage of definition, but are essentially those tests to verify that the equipment will meet EEE equipment specifications. Types of tests and test environment are shown in Figure 4-20b. It is expected that major components such as antennas will be tested by the subsystem supplier. The EEE equipment could be assembled in an RF lab, but must be tested in a shielded room or Anechoic chamber to measure low levels of sensitivity. Mechanical tests will be completed in a typical mechanical laboratory, as normally used by a spacecraft manufacturer. It follows that special tests such as thermal/vacuum will be conducted in a vacuum chamber, probably in conjunction with electrical performance tests. Test

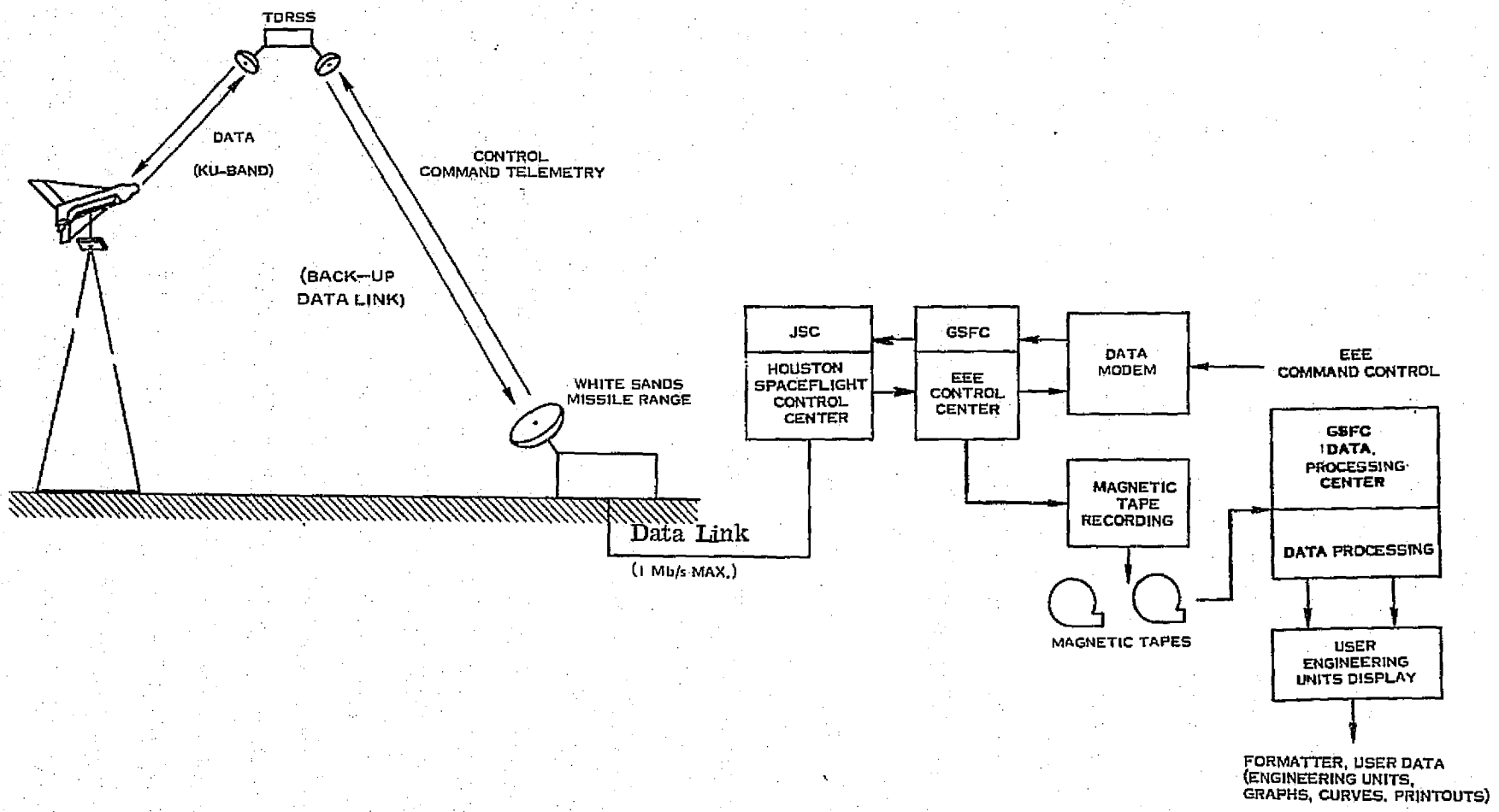

Figure 4-19. Experiment Data Processing

TEST PROGRAM

- Basic Acceptance Tests to be performed at factory
- First EEE Integration and Tests at factory
- Full Performance Tests at factory
- Calibrate built-in noise source

TEST EQUIPMENT

- Construct EEE Electrical Test Equipment - Portable Racks
- Antenna Range (120 - 2700 MHz)
- Shielded Room (120 - 2700 MHz)
- Mechanical Test Equipment including Thermal Vacuum
- Built-in Test Equipment (noise source)
- Mechanical Frame or Pallet

Figure 4-20a. EEE Factory Tests

TYPICAL TESTS	TEST ENVIRONMENT	COMMENTS
ELECTRICAL ACCEPTANCE		
- Antenna (Radiation patterns)	Range	Measured by antenna supplier
- Receivers	RF Lab	Subsystem level
- Control	RF Lab	With receivers
- Interface	RF Lab	Full subsystem
- Subsystem	Shielded room	Full subsystem, EMC
MECHANICAL ACCEPTANCE		
- Vibration	Mech. Lab	Indiv. boxes, subsystems, pallet equip. in fixture
- Shock	"	
- Acceleration	"	
- Thermal Vac	"	Indiv. boxes, subsystems
- Acoustic	"	Equip. in fixture
- Temperature	RF/Mech. Lab	Combined with elec. tests

Figure 4-20b. EEE Factory Tests

equipment for electrical performance tests will be experiment unique, and it is proposed that portable racks containing test equipment be constructed and used at various stages of test and integration. Similarly, built-in test equipment should be used in all stages of testing to calibrate the test equipment and develop experience in use of the equipment.

4.4.2 EQUIPMENT CERTIFICATION

The first level of EEE integration onto the Shuttle will be on the pallet. This phase of integration is still being defined, but could take place at a NASA center. Equipment verification will involve some basic performance tests and verification of crucial interface criteria; e.g., electromagnetic compatibility (EMC). It is proposed that these tests be performed using the portable test equipment supplied with the instrument and the built-in noise source. Figure 4-21 identifies some of the basic tests to be done at certification.

TEST PROGRAM

- Basic Performance Tests to verify equipment status
- EEE Integration Tests with Pallet Interface
- EMC Tests - Verification
- Verify built-in noise source calibration

TEST EQUIPMENT

- EEE Electrical Test equipment - Portable Racks
- Shielded Room (120 - 2700 MHz)
- Built-in Test Equipment (noise source)
- Pallet and Module Rack for integration

Figure 4-21. EEE Equipment Certification

Similarly, Shuttle integration tests are shown in Figure 4-22. Since this is the first full-up equipment and integration tests, the portable test equipment is still required, although the Spacelab equipment and built-in test equipment can be used for many of the tests. It should be noted, however, that this may be the first time that crucial integration and EMC tests are run.

4.4.3 IN-FLIGHT CALIBRATION AND TESTING

Testing and equipment calibration during the EEE flight will make use of the built-in noise source and beacons located at NASA sites shown in Figure 3-2, page 3-9 for Goldstone and Rosman. By switching in the noise source shown in Figure 4-6a, receiver sensitivity can be measured. This technique can be used to set attenuator levels as well as monitoring system noise level. Calibration of the EEE instrument, however, requires a known ground source. It is proposed that unmanned beacons emitting 10W EIRP be set up at several NASA sites. These emitters, along with other known sources, provide the sources for calibration inflight, and data received can be used in checking user data after processing. Figures 4-23 and 4-24 show the tests and test equipment suggested for these tests.

TEST PROGRAM

- Performance tests to verify equipment status
- EEE integration with module and Shuttle
- EMC tests using built-in noise source
- Experiment operation tests (Modes 1, 2, 3)

TEST EQUIPMENT

- EEE electrical test equipment - portable racks
- Built-in test equipment

Figure 4-22. EEE Integration and Prelaunch Tests

C.2

TESTS

- Monitor EEE outputs for noise power inputs
- Measure EEE outputs for On/Off noise inputs
- Calculate sensitivity and noise base

TEST EQUIPMENT

- Built-in test equipment

Figure 4-23. EEE Noise Calibration

TEST PROGRAM

- Measure 10W EIRP beacons at NASA sites
- Monitor known sources
- Operate receiver attenuators for signal reduction

TEST EQUIPMENT

- Unmanned 10W EIRP beacons

Figure 4-24. EEE In-flight Calibration with Beacons

4.5 EEE-MOD II SYSTEM DESCRIPTION

Upon completion of the EEE-MOD I design, work was directed to a consideration of expanding into the upper frequency bands from 2.7 GHz - 43 GHz. These are the band numbers designated 14 through 28 shown in Figure 4-3. Band 29 (50-65 GHz), also shown in this figure, has been designated for future space research and passive microwave sensors, and is not presently covered by this expanded configuration.

Basically, EEE-MOD I antennas and associated pallet electronics have been laid out to require less than a full pallet (see Figure 4-7). The present thinking is to design the EEE-MOD I as a unitized pallet with most of the electronics located near the antenna on the pallet. Power is provided through the pallet's Experiment Power Distribution Box (EPDB) and commands, housekeeping, and low data rate information via the Remote Acquisition Unit (RAU). The full pallet top area can be allocated for the EEE, implemented on the initial flights with EEE-MOD I antennas and related electronics. On later flights the EEE pallet may be supplemented with new upper band antennas and their associated electronics. Therefore, EEE-MOD II encompasses the MOD I frequencies and will cover the complete range of 0.121 to 43 GHz. The EEE functional concepts and its major functional parts of the experiment shown previously in Figure 4-1 remain the same and apply equally well to EEE-MOD II. The antennas and receivers, associated Spacelab equipment and interface equipment to control the experiment and transmit the data must be expanded in capability. However, the basic functions of the Payload Specialist and control modes are essentially the same as for EEE-MOD I. Operational environment and data management factors are also the same for MOD I and MOD II. Figure 4-25 is a concept of the MOD II.

The information which follows is primarily concerned with the new study considerations and hardware for the expanded frequency range of 2.7 to 43 GHz.

4.5.1 EEE-MOD II EQUIPMENT DESCRIPTION

Efforts during the latter contract period include a system definition study of EEE-MOD II equipment and design of an equipment configuration that is realizable by means of readily available components, in most cases off-the-shelf components. Where the use of off-the-

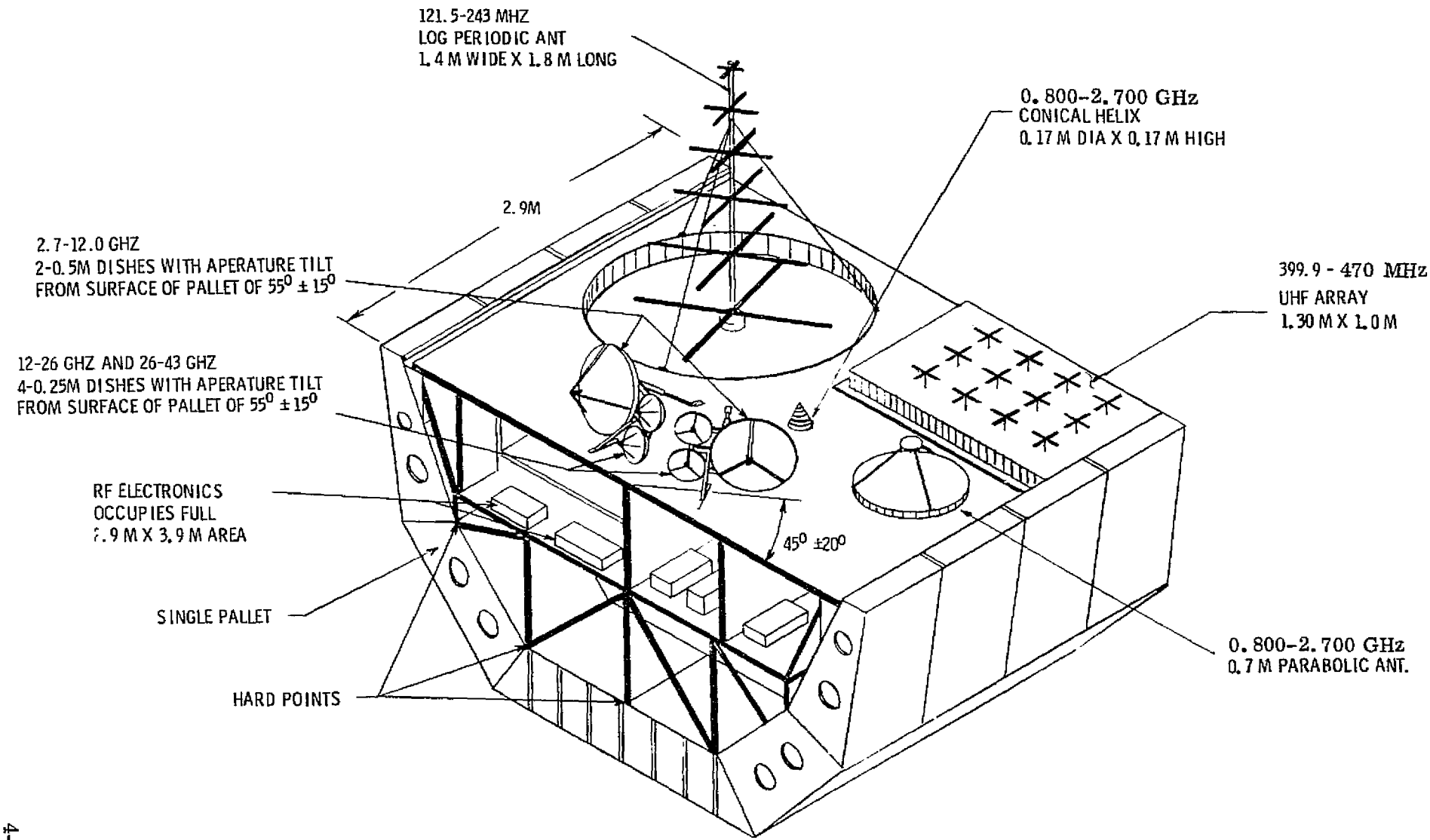

Figure 4-25. Concept Drawing of EEE-MOD II Pallet Mounted Equipment

shelf components did not appear possible or advantageous, an attempt was made to assure that the components were not excessively difficult to design. This has led to further channelization of the equipment, primarily to obtain first IF bandwidths of 4 GHz or less.

Figure 4-26 shows a system block diagram of the MOD II-EEE equipment. Antennas and related components covering the portion of the spectrum from 121.2 MHz to 2.7 GHz are identical to those described previously for the MOD I equipment.

The 2.7 to 43 GHz frequency range is covered by three pairs of antennas incorporating parabolic dish reflectors. One antenna of each pair is angled out the righthand side of the Shuttle and the other is angled out the lefthand side. One or the other is selected from each pair depending upon which gives the optimum swept antenna-pattern area on the earth in an orbital pass of the Shuttle for a particular yaw angle or spacecraft orientation. Selection of an antenna from a pair is accomplished by a switch matrix. In addition, the system is designed to enable switching in a calibration noise source to the receiver for pre-flight and in-flight testing.

Following the switch matrices, the spectrum is divided into 4 GHz (or less) bandwidth channels either by means of diplexer filters or by matrix switch selection of the filtered channel. Channels in the frequency range of 4 to 43 GHz are converted to 4 GHz first-IF bandwidths centered at either 6 or 10 GHz. Two IF switch matrices sequentially route the channel to the appropriate receivers. A sweep frequency synthesizer provides the LO input to mixers in each of the receivers. The swept LO sequentially brings the various portions of the received signal spectrum into the spectrum processor input bandwidth. In the processor the spectral power density of the input signals is measured and converted into a digital format. Tunable narrowband YIG filters are incorporated in the receiver channels to minimize image frequency response and spurious inter-modulation response errors.

FOLDOUT FRAME 1

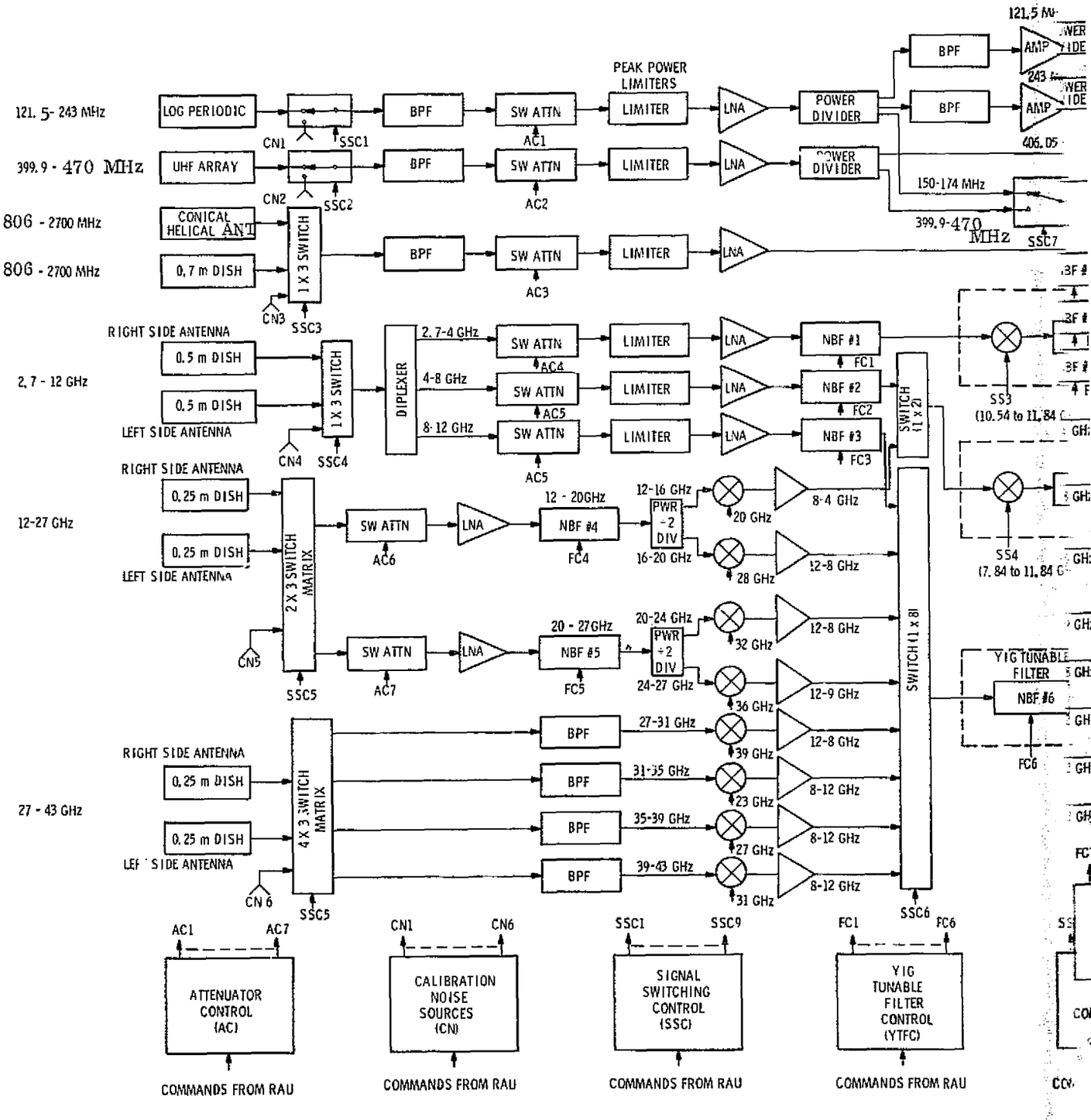

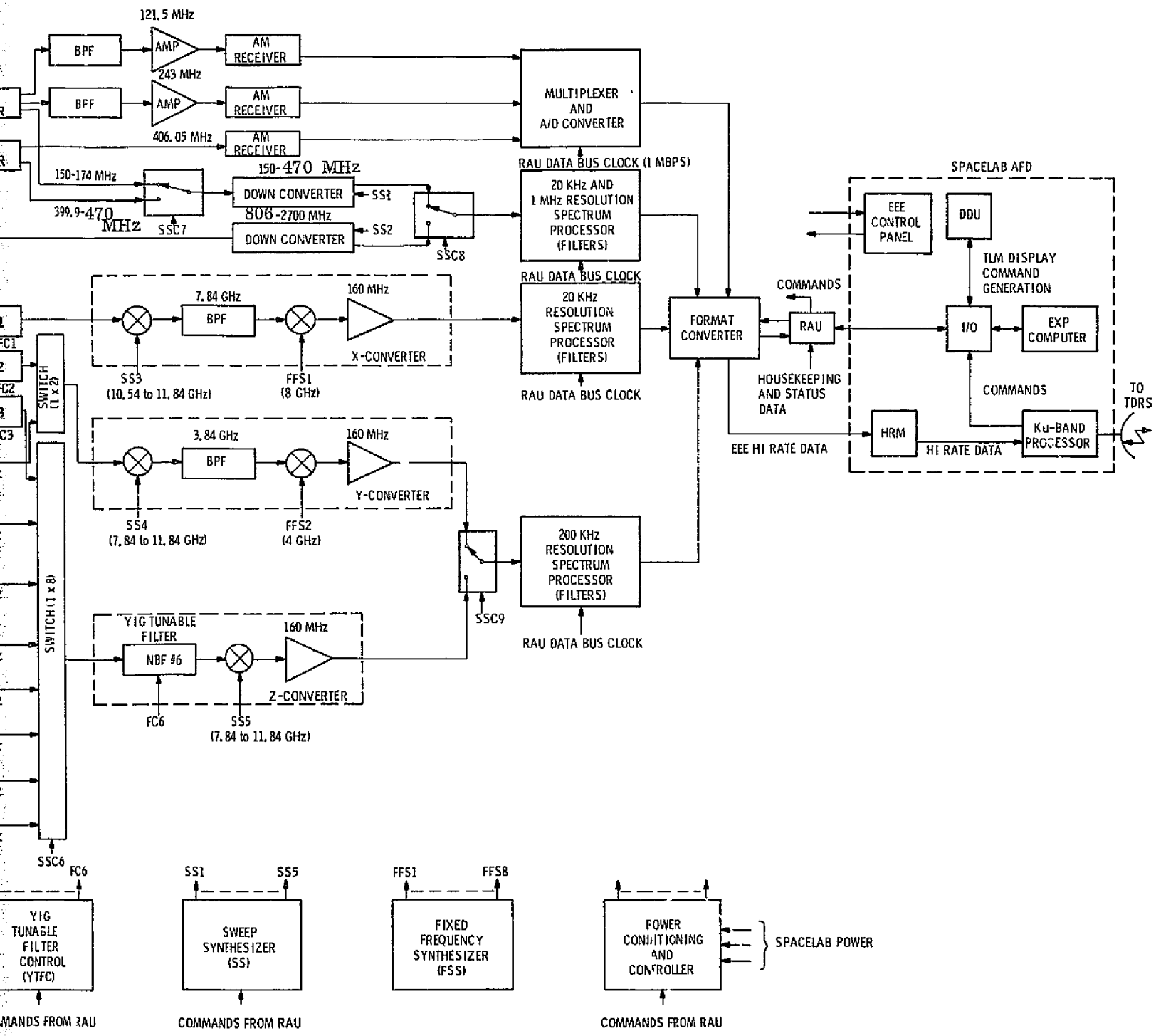

Figure 4-26. EEE-MOD II System Block Diagram

4.5.2 EEE-MOD II SENSITIVITY AND ACCURACY

Since the EEE receiving and signal processing equipment functionally is essentially a spectrum analyzer, the experiment equipment sensitivity and accuracy are dependent on the usual spectrum analyzer parameters of equipment noise performance, IF bandwidth, frequency sweep rate and video integration time. However, sensitivity in the case of the EEE can be conveniently defined in at least two ways, both of which require consideration of antenna parameters. Sensitivity can be defined in terms of the minimum EIRP of a ground emitter that can be measured to a given accuracy. This definition is convenient when considering one or a few spacially isolated emitters. An alternative definition of sensitivity is in terms of the minimum RF power-flux density, in a frequency band, that can be measured to the desired accuracy. This definition is convenient when considering many closely spaced emitters.

Both definitions introduce gain-pattern considerations of the experiment antennas. In the first case, the sensitivity is directly proportioned to antenna gain in the direction of the emitter. The usable sensitivity attainable by increased antenna gain is limited by the earth-area coverage. Gain that is too high gives a small footprint on the earth and not all the desired area will be monitored. In the second case, the sensitivity is dependent on both antenna gain and footprint area. Although the sensitivity to any single emitter increases with gain, the area covered and, hence, the number of emitters in the antenna beam decreases, giving reduced sensitivity dependence on antenna gain.

Since cases of both isolated and closely spaced emitters can be anticipated, selection of the antenna beamwidths is ultimately significantly determined by the coverage required and by the related parameter of "time-on-target" which sets the video integration time and accuracy achievable.

4.5.2.1 Sensitivity and Antenna Pattern Analysis

The EEE sensitivity in terms of the minimum detectable signal EIRP from a single emitter, is given by the standard formula, where all quantities are in dB:

$$(EIRP)_E = (S/N)_R + L + T + N_o + B - G \quad 1)$$

where,

$(EIRP)_E$ is the minimum detectable effective isotropic radiated power from a ground emitter

$(S/N)_R$ is the desired received signal-to-noise ratio

L is the path loss

T is the system noise temperature at the antenna terminals and includes the antenna input noise temperature, T_A, and the receiver system noise temperature, T_R

N_o is the noise spectral desnity for unity temperature and bandwidth = -228.6 dBW/Hz-^oK

B is the spectral processor resolution bandwidth, and

G is the receiver antenna gain

The path loss in dB is:

$$L = 20 \log f + 20 \log R_S + 32.4 \text{ dB} \quad 2)$$

where, f is the frequency of reception in MHz, and R_S is the slant range distance to the emitter in kilometers.

In order to increase the coverage area at the higher frequencies (where antenna beamwidths become small), the antennas are pointed off nadir. With such a beam configuration there is a compensating effect between the path-loss and antenna gain factors in equation 1). The path-loss and footprint area at points off nadir both increase with the angle from nadir. However, the effect of path loss is to decrease the footprint area. Therefore, equi-sensitivity contours can be defined on the earth surface. Appendix C contains illustrations of such contours. The area within such a contour, called the "footprint," is a measure of the coverage area. If the contours are specified on the basis of meeting minimum sensitivity requirements, the coverage area is defined. On the other hand, if they are defined on the basis of meeting coverage area requirements, the system sensitivity is defined.

Figure 3, from Appendix C, repeated in this section as Figure 4-27, illustrates some of the trade-offs available among antenna beamwidth, antenna pointing angle from nadir and

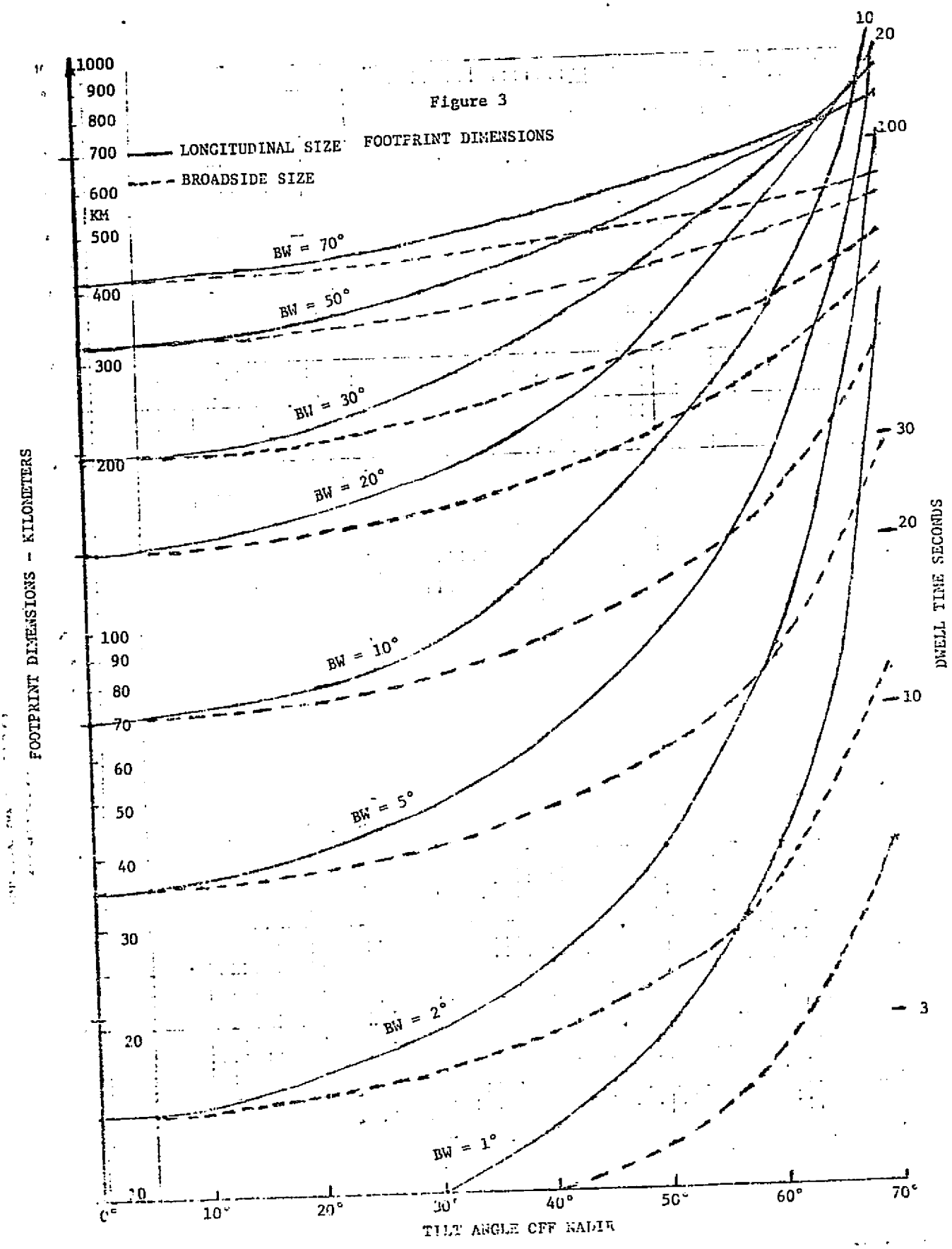

Figure 4-27. Footprint Dimensions vs. Tilt Angle Off Nadir

footprint dimensions. The latter are important because the length is indicative of how completely the earth is covered and the width determines the dwell time. Dwell time is defined as the interval between times when the spectrum must be sampled in order to provide continuous coverage along the orbital path. The footprint dimensions increase rapidly with tilt angle, for tilt angles greater than about 40°.

From Figure 2-5, page 2-9, the distance between orbits 17 and 32 at about 40°N, the approximate mid-latitude of the CONUS is seen to be about 580 km. This is the minimum length of the footprint that will give nearly complete CONUS coverage, assuming the antenna beam is perpendicular to the orbit ground track. Because the yaw angle of the Shuttle is assumed not to be controlled by the EEE experiment POCC, antenna pointing perpendicular to the ground track cannot be assured. Indeed, it is possible that an antenna beam may be pointed along the track yielding very little coverage of the earth. To avoid that situation it is planned to use antennas switchable in pairs, one pointed at an angle of $+45^{\circ}$ to the Shuttle axis and the other at -45°. The antenna giving the greatest coverage will be selected. With this antenna configuration, the worst case for coverage is when the Shuttle axis is parallel to the ground track, in which case the antenna beams are both at 45° with respect to ground track. Then for complete CONUS coverage the footprint length would have to be about 625 km. Lengths of this magnitude are obtained only for beamwidths greater than about 2° pointed near the horizon, i.e., 65° to 70° from nadir.

The antennas and antenna configurations selected for EEE-MOD II represent a compromise between sensitivity to isolated emitters and area coverage. Pointing angles from nadir of 0°, 60°, and 65° were selected, the angles increase with the operating frequency of the antenna. To increase coverage either (or both) the beamwidths and the pointing angles may be increased. Both actions tend to decrease the signal strength received from isolated sources.

Table 3, in Appendix C, summarizes the design and performance of the current EEE-MOD II design.

Using the antenna beamwidth data given there, Figure 4-27 can be used to convert the beamwidths to footprint dimensions on the earth at the various operating frequencies. These footprints are somewhat arbitrarily defined by the equi-sensitivity contour 3 dB below the maximum sensitivity. Roughly, the contours are ellipitical and as illustrated in Appendix C. Table 3 shows dwell times based on the time it takes the footprint to pass over an emitter so located to cover the maximum dimension of an antenna footprint oriented 45° to the ground track. This is the maximum time an emitter can be in the footprint. An experiment designed on the basis of that dwell time would suffer from relatively poor earth coverage. The coverage would be that of a sequence of "just touching" ellipses.

To provide increased coverage the experiment design is based on a dwell time a quarter of that represented by the minor axis of the elliptical contour. Table 4-1 shows the footprint dimensions and those of an inscribed rectangle. The narrow dimension of the rectangle is one quarter the footprint width. This dimension is a function of frequency, as shown in Table 4-1, for the six antennas of the EEE-MOD II. The assumption of an elliptical contour is used to calculate the length of the rectangle. Also shown in the table is the dwell time calculated from the rectangle dimensions. These data are shown graphically in Figure 4-28 to illustrate more clearly the dependency of the dwell time on frequency and the antenna.

From Figure 4-28 it is seen that the minimum dwell time is 1.6 seconds. This is the period between spectral density measurements at 43 GHz for continuous coverage (monitoring) of the earth for emitters at this frequency. If that period is used to perform the spectral analysis over the frequency range from 4 GHz to 43 GHz, the material in Appendix E shows that the analysis can be accomplished by a Spectrum Processor utilizing a bank of 16 filter circuits each having a resolution bandwidth of 200 KHz, an integration time of 0.125 m sec and giving an accuracy of 20%. The spectral analysis of the frequency range from 150 MHz to 4 GHz can be accomplished in 1.25 seconds, with a resolution bandwidth of 20 KHz to the 20% accuracy.

Some of the trade-offs available should be mentioned. Again assuming an elliptical footprint, the use of one quarter of its minor axis to determine the dwell time means that 97% of its major axis is used, i.e., almost all the available footprint length, as seen from

Table 4-1. However, the use of 50% of the minor axis only reduces that part of the major axis used to 87%. That is, a loss of 10% of the coverage area permits doubling the dwell time. This in turn permits halving the resolution bandwidth and increasing the sensitivity by 3 dB. This appears to be an attractive trade-off in the 4 to 43 GHz range.

Figure 4-28 suggests another possibility decreasing the resolution bandwidth and increasing sensitivity. The dwell time is seen to be a function of frequency, meaning different periods can be used between spectral analyses of different frequency intervals and still provide continuous monitoring of the emitters on the earth. For example, the frequency range from 24 GHz to 43 GHz could be analyzed every 1.6 seconds and the analysis would require 0.8 seconds in an interval could be used to perform the analysis of the 10 GHz interval from 4 to 14 GHz with a resolution bandwidth of 100 KHz. The 0.8 second portion of the next 1.6 second interval could be used to perform the same analysis of the 14 to 24 GHz band. This results in the 4 to 24 GHz band being analyzed every 3.2 seconds, which as Figure 4-28 shows, is adequate.

The above discussion of time to perform the spectral analysis is based on the equations derived in Appendices D & E, in particular equation 3 of Appendix E. For the present discussion that equation can be written:

$$T = \frac{b}{N B (v/p)^2}$$

where, T is the time required to perform the spectral analysis over a frequency interval of W Hz to a relative accuracy of v/p. B Hz is the resolution bandwidth of the spectral analysis, N is the number of contiguous filters (of bandwidth B) and detector circuits in the bank of such elements used to measure the power density, and $b = W/B$ is the number of resolution bandwidths in the W Hz frequency interval. The relative accuracy v/p is the variance of the measurement (v) divided by the actual power of the isgnal (p) in the resolution bandwidth.

Table 4 -1 . Footprint Dimensions and Dwell Time

Antenna	Frequency GHz	Footprint		Inscribed Rectangle Used		
		Length Km	Width Km	Length Km	Width Km	Dwell Time Sec
Log Periodic	0.121-0.174	420	420	407	105	14.1
	0.243	460	340	445	85	11.4
UHF Array	0.4	310	240	301	60	8.1
	0.7	180	145	174	36	4.8
S-Band	0.7	480	480	465	120	16.2
Helix	2.7	410	410	397	103	13.9
S-Band	0.7	630	370	610	93	12.5
0.7m Dish	2.7	360	165	348	41	5.5
0.5m Dish	2.7	600	250	581	63	8.5
	4.0	500	200	484	50	6.7
	8.0	320	110	310	28	3.7
	12.0	260	75	252	19	2.6
0.25m Dish	12.0	390	145	378	36	4.8
	18.0	310	105	300	26	3.5
	26.0	260	73	252	18	2.4
	43.0	155	46	150	12	1.6

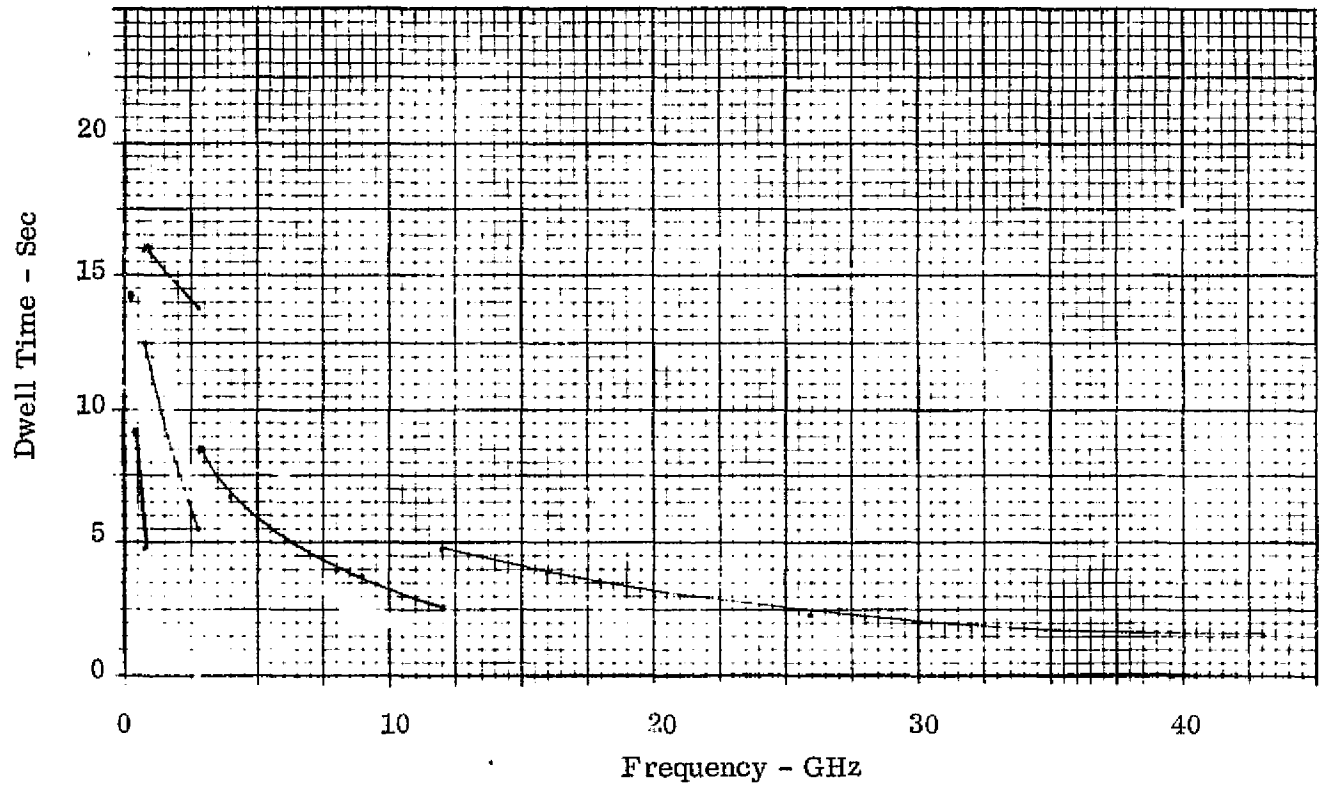

Figure 4-28. Dwell Time as a Function of Frequency

This equation can be put in the more conventional form by substituting the equation for b into the equation defining T:

$$T = \frac{W}{N\,(v/p)^2 B^2}$$

This form of the equation shows that, for a fixed number of filter detector circuits (N), and relative accuracy (v/p), the time required to perform the spectral density measurement is proportional to the reciprocal of the resolution bandwidth squared. However, in the previous discussions of trade-offs between the time to perform the spectral analysis and resolution bandwidth assume that number of circuits (N) in the filter-detector bank increases as the resolution bandwidth (B) decreases, such that the product NB is constant. In that case, the time to perform the analysis is proportional to the reciprocal of the resolution bandwidth to only the first power.

To this point the discussion has been in terms of isolated emitters. In the lower portion of the MOD II band it is expected that many emitters will be within the extended footprints. When this is the case, each of them can have a lower EIRP, and it will be possible to detect their collective power level at the Shuttle so long as it exceeds the receiver sensitivity. This means that individually they can be below the sensitivity level. This phenomenon is discussed further in Appendix C.

Summarizing, the analysis shows that there are several trade-offs available among the experiment parameters: antenna beamwidths, pointing angles, and achievable earth coverage. For a given set of antenna parameters, improved sensitivity and decreased resolution-bandwidth can be obtained by tailoring the timing of the spectral analysis of the various spectrum portions to the dwell time available at each frequency. In addition, further improvements in resolution and sensitivity can be achieved at the cost of a slight decrease in the earth area covered.

4.5.2.2 Spectral Power Density Measurement Accuracy

System noise performance, its gain stability, receiving system amplitude slope and ripple variations, interference from other Shuttle equipment, the encoding A/D conversion error and the match of the Spectral Processor characteristics to the spectrum being measured all limit the accuracy to which the spectral power density can be measured at the Shuttle.

The effects of that part of the system noise and that part of the system amplitude slope and ripple variations introduced after the antennas, can be minimized by a combination of careful design and periodic calibration. The calibration noise sources incorporated into the design provide the means for system calibration. To the extent the relevant parameters of the antenna noise, amplitude slope and ripple and interference from other Shuttle equipment is known, their effects on system accuracy can be minimized by further processing of the data from the Spectral Processor.

The determination of attainable power spectral density measurement accuracy requires further study of calibration procedures, receiving equipment performance and expected interference. The A/D conversion quantization error can be made as small as desired by increasing the number of bits in the code word. As discussed in Appendix E, the error is 1dB for a 7-bit word and 0.5dB for an 8-bit word, which is standard.

A fundamental accuracy limitation is in the design of the Spectrum Processor itself, in particular the match of the resolution-determining filters to the spectrum to be measured. Spectral power density is measured by means of the circuit shown in Figure 4-29. or its equivalent.

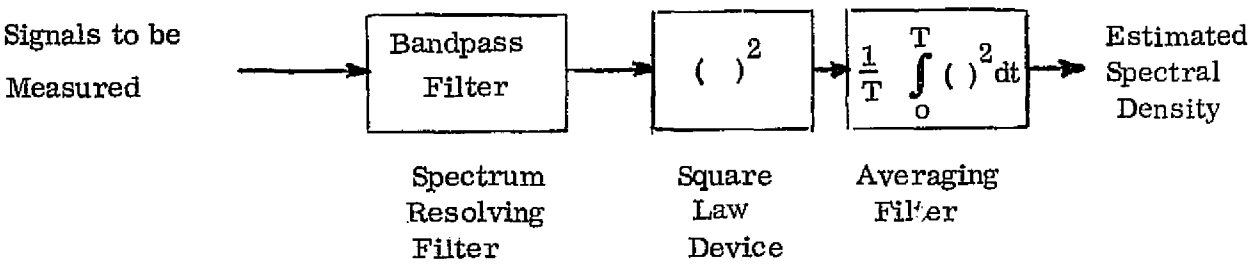

Figure 4-29. Spectral Power Density Measurement Circuit

From the material in Appendix D, assuming the input signal spectra are uniformly distributed in frequency and have a Gaussian amplitude distribution, the standard deviation of the power as measured by the circuit is less than

$$v = P \Big/ \sqrt{BT}$$

and the fractional error is less than

$$v/P = 1 \Big/ \sqrt{BT}$$

Where P is the true power of the assumed Gaussian processes; B is the bandpass filter bandwidth which is also the spectrum frequency resolution; and T is the averaging time used in the measurement. For relatively long averaging time, i.e., BT products greater than about 5, the power measurement error is approximately Gaussian. Then v has the significance of being the magnitude of the error that is exceeded in about 32% of the measurements. An error of 2 v is experienced in about 5% of the measurements.

If the amplitude distribution of the input signals in the bandwidth B is more narrowly confined than that of a Gaussian process, the measurement errors will be smaller than the above

formula suggests and, conversely, wider amplitude distributions lead to larger errors.

For what appears to be the most usual case of many emitters received within the bandwidth, the Gaussian distribution assumption is reasonably accurate. However, it is not obvious that the assumption that the signal frequency spectrum is uniformly distributed across the bandwidth will always be satisfied. FCC and other regulatory bodies tend to confine the emitters to a narrow frequency band. This can lead to cases for which the process being measured has a bandwidth, say B1, smaller than the design resolution bandwidth B. However, in the design of the Spectrum Processor a value of averaging time T has to be incorporated into the design such that BT is large enough to give the desired error. The result is that in the case of narrower spectra the error is that due to a B1 T $<$ BT or a larger error than anticipated. Table 4-2 gives a listing of the fractional error as a function of BT.

Table 4-2. Fractional Error and Averaging Time in Spectral Density Measurements

BT	Fractional Error v/P	Required Averaging Time (millisec.)		
		B= 20kHz	B=200kHz	B=1Mhz
5	0.45	0.25	0.025	0.005
10	0.32	0.5	0.05	0.010
15	0.26	0.75	0.075	0.015
20	0.22	1.00	0.1	0.02
25	0.20	1.25	0.125	0.025
30	0.18	1.5	0.15	0.03
50	0.14	2.5	0.25	0.05
75	0.12	3.75	0.375	0.075
100	0.10	5.0	0.5	0.1

A reasonable accuracy specification might be a fractional rms error of 0.2 for the power density measuring process, which corresponds to less than a 1dB rms measurement error. This requires a BT product of 25.

To illustrate the magnitude of the error involved in a mismatch between the process and the resolution bandwidths, assume the Spectrum Processor is designed for B = 1 Mhz and T = 0.025 milliseconds to give BT = 25. If the process being measured had a bandwidth of 200 kHz the actual signal bandwidth and integration time product would be $B_1T = (200 \times 10^{3})(.025 \times 10^{-3}) = 5$. From Table 4-2, it is seen that the measurement error would be more than twice that expected.

The conclusion to be drawn from this is that the error due to a mismatch between spectrum and spectral processor resolution can be significant. In the actual hardware design, this warrants either further investigation into the expected signal characteristics, or, at least for the initial experiment, the use of multiple resolution bandwidths. This would allow a comparison of results to estimate the loss of accuracy due to mismatched bandwidths.

4.6 EEE RF ENVIRONMENT SURVEY STUDY

A subcontract was awarded to the National Scientific Laboratories (NSL) for a four month study starting 1 July 1977. The study, requested by the GSFC P.I., examines the utilization of EEE frequency bands within the continental United States. From various data sources, including listings of the International Frequency Registration Board (IFRB), NSL will identify and characterize terrestrial emitters as to frequency, EIRP, modulation, radiation direction, geographical location, etc. The data from the listings will be analyzed and classified as deterministic (reliable, detailed), probabilistic (generally reliable, statistical), and indeterminate (unreliable, insufficiently detailed). The results of the study will be presented in such a manner as to aid the P.I. in evaluating the expected measurement results of the EEE experiment. Also, the study will help in interpreting the actual Shuttle experiment flight data. The computer methodology utilized may aid in the data reduction task for the large amounts of EEE flight data expected on the mission.

The results of the study will be presented graphically in NSL's Final Report in several ways, such as histograms showing the number of emitters versus frequency, and total power versus frequency. (See samples in Figures 4-30 and 4-31). The NSL Final Report will be submitted to GSFC as an amendment to the MMAP Final Report. This NSL report is due November 1, 1977.

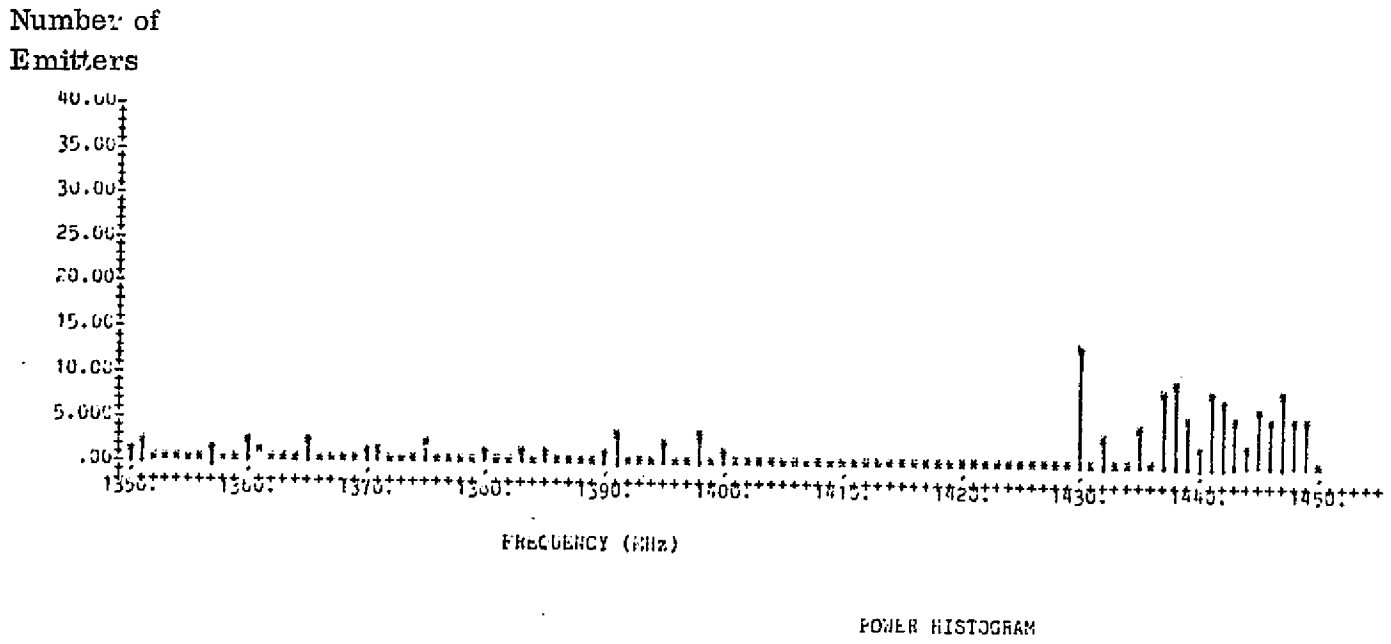

Figure 4-30. Number of Emitters versus Frequency (1350 to 1450 MHz)

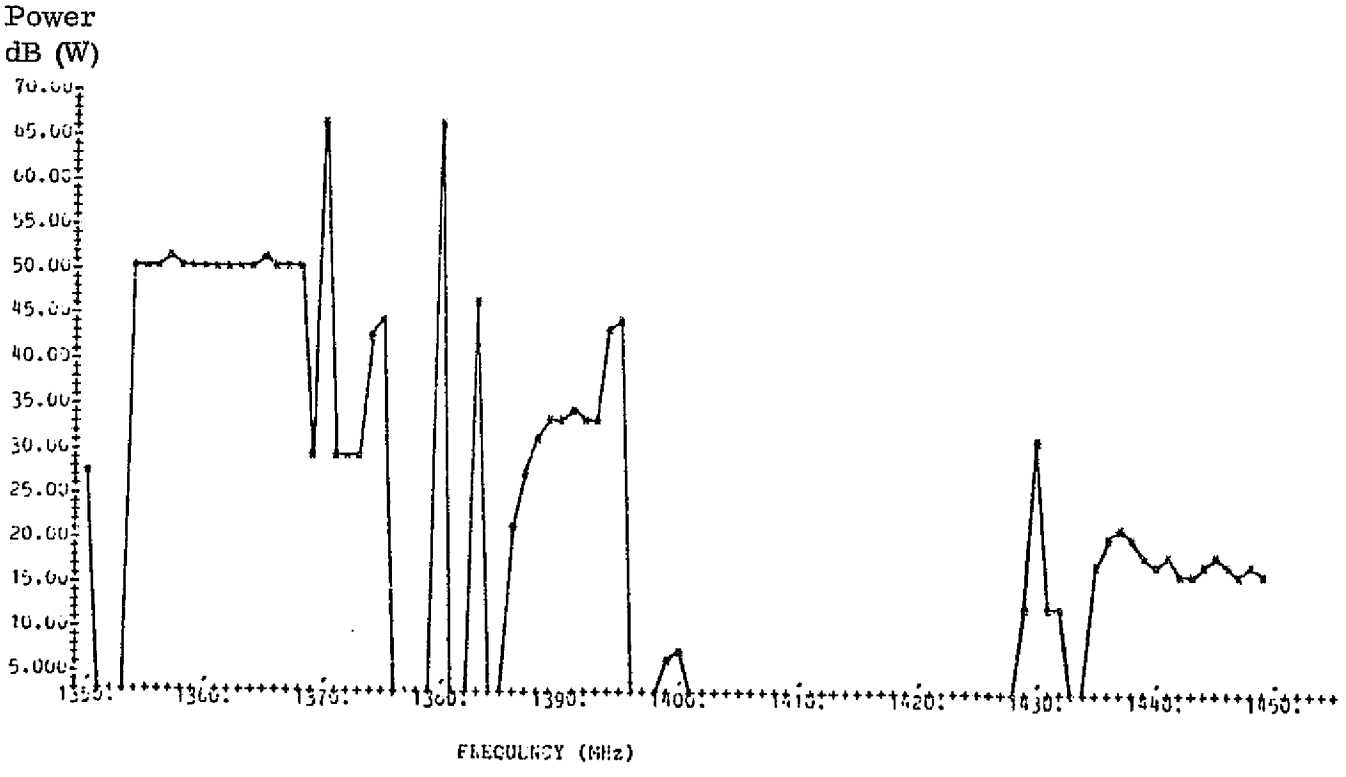

Figure 4-31. Total Cumulative Power versus Frequency (1350 to 1450 MHz)

SECTION 5

MILLIMETER WAVE COMMUNICATIONS EXPERIMENT (MWCE)

Definition of the MWCE was conducted in two phases: a MWCE-MOD I with dual transponders, steerable antenna, and monopulse tracker, and a MWCE-MOD II fixed antenna configuration with one transponder. Work completed up to March 1977 included a review of earlier studies[3], and extension of these studies to include a preliminary design of a full-up MWCE MOD I experiment using a steerable pointing antenna system. Work on experiment implementation has included study of the ground systems as well as the Shuttle equipment and a radius of operation analysis to show operating times over specific stations. Work on MOD I covered the following areas:

1. MWCE Experiment
2. MWCE -MOD I Instrument Description (Steerable Antenna)
3. Preliminary Data Reduction Analysis
4. System Performance Analysis

5.1 MWCE EXPERIMENT

In the design of space communications and microwave sensing systems at millimeter wavelengths, consideration must be given to the effects of precipitation on the earth-space propagation path. At frequencies above 10 GHz, absorption and scattering caused by hydrometeors (rain, hail, or wet snow) can cause a reduction in signal level (attenuation) which will reduce the reliability of the link. Other effects can be generated by precipitation events. They include: depolarization, amplitude and phase scintillations, and bandwidth decoherence. All of these factors can have a degrading effect on space communications and microwave sensing at millimeter wavelengths.

Over the last decade or so, direct measurements of earth-space attenuation above 10 GHz have been accomplished, first with radiometers and sun-trackers, then with the ATS earth satellites. More refined models were proposed, and the first steps in acquiring long term attenuation statistics were begun at a number of frequencies and locations. Recently, data from the ATS-5, ATS-6 and CTS satellite experiments have become available. Results from the MWCE will extend the scientific and engineering data base into the millimeter wave frequency bands, specifically the 30/20 GHz communications bands.

5.1.1 EXPERIMENT OBJECTIVES

The primary objective of the Millimeter Wave Communication Experiment (MWCE) is to evaluate advanced wideband communications techniques for space applications in the millimeter wavelength bands. The techniques will include the measurement and evaluation of digital and analog communications utilizing frequency reuse techniques. A second objective is to measure atmospheric affects and provide a data base for design of future millimeter wave communications systems.

The significant and unique aspects of the MWCE are:

1. High rate (500 Mbps capability, 50 Mbps planned for experiment) data links at 20 GHz (downlink) and 30 GHz (uplink).
2. Frequency re-use using right and left-hand circular polarized signals.
3. Provide an additional downlink for Spacelab data.
4. Data transmissions are to be evaluted as a function of local ground station elevation angle to evaluate scintillation effects and characteristics of low elevation angles.
5. Evaluate sub-synchronous communications link capabilities.
6. Wideband analog and digital techniques.

Two major advances of the MWCE are:

1. Actual wideband communications will be conducted along with beacon-type experimentation.

2. The measurements will be the first conducted from a non-synchronous orbit, thus allowing the variables of ground station elevation angle and satellite antenna pointing accuracy to be evaluated.

Results of the MWCE would be utilized in the development of system design requirements for NASA projects, for the development of spectrum utilization, frequency management and sharing criteria, and for the evaluation of domestic distribution and communications satellite questions under the GSFC TCS (Technical Consultation Services) Program.

A vast number of organizations and agencies are actively involved in the evaluation of millimeter wave data and system analysis. A partial list of these organizations interested in MWCE is presented below:

1. NASA Programs
   a. CTS, ATS - Telecommunications Users
   b. PSCS - Public Service Communication Satellite
   c. Nimbus/Landsat - Sensor Development
   d. Space Shuttle - EVAL, IUS Payload Development
   e. Next Generation NASA Operations
2. WARC Support
   a. IRAC Inputs for Position Papers
   b. Significant Interest for Frequencies Above 20 GHz
3. Technical Consultation Services (TCS)
   a. Provide support for frequency use and spectrum management under GSFC TCS Program

4. Other Government Users

   a. Federal Communications Commission (FCC)

   b. U.S. Dept. of Commerce, Office of Telecommunications, Institute for Telecommunications Sciences (OT/ITS)

   c. Office of Telecommunications Policy (OTP)

   d. National Oceanic and Atmospheric Administration (NOAA)

5.1.2 OPERATIONAL MODES

The MWCE will be flown on the Shuttle to simulate low-orbit satellite communications links from the MWCE to designated principal ground stations at GSFC, Greenbelt, Md. and GSFC, Rosman, N.C. STDN Sites. Additional ground stations might include Blacksburg, Virginia (Virginia Polytechnic Institute and State University), Columbus, Ohio (Ohio State University) and Austin, Texas (University of Texas). The location of these ground stations requires a 57^{o} inclined orbit; nominal altitude is planned for 400 km.

The operational links of the MWCE will provide a direct evaluation of critical design requirements for millimeter wave space systems. The areas of investigation include: frequency re-use techniques employing orthogonal polarization; propagation characteristics and low elevation angle effects; wideband analog and digital techniques.

The MWCE- MOD I will be operated in several modes in order to demonstrate the feasibility of high data rate, millimeter wave, satellite communication links:

1. Transponder Mode
2. Spacelab Module Mode
3. Beacon Mode

The modes are illustrated in Figure 5-1.

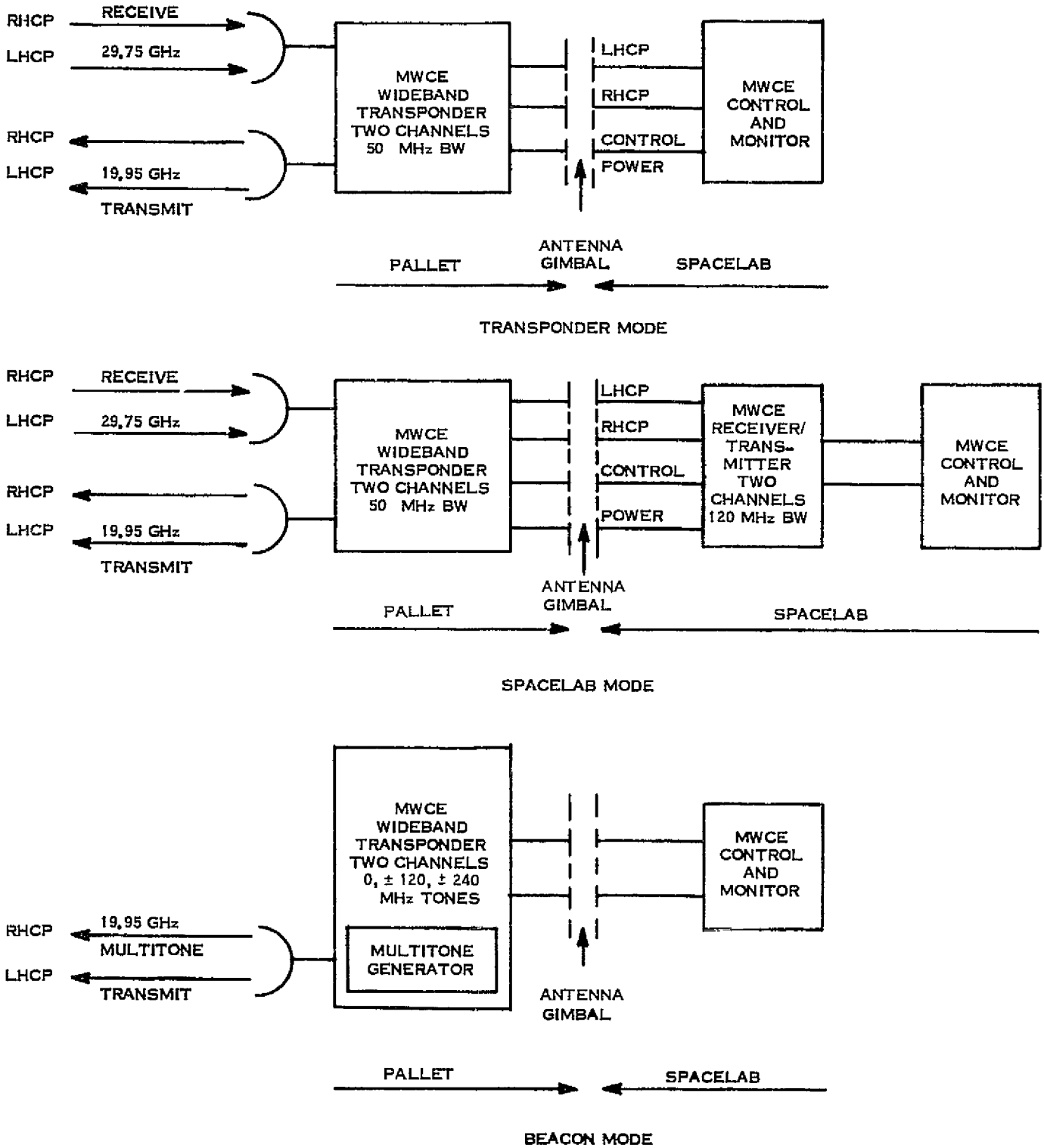

Figure 5-1. MWCE - MOD I Modes of Operation

In the Transponder mode the MWCE acts as a frequency-converting "bent-pipe" communications link. In this mode it is planned to use two circularly polarized channels each with 50 MHz bandwidth through the transponder using separate receive and transmit antennas.

In the Spacelab mode of operation the MWCE Payload Specialist (PS) will be an active participant. For example, unlinked data will be recorded, cross-correlated between channels, retransmitted via the TDRSS (limited to 50 Mbps), etc., with close coordination between the PS and the responsible ground station personnel. The PS may also be transmitting data such as random generated data, TDRSS data, video data, multitone signal, and CW. Simultaneously, antenna pointing, time sharing with other experiments, and experiment monitoring will be being conducted.

The beacon mode consists of continuously operating 20 and 30 GHz test signals (Shuttle to earth) for the evaluation of propagation and low elevation angle effects.

A summary of the principal measurement parameters is given below:

1. Transponder Mode

    a. Bit Error Rate (BER) on LHCP channel, RHCP channel no signal, channels isolation measurements

    b. BER on RHCP channel, LHCP no signal, channel isolation measurements

    c. BER on both channels, same signal and clock rate - cross-correlation between channels (a measure of channel isolation)

    d. BER on both channels, different clock rates

    e. BER as a function of elevation angle

    f. Phase lock loop lock-in, slewing, loss-of-lock

    g. Signal amplitudes

2. Spacelab Module Mode

   a. BER of known Spacelab digital data, correlate with TDRSS downlinked data, both channels

   b. BER for single channels only

   c. Spacelab data on one channel, uncorrelated data on other channel, measure BER, correlate with TDRSS downlinked data

   d. BER versus elevation angle

   e. Phase lock loop lock-in, slewing, loss-of-lock

   f. Signal amplitudes

3. Beacon Mode

   a. Attenuation and depolarization caused by rain

   b. Low elevation effects caused by the atmosphere

5.2 MWCE-MOD I INSTRUMENT DESCRIPTION

The major instrument systems of the MWCE-MOD I are illustrated in Figure 5-2. Figure 5-3 shows the MWCE pallet mounted equipment. A gimballed mount is used with $\pm 70^{o}$ FOV from NADIR. The mount will be stowed as shown in Figure 5-3 during launch and landing.

Pallet mounted equipment is enclosed in a rectangular structure of 290 x 280 x 264 centimeters. This structure is mounted on gimbals as shown in Figure 5-3 to provide $\pm 70^{o}$ field of view for ground station tracking. A light weight structure will house the two 0.7 m parabolic antennas, the two widebeam acquisition horns, and the RF electronics including the traveling wave tube amplifiers, down converters frequency synthesizer and power supplies. This arrangement provides compact packaging, weight reduction and short waveguide runs. A six inch diameter X-Y gimbal will be used to provide tracking. Flexible coaxial cables are used for IF signal connections, control signal lines, and power connections to the pallet equipment.

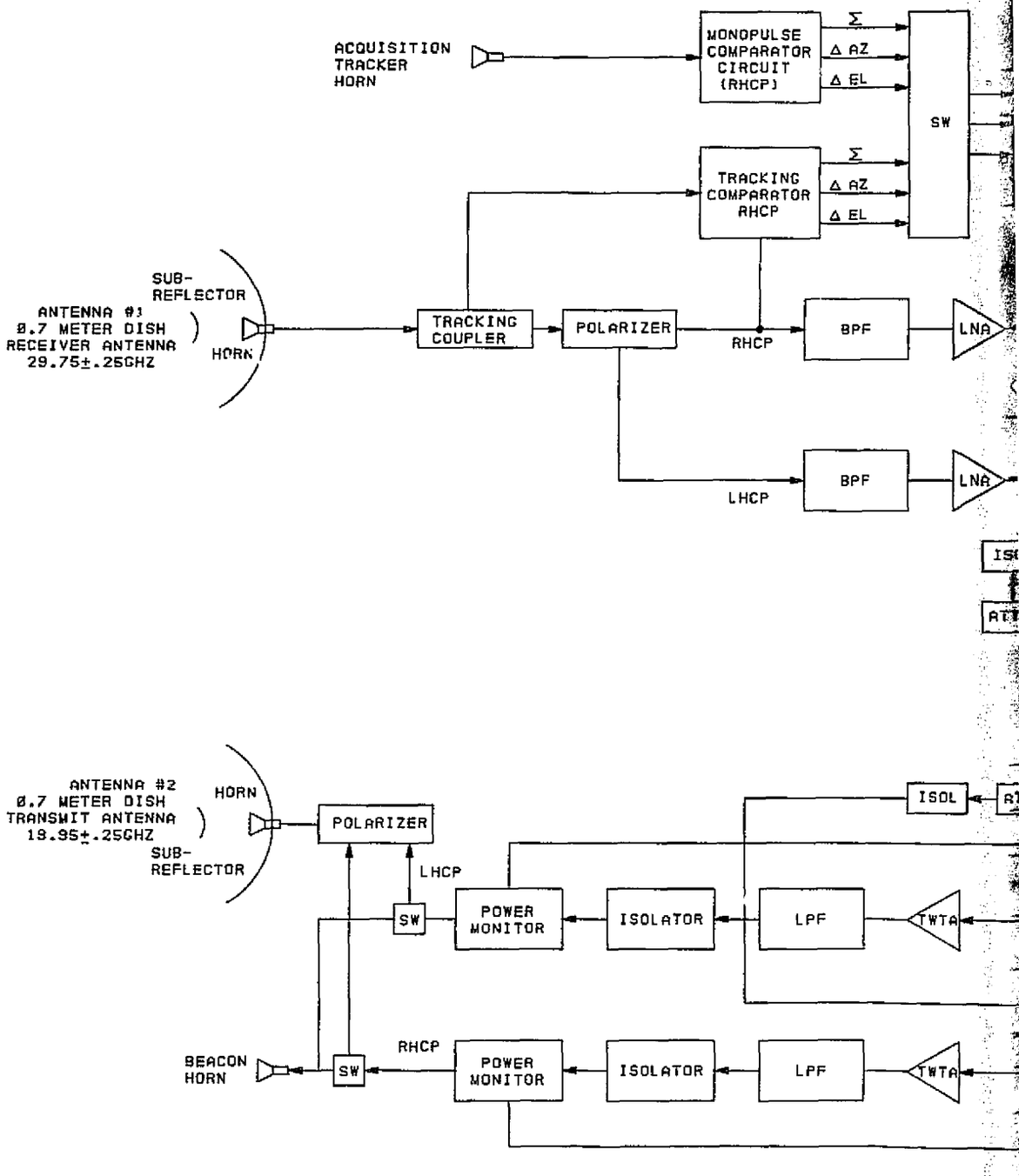

POINTER FRAME 2

PAL

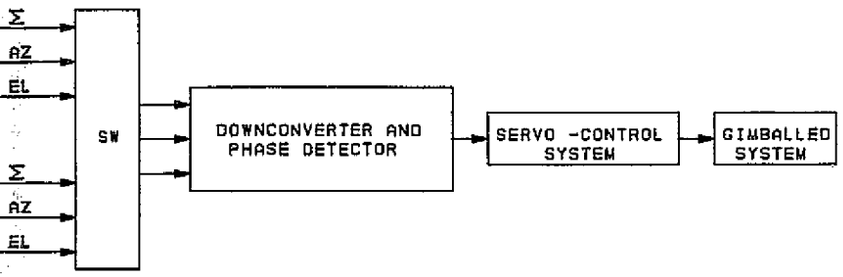

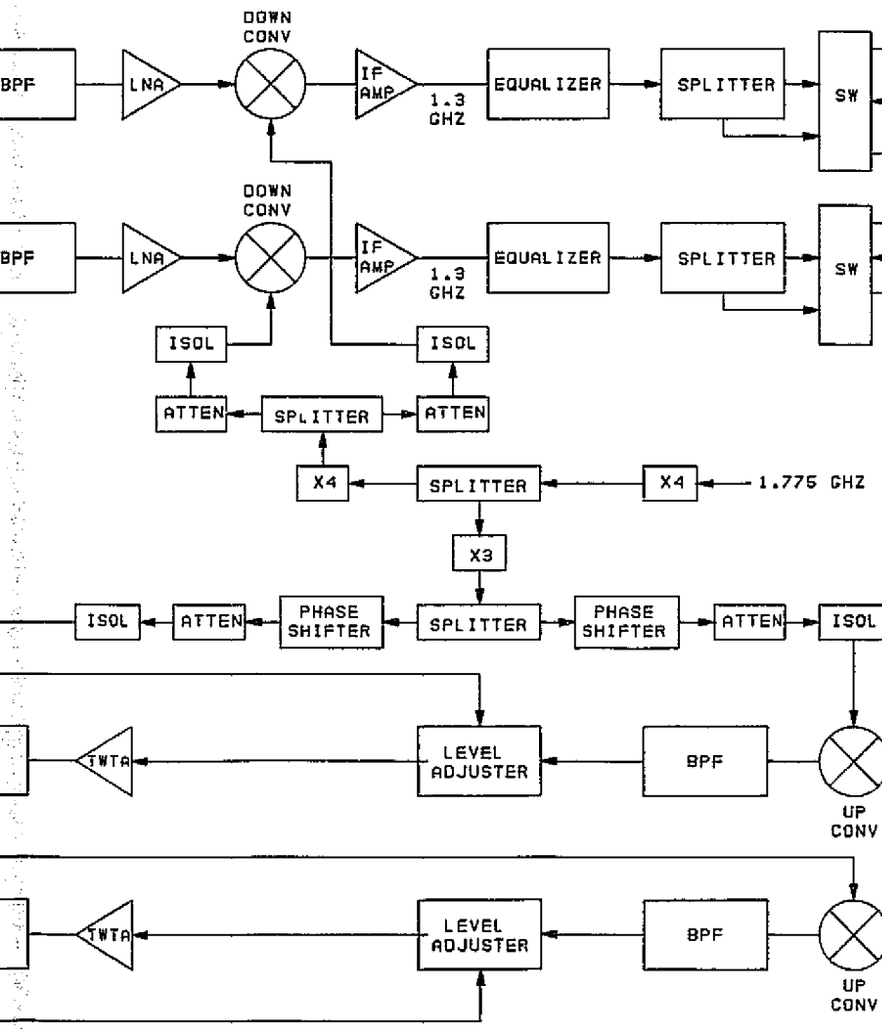

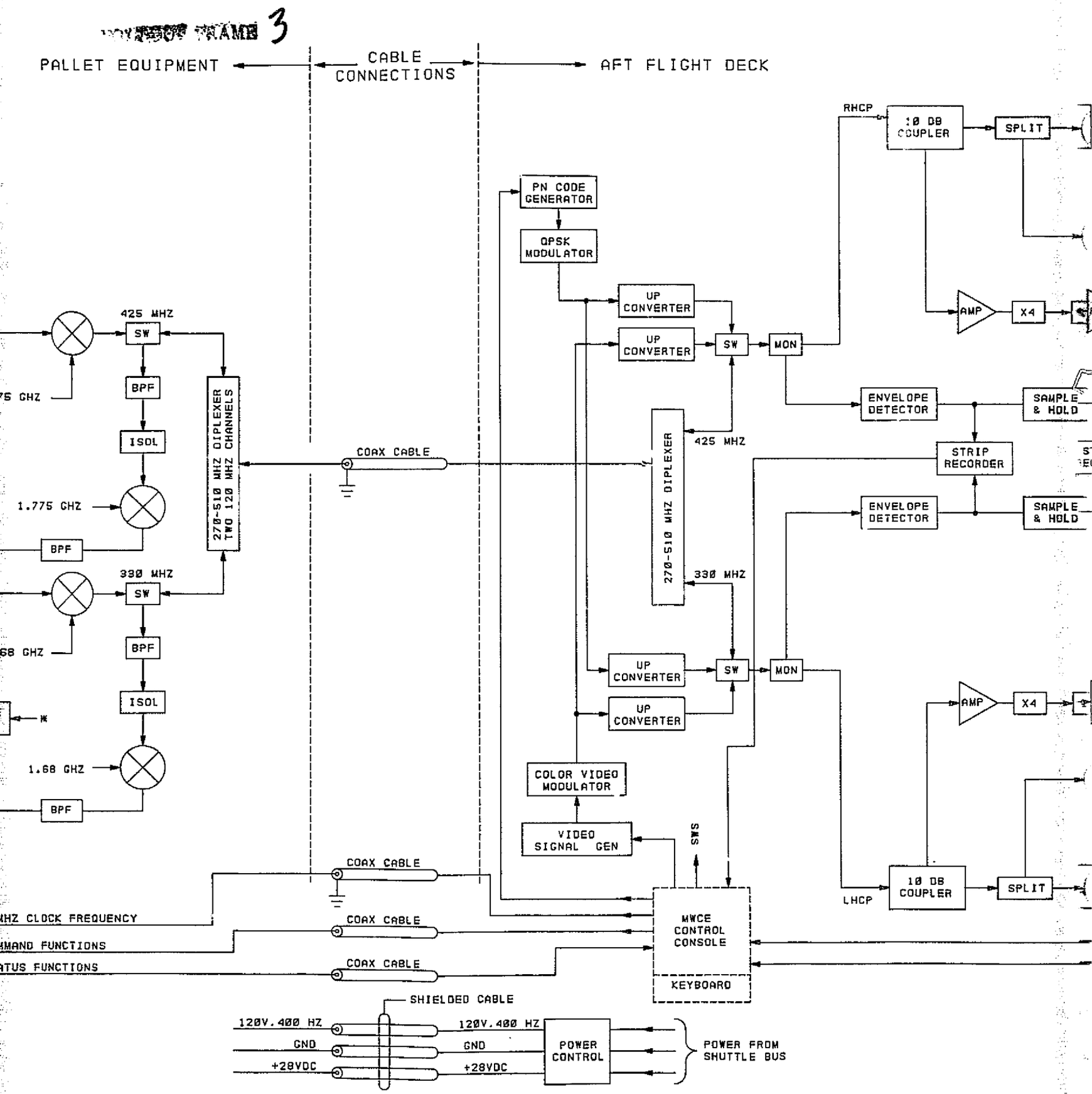
PALLET EQUIPMENT
CABLE CONNECTIONS
AFT FLIGHT DECK
425 MHZ
SW
BPF
ISOL
1.775 GHZ
BPF
330 MHZ
SW
BPF
ISOL
1.68 GHZ
BPF
270-510 MHZ DIPLEXER TWO 120 MHZ CHANNELS
COAX CABLE
PN CODE GENERATOR
QPSK MODULATOR
UP CONVERTER
UP CONVERTER
SW
MON
RHCP
10 DB COUPLER
SPLIT
AMP
X4
ENVELOPE DETECTOR
SAMPLE & HOLD
STRIP RECORDER
ENVELOPE DETECTOR
SAMPLE & HOLD
425 MHZ
270-510 MHZ DIPLEXER
330 MHZ
UP CONVERTER
UP CONVERTER
SW
MON
AMP
X4
COLOR VIDEO MODULATOR
VIDEO SIGNAL GEN
SMS
10 DB COUPLER
SPLIT
LHCP
COAX CABLE
COAX CABLE
COAX CABLE
MWCE CONTROL CONSOLE
KEYBOARD
SHIELDED CABLE
120V.400 HZ
GND
+28VDC
120V.400 HZ
GND
+28VDC
POWER CONTROL
POWER FROM SHUTTLE BUS

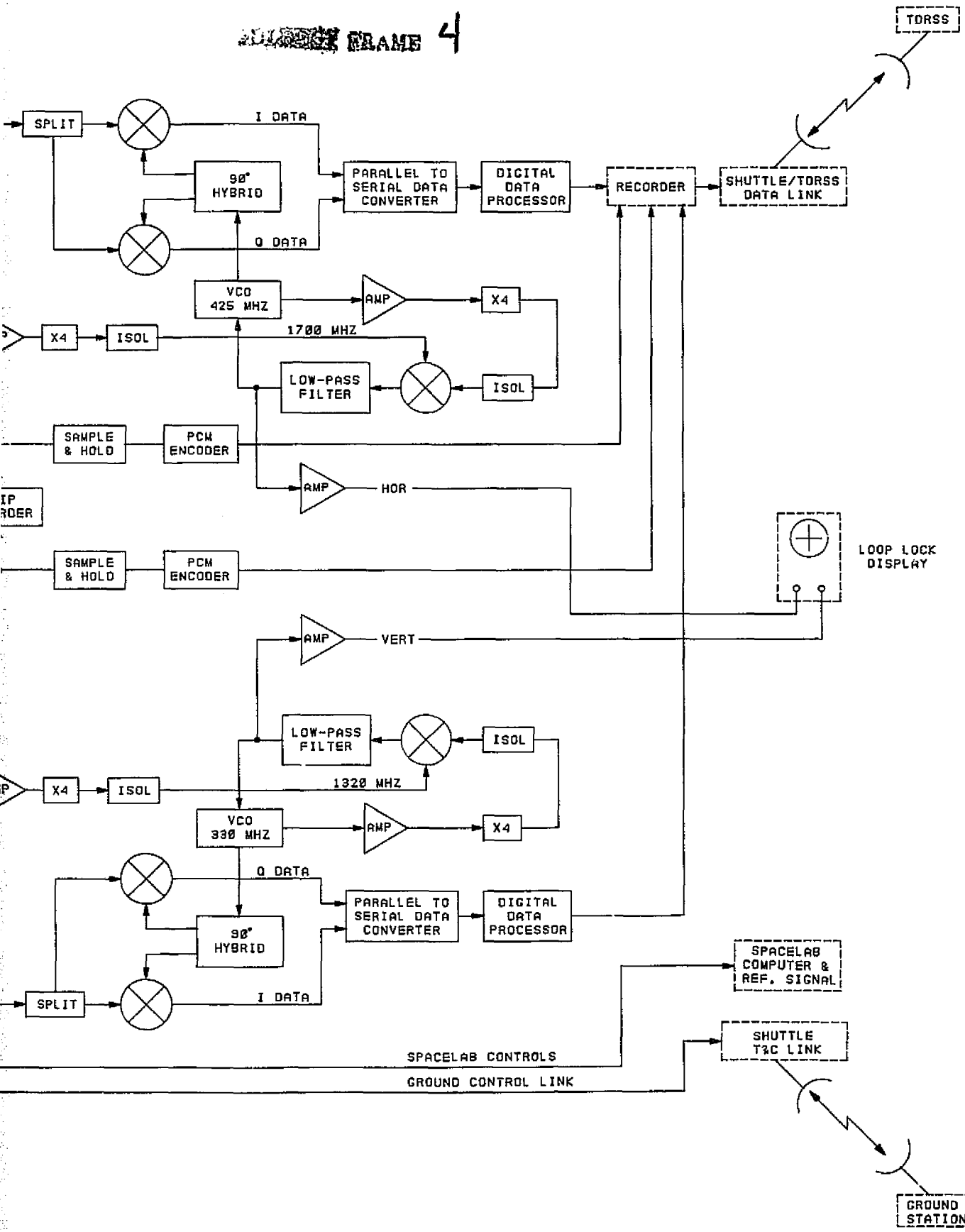

Figure 5-2. MWCE MOD-I Spacelab Equipment Block Diagram

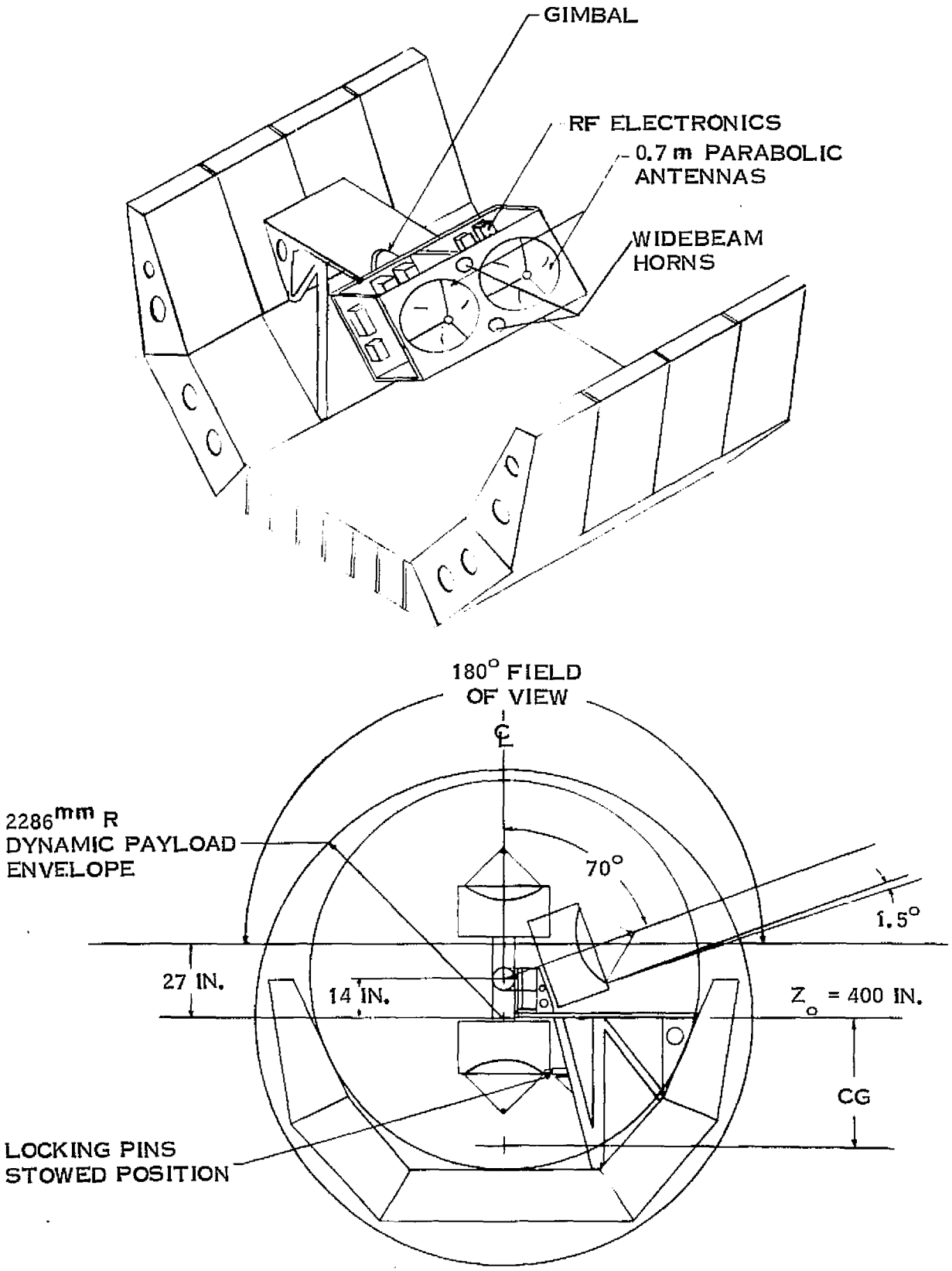

Figure 5-3. MWCE -MOD I Pallet Mounting Configuration

The $\pm 70^{o}$ FOV is obtained by mounting the pallet equipment enclosure on a cantilever structure as shown in Figure 5-3. During launch and landing the Y-axis gimbal rotates to the full down position and is locked into position. This stowed position is needed to comply with center of gravity constraints for launch and landing. Solenoid operated locking pins are used to lock the gimbal and the structure in its stowed position.

The pallet based RF systems consist of two dedicated antennas, two transponders, and two stages of IF down/up conversion. The two transponders are designed to receive at 29.75 ± 0.25 GHz and transmit at 19.95 ± 0.25 GHz. There is a separate antenna for transmitting and receiving and each antenna is capable of simultaneously handling both right- and left-hand circularly polarized signals. A passive microwave polarizer is employed to separate the polarized signals upon reception and combine the orthogonal polarizations for transmission.

The transmit antenna system consists of a Cassegrain 0.7 meter parabolic dish, 9 cm hyperbolic sub reflector, and dual polarized feed system capable of generating RHCP and LHCP. The horn aperture will be designed such as to efficiently illuminate the sub reflector for optimum aperture illumination and minimum spill over loss. The polarized section creates right-hand and left-hand circular polarizations, the quality of which is a function of power division quality, 90^{o} phase shift and internal match in the feed circuit. An axial ratio of less than 0.5 dB is achievable. Areas of concern in maintaining the polarization purity are tolerances, maintaining symmetry, reflections from the sub reflector and off axis cross polarized components introduced by the curvature of the main reflector.

The receive antenna system consists of an identical Cassegrain configuration except for the tracking mode and additional filtering which may be required. The sum mode circuit in the receive antenna (as well as in the transmit) will consist of the horn, orthogonal coupler and a short slot hybrid which creates the power combination (or division) and a 90^{o} phase differential. The quality of circular polarization is a function

of the accuracy of power division equality and 90^{o} phase shift in the short slot hybrid and the internal match in the feed circuit.

In the transponder mode of operation each transponder acts as a double conversion RF/IF/RF repeater with a 1.35 GHz IF frequency. After conversion the received dual polarized signals are retransmitted by a 10W TWTA operated at saturated power. Because of the high data rates to be transmitted, i.e., up to a maximum of 500 Mbps, the amplitude and phase characteristics of the transponder components must be designed for minimum distortion. In the Spacelab mode, additional IF conversion stages translate the received left-hand circularly polarized signal (LHCP) to an IF frequency of 425 MHz and the right-hand circularly polarized signal (RHCP) to an IF frequency of 330 MHz. The two orthogonal polarized signals are then sent to the display console for analysis by the Payload Specialist. Similarly, digital or analog signals generated at the control console by the Payload Specialist are converted to 425 MHz and 330 MHz IF frequencies for LHCP and RHCP signals, respectively, and then translated to the 1.35 GHz IF frequency for transmission to the ground stations.

In the Beacon mode of operation, a CW beacon or a multitone generator will supply signals at 1.35 GHz which are then up-converted for transmission to the ground station. The CW beacon frequency is 19.95 GHz and the tones generated are spaced around the center frequency of 19.95 GHz at $\pm$120 MHz and $\pm$240 MHz.

In the console control area there are five specific experiment display and control functions under the supervision of the Payload Specialist during the Spacelab mode of operation. For each circularly polarized signal there is a QPSK demodulator with phase lock loop. The constituent quadrature I and Q channel data streams are processed to determine the overall BER and the resulting BER is recorded. Alternately, the quadrature data streams can be recorded or retransmitted via TDRSS. The phase lock loop error signal is displayed to determine lock-in or loop lock loss. The received signal amplitude variation is determined by an envelope detector. An analog strip-chart

recorder (optional) for recording the amplitude variations may be available to the Payload Specialist. The signal amplitude is also sampled, digitized in a PCM format and recorded for later analysis.

There are two transmitted information signals under the direct control of the Payload Specialist, a video signal that originates in the shuttle and a coded QPSK modulated data stream. In the former case, various parameters of the video signal are controlled directly by the Payload Specialist, e.g., the type of test pattern transmitted. The modulation format for the video information can be chosen to be some form of angle modulation (FM, PM, etc.). In the digital transmission mode, a PN code generator and its effective data rate are controlled by the Payload Specialist to determine variation of channel BER with respect to data rate.

5.3 DATA REDUCTION AND ANALYSIS

Due to the high data rates that will be transmitted, storage of the received 50 Mbps digital signal originating from the ground or the Shuttle will be prohibitive. Consequently, all high digital data rate information must be processed and the processed information stored. For example, the BER results can be digitized and stored rather than storing the received digital stream. The amplitude variations of the received signals are strip-chart recorded directly and sample digitized in a PCM format and stored.

Data received by the MWCE will be sent to the ground control/processing center in real time via the TDRSS and existing land lines. Figure 5-4 shows the steps to be taken to process data received at the control center. All data are expected to be initially recorded on magnetic tapes for storage and eventually transferred to GSFC Information Processing Division (IPD) data processing system. Similarly, data received at the tracking stations will be recorded and sent to the GSFC IPD.

Additional information on MWCE data handling is given in the task report, CI 10.

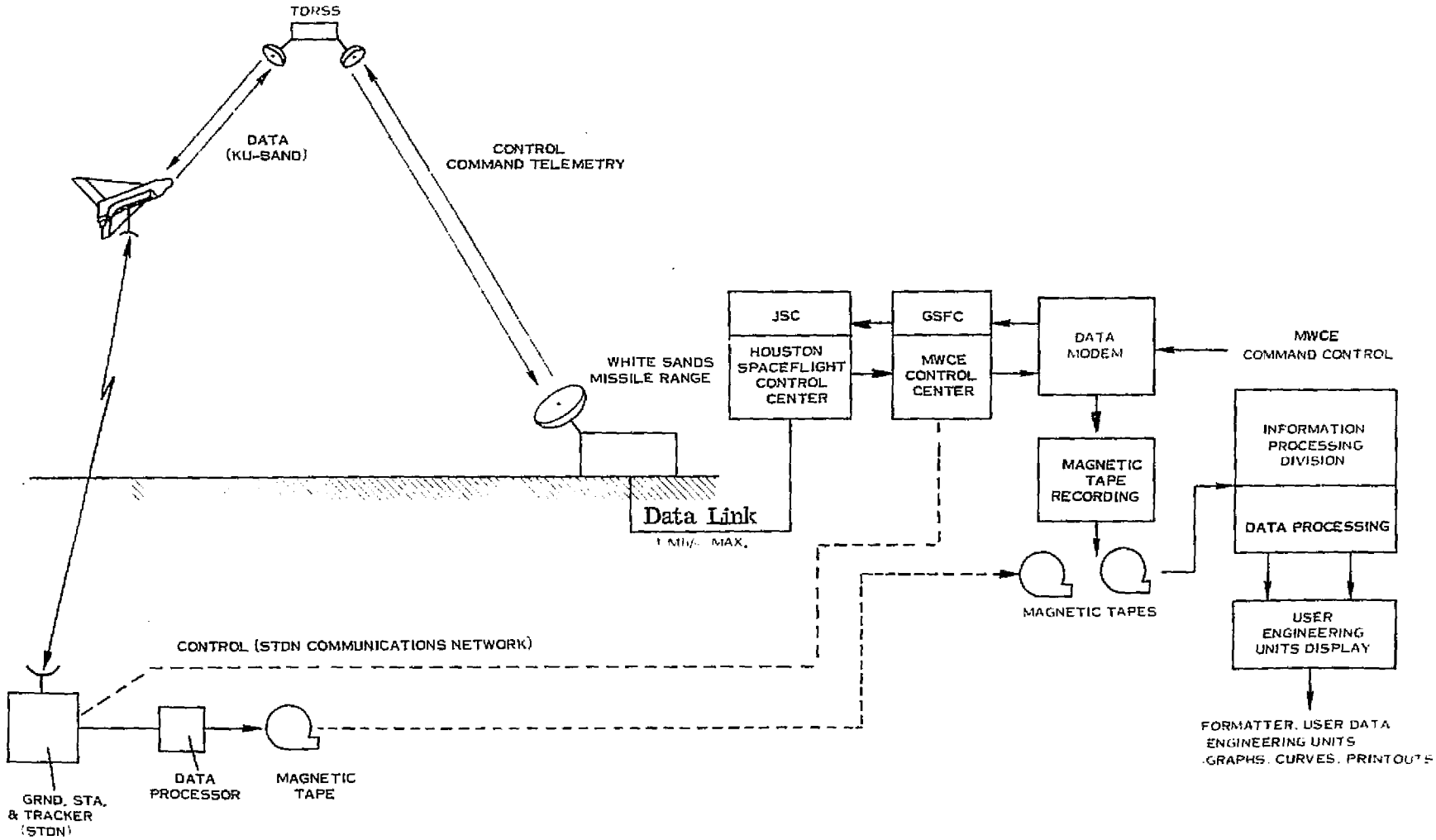

Figure 5-4. MWCE Data Processing

5.4 SYSTEM PERFORMANCE ANALYSIS

5.4.1 RADIUS OF OPERATION AND OPERATIONAL TIME

The radius of operation is defined as the maximum great circle arc distance from an earth station at which a desired communication system performance is achieved. The radius of operation can be limited either by geometrical factors such as the maximum allowable ground station elevation angle or the maximum shuttle antenna viewing angle, or by communication performance parameters such as receiver sensitivity or antenna gain. The practical operating elevation angle for most ground stations is about 5^{o}. For ground stations located in very flat areas with no ground obstructions such as trees or mountains, it may be possible to operate at or near 0^{o} elevation angle. For most stations the radius of operation is the great arc circle distance to the sub-shuttle point for a 5^{o} ground station elevation angle. The Shuttle-Ground Station geometry is illustrated in Figure 5-5.

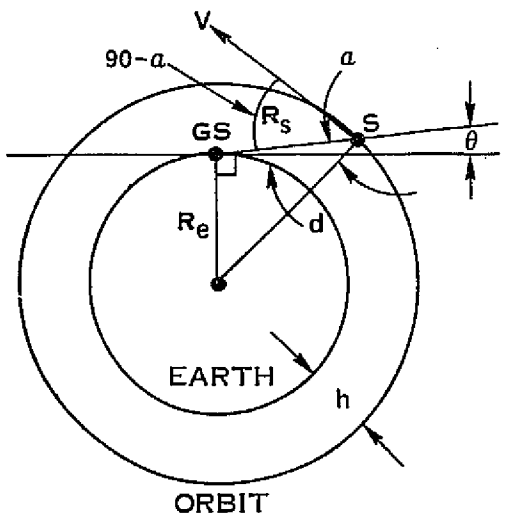

S = SHUTTLE
GS = GROUND STATION
R_e = EARTH RADIUS = 6374 km
h = SHUTTLE ALTITUDE
θ = ELEVATION ANGLE
a = MWCE ANTENNA VIEWING ANGLE
R_s = SLANT RANGE
d = ARC DISTANCE TO SUB-SHUTTLE POINT ON EARTH'S SURFACE

Figure 5-5. Satellite-Ground Station Geometry

For a given ground station elevation angle the MWCE antenna view angle from Figure 5-5 can be expressed as

$$\alpha = \sin^{-1}\left[\frac{R_e}{R_e + h}\left(\cos\theta\right)\right] \tag{1}$$

where

α is the MWCE antenna view angle from nadir

R_e is the earth's radius = 6374KM

h is the Shuttle altitude

θ is the ground station elevation angle.

The slant range one-way communication distance between the shuttle and the ground station is

$$R_s = \frac{\cos(\theta + \alpha)}{\cos\theta}(R_e + h) \tag{2}$$

where R_s is the slant range distance between the shuttle and the ground station. The great-arc distance between the ground station and the sub-shuttle point is

$$d = \frac{\pi R_e}{180}(90 - \theta - \alpha) \tag{3}$$

and the radius of operation r, is given by

$$\gamma = d(\theta_{MAX}) \tag{4}$$

The radius of operation and the MWCE antenna view angle from NADIR are given in Table 5-1 for various values of the maximum ground station elevation angle. Also, the same results are presented in graphical form in Figures 5-6 and 5-7.

Table 5-1. Radius of Operation and Total Link Margin for Various Ground Station Elevation Angles*

ELEVATION ANGLE (°)	ANTENNA VIEW ANGLE FROM NADIR (°)	REQUIRED S/N (dB)	RECEIVED S/N (dB)	MARGIN (dB)	RADIUS OF OPERATION (km)
5	69.6	15.7	29.5	13.8	1713 (925 nm)
10	67.9	15.7	34.0	18.3	1344 (726 nm)
20	62.2	15.7	38.5	22.8	873 (471 nm)
30	54.6	15.7	41.3	25.5	603 (326 nm)
40	46.1	15.7	43.3	27.6	431 (233 nm)
45	41.7	15.7	44.1	28.4	366 (198 nm)

* ORBIT: 400 KM, 57° INCLINATION

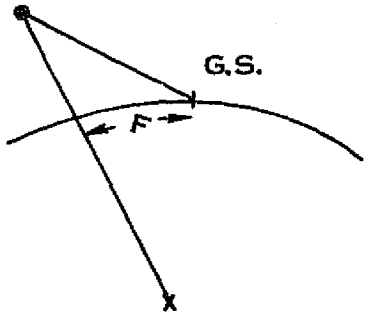

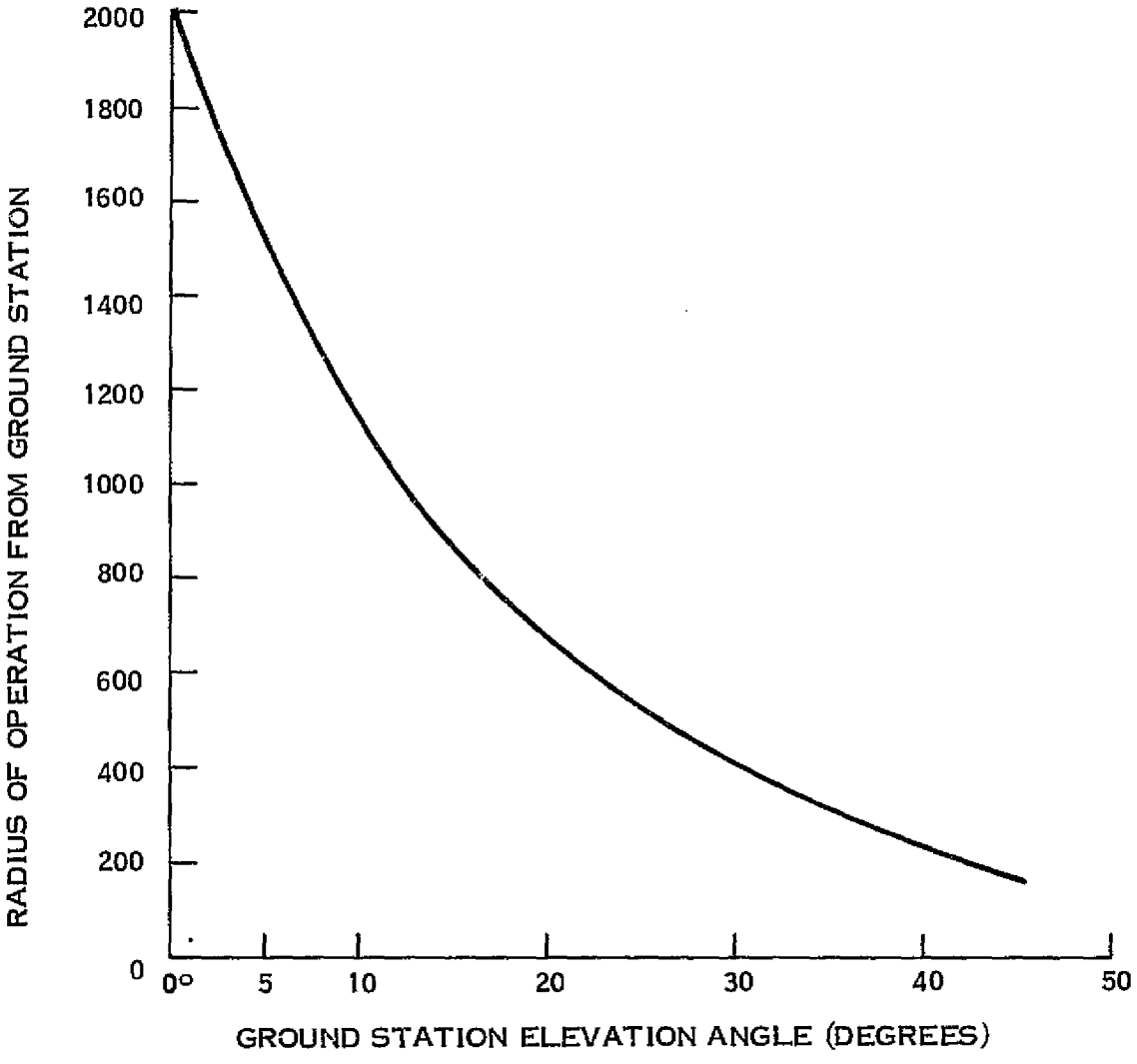

Figure 5-6. MWCE Maximum Radius of Operation as a Function of Ground Station Elevation Angle

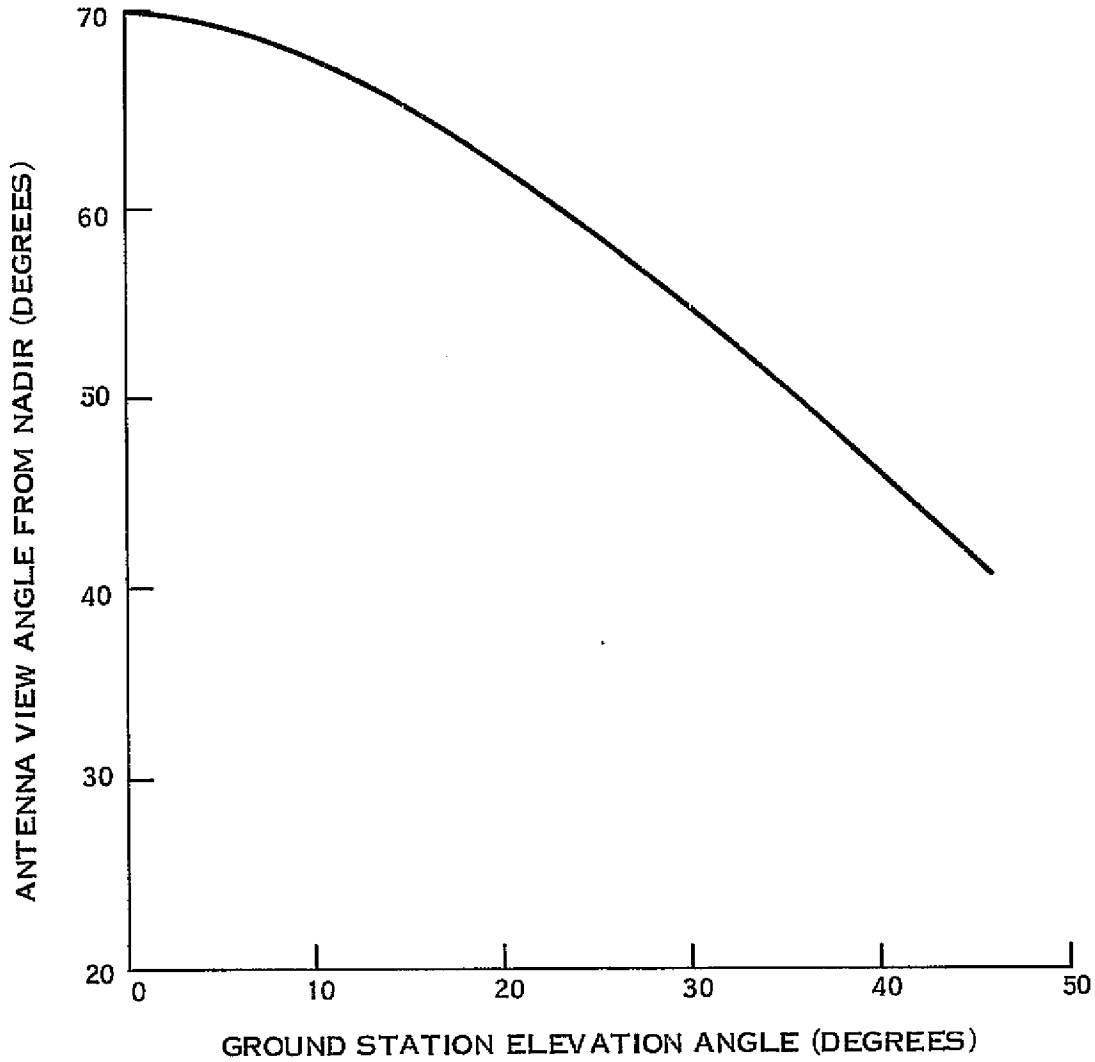

Figure 5-7. MWCE Antenna View Angle from NADIR as a Function of Ground Station Elevation Angle

The extent of the radii of operation for the Rosman, N.C. and Austin, Texas ground stations is illustrated in Figure 5-8. The radii of operation, corresponding to a 5^{o} elevation angle (1713 km), were drawn around the both ground stations and a radius of operation, corresponding to a 20^{o} elevation angle (873 km), was drawn around the Rosman, N.C. facility. The CONUS shown in the figure as well as the longitudinal and latitudinal scales are MERCATUR projections of their actual spherical shapes.

The cross-hatched lines represent the orbital paths of the Shuttle for a 400 km orbit with a 57^{o} inclination traced over a full, six day period. Approximately 94 orbits are traced in a six day mission with an orbitral period 92.65 minutes. The numbers at the bottom of Figure 5-8 correspond to the sequential orbit number of the trace. The operational time for a particular ground station represents the total orbital time within the radius of operation of the ground station, that is, the sum of all of the orbit trace times within the radius of operation. The operation time is determined by first computing the great arc circle length of each orbital trace of interest.

The calculation of the great arc circle length is illustrated in Figure 5-9. The points A and B are the intersection points of the orbital trace and the radius of operation and $\hat{p}$ is the great circle arc distance between the intersection points. The coordinates of A are given by λ_a and η_A and those of B are given by λ_B and η_B. The terms $\hat{a}$ and $\hat{b}$ are minor arcs of a great circle and together A, B and point P, the North Pole, form a spherical triangle. The great-circle arc distance is given by

$$\hat{p} = \cos^{-1} \left[\cos \hat{a} \cos \hat{b} \times \sin \hat{a} \sin \hat{b} \cos \hat{P}\right] \tag{5}$$

where

$$\hat{a} = \pi/2 - \lambda_A \tag{6}$$

$$\hat{b} = \pi/2 - \lambda_B \tag{7}$$

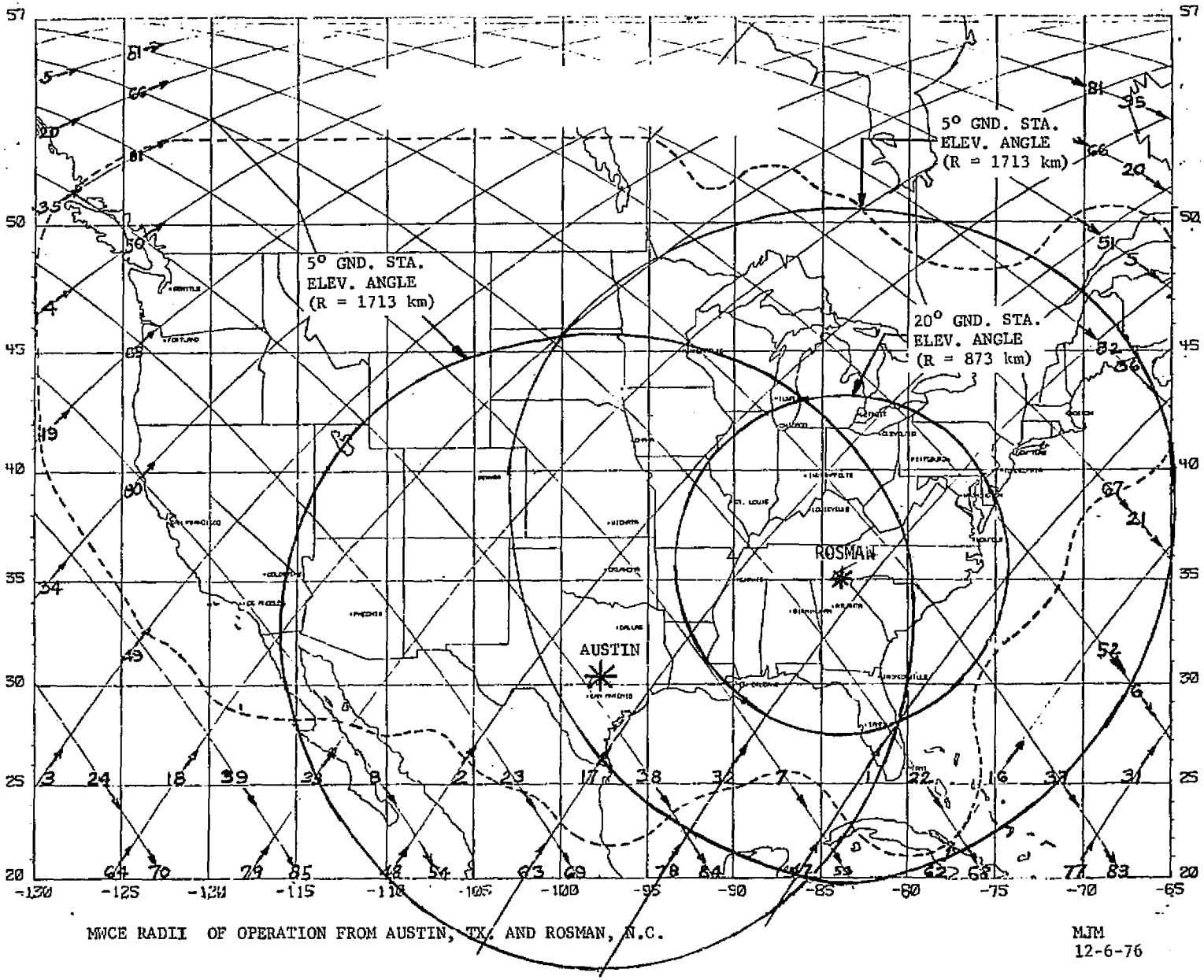

Figure 5-8. MWCE Radii of Operation from Austin, TX. and Rosman, N. C.

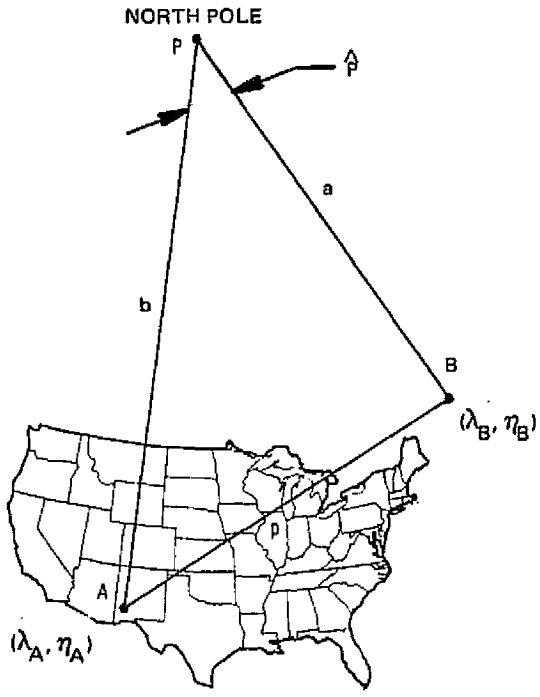

Figure 5-9. Spherical Geometry for Computation of Orbital Trace Time

and

$$\hat{p} = \left| \eta_B - \eta_A \right| \tag{8}$$

The operational time corresponding to the great-circle arc length $\hat{p}$ is

$$t = \frac{\hat{p}}{\pi} T \tag{9}$$

where

t is the operational time

$\hat{p}$ is the arc length in radians

and

T is the orbital period

The total operation times for the Rosman N. C. Facility for a 20^{o} and a 5^{o} ground station elevation angles is presented in Tables 5-2 and 5-3, respectively. It can be seen that the operation time increases considerably when going from a 20^{o} elevation angle (873 km) to a 5^{o} elevation angle (1713 km). The operating time over Austin, Texas is shown in Table 5-4 and is slightly less than the operating time over Rosman, N. C. The operating time for a given elevation angle should not vary widely with respect to the particular ground station location. The operating time using both ground stations is presented in Table 5-5.

5.4.2 COMMUNICATION PERFORMANCE ANALYSIS

Of the three modes of operation the transponder mode of operation for QPSK represents the worst-case operation in terms of overall link performance; consequently, only this case will be analyzed. It was assumed that a bit error rate (BER) of 10^{-5} was the desired probability of error performance. The required bit energy to noise density ratio to obtain a 10^{-5} BER for ideal QPSK detection is 9.6 dB. Since there are two bits of information for every QPSK symbol, the ideal detection signal-to-noise ratio for QPSK is given by adding 3.0 dB to the required E_b/N_o ratio. From General Electric's experience in the design, testing, and simulation of QPSK modems, it is known that the ideal performance is not difficult to achieve. Due to the practical implementation of QPSK detection and non-linear amplification there is a difference between the actual versus the ideal BER performance. It has been found that there is a 3.1 dB difference between actual and ideal BER performance. Some of the causes for this "digital demodulation loss" are intersymbol interference, carrier recovery phase errors, non-linearities in the MWCE/Shuttle TWTA, sampling jitter noise, etc. Thus, the total signal-to-noise ratio needed at the input to the detector is 15.7 dB and the results are presented in Table 5-6.

All of the equations needed to determine the system performance will now be derived. The actual received signal-to-noise ratio is determined by combining the noise contributions produced by the up-link transmission and reception in the shuttle and by the

Table 5-2. MWCE Operating Time Over Rosman, N.C. for 20° Ground Station Elevation Angle

DAY 1		DAY 2		DAY 3		DAY 4		DAY 5		DAY 6	
ORBIT	TIME (MIN.)	ORBIT	TIME (MIN.)	ORBIT	TIME (MIN.)	ORBIT	TIME (MIN.)	ORBIT	TIME (MIN.)	ORBIT	TIME (MIN.)
1	2.2	17	3.3	37	3.8	52	1.9	68	3.8	83	3.8
6	1.9	22	3.8	47	2.2	63	3.3	78	3.9		
		32	3.9								
TOTAL	4.1		11.0		6.0		5.2		7.7		3.8

SIX DAY TOTAL: 37.8 MINUTES

ORBIT: 400 KM, 57° INCLINATION

Table 5-3. MWCE Operating Time Over Rosman, N.C. for 5° Ground Station Elevation Angle

DAY 1		DAY 2		DAY 3		DAY 4		DAY 5		DAY 6	
ORBIT	TIME (MIN.)	ORBIT	TIME (MIN.)	ORBIT	TIME (MIN.)	ORBIT	TIME (MIN.)	ORBIT	TIME (MIN.)	ORBIT	TIME (MIN.)
1	7.5	16	4.9	33	5.0	48	6.7	64	1.3	79	5.0
2	6.7	17	7.5	36	2.8	52	7.0	67	5.4	82	2.8
6	7.0	18	1.3	37	7.8	53	6.8	68	8.0	83	7.8
7	6.8	21	5.4	38	3.5	62	4.9	78	8.0	84	3.5
		22	8.0	47	7.5	63	7.5				
		32	8.0								
TOTAL	28.0		35.1		26.6		32.9		22.7		19.1

SIX DAY TOTAL: 164.4 MINUTES

ORBIT: 400 KM, 57° INCLINATION

Table 5-4. MWCE Operating Time Over Austin, TX. for 5^{o} Ground Station Elevation Angle

DAY 1		DAY 2		DAY 3		DAY 4		DAY 5		DAY 6	
ORBIT	TIME (MIN.)	ORBIT	TIME (MIN.)	ORBIT	TIME (MIN.)	ORBIT	TIME (MIN.)	ORBIT	TIME (MIN.)	ORBIT	TIME (MIN.)
1	3.0	17	7.8	32	6.9	48	7.8	64	4.7	79	6.8
2	7.8	18	4.7	33	6.8	53	7.7	68	6.2	83	3.6
7	7.7	22	6.2	37	3.6	54	4.6	69	7.2	84	8.0
8	4.6	23	7.2	38 47	8.0 3.0	63	7.8	78	6.9		
TOTAL	23.1		25.9		28.3		27.9		25.0		18.4

SIX DAY TOTAL: 148.6 MINUTES

ORBIT: 400 KM, 57^{o} INCLINATION

Table 5-5. MWCE Two-Station Operating Time Over Austin, TX. - Rosman, N. C. for 5° Ground Station Elevation Angle

DAY 1		DAY 2		DAY 3		DAY 4		DAY 5		DAY 6	
ORBIT	TIME (MIN.)	ORBIT	TIME (MIN.)	ORBIT	TIME (MIN.)	ORBIT	TIME (MIN.)	ORBIT	TIME (MIN.)	ORBIT	TIME (MIN.)
1	8.1	16	4.9	33	9.0	48	10.2	64	5.9	79	9.0
2	10.2	17	10.8	36	2.8	52	7.0	67	5.4	82	2.8
6	7.0	18	5.9	37	7.8	53	8.2	68	8.0	83	7.8
7	8.2	21	5.4	38	8.0	54	4.6	69	7.2	84	8.0
8	4.6	22	8.0	47	8.1	62	4.9	78	9.8		
		23	7.2			63	10.8				
		32	9.8								
TOTAL	38.1		52.0		35.7		45.7		36.3		27.6

SIX DAY TOTAL: 235.4 MINUTES

ORBIT: 400 KM, 57° INCLINATION

Table 5-6. Transponder Mode of Operation

SIGNAL-TO-NOISE RATIO

REQUIRED FOR BER = 10^{-5}

(TOTAL LINK)

REQUIRED E_b/N_o (IDEAL)	=	9.6 dB
CONVERSION TO QPSK*	=	3.0 dB
DIGITAL DEMODULATION LOSS**	=	3.1 dB
		15.7 dB

* NUMBER OF BITS/SYMBOL

** INTERSYMBOL INTERFERENCE, CARRIER RECOVERY PHASE ERRORS, SAMPLING JITTER NOISE, MODULATOR AMPLITUDE IMBALANCE, ETC.

down-link shuttle transmission and ground station reception. The total received signal-to-noise ratio for the transponder mode of operation is given by

$$(S/N)_{TOTAL} = \frac{S}{N_{UPLINK} + N_{DOWNLINK}} \tag{10}$$

or

$$(S/N) = \frac{1}{1/(S/N)_{UPLINK} + 1/(S/N)_{DOWNLINK}} \tag{11}$$

The uplink signal-to-noise ratio is given by

$$(S/N)_{UPLINK} = (EIRP)_E - L_T + (G/T)_{S/C} - BW - N_o \tag{12}$$

where

$(EIRP)_E$ is the effective isotropic radiated power of the ground station

L_T is the total path loss for the up-link transmission

$(G/T)_{S/C}$ is the ratio of the gain of the MWCE spacecraft antenna to the noise temperature of the MWCE receiver

BW is the received signal bandwidth

N_o is the thermal background noise power density for unit temperature.

Similarly, the downlink signal-to-noise ratio is given by

$$(S/N)_{DOWNLINK} = (EIRP)_{S/C} - L_T + (G/T)_E - BW - N_o \tag{13}$$

where

$(EIRP)_{S/C}$ is the effective isotropic radiated power of the MWCE on-board the spacecraft

L_T is the total path loss for the downlink transmission

$(G/T)_E$ is the ratio of the ground station antenna gain to the noise temperature of the ground station receiver.

The total path loss is the sum of four components and is given as

$$L_T = L_f + L_p + L_A + L_{po} \tag{14}$$

where

L_f is the free-space loss

L_{po} is the pointing loss and is caused by the transmit and receive antennas not being pointed on boresight

L_p is the polarization loss due to polarization alignment mismatches between the receive and transmit antennas

L_A is the atmospheric loss due to oxygen and water vapor absorption

An empirical formula[3] for the atmospheric loss is

$$L_A\,(20\ \text{GHz}, \theta) = .71\,(.6)/\sin\theta \tag{15}$$

$$L_A\,(30\ \text{GHz}, \theta) = .71\,(.45)/\sin\theta \tag{16}$$

where θ is the elevation angle.

The effective isotropic radiated power is given by

$$(\text{EIRP}) = G - L_\ell - P_T \tag{17}$$

where

G is the antenna gain referred to an isotropic antenna

L_ℓ is the total line loss between the transmitter and the antenna

P_T is the total transmitted signal power.

The total system noise temperature of a receiver is

$$T_S = T_a + T_o (L_\ell - 1) + L_\ell \, T_o (NF-1) \qquad (18)$$

where

T_a is the antenna temperature.

T_S is the total receiver system noise temperature referred to the input antennas terminals

T_o is the standard noise reference temperature = 290^oK

L_ℓ is the total line loss between the antenna and the receiver

NF is the noise figure of the receiver.

The uplink and downlink transmission parameters employed in the analysis are presented in Figures 5-10 and 5-11. The transmitter powers, the antennas, and the receiver noise figures employed were the same parameters recommended in a previous report (Reference 3). The total line losses employed represent worst-case values. The EIRP's and (G/T)'s of the transmitter and receiver systems is also indicated. The complete system performance calculations for the transponder mode for ground station elevation angle of 45^o, 20^o, and 5^o is presented in Tables 5-7, 5-8 and 5-9 respectively. The complete system performance summary is given in Table 5-1.

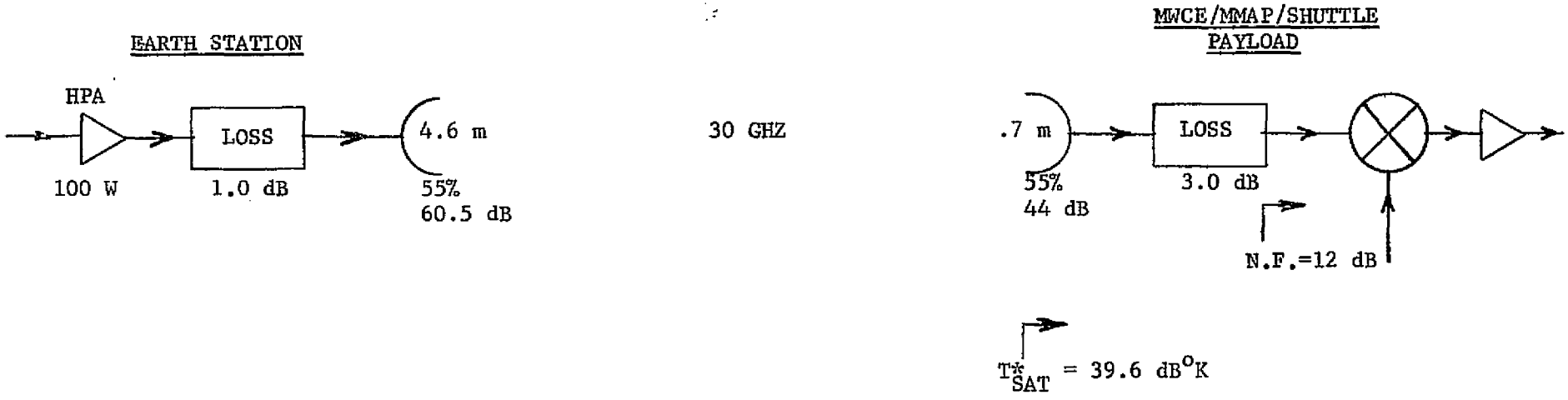

$(EIRP)_E$ = 78.5 dBW

$L_T = L_f + L_p + L_A + L_{po}$

L_T = TOTAL LOSS

L_f = FREE SPACE LOSS

L_{po} = POINTING LOSS

L_p = POLARIZATION LOSS

L_A = ATMOSPHERIC LOSS

$(G/T)_{SAT}$ = 4.4 dB/°K

$$(S/N)_{UPLINK} = (EIRP)_E - L_T + (G/T)_{S/C} - BW - N_o$$

* INCLUDES LINE LOSS

Figure 5-10. Uplink Transmission Parameters

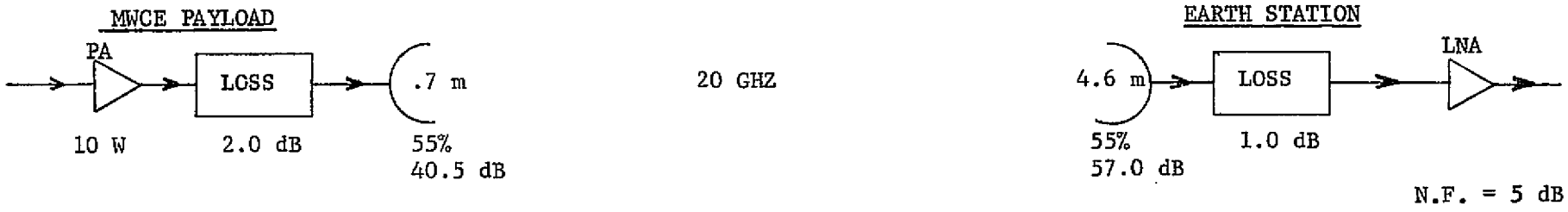

$T_E^* = 29.5\ dB^oK$

$$L_T = L_f + L_p + L_A + L_{po}$$

$(EIRP)_{S/C} = 48.5\ dBW$

$(G/T)_E = 27.5\ dB/^oK$

$$(S/N)_{DOWNLINK} = (EIRP)_{S/C} - L_T + (G/T)_E - BW - N_o$$

Figure 5-11. Downlink Transmission Parameters

Table 5-7. 30 GHz Uplink Budget for a 45° Elevation Angle

EARTH STATION TRANSMITTER POWER (dBW)	20.0
EARTH STATION RF LOSSES (dB)	2.0
EARTH STATION ANTENNA GAIN (dBi)	60.5
EARTH STATION EIRP (dBW)	78.5
LOSSES	
FREE SPACE LOSS (dB)	176.8
POLARIZATION (dB)	.5
ATMOSPHERIC (dB)	.5
POINTING LOSS (TX ANT.) (dB)	.5
TOTAL LOSSES (dB)	178.3
SATELLITE RECEIVE SYSTEM G/T* (dB/°K)	4.4
SIGNAL BANDWIDTH (dB-Hz)	84.0
BOLTZMAN'S CONSTANT (dBW/Hz-°K)	-228.6
C/N UPLINK TOTAL (dB)	49.3

$T_{SAT} = T_a + T_o (L_\ell - 1) + L_\ell T_o (NF - 1)$
$T_{SAT} = 290^o + 290^o (1) + (2) (290^o) (14.8)$
$T_{SAT} = 9192^oK = 39.6\ dB^oK$
*INCLUDES LINK LOSS

Table 5-7. 20 GHz Downlink Budget for a 45° Elevation Angle (Cont'd)

TRANSMITTER POWER (dBW)	10.0
RF LOSSES (dB)	2.0
ANTENNA GAIN (dBi)	40.5
EIRP (dBW)	48.5
LOSSES	
FREE SPACE LOSS (dB)	173.3
POLARIZATION (dB)	.5
ATMOSPHERIC (dB)	.6
POINTING LOSS (dB)	.5
TOTAL LOSSES (dB)	174.9
EARTH STATION RECEIVE SYSTEM G/T* (dB/°K)	29.5
SIGNAL BANDWIDTH (dB-Hz)	84.0
BOLTZMAN'S CONSTANT (dBW/H_z-°K)	-228.6
C/N DOWNLINK TOTAL (dB)	45.7
C/N UPLINK (dB)	49.3
C/N TOTAL (UP LINK + DOWN LINK) (dB)	44.1

$T_E = T_a + T_o (L_\ell - 1) + L_\ell T_o (NF - 1)$
$T_E = 35°K + 290° (.26) + 290° (1.26) (2.16)$
$T_E = 900°K = 29.5$ dB°K
*INCLUDES LINE LOSS

Table 5-8. 30 GHz Uplink Budget for a 20° Elevation Angle

EARTH STATION TRANSMITTER POWER (dBW)	20.0
EARTH STATION RF LOSSES (dB)	2.0
EARTH STATION ANTENNA GAIN (dBi)	60.5
EARTH STATION EIRP (dBW)	78.5
LOSSES	
FREE SPACE LOSS (dB)	181.8
POLARIZATION (dB)	.5
ATMOSPHERIC (dB)	.9
POINTING LOSS (TX ANT.) (dB)	.5
TOTAL LOSSES (dB)	183.7
SATELLITE RECEIVE SYSTEM G/T* (dB/°K)	4.4
SIGNAL BANDWIDTH (dB-Hz)	84.0
BOLTZMAN'S CONSTANT (dBW/Hz-°K)	-228.6
C/N UPLINK TOTAL (dB)	43.8

$T_{SAT} = T_a + T_o (L_\ell - 1) + L_\ell T_o (NF - 1)$
$T_{SAT} = 290^o + 290^o (1) + (2) (290^o) (14.8)$
$T_{SAT} = 9192^oK = 39.6\ dB^oK$
*INCLUDES LINE LOSS

Table 5-8. 20 GHz Downlink Budget for a 20° Elevation Angle (Cont'd)

TRANSMITTER POWER (dBW)	10.0
RF LOSSES (dB)	2.0
ANTENNA GAIN (dBi)	40.5
EIRP (dBW)	48.5
LOSSES	
FREE SPACE LOSS (dB)	178.3
POLARIZATION (dB)	.5
ATMOSPHERIC (dB)	1.3
POINTING LOSS (dB)	.5
TOTAL LOSSES (dB)	180.6
EARTH STATION RECEIVE SYSTEM G/T* (dB/°K)	29.5
SIGNAL BANDWIDTH (dB-Hz)	84.0
BOLTZMAN'S CONSTANT (dBW/H_z-°K)	-228.6
C/N DOWNLINK TOTAL (dB)	40.0
C/N UPLINK (dB)	43.8
C/N TOTAL (UP LINK + DOWN LINK) (dB)	38.5

$T_E = T_A + T_o (L_\ell - 1) + L_\ell T_o (NF-1)$
$T_E = 35°K + 290° (.26) + 290° (1.26) (2.16)$
$T_E = 900°K = 29.5\ dB°K$
*INCLUDES LINE LOSS

Table 5-9. 30 GHz Uplink Budget for a 5° Elevation Angle

EARTH STATION TRANSMITTER POWER (dBW)	20.0
EARTH STATION RF LOSSES (dB)	2.0
EARTH STATION ANTENNA GAIN (dBi)	60.5
EARTH STATION EIRP (dBW)	78.5
LOSSES	
FREE SPACE LOSS (dB)	187.2
POLARIZATION (dB)	.5
ATMOSPHERIC (dB)	3.7
POINTING LOSS (TX ANT.) (dB)	.5
TOTAL LOSSES (dB)	191.9
SATELLITE RECEIVE SYSTEM G/T* (dB/°K)	4.4
SIGNAL BANDWIDTH (dB-Hz)	84.0
BOLTZMAN'S CONSTANT (dBW/Hz-°K)	-228.6
C/N UPLINK TOTAL (dB)	35.6

$T_{SAT} = T_a + T_o (L\ell - 1) + L\ell\ T_o(NF-1)$
$T_{SAT} = 290^o + 290^o (1) + (2) (290^o) (1.8)$
$T_{SAT} = 9192^oK = 39.6\ dB^oK$
*INCLUDES LINE LOSS

Table 5-9. 20 GHz Downlink Budget for a 5° Elevation Angle (Cont'd)

TRANSMITTER POWER (dBW)	10.0
RF LOSSES (dB)	2.0
ANTENNA GAIN (dBi)	40.5
EIRP (dBW)	48.5
LOSSES	
FREE SPACE LOSS (dB)	183.7
POLARIZATION (dB)	.5
ATMOSPHERIC (dB)	4.9
POINTING LOSS (dB)	.5
TOTAL LOSSES (dB)	189.6
EARTH STATION RECEIVE SYSTEM G/T* (dB/°K)	29.5
SIGNAL BANDWIDTH (dB-Hz)	84.0
BOLTZMAN'S CONSTANT (dBW/H_Z-°K)	-228.6
C/N DOWNLINK TOTAL (dB)	31.0
C/N UPLINK (dB)	35.6
C/N TOTAL (UP LINK + DOWN LINK) (dB)	29.5

$T_E = T_a + T_o (L_\ell - 1) + L_\ell T_o (NF-1)$
$T_E = 35°K + 290° (.26) + 290° (1.26) (2.16)$
$T_E = 900°K = 29.5\ dB°K$
*INCLUDES LINE LOSS

5.5 MWCE-MOD II INSTRUMENT DESCRIPTION

This configuration, a simplified version of MWCE-MOD I, is designated as the MWCE-MOD II. It is characterized by a non-steerable and non-deployable fixed set of antennas and a single wideband transponder, switchable to either RHCP or LHCP. The flexibility of the three operational modes is retained along with all essential features of the system design and hardware complement. The MWCE-MOD II is considered a cost-effective approach to meeting the Shuttle experiment objectives.

Figure 5-12 illustrates the MWCE-MOD II modes of operation and may be related to Figure 5-1 for MOD I.

A summary of the principal measurement parameters is given below:

1. Transponder Mode (RHCP and LHCP)
   a. BER tests on Mbps versus elevation angle on RHCP
   b. BER tests on 50 Mbps versus elevation angle on LHCP
   c. Signal strength measurements, 30 GHz uplink
   d. Signal strength measurements, 20 GHz downlink
   e. Digital/Analog video transmission quality
2. Module Mode (RHCP and LHCP)
   a. BER on uplink data in conjunction with transponder mode BER tests at ground station on same data versus elevation angle
   b. Uplink BER tests on 30 GHz link versus elevation angle
   c. Downlink BER tests on 20 GHz link versus elevation angle
   d. Signal strength measurement, 30 GHz uplink
   e. Optional downlink digital video versus analog video quality tests
3. Beacon Mode (RHCP and LHCP)
   a. Attenuation and depolarization caused by rain
   b. Low elevation effects caused by the atmosphere

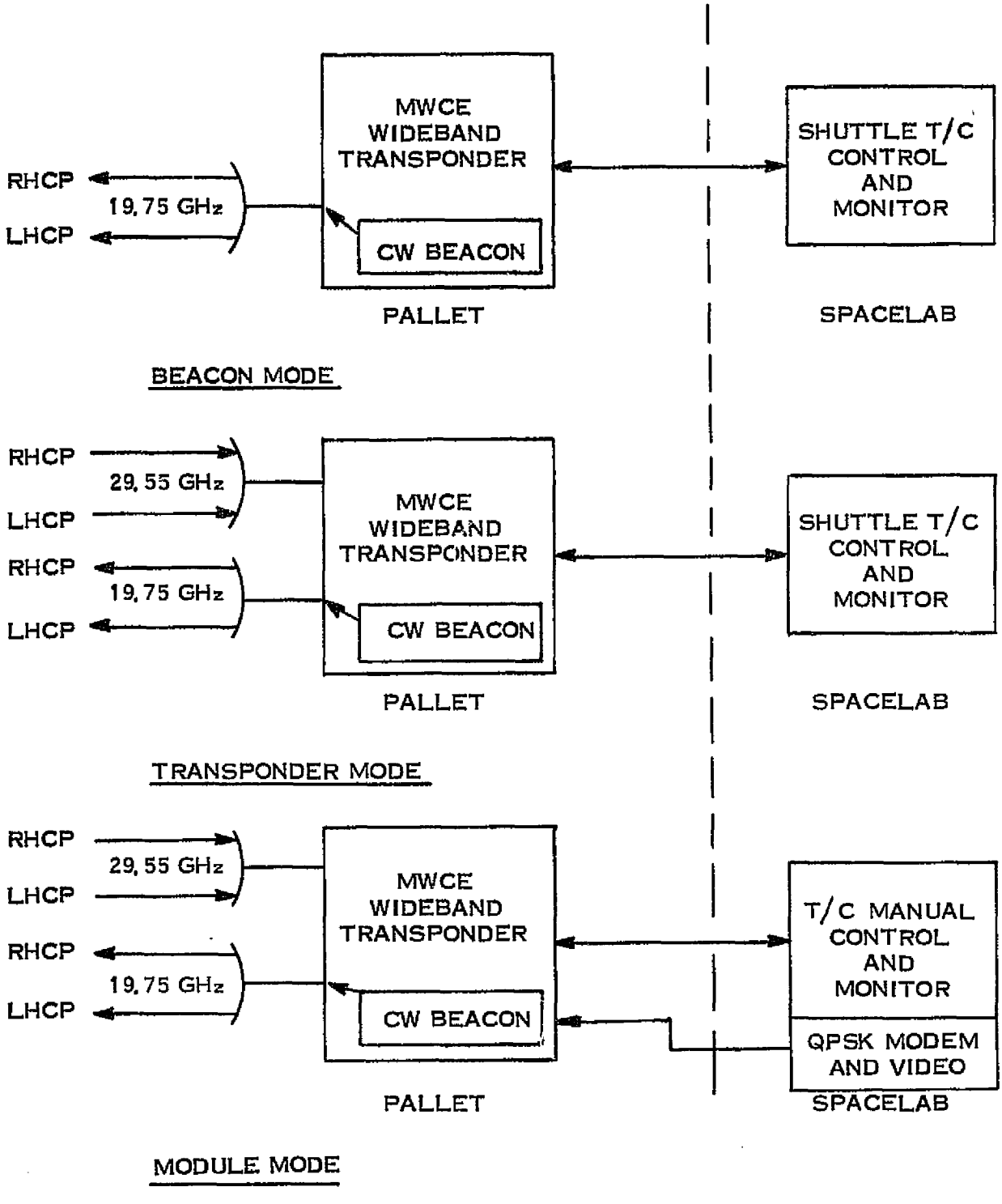

Figure 5-12. MWCE-MOD II Modes of Operation

5.5.1 LINK REQUIREMENTS

Communications Link

The following requirements have been established for this phase of the communication experiment:

1. Data Rate, 50 Mbps
2. BER, 1×10^{-5}
3. Margin, 10 dB
4. Transponder bandwidth capability, 500 MHz minimum

Assuming a 3 dB demodulation loss, the required signal-to-noise ratio in a bandwidth equal to the bit rate is 22.7 dB including the 10 dB margin. This amounts to a total signal-to-noise density ratio of $C/N_0 = 99.7$ dB-Hz.

Using the above requirements, a 400 km orbiting Shuttle and realizable models of the up-link and downlink equipment, an analysis was performed to determine the minimum 30 GHz and 20 GHz Spacelab antenna gain pattern required for the experiment. This analysis is included in Appendix B. Figure 5-13 summarizes the results.

The gain pattern shown, though not physically realizable with a single passive antenna, can be achieved using beam steering or beam switching techniques.

Beacon Link

The downlink beacon will operate in two modes – the normal/tracking mode and the acquisition/propagation mode. In the acquisition/propagation mode, the beacon will utilize the full power of the transmitter, and the communication signal will be turned off. Since this is a one-way uplink only, the signal-to-noise density available on the ground will be slightly greater than that available for the communication signal through the transponder, or in the order of $CN_0 \approx 100$ dB-Hz. The high signal levels available in this mode will be utilized for initial acquisition at low elevation angles, and for propagation studies at low elevation angles and during adverse weather conditions.

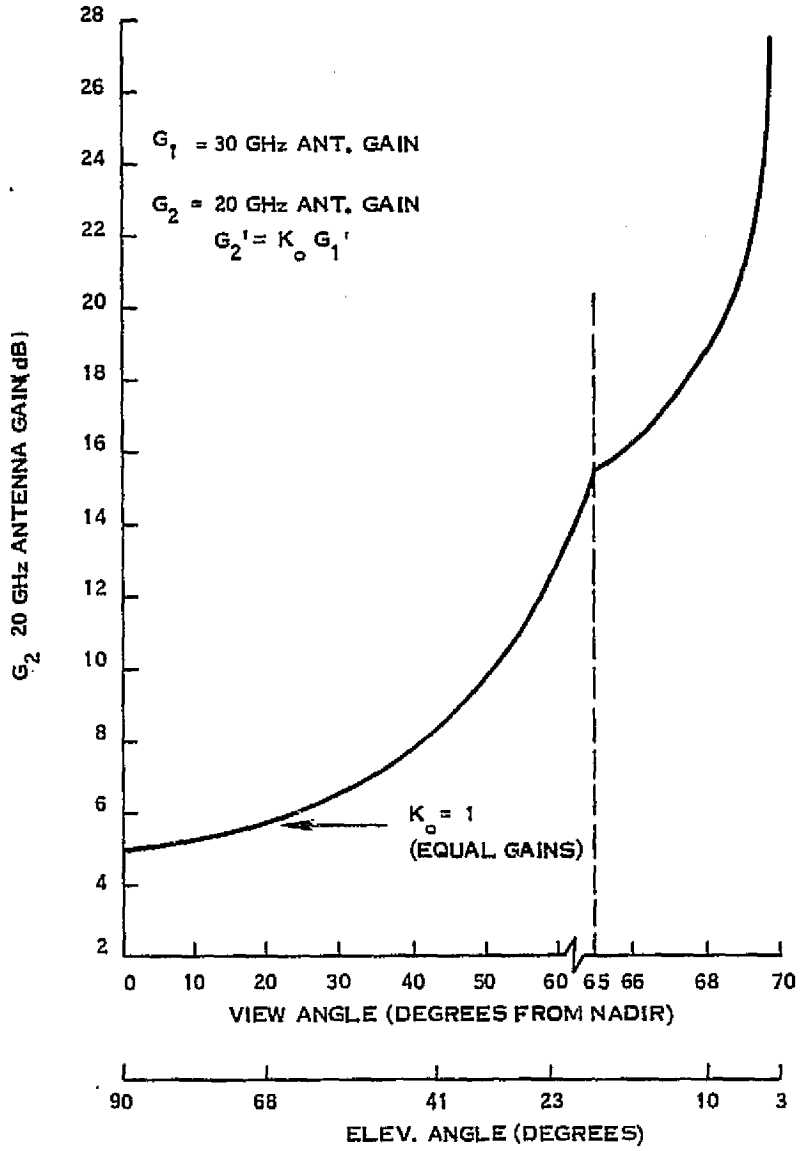

Figure 5-13. MWCE-MOD II Antenna Gain Requirements for Two-Way Transmission Link

The normal/tracking mode of beacon operation will occur simultaneously with the communication experiment and will share the transmitter power with the communications signals. The available signal level will be 20 dB less in this mode, for a nominal C/N_O = 80 dB-Hz at the ground station.

Table 5-10 summarizes the downlink beacon capabilities.

Table 5-10. Beacon Link Summary

Parameter	Acquisition Propagation Mode		Normal/ Tracking
	Acquisition	Propagation	
C/N_O Available	100 dB-Hz	100 dB-Hz	80 dB-Hz
Bandwidth	50 dB-Hz	30 dB-Hz	30 dB-Hz
Threshold SNR	10 dB	10 dB	10 dB
Acquisition Fade Margin	40 dB		
Operational Fade Margin		60 dB	40 dB

The data in the table above applies to a pilot phase lock receiver for signal acquisition. The 1 kiloHertz tracking bandwidth refers to a second order loop and offers margin in tracking a maximum rate of Doppler of 24 kHz/sec. The requirements for a monopulse antenna tracking receiver may require use of some of the fade margin listed above.

Frequency Plan

The proposed uplink frequency plan is shown in Figure 5-14. Both the uplink and downlink bands are based on currently assigned operational frequency allocation by the Federal Communications Commission. The specific band allocated by the FCC for Fixed Satellite, Earth-toSpace is 29.5 GHz to 30 GHz. A potential interference problem, however, exists in the second harmonic of the Shuttle TDRS Ku-band transmitter which is centered at 30.0068 GHz, as shown, The data rate of the Shuttle to TDRS signal can be anywhere from 1 kbps to 300 Mbps. At the high data rates, considerable second harmonic spillover into the MWCE channel can occur. To minimize the TDRS interference, the MWCE frequency plan was established as shown in Figure 5-14 where the 50 Mbps uplink data is spaced at the low

end of the band. Also, even though the intrinsic design of the MWCE transponder is wide-band to handle 500 MHz, the IF bandwidth for this experiment is specified at 200 MHz to prevent retransmission of the TDRS second harmonic. Further control of the TDRS interference can be imposed by the MWCE experiment in its requirement and specification of the Shuttle to TDRS data rate and time of transmission.

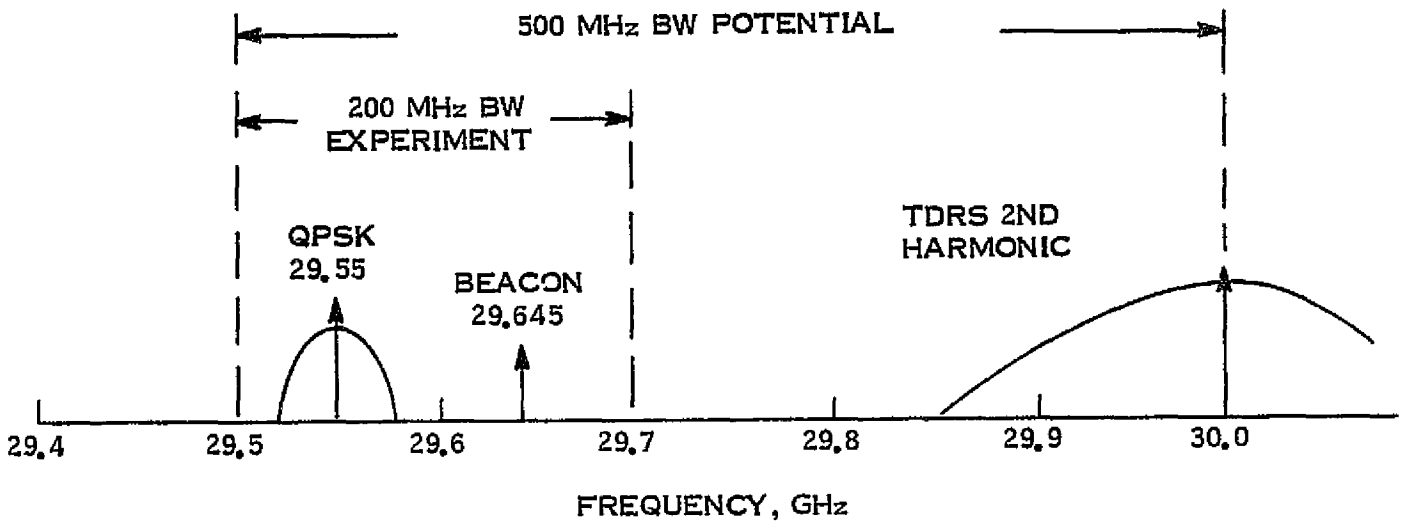

Figure 5-14. Uplink Frequency Plan

The uplink beacon signal, shown at 29,648 GHz, is transmitted when required for round trip propagation measurement, ground station Doppler compensation for bent-pipe data transmission, or for Space Shuttle beamswitching or steering.

The downlink frequency plan is shown in Figure 5-15. For the bent-pipe transponder mode of operation, it consists of the uplink signal translated 9.8 GHz down in frequency.

The downlink beacon signal is always present for ground station antenna tracking, as well as for propagation measurements.

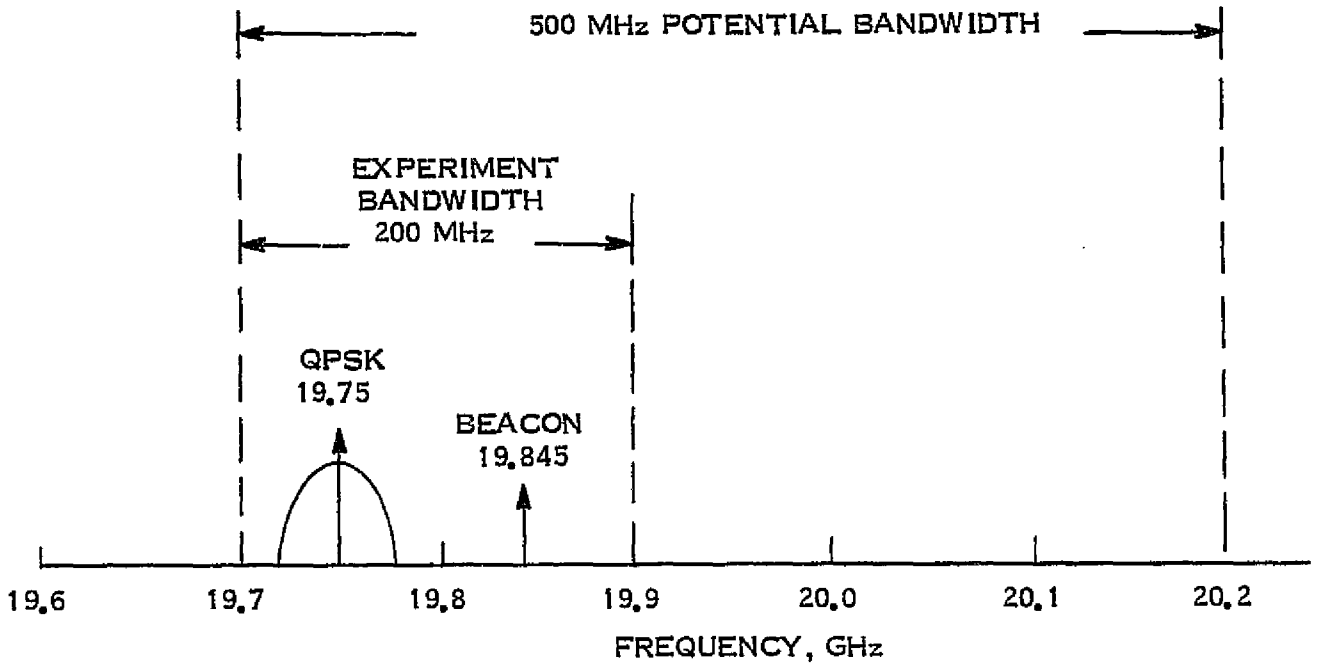

Figure 5-15. Downlink Frequency Plan

5.5.2 EXPERIMENT SYSTEM - ELECTRICAL DESIGN

Figures 5-16 and 5-17 show a block diagram of the MWCE-MOD II Shuttle equipment. The experiment operates in one of the three following modes:

1. Transponder mode
2. Module mode
3. Beacon mode

In the transponder mode, the uplink communication signal is received at 29.55 GHz and converted to an IF frequency of 1.375 GHz by means of a low noise image recovery mixer. The signal is then filtered, amplified and up-converted to the downlink frequency of 19.75 GHz. Finally, it is amplified to a level of 10 watts in a TWT amplifier.

The transponder signals will consist of wideband analog or digital signals and a beacon signal which is received from the ground station or is originated in the transponder.

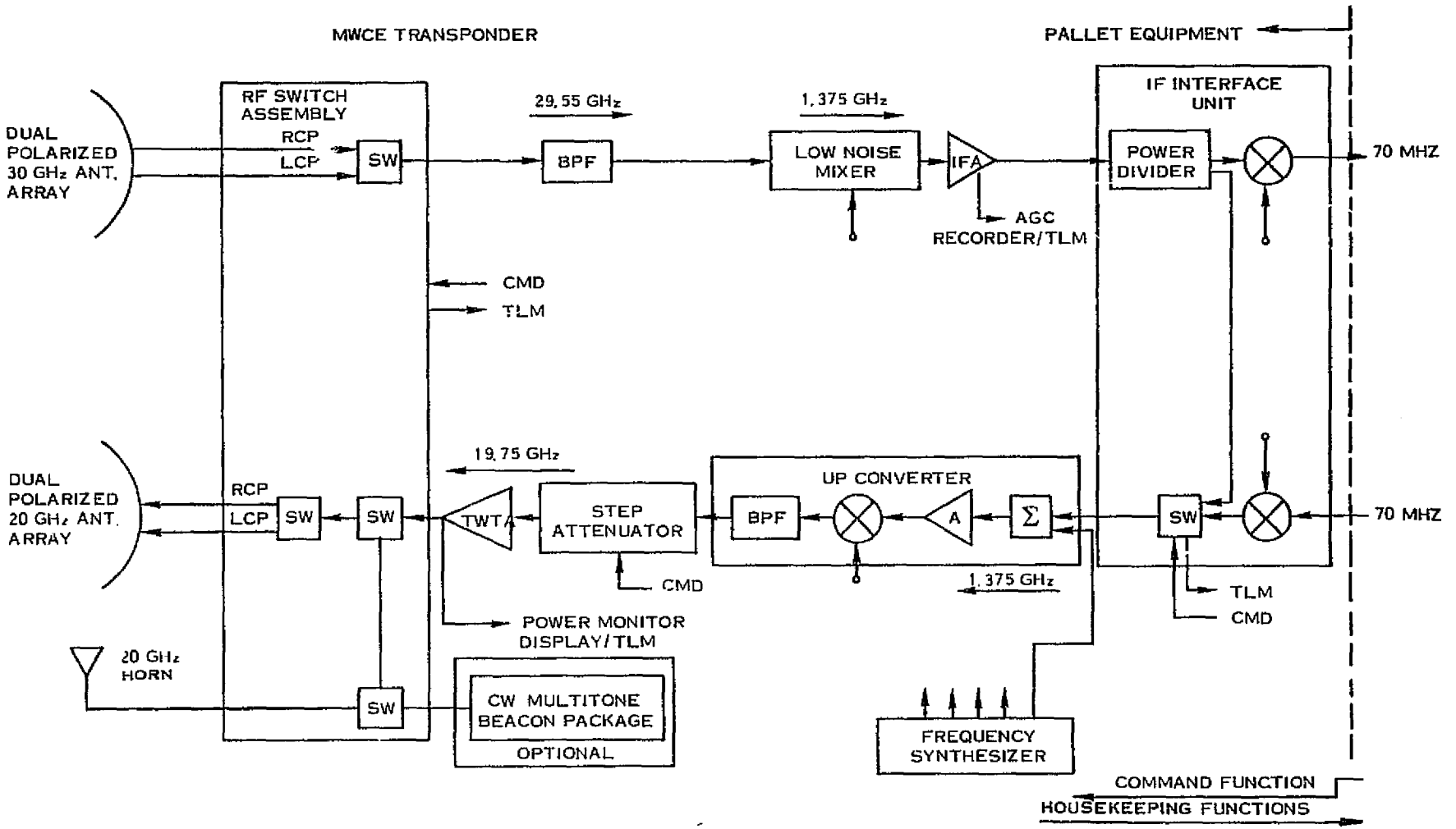

Figure 5-16. MWCE-MOD II Experiment Configuration (RF Portion)

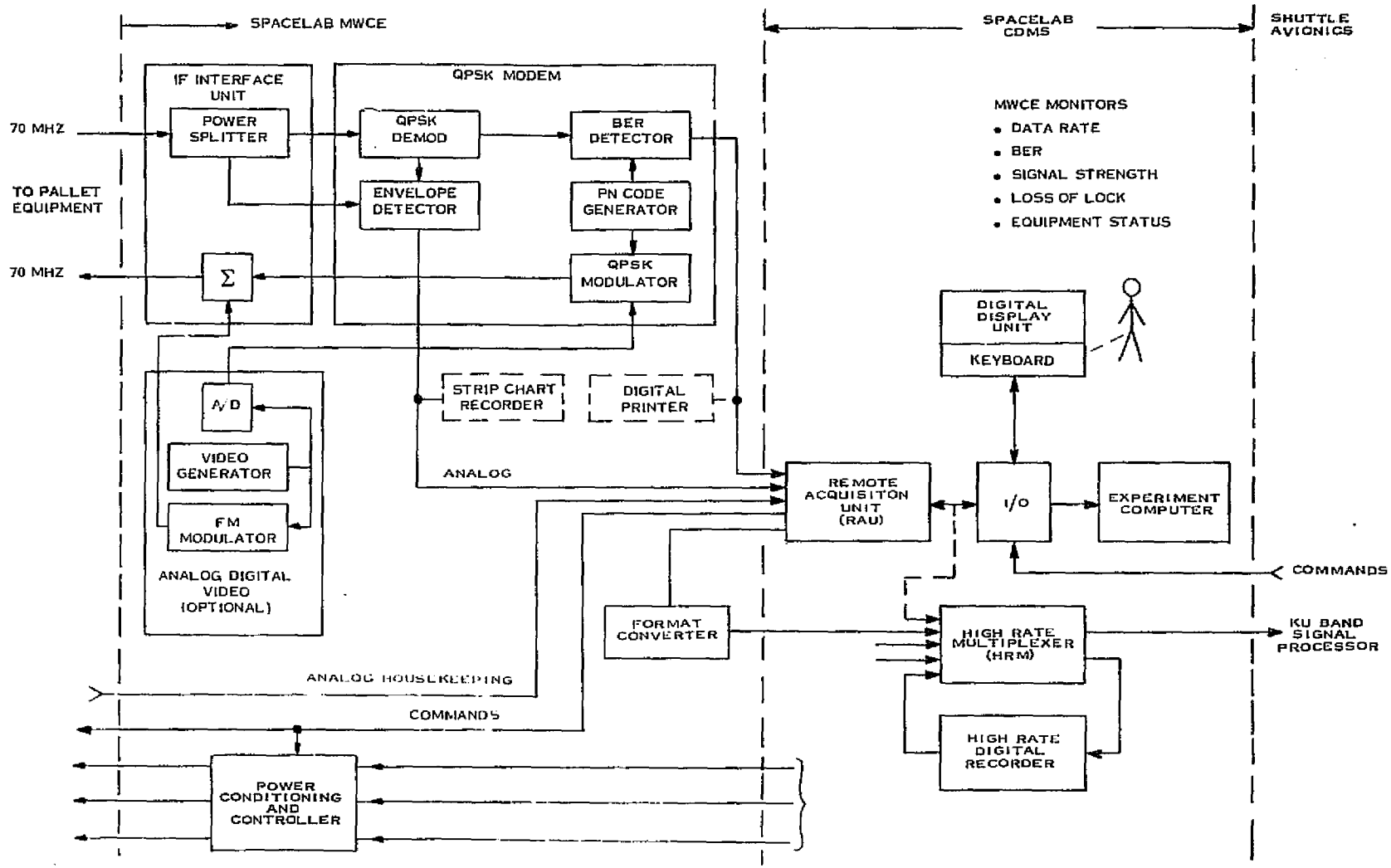

Figure 5-17. MWCE-MOD II Experiment Configuration (Control and Monitoring Portion)

Either RHC or LHC polarization can be selected by means of receive and transmit switches.

When operative in the Spacelab mode, uplink signals are converted to an IF frequency of 70 MHz and transferred to the Spacelab module as shown. Downlink signals which originate in the Spacelab module are transferred to the pallet equipment at 70 MHz and then converted to the IF frequency of the transponder.

The Module mode of operation may consist of independent uplink and downlink signals. For example, a 50 Mbps signal may be demodulated in the Spacelab QPSK demodulator and BER tests may be performed at the same time a different QPSK signal or analog signal is transmitted to the ground station.

BER tests may also be performed in the Spacelab on uplink signals at the same time BER tests are run at the ground station on the downlink transponder signal.

Operation in the normal Beacon mode may occur simultaneously with operation in the Transponder mode or Module mode. In this case, the Beacon signal is 20 dB below the level of the communication signal. In most cases, however, important propagation characteristics will be obtained during beacon operation at the high power level as shown in Table 5-13. As shown in the block diagram of Figure 5-16, the downlink beacon signal originates in the frequency synthesizer and is injected into the downlink at the IF frequency at two different levels. The two levels of beacon signal are switch selectable. The low level is for normal operation and the high level is for the acquisition and propagation mode.

The beacon signal can also be switched to a broad beam horn antenna when downlink signals are desired at more than one ground station or during handover from one station to another.

An optional multitone beacon package is shown in the block diagram of Figure 5-16, which could be GFE equipment, should the need arise.

5.5.3 EXPERIMENT SYSTEM-HARDWARE DESIGN

Hardware Description

The hardware comprising the MWCE-MOD II is made up of pallet-mounted equipment and Spacelab Module equipment. Concept mechanical configurations are shown in Figures 5-18 and 5-19. In the Transponder mode and Beacon mode, the pallet-mounted equipment can operate independently of the Spacelab Module equipment, except for TT&C housekeeping and power control equipment. The two assemblies mounted on the pallet are the antenna subsystem and the transponder subsystem.

Antenna Subsystem

The antenna subsystem consists of a 30 GHz dual polarized antenna/array, a 20 GHz dual polarized antenna/array and a broad beam horn with a 4 dB beamwidth of 140 degrees.

The antenna subsystem will be a subcontract item which may or may not be supplied by the prime MWCE contractor. By program definition, this task considers only mechanically fixed antennas. The design of the MWCE-MOD II antenna subsystem is beyond the scope of this contract and will be addressed in a separate antenna design study. The desired pattern, Figure 5-13, is not feasible using a single passive antenna. The most cost effective approach may be to reduce or eliminate the requirements for low elevation angle coverage, accept a shorter mission test time, and use a switchable multibeam antenna system or similar design. Table 5-11 shows typical operating time starting at 5^{o} elevation angle from Rosman, North Carolina.

Shuttle Interface Electronics

The Shuttle Interface Electronics Unit consists of encoding and decoding equipment required to process and interface all command and telemetry signals with the Shuttle TT&C equipment and with the Spacelab display and control equipment.

Equipment Summary

The hardware matrix chart (Table 5-12) lists all the proposed equipment for the MWCE-MOD II experiment, with estimates of the size, weight and power requirements of each.

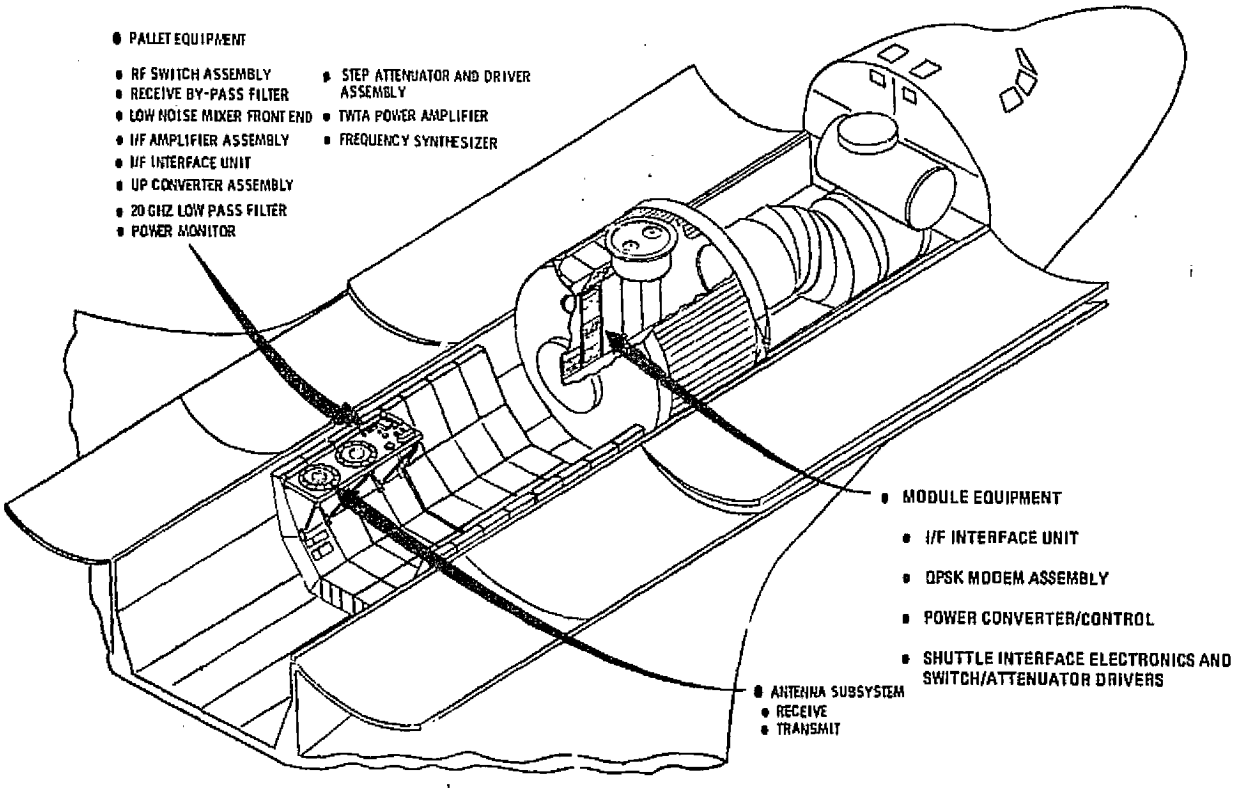

Figure 5-18. Concept of MWCE-MOD II Installed in Spacelab/Shuttle

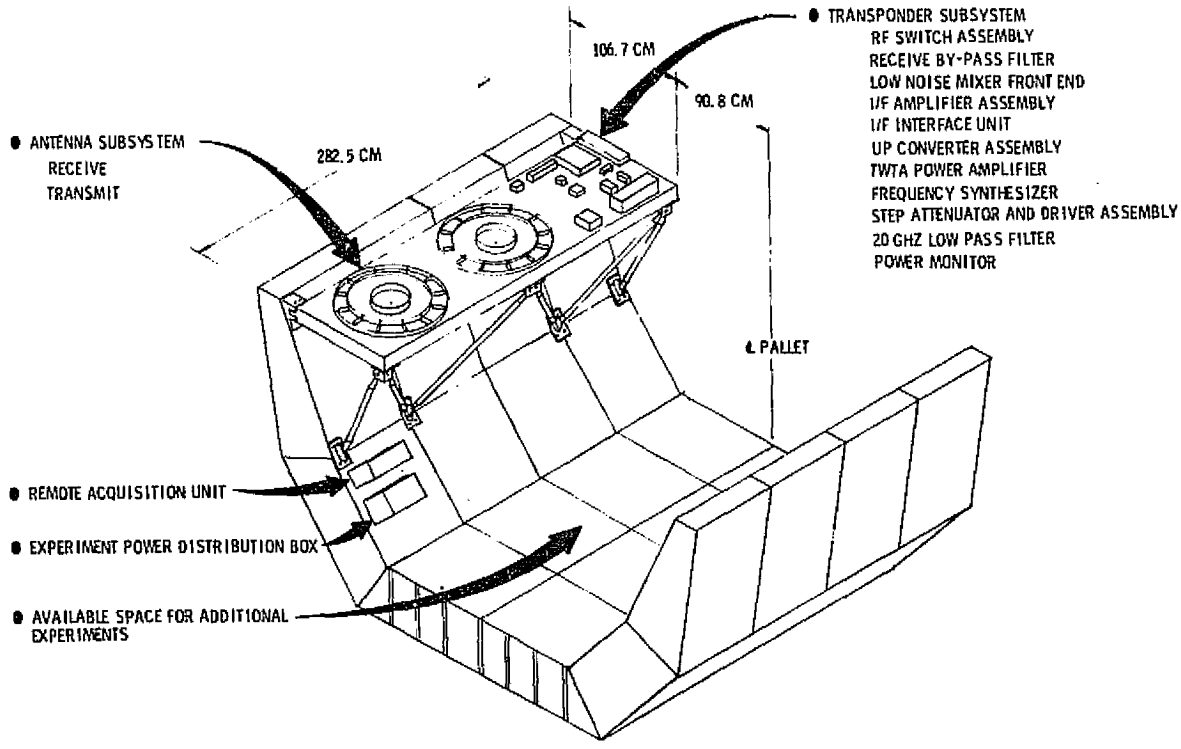

Figure 5-19. MWCE-MOD II Experiment Pallet Equipment

Table 5-11. MWCE Operating Time Over Rosman, N.C.
for 5° Ground Station Elevation Angle

Day 1		Day 2		Day 3		Day 4		Day 5		Day 6	
Orbit	Time (Min.)	Orbit	Time (Min.)	Orbit	Time (Min.)	Orbit	Time (Min.)	Orbit	Time (Min.)	Orbit	Time (Min.)
1	7.5	16	4.9	33	5.0	48	6.7	64	1.3	79	5.0
2	6.7	17	7.5	36	2.8	52	7.0	67	5.4	82	2.8
6	7.0	18	1.3	37	7.8	53	6.8	68	8.0	83	7.8
7	6.8	21	5.4	38	3.5	62	4.9	78	8.0	84	3.5
		22	8.0	47	7.5	63	7.5				
		32	8.0								
Total	28.0		35.1		26.6		32.9		22.7		19.1

Six-Day Total: 164.4 Minutes
Orbit: 400 km, 57° Inclination

Table 5-12. MWCE-MOD II Hardware Matrix

ITEM	SIZE CM	WEIGHT Kg	POWER (WATTS)
PALLET EQUIPMENT		41.55	117.6
• ANTENNA SUBSYSTEM	ESTIMATE →	25	→ 20
• TRANSPONDER SUBSYSTEM		16.55	97.6
- RF SWITCH ASSEMBLY	20 x 25 x 6.4	2.0	10
- RECEIVE BP FILTER	10 x 2.5 x 2	0.2	-
- LOW NOISE MIXER FRONT END	8 x 3 x 3	0.2	-
- IF AMPLIFIER ASSEMBLY	25 x 5 x 5	1.5	2.9
- IF INTERFACE UNIT	5 x 5 x 10	.6	-
- UP CONVERTER ASSEMBLY	10 x 6 x 6	.75	2.5
- STEP ATTENUATOR AND DRIVER ASSEMBLY	22 x 12 x 5	1.5	2.0
- TWTA	33.7 x 10.7 x 9.0	2.8	50
- 20 GHz LOW PASS FILTER	5 x 2.5 x 2	0.2	-
- POWER MONITOR	5 x 5 x 3	0.3	.2
- MSC HARNESS & RF CABLING WAVEGUIDE, PANEL, ETC.		4.5	-
- FREQUENCY SYNTHESIZER	15.25 x 5 x 11.5	2.0	30
SPACELAB MODULE EQUIPMENT		73.2	311
• QPSK MODEM ASSEMBLY			
- QPSK MODEM	48.25 x 50.5 x 13.3	15.9	30
- PN GENERATOR AND BER DETECTOR	48.25 x 50 x 5	4.0	10
- SIGNAL STRENGTH MODIFICATION TO MODEM		1.0	1.0
• INTERFACE UNIT		1.0	-
• STRIP CHART RECORDER	17.8 x 43.2 x 34	12.3	120
• SHUTTLE INTERFACE ELECTRONICS AND SWITCH/ATTEN DRIVERS	48.25 x 50 x 14	16	30
• POWER CONVERTER/CONTROL	48.25 x 50 x 14	16	20
• DIGITAL PRINTER	21.6 x 17.8 x 35.6	7.0	100

5.5.4 GROUND STATION CONSIDERATIONS

Several modifications may be necessary to existing ground stations to participate in the MWCE-MOD II experiment. First, a nominal G/T of 30.1 dB/^{O}K was used as the figure of merit for the ground station receiving equipment in the following link analysis. This figure is achieved with a 3 dB parametric amplifier preceded by 1 dB of loss and a high elevation angle antenna temperature of 50^{O}K.

Second, in the Transponder mode of operation, the uplink Doppler shift of $\pm$ 750 kHz adds to the downlink Doppler shift of $\pm$500 kHz for a total Doppler of $\pm$1.25 MHz at a maximum rate of change of 24 kHz per second.

These Doppler rates and offsets are not problems in high data rate system where the recovered carrier has a high signal-to-noise density content and where tracking loop bandwidths are high. The communications experiment at 50 Mbps may not be performed during adverse weather conditions and low elevation angles. In order to provide large fade/loss margin, narrow detection bandwidths must be used for the beacon signal, which in turn require the use of tracking receivers.

Since a tracking pilot receiver is necessary to track the beacon, the tracking of the full Doppler by the QPSK demodulator can be relaxed since most of the Doppler will be removed by the pilot receiver. However, this is only true when the source of the beacon signal is collated with the source of the QPSK signal. If this is not always true, then the QPSK demodulator must be capable of tracking the residual Doppler in the received signal, which may include the entire uplink Doppler shift, if the beacon originates in the Spacelab and the QPSK signal originates at the ground station. Figure 5-20 shows a conceptual block diagram of the ground station receiving system using a pilot receiver.

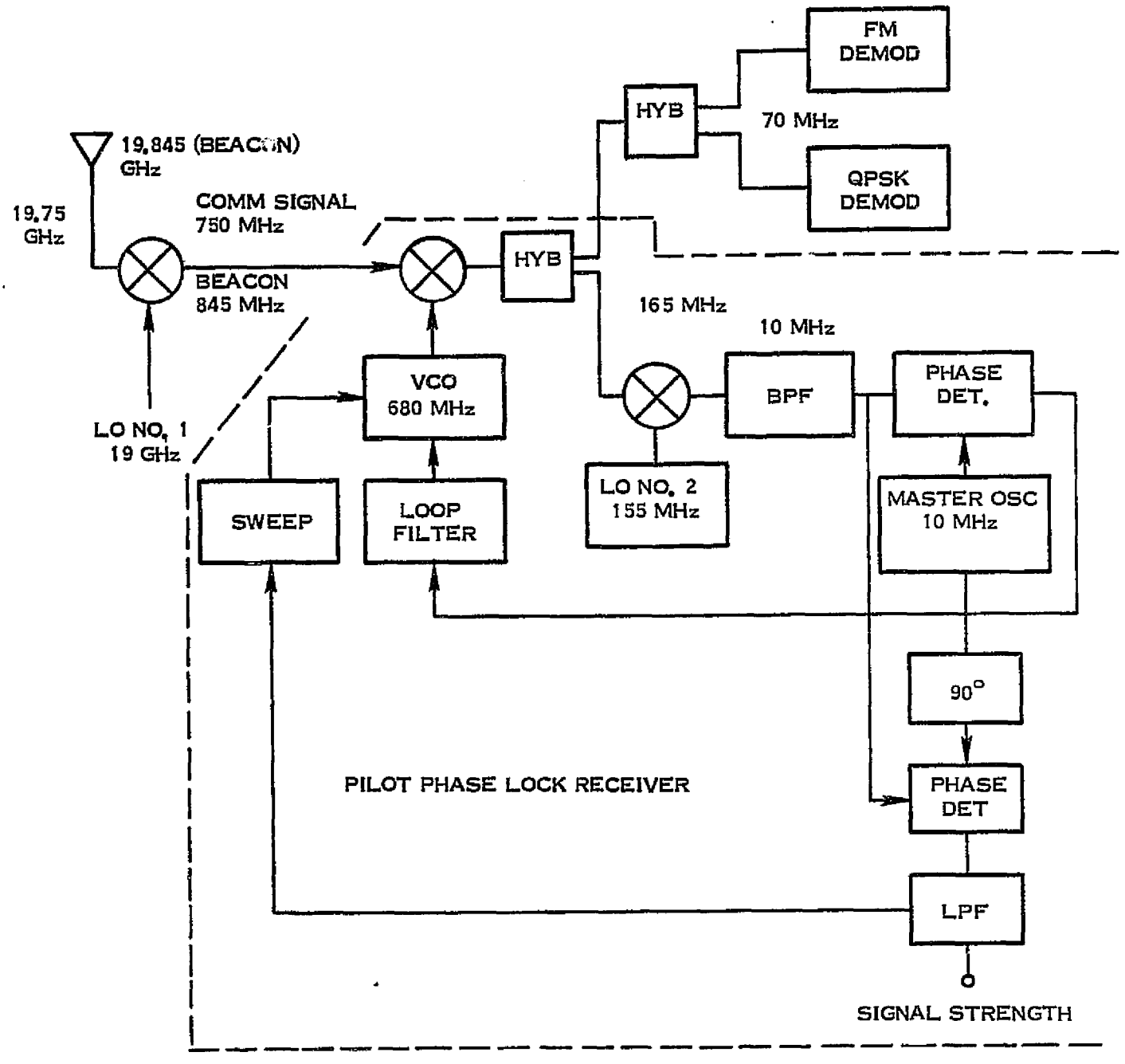

Figure 5-20. Conceptual MWCE-MOD II Ground Station Receiver

SECTION 6

OTHER CANDIDATE MMAP EXPERIMENTS

At the outset of this study, as explained in the Introduction (Section 1), a number of other candidate experiments were to be considered other than AMPA, EEE, and MWCE. The objective was an attempt to identify a commonality in the antenna subsystem, electronics subsystem, power and control subsystems, and data handling subsystems. From this design commonality, theoretically it is possible to configure a number of related MMAP experiments such as those listed on page 1-1 (duplicated below with number 9 added):

1. EEE
2. AMPA
3. MWCE
4. Orbiting Standards Platform (OSP)
5. Antenna Range Experiment (ARE)
6. Cooperative Surveillance Spacelab Radar (CSSR) Experiment
7. Data Collection with Multibeam (DCMB) Experiment
8. NAVSTAR GPS Experiment (GPS)
9. Position Location Interferometer (PLI)

The study revealed that the experiments are each virtually unique with respect to one another in their antenna, transmitting, receiver, and signal processing requirements. Each one must be optimally designed as a aprtial or total pallet-experiment hardware package. However, the Shuttle-provided data handling, control, and monitoring subsystem (CDMS) and the power subsystem (EPDB) etc., may be used for all experiments.

By direction from GSFC, emphasis was placed on the first three experiments listed. In the last interim report it was indicated that the PLI would be considered. This was subsequently dropped by GSFC as a potential Spacelab experiment.

During the later phases of the MMAP contract, the OSP has emerged as a good potential Spacelab experiment for future flights, perhaps after 1982.

The remaining portion of this section is devoted to a brief overview of the work done to date on OSP as a result of the Preliminary User Requirement Study accomplished by OT/ITS (Office of Telecommunications/Institute for Telecommunications Sciences), Boulder, Colorado, and NASA, with active GE support. An informative data package and questionnaire has been sent to prospective government and commercial users of OSP. Participants in the working group, chaired by John Woodruff, included:

R. Baird	- NBS
H. T. Dougherty	- OT/ITS
G. Ehrlich	- NASA/Hdqts.
A. J. Estin	- NBS
A. Kampinsky	- NASA/GSFC
R. W. Kreutel	- Comsat Labs
W. L. Morgan	- Comsat Labs
J. Woodruff	- NASA/GSFC

Following is a brief description of the proposed OSP experiment.

6.1 EXPERIMENT OBJECTIVE AND JUSTIFICATION OF THE SPACELAB OSP EXPERIMENT

The objective is to develop, test and demonstrate on a Spacelab. The OSP concept is to deploy at synchronous orbits, a family of dedicated-standards beacons and receivers to provide signal sources and receivers of well-defined frequency, spectral power, noise, and polarization properties for the measurement of long-term propagation statistics and the measurement and calibration of antennas. It is necessary to characterize accurately and precisely the ground station antennas and propagation paths for optimum utilization of the available spectrum on earth/satellite links. For a significant user community, the use of synchronous satellite pattern range is the only cost-effective means of precisely measuring large antenna gain, pattern and polarization characteristics. These needs require dedicated signal sources and receivers as described above, and/or long, continuous periods of propagation measurements (adequate to provide meaningful statistics) to synchronous orbit. The Shuttle provides a significantly softer ride into orbit of standards-quality devices, checked, tested, and thermally evaluated while in low orbit and softly inserted into a synchronous orbit.

The current trend towards re-utilization of frequencies and utilization of higher frequencies requires improved characterization of both the propagation path and the ground station antennas that can only be done effectively using a "standard source" at synchronous orbit. Present capability is limited to natural sources (e.g., radio stars). System margins on satellite/earth links have to be made larger; pattern and gain control on physically or electrically large antennas and tighter controls on polarization, for example, are almost impossible to effectively invoke in the absence of such a facility (standard source).

6.2 TECHNICAL APPROACH FOR THE OSP EXPERIMENT

The approach is to develop Orbiting Standards Platforms consisting of simple dedicated payloads brought up to low orbit by the Space Transportation System (STS) in a package attached (one per mission) on dedicated free-flyers, checked out and tested in space and then inserted gently into synchronous orbit. Free-flyers would be retrieved and re-used, payloads modified and/or replaced during the missions. The OSP will have antennas of precisely known gain, pattern, and polarization servicing a variety of signal sources and receivers. The sources and receivers will operate in modes such as: commanded center-frequency and bandwidth, swept frequency, commanded coherent tones, and spectrally pure discrete frequency. The sources will have synthesizer/modular capability and precisely controlled power outputs. The receivers will have precision phase and amplitude measurement capability. Receiver outputs will be encoded and transmitted to earth along with other monitoring and control data.

6.3 BASIC OSP EXPERIMENT REQUIREMENTS

Initial experiments will probably involve pallet-mounted antennas and electronic hardware in the Shuttle bay area much as planned for the EEE, AMPA, and MWCE experiments. This will enable basic checkout of all fundamental experimental work to be done with the Shuttle low orbits in conjunction with various user terminals.

The ultimate experiment requires the Orbiter/Shuttle for checkout and test; soft insertion (2G) into synchronous orbit; and packaging for (2G) launch to orbit. The experiment

hardware includes a free-flyer package with appropriate attitude control and prime power (≈1 kW) for a minimum two-year mission, T&C channel capacity to monitor and control OSP, NBS-calibrated antennas (earth coverage), frequency standards, signal source control and monitoring, signal sources, etc. On-board support by the Payload Specialist involves onboard checkout of OSP, adjustment and modification of OSP for re-use, insertion of OSP into a free-flyer mode, and later retrieval of OSP for low-orbit testing.

Initially, multi-mission coverage using discrete segments of the frequency range 100 MHz to 100 GHz would meet most needs. Expansion to segments in the range 10 MHz to 300 GHz would be ultimately desirable. A set of dedicated narrowband frequencies spread over the spectrum that can exceed the approximate -150dBW/m^2/4 kHz flux limit appears desirable and should be sought at the upcoming international conferences.

SECTION 7

NEW TECHNOLOGY

Work on this contract during the contract period of September 1976 through September 1977 has not resulted in the evolution of new technology.

SECTION 8
CONCLUSIONS

At the end of the MMAP Systems Definition Study, some preliminary conclusions may be drawn. The effectiveness of the study benefited by the highly responsive posture that has been maintained during the course of the contract with the Technical Officer, J. Woodruff, the various Principal Investigators, and with NASA support personnel. Examples include timely responses to the Spacelab Experiment Announcement of Opportunities (AO's) which resulted in the preparation of several Spacelab proposals written in NASA's context. Also included is the detailed technical consideration of a multiplicity of experiment design and system variations, many suggested by the Principal Investigators.

Work completed during the interim period September 1976 to July 1977 has resulted in two experiment designs, the EEE-MOD I and the MWCE-MOD I. Operational parameters were studied and applied to the AMPA Experiment. A 400 km, 57^{o} inclination orbit profile was selected as a typical one to define the operational parameters for the experiments.

The AMPA and EEE-MOD I instruments have been completed in this feasibility and systems definition study and may now progress to the next phase of NASA's experiment hardware procurement. As a cost effective technique, some of the work was based on completed contracts [1,2] and on current AMPA contractual work being conducted for NASA by the Airborne Instrument Laboratories. The General Electric studies provided the basis for the AMPA Concept Review held at NASA-GSFC in February 1977. Work on defining the AMPA experiment's operational modes has shown that at least a $\pm 70^{o}$ viewing angle from the Shuttle is needed to provide an experiment operating time of 6-8 minutes. Details of the experiment operation are included in Section 3 of this report along with a trade-off study of viewing angle versus operating time.

The MWCE-MOD I concept design was completed for a system using a steerable antenna mount. This system represents a full-up MWCE, found to be too expensive for the initial implementation. An analysis of the MWCE radius of operation reveals that operation to

ground terminals with at least a 5^{o} ground-elevation angle is needed to achieve practical operational times, in the order of 6-8 minutes. Therefore, it appears essential to employ a high gain ground antenna in order to achieve a satisfactory carrier-to-noise (C/N) ratio at low antenna elevation angles.

A lower cost MWCE-MOD II concept design was completed during the period March 1977 to June 1977, which promises to meet essentially all of the experimental requirements.

System definition of the EEE-MOD I (121.5 MHz to 2700 MHz) and EEE-MOD II (121.5 MHz to 43 GHz) are complete. Equipment layouts indicate the requirement for one standard pallet and moderate-size electronics packages in the Spacelab Module or AFD. Data handling requirements were studied and reported in a separate task report (C.I. 10) involving the transmission of real-time data via the TDRSS links. Flexibility of experiment control is afforded by three optional operational modes: remote control via TDRSS, automatic programmed control, or manual control by the Payload Specialist. Analysis work was done to evaluate the effects of antenna pattern coverage with the higher gain, higher frequency antennas above 2.7 gHz. Tilting the antennas forward and off nadir produces an optimum coverage of terrestrial emitters.

SECTION 9

REFERENCES

1. J.B. Horton, M.S. Afifi, G.A. Dorfman, H. Jankowski, Shuttle/Spacelab Electromagnetic Environment Experiment, Phase B Definition Study, Final Report, NAS 5-22469, April 1976 (GE).

2. C.C. Allen, S.P. Applebaum, W.J. Papowsky, G. Wouch, Adaptive Multibeam Antennas for Spacelab, Phase A Feasibility Study, Final Report, NAS 5-22425, February 1976.

3. R. Kaul, Experiment Definition Report on the Millimeter Wave Communications Experiment, Final Report, NAS 5-24034, January 1976 (ORI).

4. Space Shuttle Level II Program Definition and Requirements, JSC-07700, NASA, JSC, Houston, Texas, July 3, 1974.

VIII	Mission Operations
IX	Ground Operations
X	Flight and Ground Specifications
XI	Crew Operations
XII	Integrated Logistics Requirements
XIV	Space Shuttle System Payload Accommodations
XVIII	Computer Systems Software

5. Spacelab Payload Accommodation Handbook, NASA/ESRO, ESTEC REF. No. SLP/2104, May 1975.

6. R.E. Taylor and J.S. Hill, "0.4 to 10 GHz Airborne Electromagnetic Environment Survey of U.S.A. Urban Areas," IEEE International Symposium on Electromagnetic Compatibility (EMC), Session 2B, Washington, D.C., 13-15 July 1976, NASA Accession No. N76-23460.

APPENDICES

A - MWCE ANTENNA POINTING SYSTEM PRELIMINARY DESIGN

B - MWCE-MODD II ANTENNA REQUIREMENTS ANALYSIS

C - EEE ANTENNA PATTERN AND FOOTPRINT ANALYSIS

D - ANALYSIS OF EEE SPECTRUM PROCESSOR ACCURACY

E - EEE SPECTRAL PROCESSOR DESIGN

APPENDIX A

MWCE-MOD I ANTENNA POINTING SYSTEM PRELIMINARY DESIGN

1.0 FUNCTIONAL DESCRIPTION

The MWCE Antenna Pointing System (APS) has two modes of operation: Acquisition and Tracking. The APS functional block diagrams for the acquisition and tracking modes are shown in Figures 1 and 2 respectively. In the acquisition mode the gimbal orientation required to point the monopulse antenna at the desired ground station is determined by the MWCE controller and applied to the APS controller. The commanded gimbal orientation is compared with the actual gimbal orientation as measured by the gimbal potentiometer. The gimbal orientation error is then used to command the gimbal torquer such that the gimbal orientation error is nulled.

When the monopulse system has acquired and is tracking the ground station, the MWCE controller switches the APS from the acquisition to the tracking mode. In the tracking mode (see Figure 2), the monopulse processing electronics generate signals that are proportional to the antenna pointing error relative to the ground station. These signals are processed to generate the appropriate gimbal commands to null the antenna pointing error.

The APS is comprised of two major components. The gimbal assembly and the APS controller. The gimbal assembly contains the gimbal structure, drive motors, bearings, and potentiometers. The APS controller contains the electronics required to process the gimbal pointing error signals and generate the appropriate gimbal motor drive signals.

The APS gimbal assembly mounted in the Spacelab pallet is shown in Figure 3. The gimbal concept is a two axis, X-Y direct drive gimbal similar to that used on the S-193 Skylab experiment. The MWCE mounting arrangement allows the MWCE to be

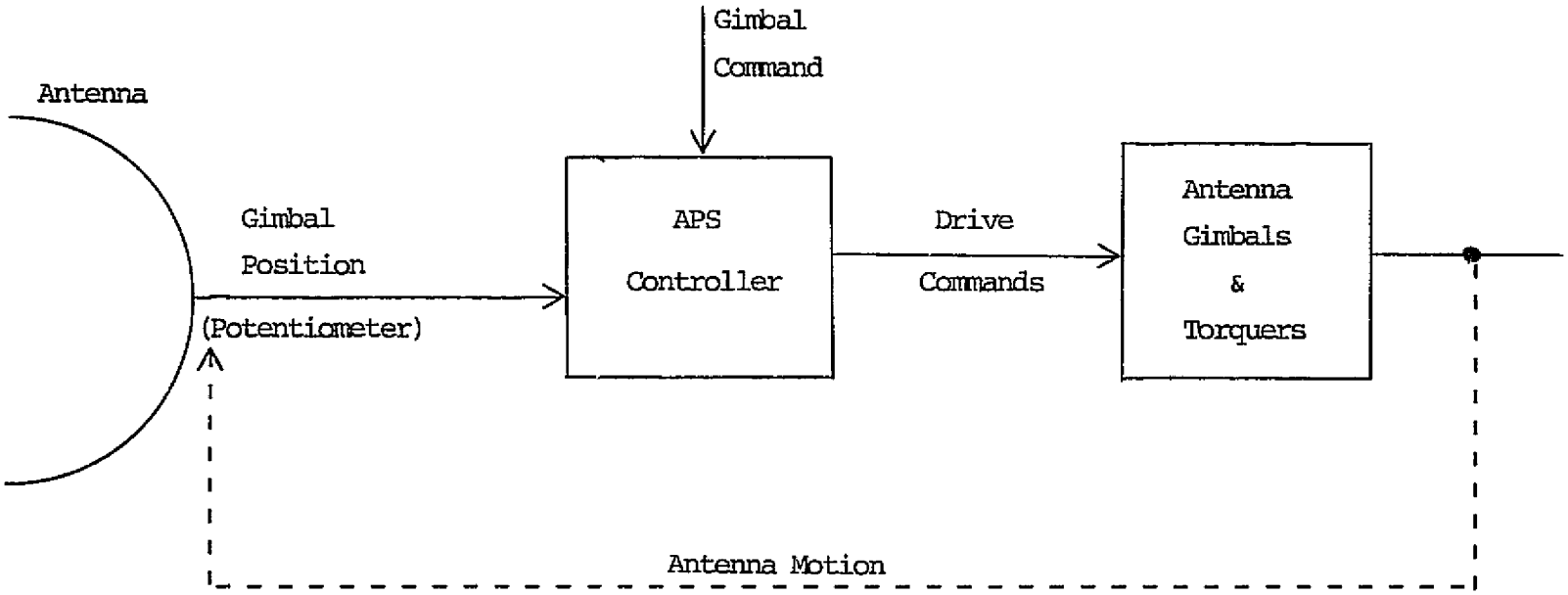

Figure 1 MWCE APS Acquisition Mode Functional Block Diagram

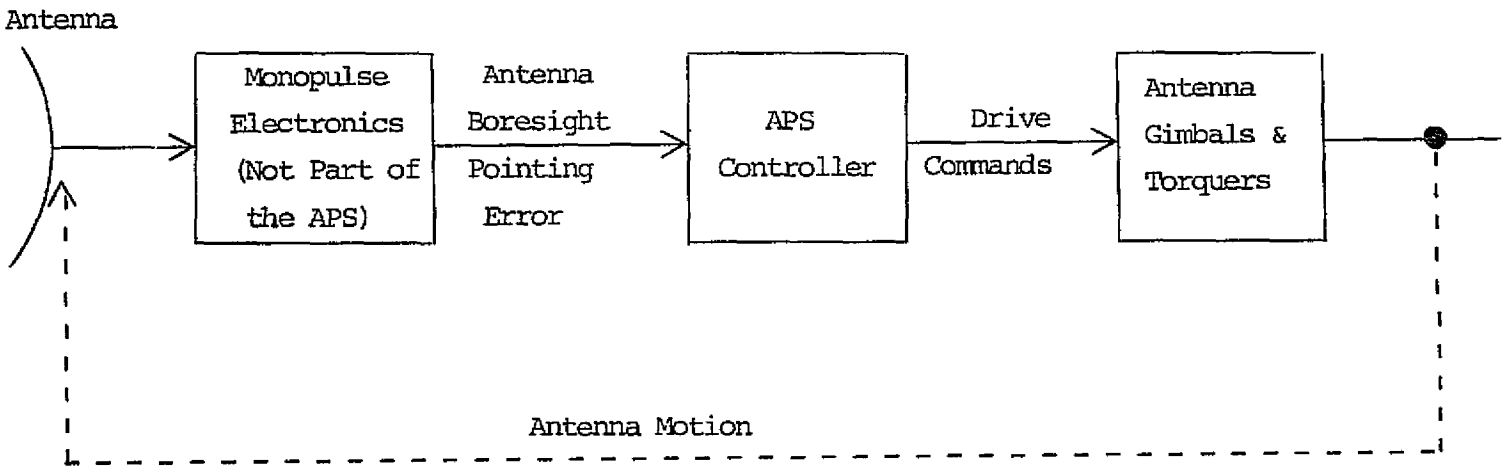

Figure 2 MWCE APS Tracking Mode Functional Block Diagram

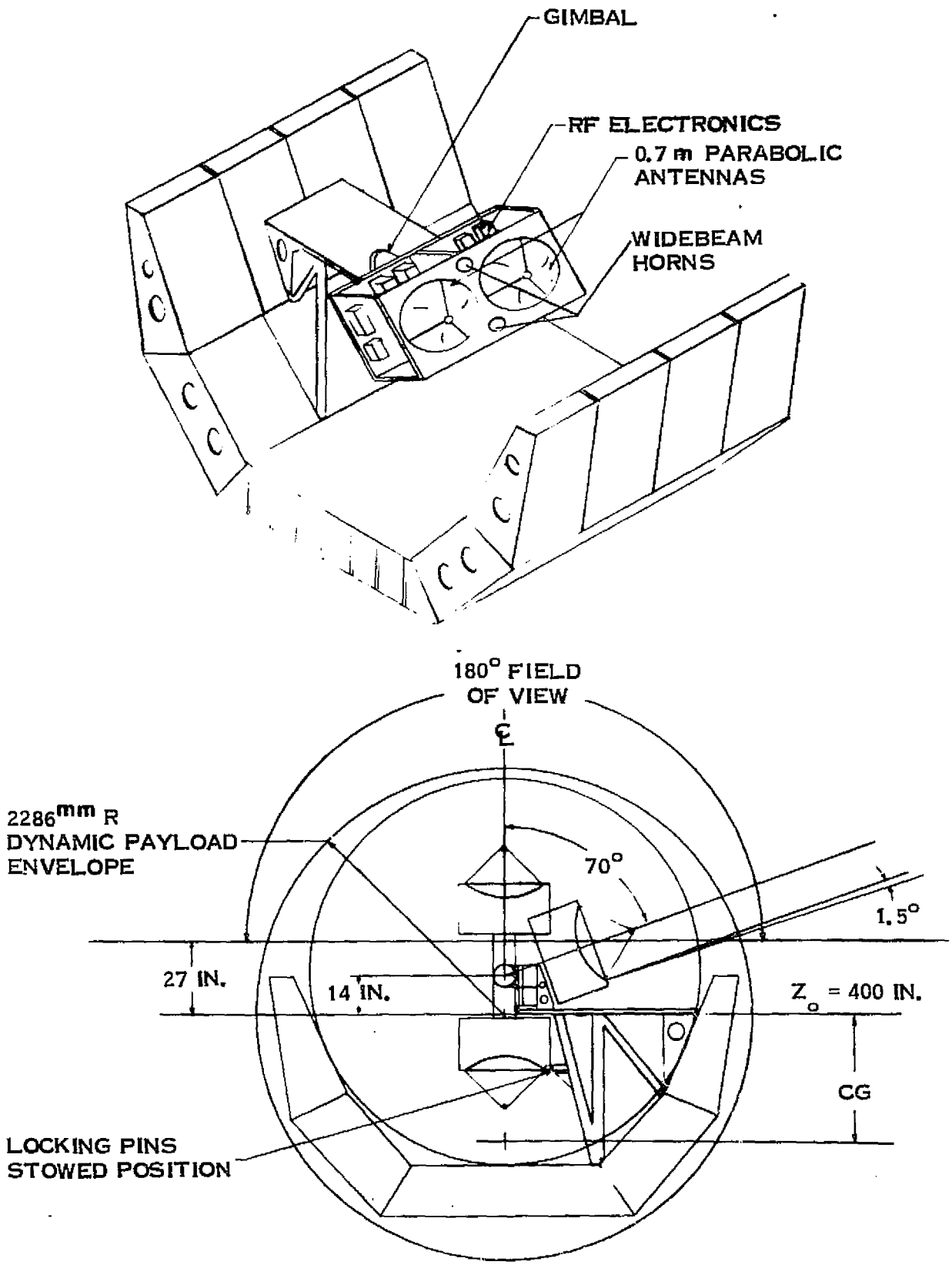

Figure 3 . MWCE Pallet Mounting Configuration

stowed with a low c.g. relative to the shuttle but swing up to obtain the ±70 deg (in both directions) clear field-of-view required for the MWCE.*

A cutaway drawing of the gimbal assembly is shown in Figure 4. Two Inland 7200 DC torque motors provide gimbal control torques. For the nominal mass properties, this results in a 0.34 rad/sec^2 angular acceleration capability*

The APS controller functional block diagram is shown in Figure 5. This APS controller design is based upon the design analysis described in Section 3. The same control loop compensation is used for both the acquisition and tracking modes. Thus, mode selection consists essentially of specifying the pointing error source. It is assumed that the mode commands and acquisition gimbal commands are generated external to the APS.

2.0 Requirements

This section contains the preliminary MWCE APS requirements that were used to guide the design effort. All requirements are 3σ. It can be anticipated that these requirements will be modified as the MWCE design is refined.

2.1 Acquisition Mode

Pointing Accuracy

The APS shall point the antenna boresight within 2 deg of the commanded attitude after the slew and settling time.

Slew Duration

The APS shall execute a commanded 60 deg reorientation with a total slew and settling time less than 10 sec.

2.2 Tracking Mode

Tracking Accuracy

When using the narrow beamwidth monopulse, the antenna boresight shall point within 0.10 deg of the ground station.

Transient Response

An initial 10 deg attitude error at monopulse acquisition shall be reduced to within the tracking accuracy limits within 10 sec.

3.0 Design and Performance Analysis

3.1 Acquisition Mode

The preliminary acquisition mode single axis gimbal control loop is shown in Figure 6. For the preliminary design no slew command shaping/feedforward control has been included. For large angle slews, the gimbal drive motor will be saturated

---

* The MWCE gimbal and support structure configuration was designed by John Zemany; the detail gimbal design was provided by Rae Stanhouse.

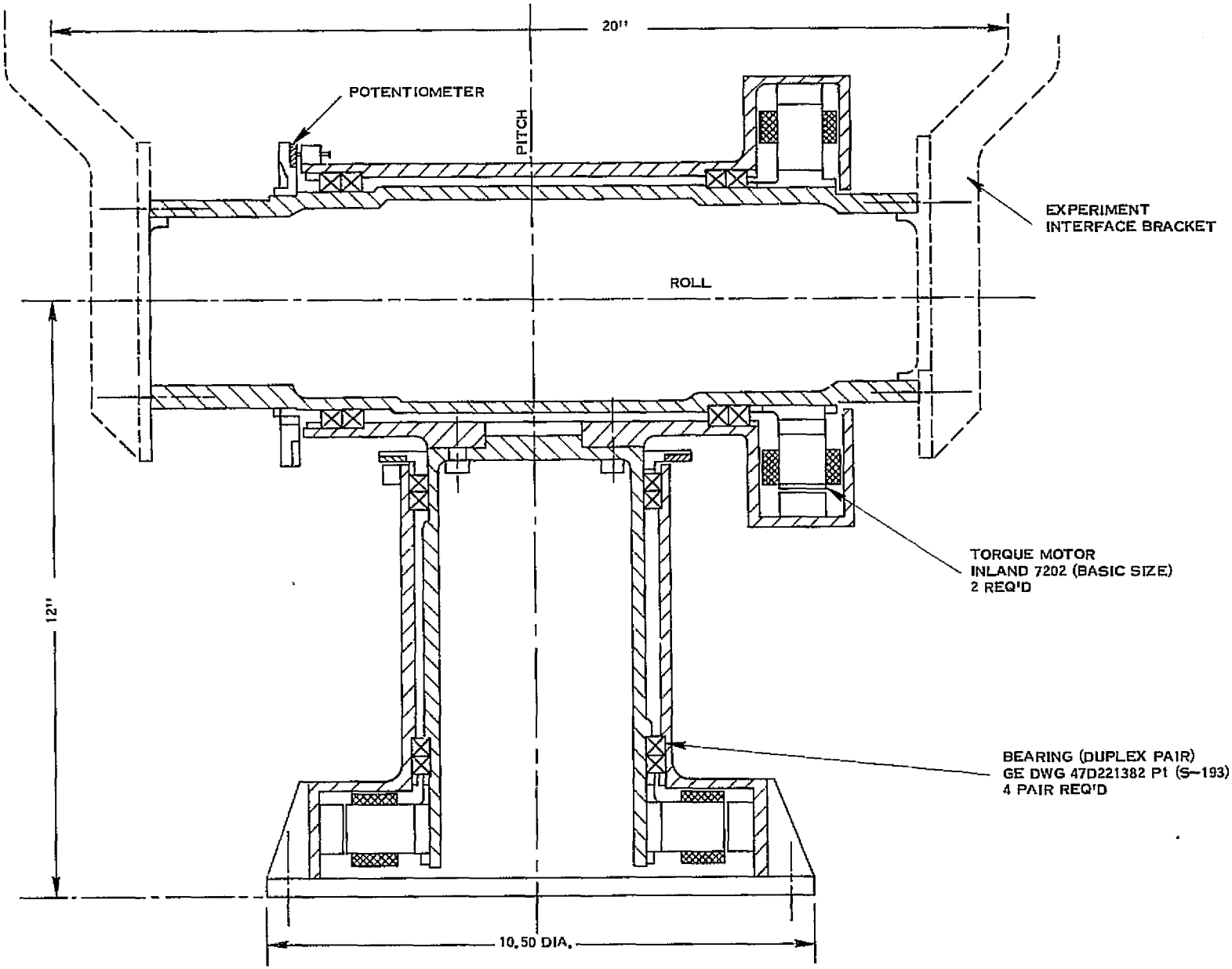

Figure 4. MWCE Gimbal Concept

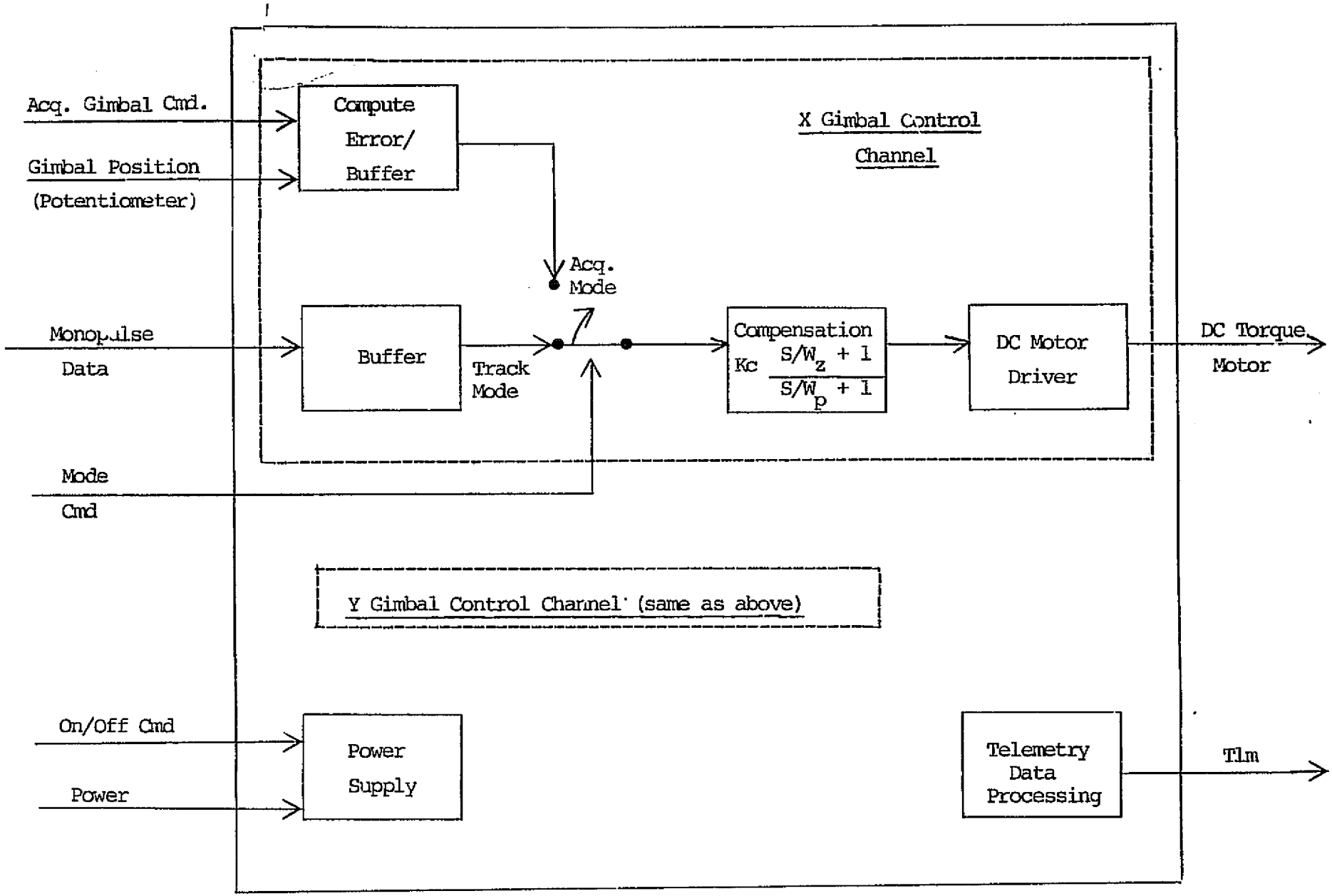

Figure 5 MWCE APS Controller Functional Block Diagram

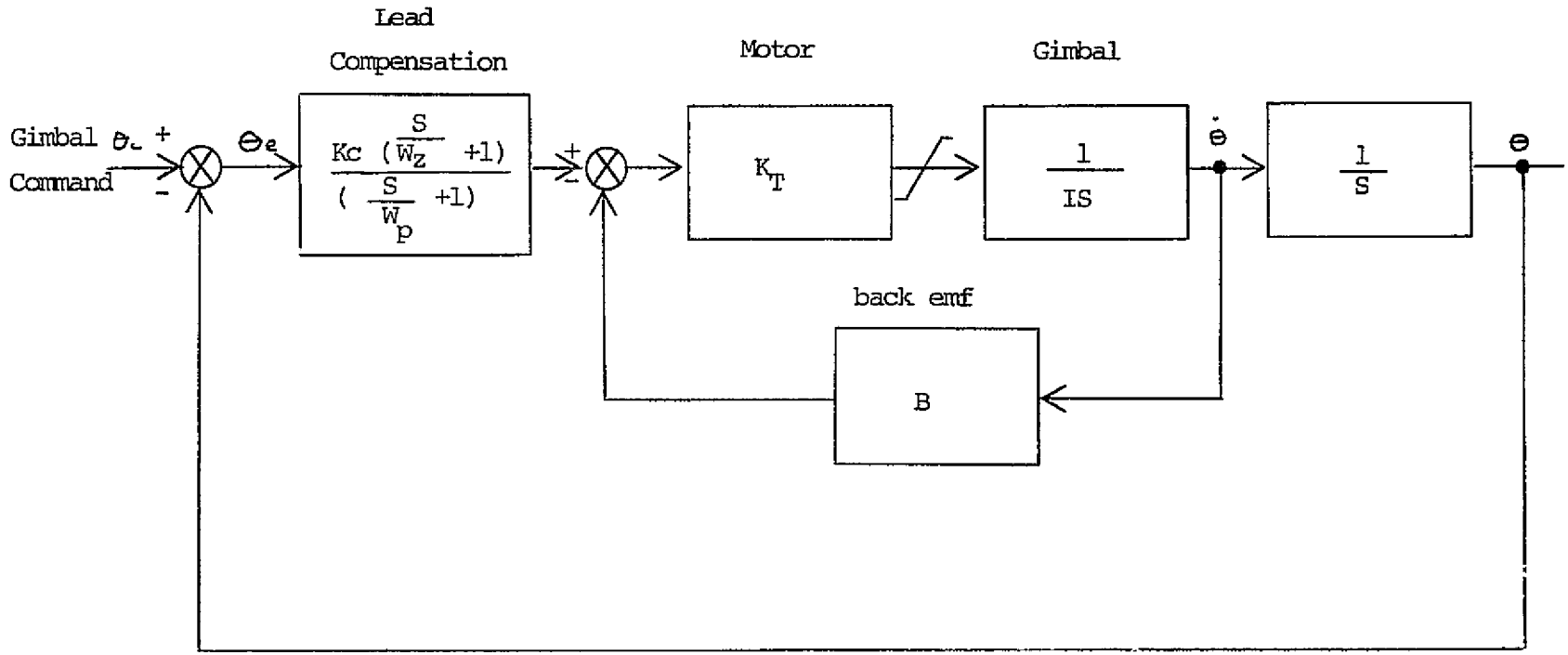

Figure 6 Acquisition Mode Gimbal Control Loop Block Diagram

yielding a maximum gimbal acceleration of 0.34 rad/sec^2. With this acceleration capability, an optimal 60 deg slew can be completed in 3.5 sec. The acquisition control loop shown in Figure 6 will not yield an optimal (i.e., minimum time) slew maneuver; however, it is anticipated that the 60 deg slew maneuver can be completed well within the 10 sec requirement.

The accuracy of the slew maneuver is determined by the gimbal potentiometer angular readout accuracy. Meeting the 2 deg acquisition mode pointing requirement should not present a problem. It should be realized that other attitude error sources external to the gimbal servo loop (e.g. shuttle attitude errors, gimbal command errors, etc.) will also cause errors in the antenna boresight pointing.

3.2 Tracking Mode

There are several conflicting factors in the design of the tracking mode APS. Low tracking errors, fast response and the reduction of the effects of disturbance torques, gimbal bearing friction, and shuttle motion are accomplished with a high gain, high bandwidth control loop. On the other hand, the undesirable effects of monopulse noise on pointing error are agravated by increasing the control loop bandwidth. A preliminary tracking mode control loop design was performed to evaluate these conflicting factors and evaluate the feasibility of the APS design approach.

The tracking mode gimbal control loop block diagram is shown in Figure 7. A series compensated control loop has been selected for the baseline design. This represents the simplest (and least expensive) approach for the APS design. The parameter values for the baseline control loop design are given in Table 1. The motor parameters are based on similar DC torque motors. The MWCE moment of inertia is based on preliminary mass properties data. Single axis, rigid body dynamics have been used for the preliminary design analysis. In view of the relatively low angular rates and control loop bandwidth for the APS, gimbal cross coupling and flexible structure dynamics should not significantly impact the baseline design.

Summary

The principle conclusion of the preliminary design and performance analysis is that the 0.1 deg tracking mode pointing accuracy requirement can be satisfied by the baseline APS design. Table 2 contains a summary of the baseline APS performance.

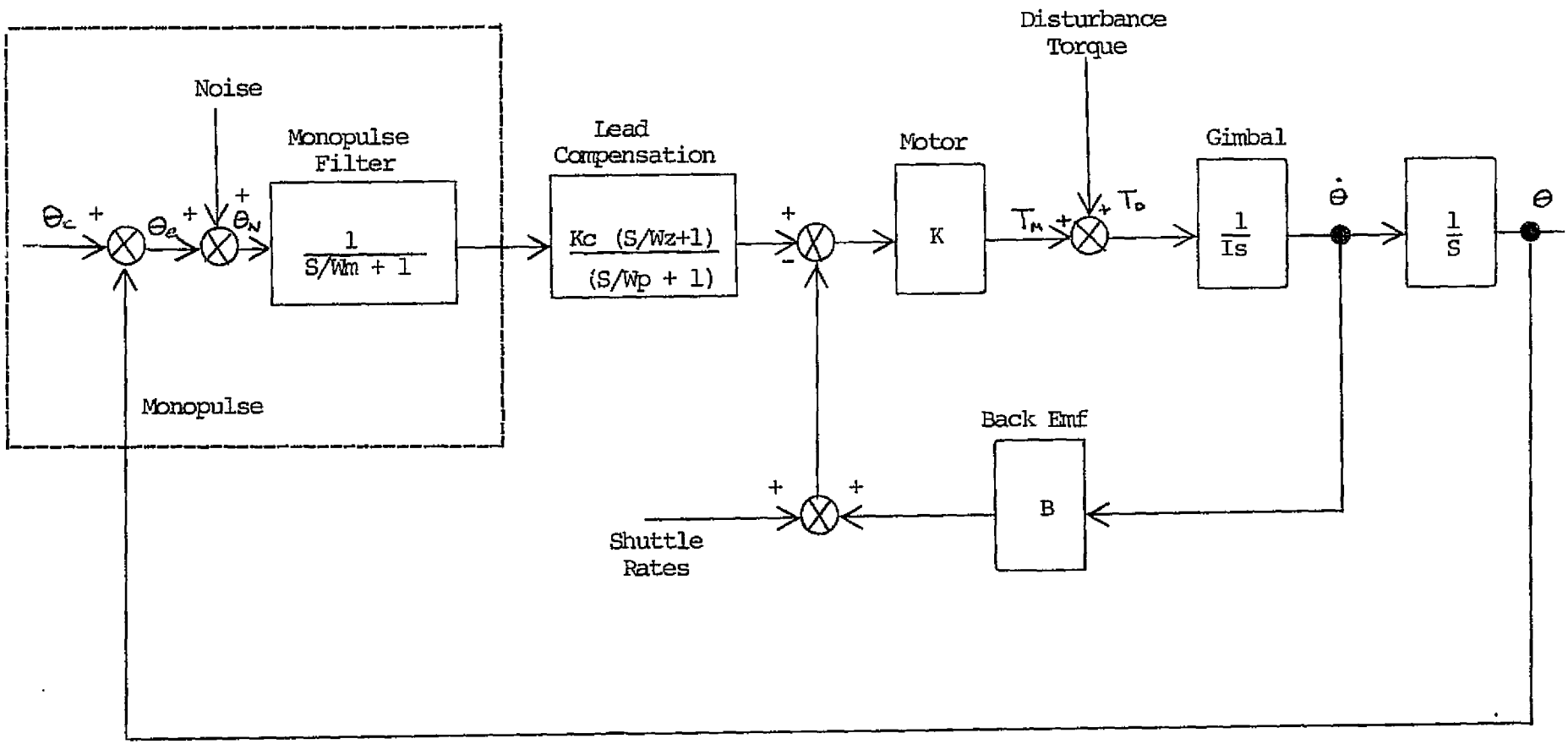

Figure 7 Tracking Mode Gimbal Control Loop Block Diagram

Table 1 Antenna Pointing System Parameters

Symbol	Definition	Value	Units
I	Moment of inertia of gimbal and experiment	31.	slug ft^2
K_c	Compensation gain	1000	volts/rad
W_z	Compensation lead break frequency	1	rad/sec
W_p	Compensation lag break frequency	40	rad/sec
W_m	Monopulse noise filter break frequency	not used	rad/sec
K_T	Motor torque constant	0.25	ft.lb/volt
B	Motor back emf coefficient	1	volt/rad/sec

Table 2 Baseline APS Performance Summary

Performance Criteria	Performance Level	Comments
Steady state pointing error caused by 1 deg/sec ramp input	0.001 deg	Indicates that tracking error due to relative ground station motion will be small
Pointing error caused by monopulse noise	0.001 deg	Based on monopulse noise level of 0.00048 deg (3σ)
Response to disturbance torques cause by shuttle motion	0.06 deg	Can be reduced by increasing loop gain/bandwidth; however, this increases the effects of monopulse noise and flexible structure, control loop interaction
Linear step response settling time (time to move within $\pm$5% of final value)	1.2 sec.	Represents nulling of initial error (i.e., acquisition). Large initial errors (> 1.5 deg) will cause motor saturation and an increase in the response time.
Pointing error cause by bearing friction	0.03 deg	Based on 0.2 ft. lb. bearing friction. Can be reduced by integral compensation
Response to shuttle angular rate	TBD	Not yet evaluated; however, the relatively low shuttle angular are not expected to cause significant control disturbances.

Stability

Of prime consideration in any control loop design is stability. Figure 8 shows the open loop bode plot for the baseline APS. The lead compensation break frequencies have been selected to yield a relatively large phase margin of 72 deg. This results in an overdamped control loop response which has the advantage of reducing the effects of monopulse noise. The possibility of including a monopulse noise filter was incorporated in the baseline design (see Figure 7). The preliminary analysis indicated that the noise filter did not significantly improve performance and consequently it is not included in the final baseline design.

The closed loop frequency response for the baseline APS is shown in Figure 9. The closed loop bandwidth is 11 rad/sec.

Step Response

The unit step response is shown in Figure 10. In general, the step response shows the manner in which an initial error is nulled; i.e., it describes the acquisition response. However, the loop gain is such that motor torque saturation will occur when the initial error is greater than about 1.5 deg. If the motor saturates, the step response rise and settling time will be increased. However, the motor acceleration capacity is such that the 10 sec requirement for nulling an initial 10 deg acquisition attitude error should be satisfied.

Bearing Friction Effects

S-193 gimbal experience indicates that the gimbal bearing friction will be on the order of 0.2 ft. lb. For the baseline APS gains, the pointing error required to overcome the friction is 0.03 deg. This value appears acceptable; however, it desired, it could be reduced by the incorporation of an integral compensation term in APS control compensation. If the friction level goes up, then it will be necessary to add the integral compensation. This will not be a significant impact to the design.

Steady State Tracking Error

For the baseline APS, the steady state pointing error response to a ramp input is given by:

$$\theta_{es} = \frac{B}{K_c} \dot{\theta}_c$$

where $\dot{\theta}_c$ is the gimbal command ramp rate.

The maximum tracking angular rate for the MWCE is about 1 deg/sec. For the baseline APS, a constant 1 deg/sec angular rate input causes a steady state error of 0.001 deg. During actual operation, the input to the APS will not have

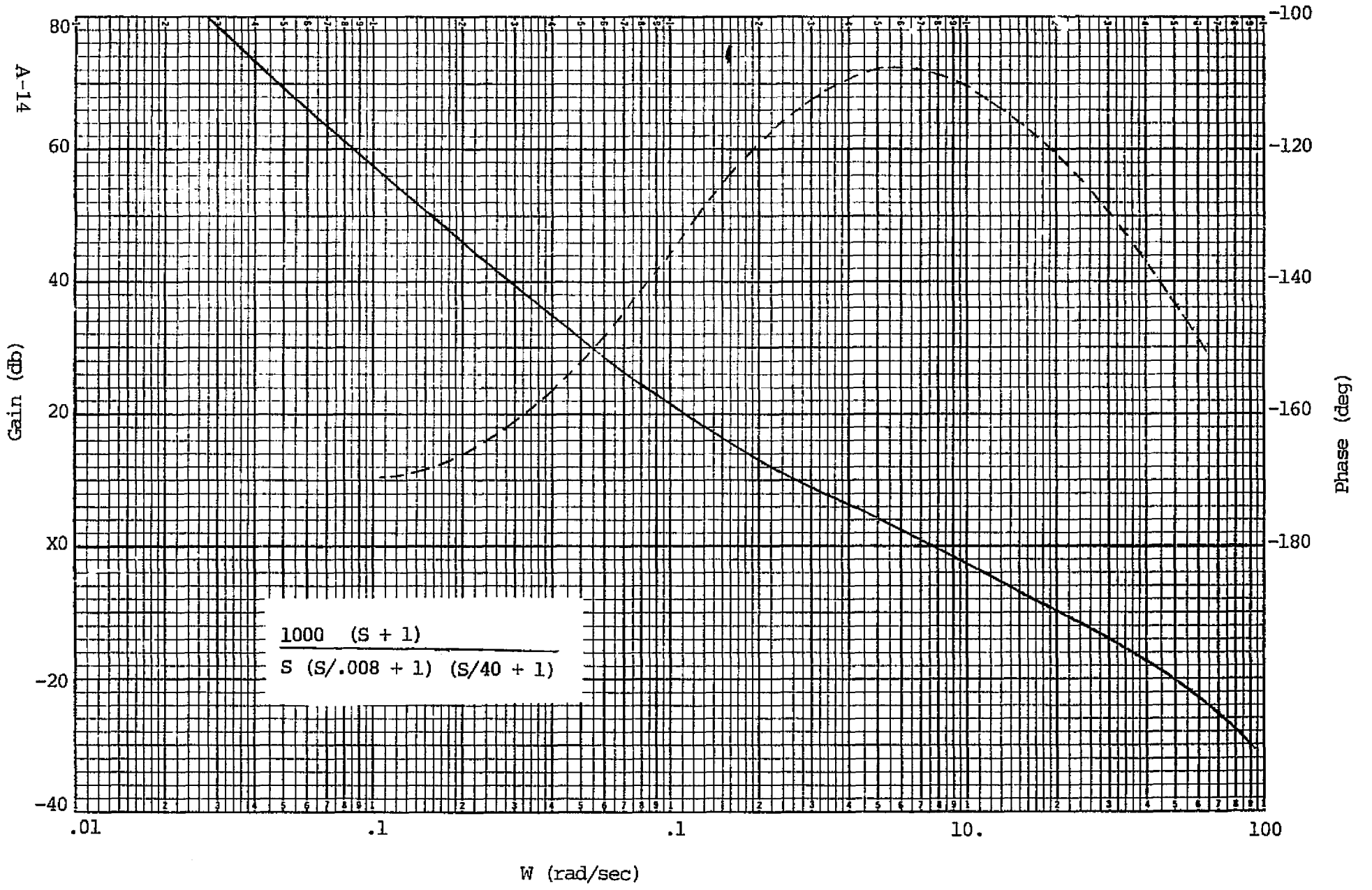

Figure 8 Baseline APS Open Loop Frequency Response

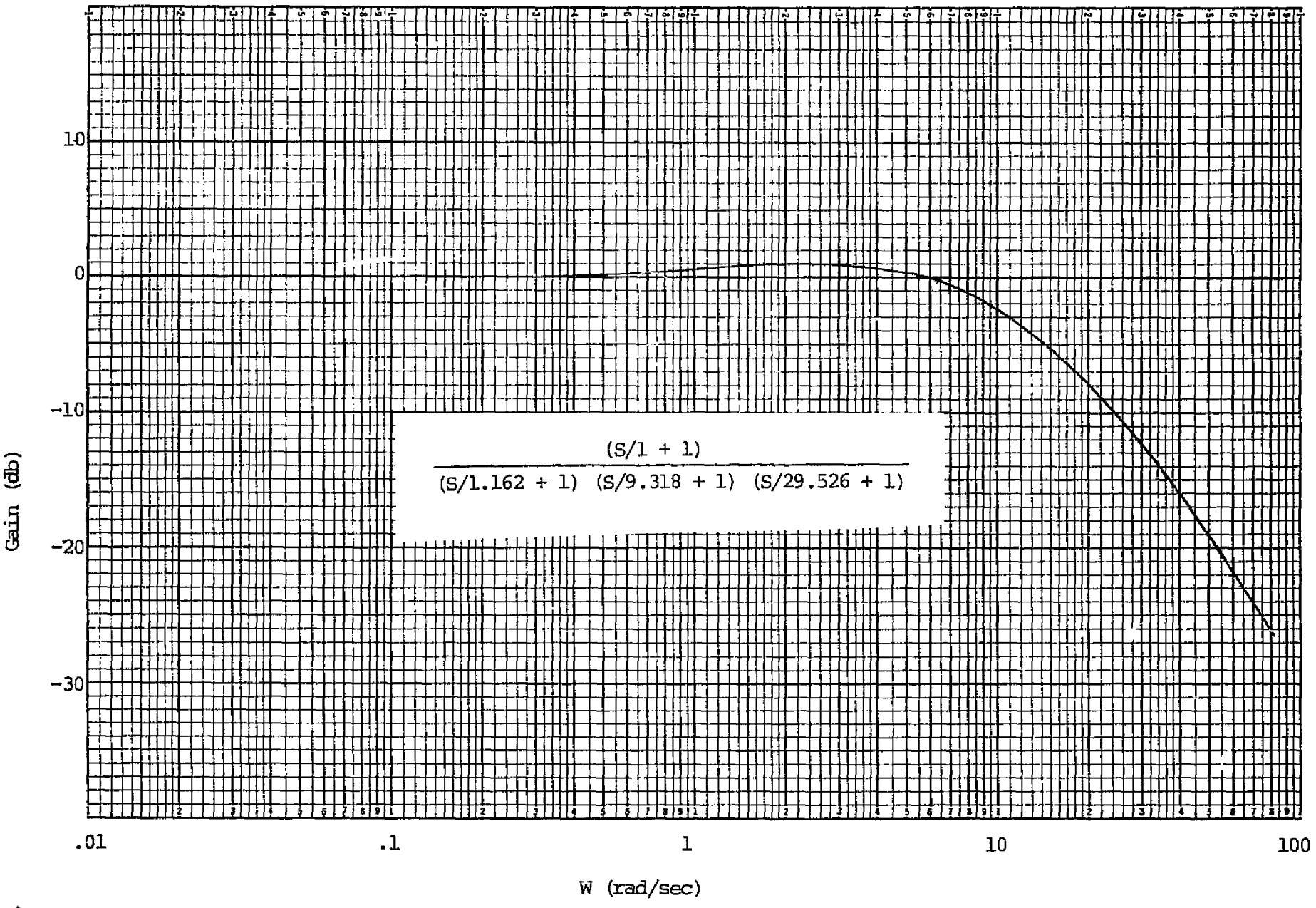

Figure 9 Closed Loop Frequency Response

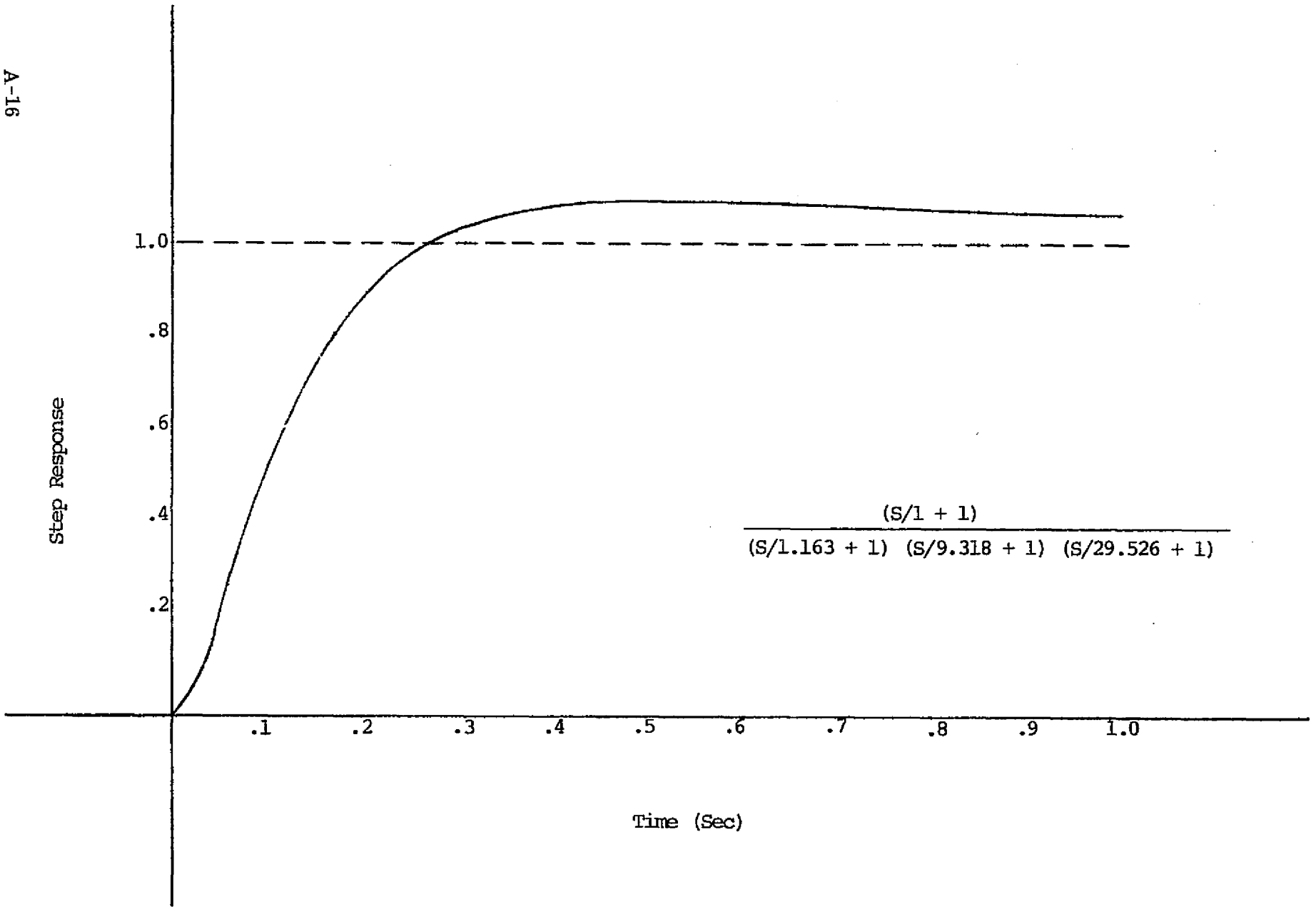

Figure 10 Unit Step Response

a constant angular rate; i.e., keeping the antenna boresight aligned with the ground station will require some angular acceleration. This angular acceleration will cause some increase in the tracking error; however, the angular acceleration is low and the above result indicates that the tracking error caused by the target motion will be small.

Disturbance Torque Response

An important consideration in the MWCE APS is the effect of disturbance torques introduced by shuttle motion. It is assumed that the shuttle is limit cycling between attitude error limits. When the attitude error limit is reached, thrusters are fired to reverse the shuttle angular rate. These thruster pulses generate shuttle motion that results in disturbance torques being applied to the APS gimbals.

The disturbance torque caused by shuttle motion can be shown to be:*

$$Td = l_E \, m \, \ddot{Z}g$$

where Td is the disturbance torque

l_E is the distance from the experiment center of mass and the gimbal axis

m is the mass of the experiment

$\ddot{Z}g$ is the gimbal acceleration.

$\ddot{Z}g$ depends on the shuttle motion and is given by:

$$\ddot{Z}g = \left(\frac{1}{m_s} + \frac{l_g \, l_t}{I_s} \right) F_t$$

where F_t is the thruster force used to control the shuttle attitude.

l_t is the moment arm from the thruster to the shuttle c.g.

l_g is the moment arm from the shuttle c.g. to the gimbal axis.

I_s is the shuttle moment of inertia.

m_s is the shuttle mass.

---

*This disturbance torque analysis is based on a similar analysis performed by Ball Bros. Research Corp. for the shuttle Small Instrument Pointing System (SIPS).

The following numberical values are used:

m_s = 5925 slugs

I_s = 5.8099 E6 slug ft^2

F_t = 36 lb.

l_t = 66 ft.

l_g = 30 ft.

l_E = 3 ft.

m = 6 slugs

yielding

$\ddot{Z}g$ = 0.0184 ft/sec^2

and

Td = .33 ft.lb.

The disturbance torque is not a step but rather a short duration pulse. The duration of the pulse can be determined from the time required to change the shuttle angular rate from +0.01 to -0.01 deg/sec. which yields a pulse duration of 0.86 sec.

To find the approximate gimbal attitude error caused by the shuttle motion, the disturbance torque pulse will be approximated by an impulse with strength (.33) (.86) = .28 ft. lb.

The response to the shuttle induced 0.28 ft. lb. disturbance torque impulse is shown in Figure 11. It can be seen that the peak antenna pointing error is about 0.06 deg. This is acceptable; however, for the preliminary design phase it would be desirable to have a slightly lower disturbance torque response. The disturbance torque induced pointing error can be reduced by increasing the control loop gain and bandwidth. This also increases the errors introduced by monopulse noise; however, the monopulse noise analysis indicates that there is some margin for increasing the bandwidth.

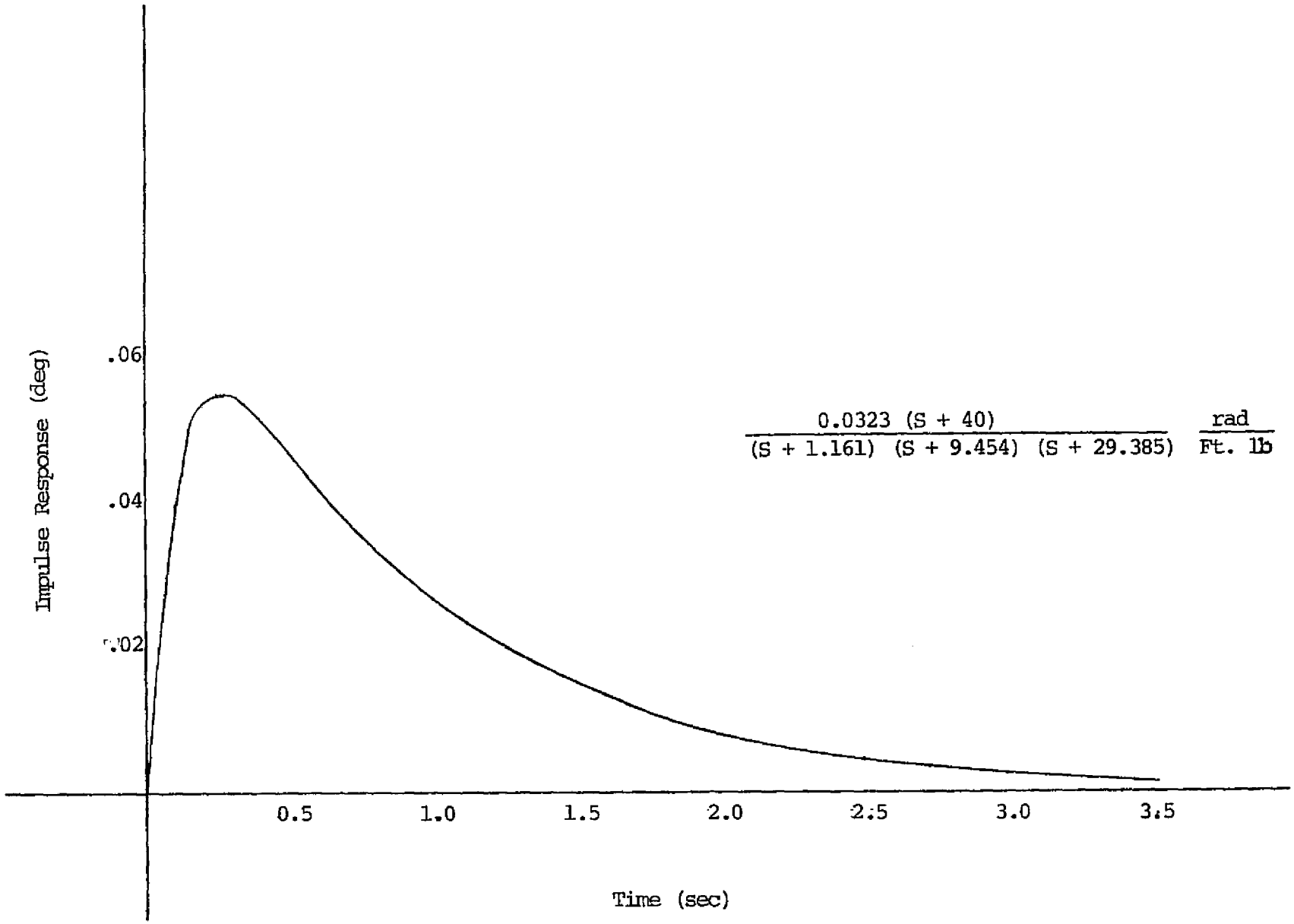

Figure 11 Disturbance Torque Impulse Response

Monopulse Noise Response

The antenna pointing error response to monopulse noise is given by the APS closed loop response.

$$\frac{\theta}{\theta_n}(s) = G_c(s)$$

It will be assumed that the monopulse noise is white with strength σ_n^2; thus the monopulse noise power spectral density (PSD) is uniform with frequency and has magnitude σ_n^2.

The 1σ pointing error caused by the monopulse noise, σ_θ, is then computed by:

$$\sigma_\theta = \sigma_n \left[\frac{1}{2\pi} \int_{-\infty}^{\infty} |G_c(j\omega)|^2 d\omega \right]^{1/2}$$

The integral in the brackets has been tabulated for rational algebraic transfer functions. For the baseline APS, the monopulse noise response can be computed to be:

$$\sigma_\theta = 2.15\, \sigma_n$$

A preliminary analysis of the MWCE monopulse tracking accuracy indicates that the monopulse noise will be quite low - 0.00016 deg (1σ). Thus, the 3σ antenna pointing error caused by monopulse noise is 3 (2.15) (.00016) = .001 deg for the baseline APS.

Other Considerations

1. Effects of Shuttle Angular Rate

Shuttle angular rates cause antenna pointing disturbance through the motor back emf (as shown in Figure 7) and through the bearing friction (not shown in Figure 7). Because of the relatively low shuttle angular rates, these disturbances are not expected to produce significant antenna pointing errors.

2. Antenna Stowing Maneuver

The MWCE antenna must be stowed and latched prior to shuttle deorbit and landing. The important requirement for the stowing maneuver is that the antenna be guided into the proper position for engaging the retention mechanism without striking any of the support structure. It appears that the baseline APS can support this requirement by employing the acquisition mode control configuration (i.e., control using the potentiometer) and selecting a proper sequence of control commands.

First the antenna would be oriented such that a single gimbal axis maneuver is required to complete stowing. The final stowing maneuver would then be executed as a series of small steps or a slow rate ramp until the antenna is in the desired position. This approach would avoid any significant control loop overshoot that would bump the antenna into the support structure.

An alternate approach for the final (i.e., single axis) stowing maneuver would be to modify the control loop compensation such that the loop is highly overdamped and responds to command inputs with zero overshoot. This approach would complicate the APS controller somewhat but simplify the stowing maneuver commanding.

3. MWCE/Spacelab Cable

The current MWCE design employs a flexible cable to provide power and signal communication between the gimbal mounted MWCE and the Spacelab. Care must be taken in the design of this cable to ensure that the cable induced disturbance torques do not generate large pointing errors.

APPENDIX B

MWCE-MOD II ANTENNA REQUIREMENTS ANALYSIS

The MWCE (Millimeter Wave Communications Experiment) must be capable of operating in various modes, including independent up and downlink modes, as well as bent-pipe transponder mode, where the uplink 30 GHz signal is translated to 20 GHz and retransmitted back to the ground. The transponder mode of operation sets the minimum gain requirements on the receiving and transmitting antennas, since this mode includes the tandem link loss of the cascaded up and down links.

The total round trip signal to noise ratio is expressed by the following equation:

$$SNR_T = \frac{SNR_1 \, SNR_2}{SNR_1 + SNR_2} \tag{1}$$

where, SNR_1 = Uplink minimum SNR

SNR_2 = Downlink minimum SNR

But, $SNR_1 = SNR_2 = 22.7$ dB, as defined by the requirements given earlier. Now if SNR_T is to be made equal to 22.7, then SNR_1 and SNR_2 must be increased by G'_1/G_1 and G'_2/G_2 respectively as shown in equation (2).

$$SNR_T = \frac{SNR_1 \, (G'_1/G_1) \, SNR_2 \, (G'_2/G_2)}{SNR_1 \, (G'_1/G_1) + SNR_2 \, (G'_2/G_2)} \tag{2}$$

where G_1 = One-way uplink 30 GHz antenna gain

G_1 = Two-way 30 GHz antenna gain requirement

G_2 = One-way downlink 20 GHz antenna gain

G'_2 = Two-way 20 GHz antenna gain requirement

Now since $SNR_T = SNR_1 = SNR_2 = 22.7$ dB, equation (2) becomes,

$$1 = \frac{G'_1 \, G'_2}{G_2 \, G'_1 + G_1 \, G'_2} = \frac{G_2}{G'_2} + \frac{G_1}{G'_1} \tag{3}$$

Now let $G'_1 = G'_2/K_o$ and substitute into (3)

Therefore,

$$G'_2 = G_2 + G_1 K_o \tag{4}$$

and

$$G'_1 = G_1 + G_2/K_o \tag{5}$$

Equations (4) and (5) show that the minimum two-way (30 GHz and 20 GHz) antenna gain requirements for the transponder mode is a function of both the uplink and downlink minimum gain requirements for the one-way links. For the equal gain case, where $K_o = 1$, the minimum gain requirement for the two-way link is simply the sum of the one-way link antenna gain ratios, or,

$$G_1' = G_2' = G_1 + G_2$$

The analysis which follows is performed to determine the one-way uplink and downlink antenna gains (G_1 and G_2) as a function of elevation angle, and angle off Nadir for an orbiting Shuttle at 400 km altitude. The results are plotted in Figure B-1.

Using the results in Figure B-1, the 30 GHz and 20 GHz antenna gain requirements for the two-way link are plotted in Figure B-2, for equal gain case, or $K_o = 1$.

Figure B-2 shows the equal aperture case when $K_o = 1/2.25$.

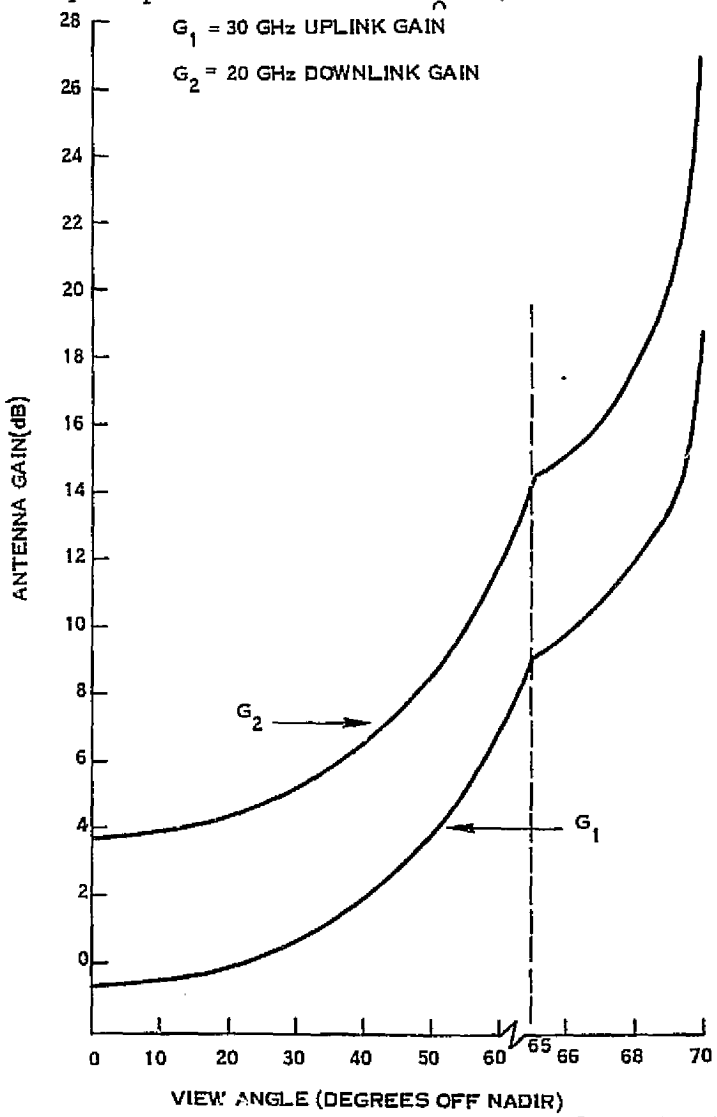

Figure B-1. Antenna Gain Requirements for One-Way Links Only

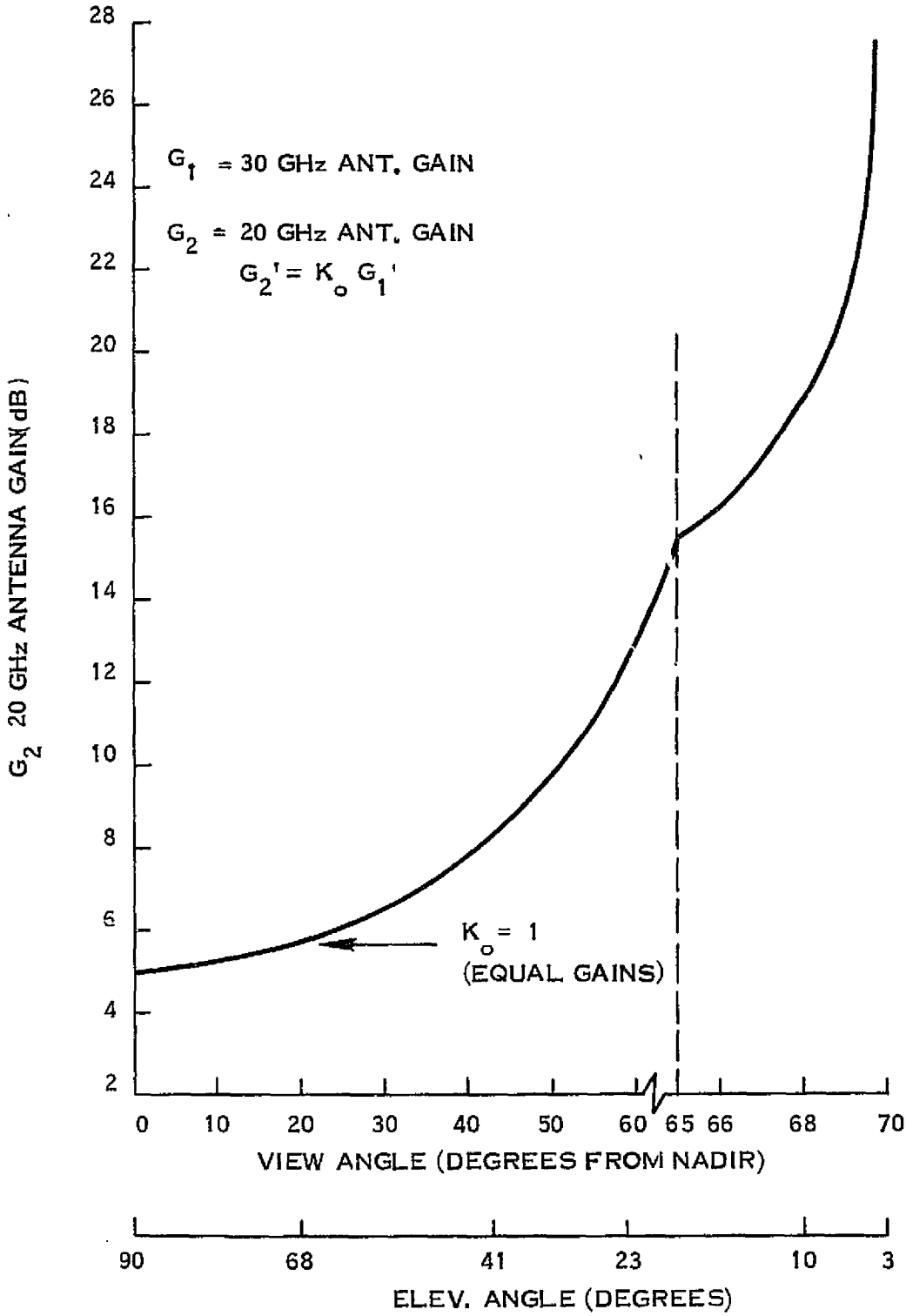

Figure B- 2. Antenna Gain Requirements for Two-Way Transmission Link, Equal Aperture Case

G_1 = SNR + BW - 228.6 (Boltzman's Constant) + T_s + L + L_p - EIRP

Parameters

G_1 = 30 GHz Receiving antenna gain

SNR = 22.7 dB in 50 MHz bandwidth

BW = Signal bandwidth, 77 dB-Hz

T_s = System effective receiving temperature, 32.8 dB-^oK

T_L = 0.5 dB, antenna pointing loss

EIRP = Ground station uplink signal EIRP = 79.5 dBW

L = Total link losses, including the following,

-10 log $(1/4\ \pi\ R^2)$, Path spreading loss, dB

-10 log $(\lambda^2/4\pi)$, effective area, isotropic antenna

$\frac{0.3195}{\sin\theta}$, atmospheric loss, dB (to 3^o Elevation)

where

$R = \cos(\theta + \alpha)/\cos\theta\ (R_e + h)$, range in km

$\alpha = \sin^{-1}\left(\frac{R_e}{R_e + H}\right)\cos\theta$, degrees, view angle off Nadir

θ = Elevation angle, degrees

R_e = Earth's radius, 6374 km

h = Shuttle altitude, 400 km

or

$G_1 = 175.1 - 10 \log (1/4\ \pi\ R^2) - 10 \log (\lambda^2/4\ \pi) + 0.3195/\sin\theta$, (dB)

$= -175.1 + L$ (dB)

Atmospheric Loss = $A_L = .43/\sin\theta$, dB

Atmospheric Loss Ratio = $A_R = 10^{A_L/10}$, Ratio

Ground System Effective Temperature = $T_S = \frac{(A_R-1)}{A_R}$ $290 + 50^{\circ} + (NF-1)\ 290$

or $T_S = \frac{(A_R-1)}{A_R}$ $290 + 488$

Therefore,

$$G/T = 57 - 10 \text{ Log } T_S$$

Downlink Antenna Gain

$$G_2 = -P_O + L_L + L + L_p - G/T - 228.6 + BW + SNR + \text{Transponder Loss}$$

Where

P_O = 10 dBW (Saturated TWT)

L_L = Line Loss, 1.0 dB

L_p = Pointing Loss 0.5 dB

L = Space Loss at 20 GHz including atmospheric loss at $0.43/\sin\theta$, dB

Transponder Loss = $\frac{SNR_{TR}}{SNR_{TR}+1}$ = 0.2 dB for 500 MHz Transponder (Power Robbing of Transponder EIRP by Noise for Saturated TWT) or $G_2 = 137.2 - G/T + L$ (dB)

APPENDIX C

EEE ANTENNA PATTERN AND FOOTPRINT ANALYSIS

The beam formations and antenna arrangements of the Electromagnetic Environmental Experiment (EEE) on board the Space Shuttle are used to monitor RF radiation from emitters located on the earth. The antenna arrangements selected use as much existing hardware as possible. The EEE-MOD II antennas handle the frequency bands of 0.1215 - 2.7 GHz plus the 2.7 - 43.0 GHz range. Sketches of the EEE-MOD II antenna arrangement are shown in Section 3.0. Sections 1.0 and 2.0 describe the RF parameters and the specific levels of radiation.

1.0 SENSITIVITY ANALYSIS

The EEE antennas receive signals (at specific frequency bands) from many sources of radiation. These sources include harmonics of other sources, residues of spectra of other bands, intermodulation components, etc., with signals which vary considerably in amplitudes, phases and directions of arrival.

A source signal field level may be represented by

$$\bar{A} = \bar{A}_n \, e^{i\varphi n} \qquad 1)$$

Where $\bar{A}_n$ is the amplitude vector of the source signal and ϕn is its phase. The total received level, from numerous sources in the antenna field of view at the antenna terminals is given by

$$\bar{A}_s = \sum_{n=1}^{N} \bar{A} \, D_n \, \frac{e^{ik \, Tn}}{Tn} \quad , \qquad 2)$$

where Dn is the antenna gain in the direction of the source of radiation, $k = 2\pi/\lambda$, Tn is the path length distance to the source, N is the total number of sources and λ is the wave length of electromagnetic radiation.

If $T_n = T_o + tn$,

where T_o is the path length from the antenna phase center to a point of observation on earth along the direction of the main beam, and tn is the differential path length to other points of observation away from that direction, the signal level at the antenna terminal is given by

$$\bar{A}_s = e^{ikTo} \sum_{n=1}^{N} \frac{\bar{A}n\ Dn}{Tn} e^{i\ (\varphi n + kt_n)} \qquad 3)$$

In case of uniformly distributed sources of equal amplitudes, neglecting phase and path length variations among the sources, the received signal level is

$$\bar{A}_s = e^{ikTo} \sum_{n=1}^{N} SnD_n = \bar{K} \iint_{\Omega} Dn\ dS, \qquad 4)$$

where $\bar{K}$ is a representation of elementary signal amplitude and polarization, $\bar{K}$ is equal to $\left(\frac{\bar{A}n e^{ikTo}}{T_o}\right)$, dS is the elementary source sampling area and Ω is the solid angle of the antenna pattern, in the field of view.

Equation (4) represents the conventional antenna far field pattern, the gain of which is given by

$$G = \frac{4\pi}{|\bar{K}|^2 \iint_{\Omega} (Dn)^2\ dS} \qquad 5)$$

The smaller the value of the integration the higher the antenna gain. When the path length of the signal is taken into consideration (with uniform amplitude and phase of sources)

$$\bar{A}_{st} = \frac{\bar{A}\ e^{ikTo}}{T_o} \sum_{n=1}^{N} \frac{D_n}{K_T} e^{iktn}\ , \qquad 6)$$

where K_T is the relative path length variation factor. The amplitude variations reflected in the path length factor K_T reduces the signal level from sources of radiation away from nadir. This reduces the footprint length and gives an effect similar to an enhancement of the antenna gain.

When the sources of radiation may be considered to be a large number of random amplitude and phase distributed emitters, the RMS value of $\bar{A}_S$ is:

$$\bar{A}_{sm} = \frac{1}{\sqrt{2}} \left(\sum_{n=1}^{N} \bar{A}_{sn}^2 \right)^{1/2}$$

$$= \sqrt{\frac{N}{2}} \; \bar{A}_{so} \quad ,$$

where $\bar{A}_{So}$ is the RMS value of $\bar{A}_S$. This RMS value is strongly affected by the path length variation.

In evaluating the sensitivity requirements of the EEE receivers two different sensitivity values are convenient. The simplest is the sensitivity to isolated sources. The second is that applicable when the antenna footprint is occupied by huge mass of radiators, distributed over the area.

For this reason evaluations are made of equal sensitivity lines defining the footprints of the EEE beams to determine their coverage areas on the ground and their coverage area relative to nadir pointing beam footprints. The analysis is based on the outline configuration of Figure 1. Summary charts which give complete information on the footprint configurations are shown in Figures 2, 3, 4, 5, 6, 7, and 8. These charts are generated using a computer program (EEEDBX) which determines the equal sensitivity contour of the antenna at any chosen level relative to its peak sensitivity. The program determines the level of the peak and its relative location to nadir. The input parameters to the program are the beam tilt angle (off nadir) and the 3 dB beamwidth. These charts show that the extent of the equal sensitivity lines of the footprint is more sensitive to the beam tilt angle for smaller beamwidths.

Figure 1. Geometry of Footprint Configuration

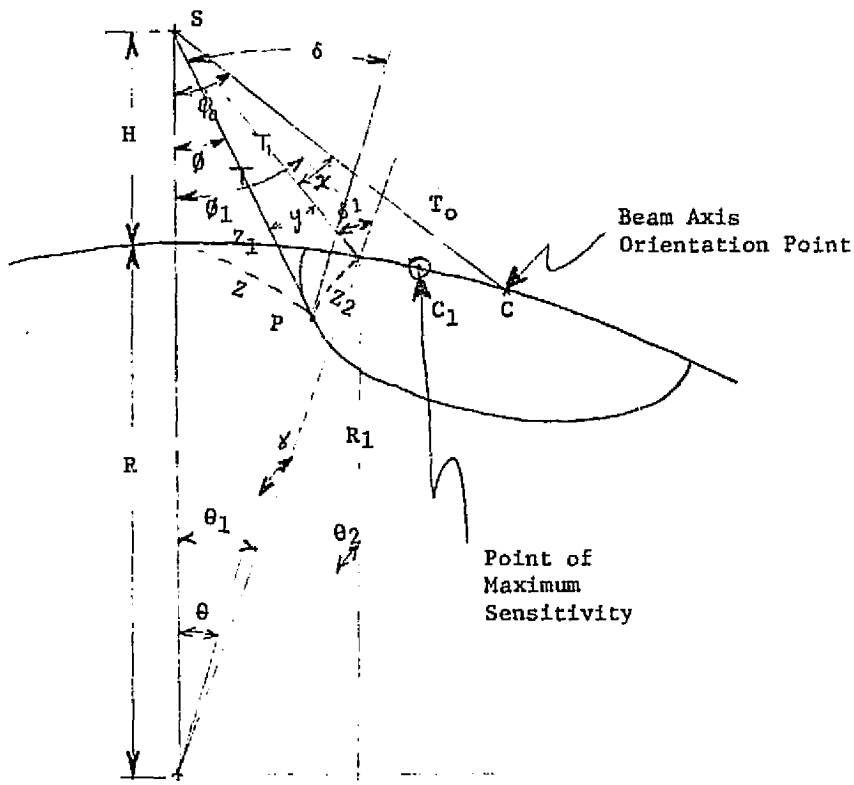

R = Radius of Earth
H = Height of the Shuttle
T_o = Free Space Distance Between the Shuttle and the Beam Axis Orientation Point (C) of the Beam = $R \sin\left\{\sin^{-1}\left[\left(\frac{R+H}{R}\right)\sin\phi_o\right] - \phi_o\right\}/\sin\phi_o$

ϕ = Angle from Nadir to any Point on the Footprint (P)
$= \cos^{-1}(\cos\phi_1 \cos y)$
x and y are the elevation and azimuth angles off the beam axis.
z = Arc Distance OP = $R\theta$, $Z1 = R\theta_1$ and $Z_2 = R$
$\theta = \sin^{-1}\left[\left(\frac{R+H}{R}\right)\sin\phi - \phi\right]$
Z_1 and Z_2 are the Arc Length Coordinates of P, on the Surface of the Earth
The Radiation Pattern (Centered at C_1) is given by

$$E = -3\left(\frac{\sin\left(\sqrt{x^2 + y^2}\right)}{\sin(\alpha/2)}\right)^2 T_o/T,$$

α = 3 dB Beamwidth,
and $T = SP = R \sin\left\{\sin^{-1}\left[\left(\frac{R+H}{R}\right)\sin\phi\right] - \phi\right\}/\sin\phi$

Figure 2

FOOTPRINT AREA AS FUNCTION OF
THE TILT ANGLE OFF NADIR

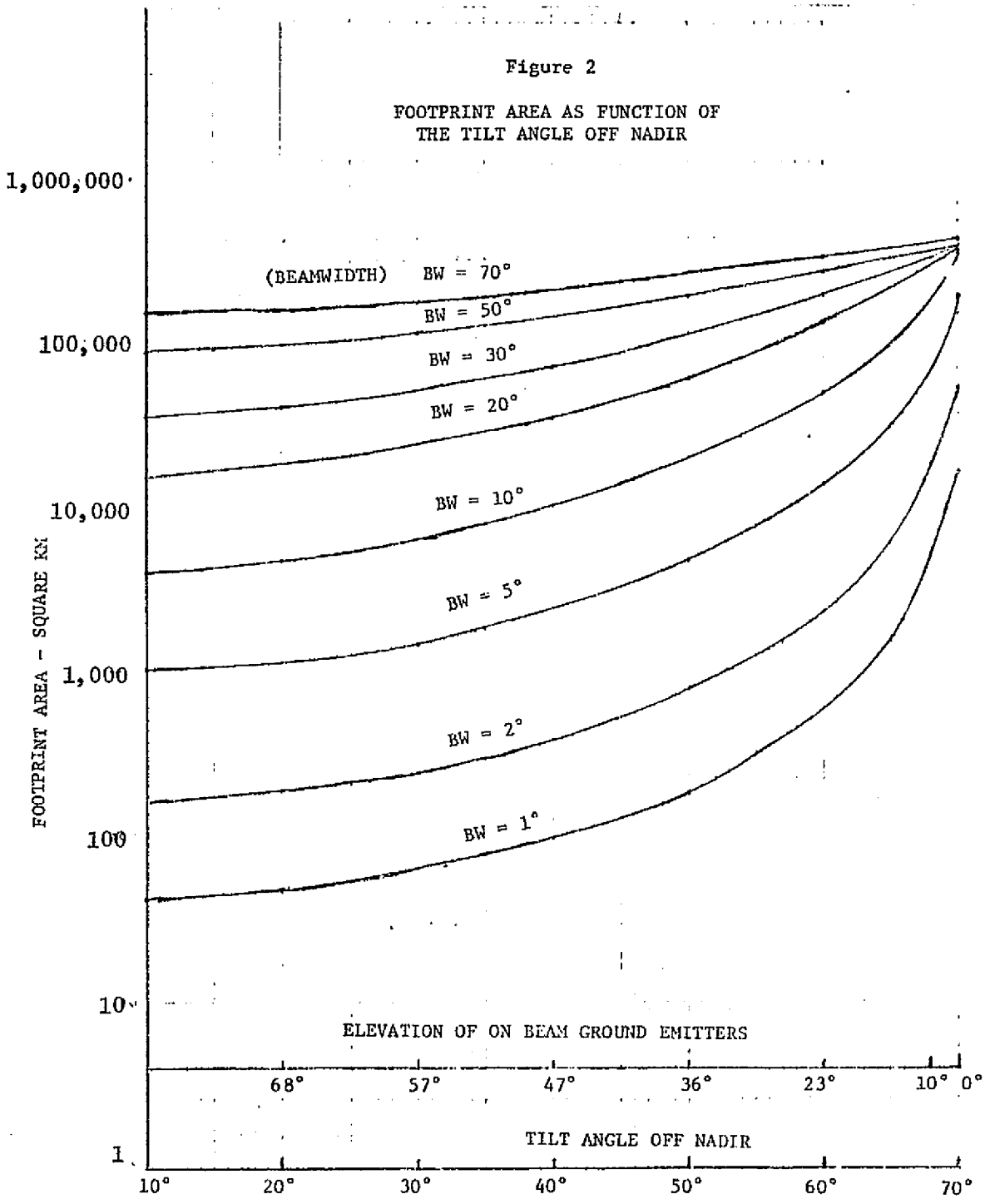

Figure 3

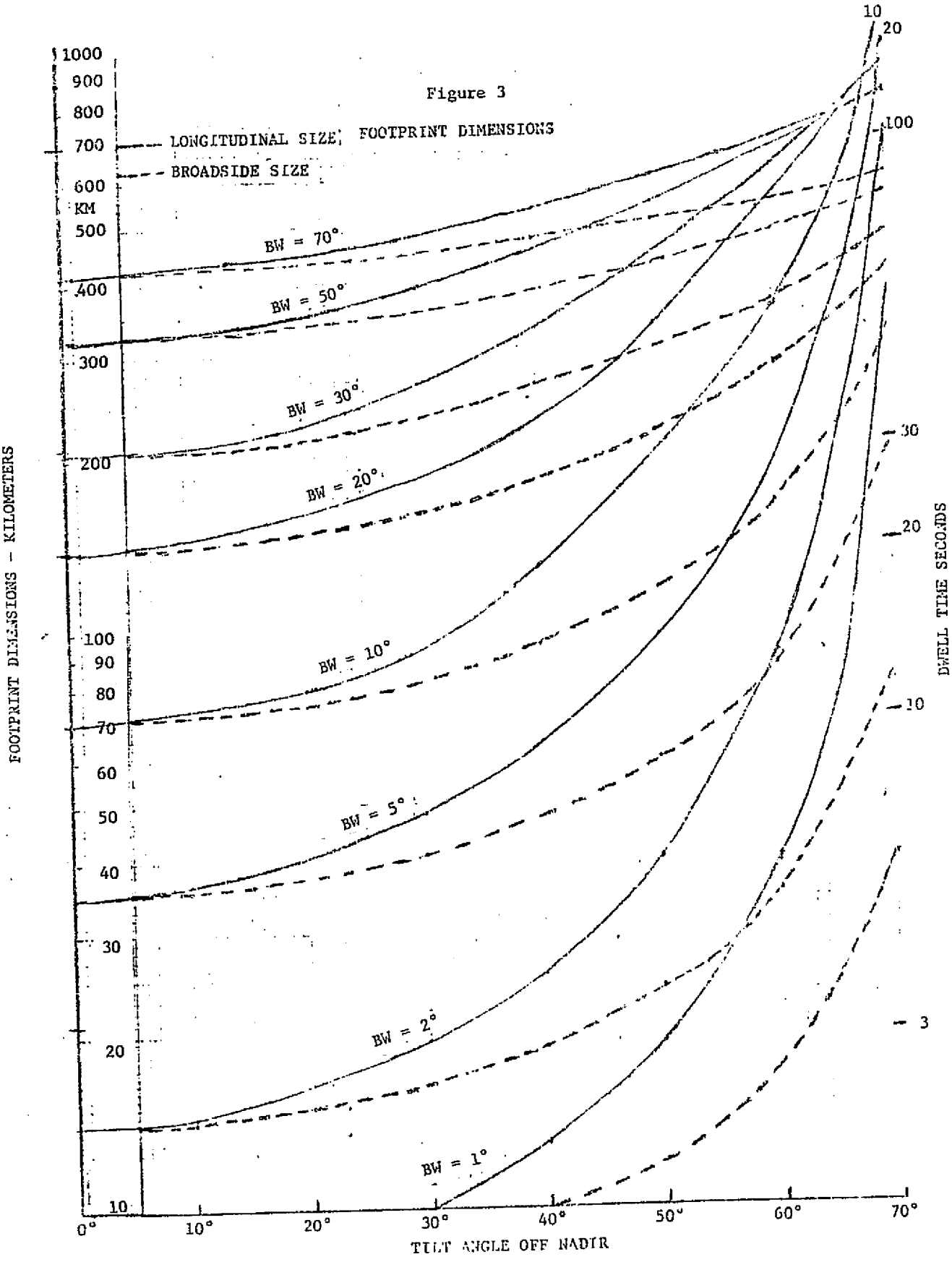
LONGITUDINAL SIZE, FOOTPRINT DIMENSIONS
BROADSIDE SIZE
BW = 70°
BW = 50°
BW = 30°
BW = 20°
BW = 10°
BW = 5°
BW = 2°
BW = 1°
1000
900
800
700
600
KM
500
400
300
200
100
90
80
70
60
50
40
30
20
10
10
20
100
30
20
10
3
0°
10°
20°
30°
40°
50°
60°
70°
TILT ANGLE OFF NADIR
FOOTPRINT DIMENSIONS - KILOMETERS
DWELL TIME SECONDS

Figure 4

ANGLE FROM BEAM AXIS TO DIRECTION
OF MAXIMUM SENSITIVITY

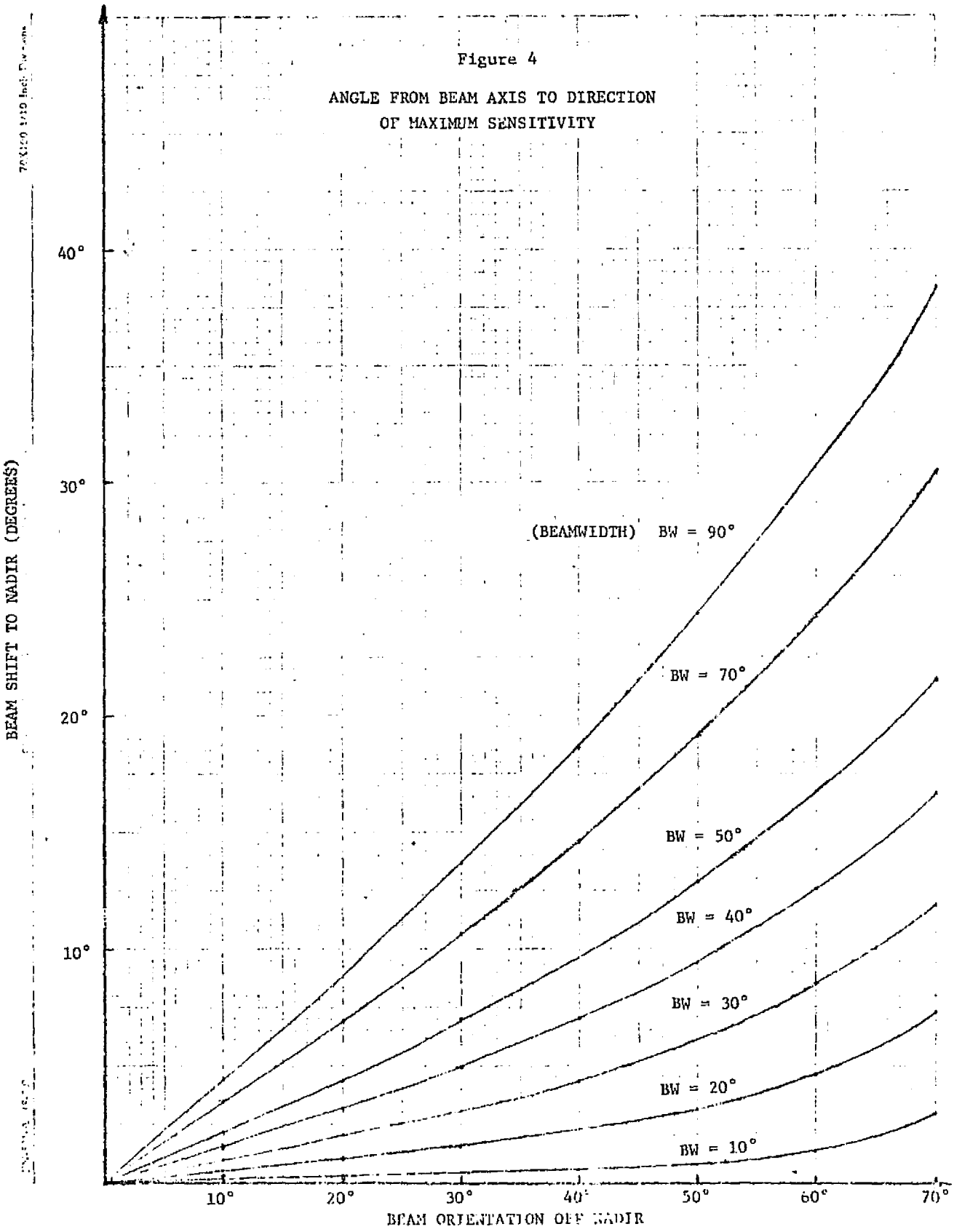

Figure 5

ANGLE FROM BEAM AXIS TO DIRECTION OF MAXIMUM SENSITIVITY

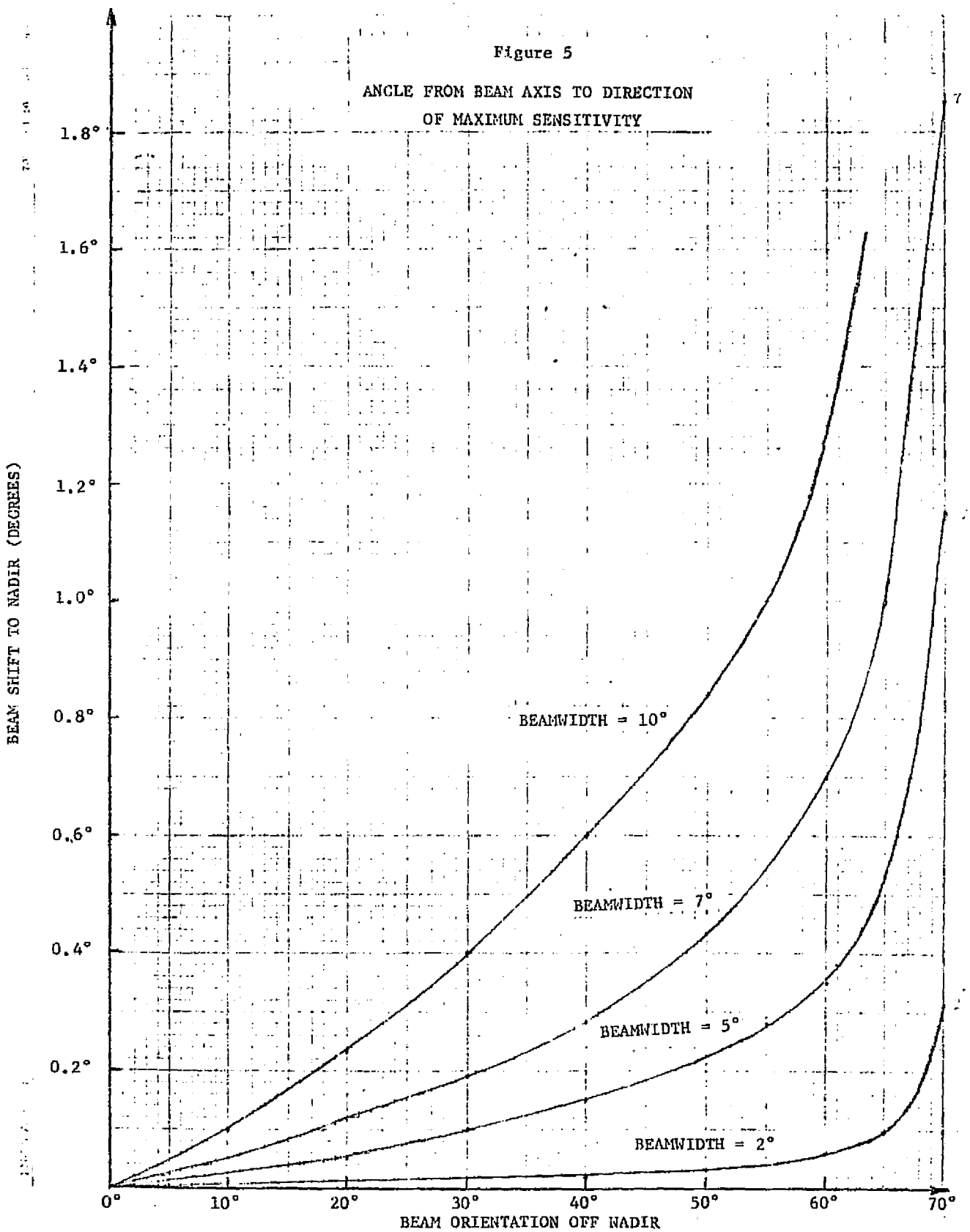

Figure 6

DIAMETER OF NADIR - POINTING ANTENNA FOOTPRINT

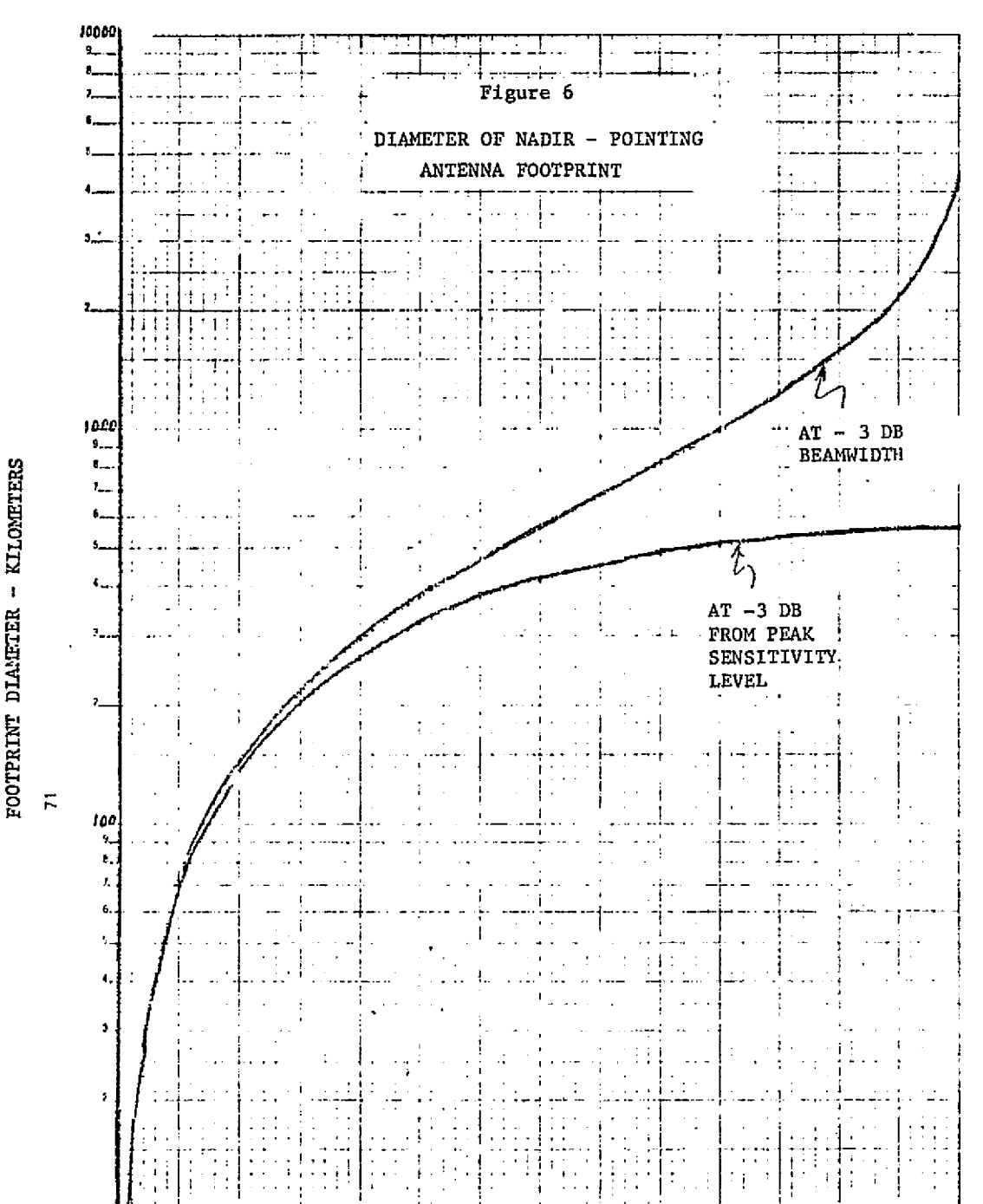

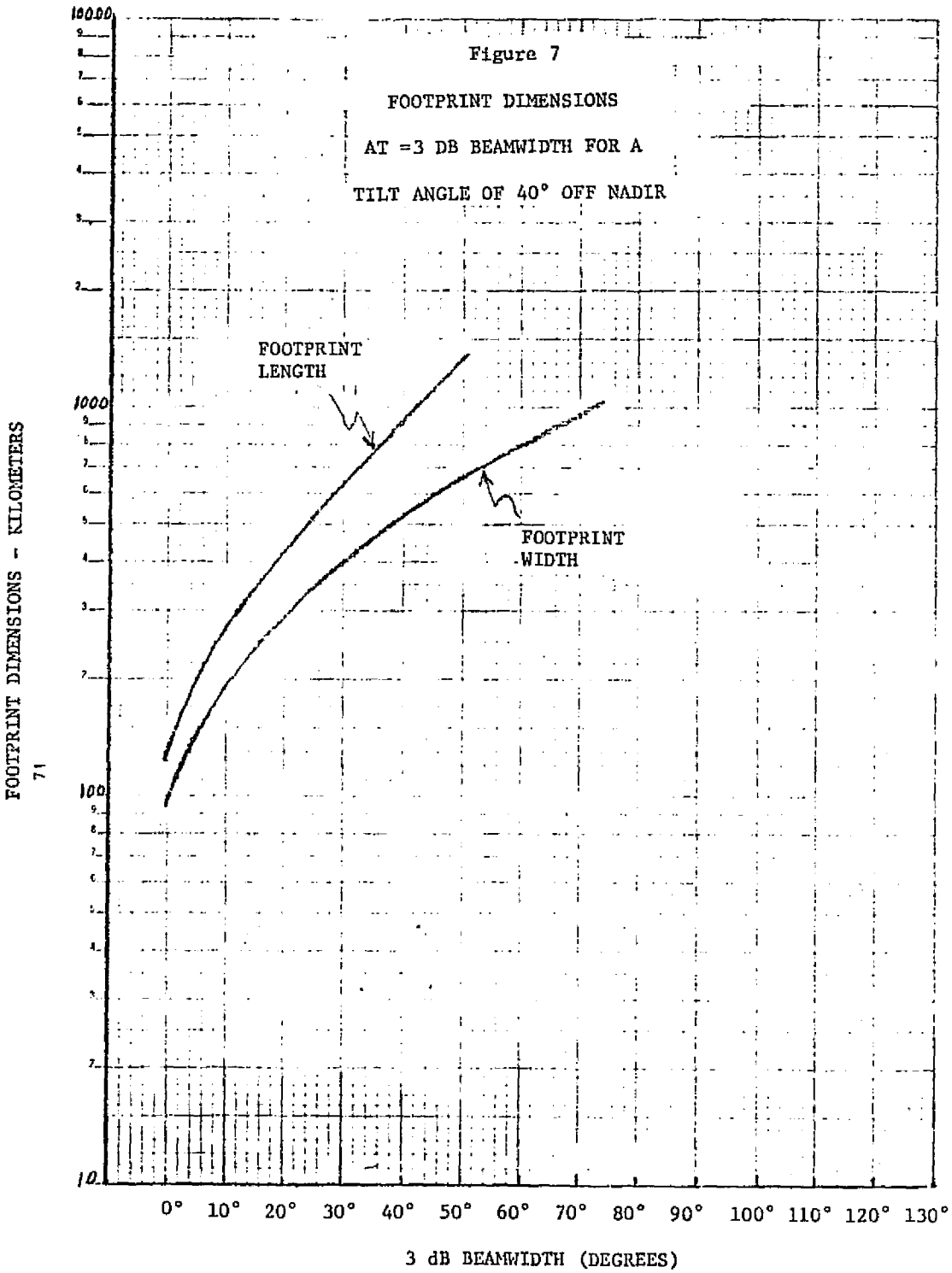
Figure 7
FOOTPRINT DIMENSIONS
AT =3 DB BEAMWIDTH FOR A
TILT ANGLE OF 40° OFF NADIR
FOOTPRINT LENGTH
FOOTPRINT WIDTH
FOOTPRINT DIMENSIONS - KILOMETERS
71
10000
1000
100
10
0° 10° 20° 30° 40° 50° 60° 70° 80° 90° 100° 110° 120° 130°
3 dB BEAMWIDTH (DEGREES)

Figure 8

-3 dB SENSITIVITY FOOTPRINT AS FUNCTION OF BEAMWIDTH FOR A TILT ANGLE OF 40° OFF NADIR

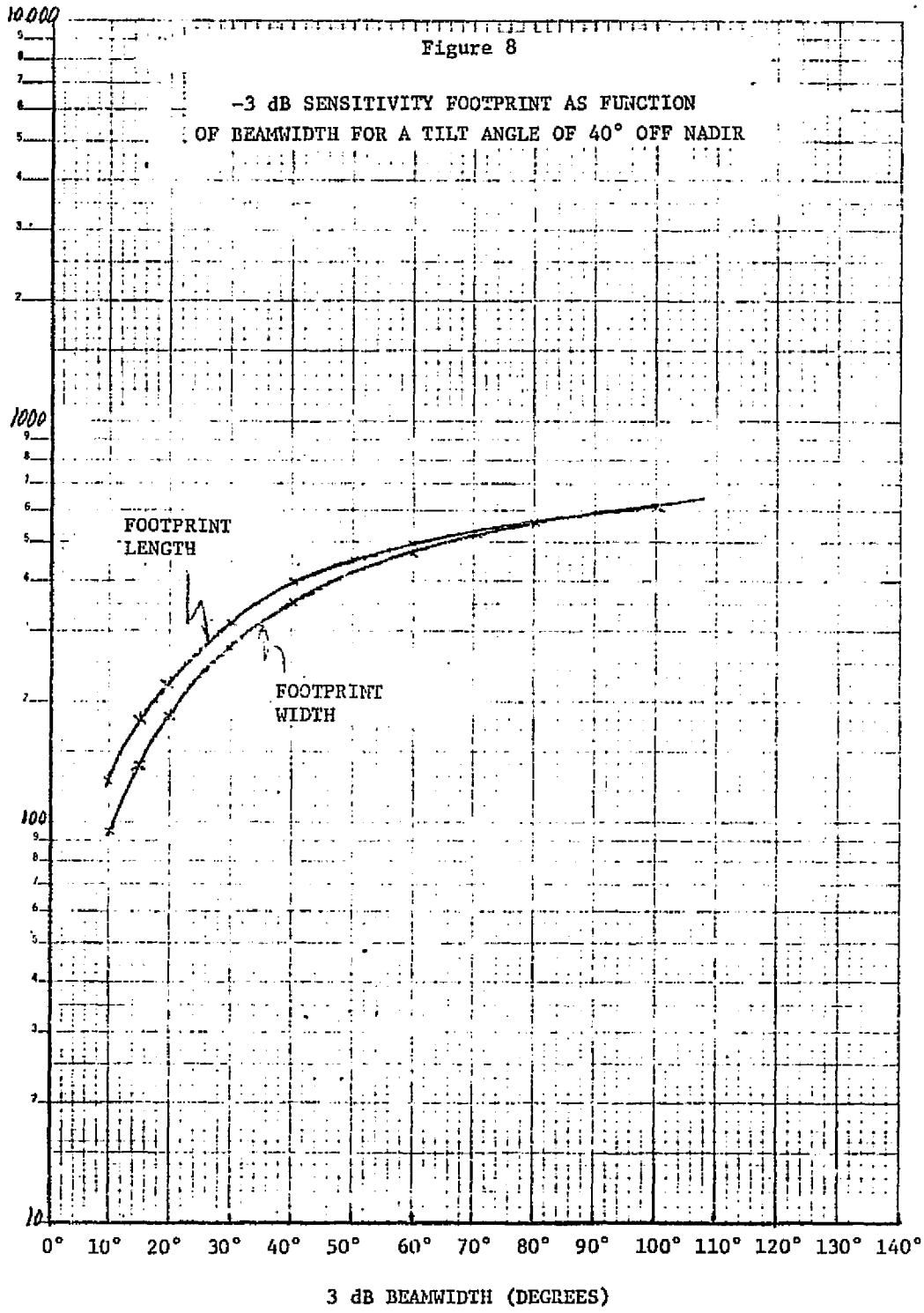

Another computer program has been developed to determine the equal sensitivity contours of specific antennas (mainly reflector antennas). In addition this program (EEEFF) performs an integration of the area within the equal sensitivity contour for the evaluation of effective sensitivity improvements due to a multiplicity of sources. A third program (DWELL 4) calculates the link parameters, including the dwell time on targets at any equal sensitivity level, the EIRP level (in dBW) and the power flux density associated with any antenna configuration (especially reflector antennas).

In order to calculate the sensitivity of the EEE at specific frequencies, several factors must be taken into consideration:

1. The dwell time is determined by the size of the equal-sensitivity (-3 dB) footprint contour lines. This is evaluated from the tilt angle off nadir and the choice of the antenna configuration and aperture size.

2. At low frequencies, where many sources of radiation are expected within the beam footprint, and where the noise figure and path loss are relatively low, wide beams looking near nadir are expected to yield adequate performance.

3. At higher frequencies the high path losses and noise figures of the receivers required higher gain antennas with narrow beamwidths, which reduce considerably the dwell times on the sources. To overcome this problem an antenna tilted in angle from nadir is desirable. The tilt angle enhances the intersection probability of radiating sources because of the larger footprint generated. This, however, is accompanied by increase in the path loss of the signal and an "optimum tilt angle" gives the best compromise.

2.0 DESCRIPTION OF CURRENT EEE PARAMETERS

2.1 EEE-MOD I ANTENNA ARRANGEMENTS

The EEE-MOD I configuration uses four antennas as shown in Figure 4-7. The main RF parameters of these are described in Table 1. The radiation patterns and the corresponding equal sensitivity lines, of the 0.7 meter dish, are computed (using the EEEFF computer program) and projected as footprints on the earth surface, from the Shuttle altitude of

TABLE 1

MOD I ANTENNA PARAMETERS*

ANTENNA TYPE	FREQUENCY RANGE MHz	NOMINAL GAIN DBI	NOMINAL 3 DB BEAMWIDTH
VHF Log Periodic 1.3 m x 1.5 m	121.5 - 243	7	65° x 95°
UHF Array 1.0 m x 1.3 m	399.9 - 470	12.5	43° x 22°
S-Band 0.7 m Dish (with a cavity backed spiral as a feed, preliminarily selected AEL "ASN113A"	806 - 2700	12-23	32° - 10° (or 40° - 10°)**
S-Band Conical Helix 0.17 m Conical Spiral, wide beam	600 - 2700	8	70°

*All the antennas handle right hand circular polarization.

**The large beamwidths are applicable to an offset antenna configuration with minimal blockage.

400 Km. (The available MOD I parameters were used in the initial program to prove its validity.) A tilt angle of this antenna may be selected in order to optimize its earth coverage at the high frequencies. At low frequencies, with large beamwidths, the nadir orientation of MOD I antennas, especially the log periodic, appears to be adequate. As an example of this situation, from Figure 3, equal sensitivity circles of 320-420 Km correspond with 50°-70° beams looking at nadir. In order to increase the size of this footprint to 500 Km, which is the approximate separation distance between the orbital tracks of the Space Shuttle, a beam tilt angle of more than 45° is needed. With such an antenna tilt angle, the sensitivity at the -3 dB level produces the same result as the sensitivity at the -6.5 dB level of the nadir looking beams. The -6.5 dB line of the nadir looking beams is at a beamwidth of 75° and occurs at a footprint diameter of 618 Km, which is larger in size than the footprint size at the tilt angle of 45°.

The narrower the beamwidth the greater the area gain resulting from the use of tilted beams. At a beamwidth of approximately 20° the area gain factors of the tilted beams are almost equivalent to the space attenuation factors. For narrower beams the area gain factors increase faster than the space attenuation factors. This phenomenon is easily recognizable from the area factors of Figure 2 for several antenna beamwidths.

The 0.7 meter dish has range of beamwidths of 40°-10° which yield high-tilt gains at high frequencies and flat-tilt gains at low frequencies. This effect, added to the gain factor considerations of the antenna beam, yields EIRP sensitivity levels which have minor differences between high and low frequencies (at nadir or at 60° tilt angle). The major advantage at tilt angles is the capability of receiving multiple signals (especially at high frequencies) due to multipath effects and hence increases the probability of using the higher multiple-source signal-gain factors. (The multiple-source gain of the antenna = the nominal gain plus beamwidth gain factor plus the footprint area-gain factor).

2.1.1 Antenna Dish Configuration Used

1. A 0.7 m center-fed dish with (F/D) = 0.5 is used.

2. The feed tentatively selected is the AEL "ASN113A," cavity-backed Archimedes spiral, having a diameter of 8.88 in. (25.55 cm).

2.1.2 Pattern and Footprint Computations

A radiation pattern computer program (EEEFF) handled the following:

1. Parameters of a circular feed, focused at all the frequencies, with effective diameters as follows:

Frequency (GHz)	0.806	1.215	1.3	1.74	2.43	2.7
Feed Diameter (Cm)	30.48	26.67	25.40	21.59	15.24	12.70

2. Radiation feed patterns similar to the H-plane patterns of horns having the diameters of the previous table are used. Comparison is shown in Figure 9 between the computed gains and the practical gains of AEL ASN113A cavity backed spiral.

3. Radiation pattern computations (with or without the path loss considerations) with any arbitrary central blockage. (The blockage used is 22.9 cm of a central disk).

4. In addition to computations of the illumination efficiency (which contains the aperture taper, spillover and blockage losses) a 90% efficiency is assumed for design defects (such as surface roughness, defocusing, VSWR, etc.). Moreover, a 1 dB is subtracted to accommodate for feed line and antenna feed losses. The final gain numbers at different frequencies are tabulated in Figure 10.

5. Computations of the earth surface coordinates (related to the nadir point), which correspond to the dB level of the antenna pattern (at any tilt angle from nadir). This is shown in Figure 11.

Figure 9

GAIN PERFORMANCE OF CAVITY BACKED SPIRAL FEED

OF THE 0.7M DISH OF MOD I EEE

CENTER FED ANTENNA

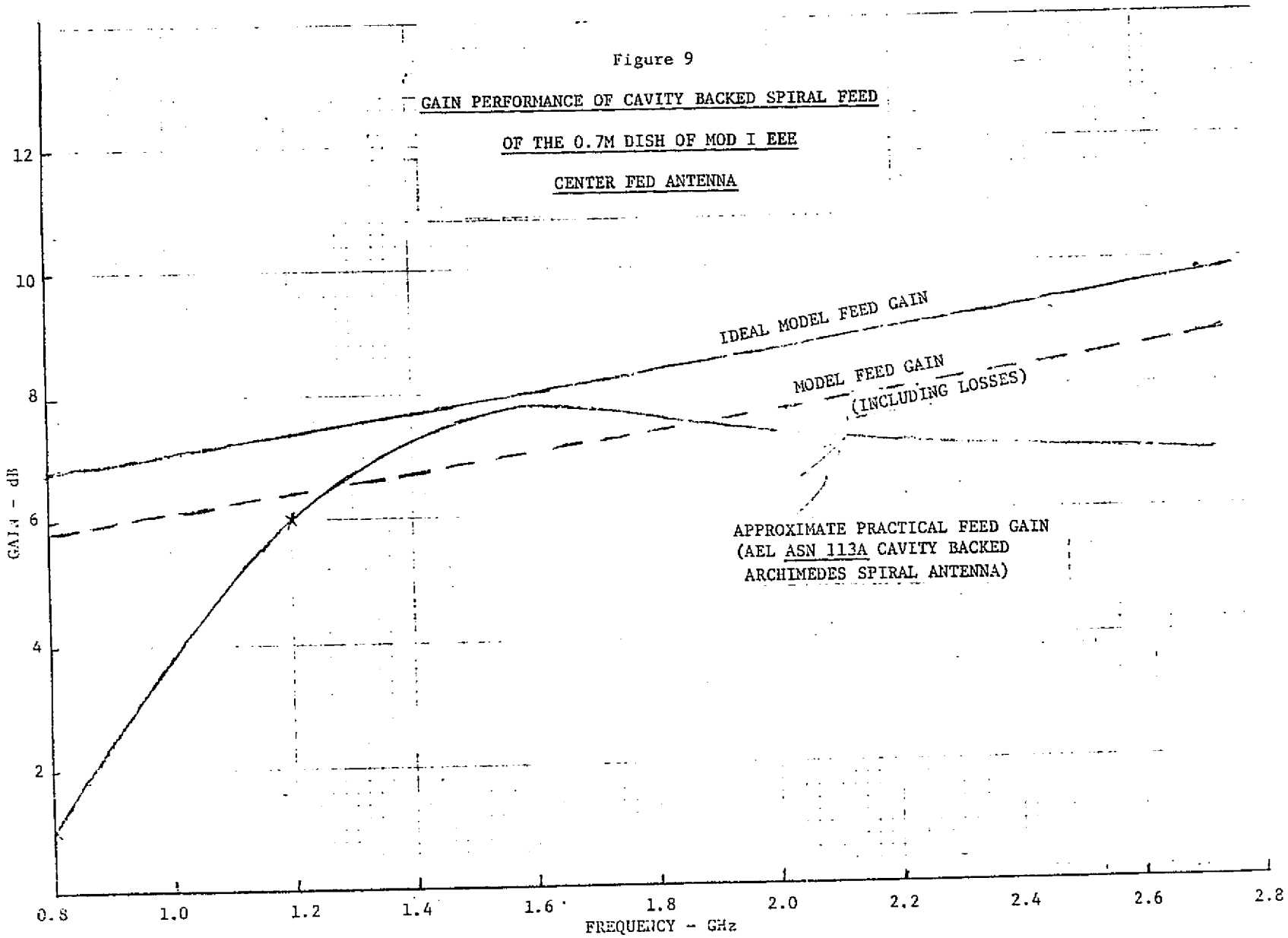

Figure 10

SENSITIVITY GAIN IMPROVEMENT OF 0.7M DISH
USING PATTERN INTEGRATION AND
INCLUDING PATH LENGTH EFFECTS
(ASSUMING UNIFORMLY DISTRIBUTED EMITTERS)

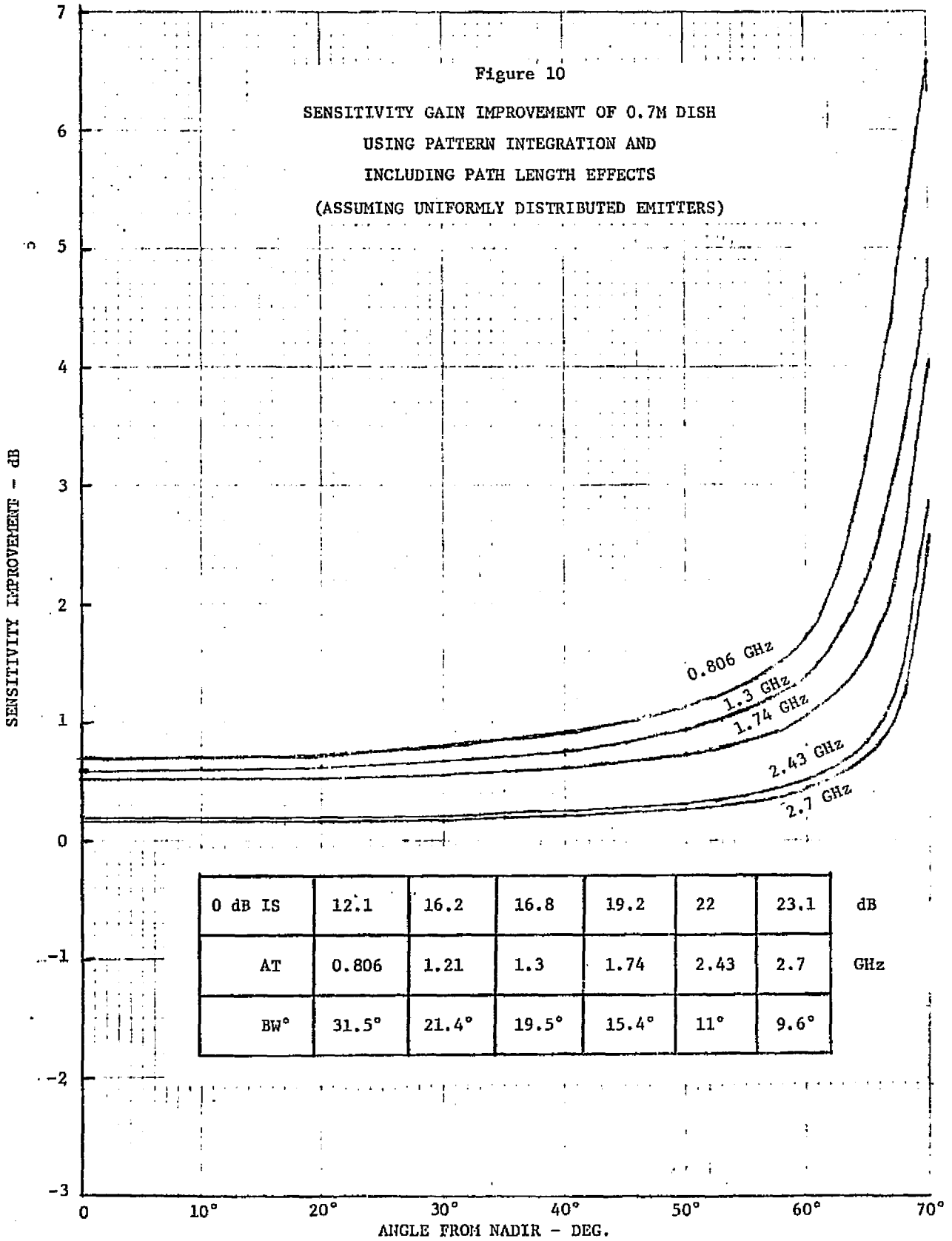

0 dB IS	12.1	16.2	16.8	19.2	22	23.1	dB
AT	0.806	1.21	1.3	1.74	2.43	2.7	GHz
BW°	31.5°	21.4°	19.5°	15.4°	11°	9.6°	

Figure 11

EFFECT OF SENSITIVITY GAIN IMPROVEMENTS
ON THE FREE SPACE SIGNAL LOSS (RELATED TO NADIR LEVEL)
FOR MOD I 0.7M DISH

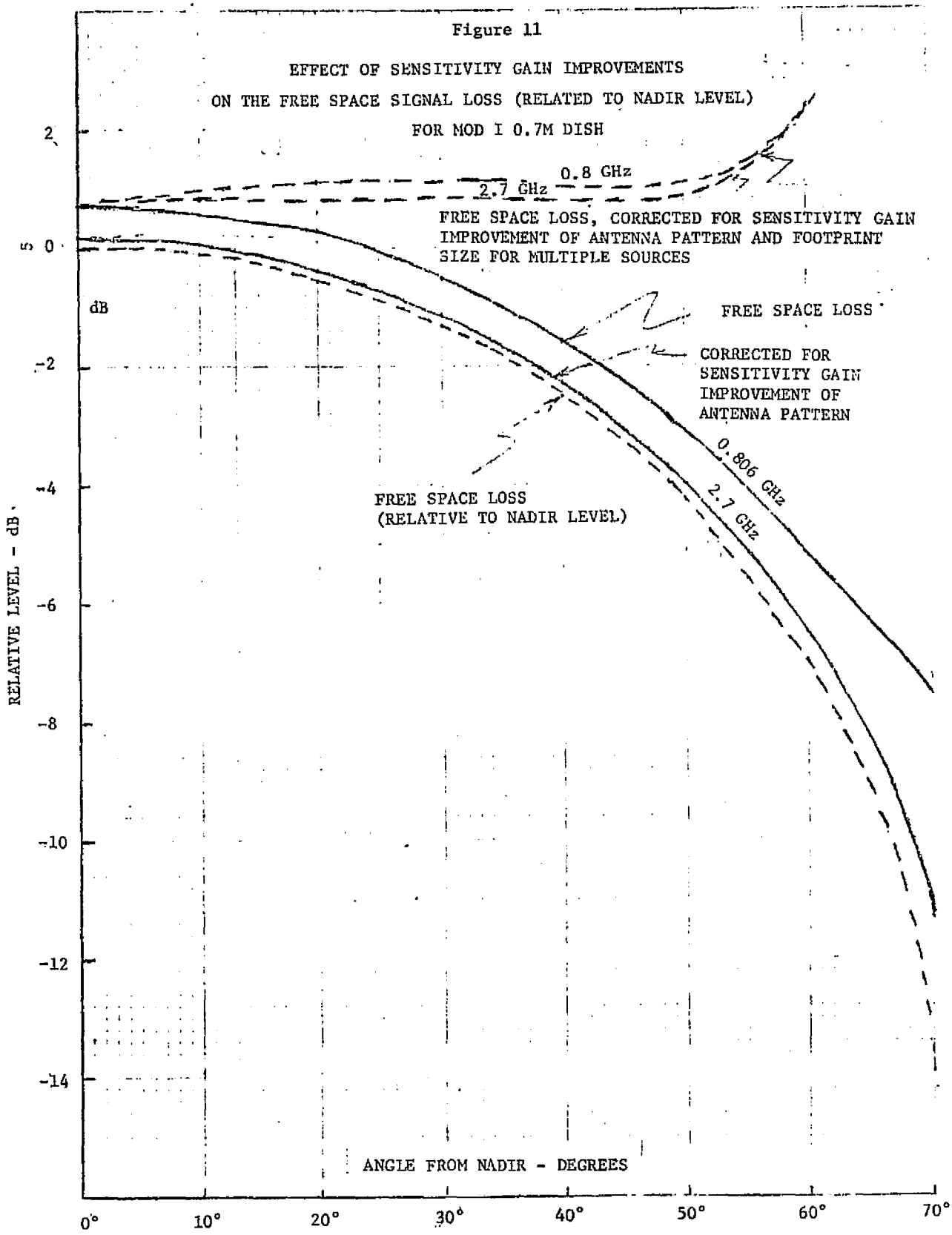

6. Integration of the radiation pattern at any limits within the earth-projection of the beam on a rectangular grid, to determine the gain for absolute or comparison purposes.

7. Automated plots of antenna footprints at any number of dB levels. Examples of the footprints of this antenna (with equal sensitivity lines at -3, -10 and -20 dB) are shown in Figures 12, 13, 14, 15, 16, and 17, at an antenna tilt angle of 40^{o} off nadir.

Figure 10 given previously shows the dB-level improvements of the antenna gain (due to path length variation effects) using pattern integration, up to the first sidelobe, without consideration of beam shift effects caused by path length propagation effects to the surface of the earth. When taking these beam shifts into consideration, more gain improvements are expected, especially near to the horizon as shown in Table 3. Gain improvements at low frequencies cause the EIRP levels to increase. An illustration for this increase was shown in Figure 11 (without beam shift corrections).

High sidelob levels require careful design consideration, especially when the beam is pointed towards the horizon. The first sidelobe level increases from -14 dB when the antenna is pointing at nadir to -7 dB when the beam is at the horizon. These high sidelobe levels are a combination of blockage and range-propagation effects.

2.2 EEE-MOD II ANTENNA ARRANGEMENTS

The EEE-MOD II configuration for 2.7- 43 GHz uses six reflector antennas. The main RF parameters of these are described in Table 2. High gain antennas are needed at the high frequencies in order to make up for the increased path loss of signals, for the high noise figures of their associated receivers, for the high insertion losses of feed lines, and for atmospheric attenuation. High gains and accompanying narrow beamwidth reduce the dwell times on emitter sources and hence reduce the probability and the accuracy of recognition of signals. These considerations make it necessary to use the antenna tilt angle effects (off nadir) to increase the dwell time of footprints on sources and to increase the possibility of multiple-source gain effects. Multiple source gain effects are more probable near the horizon due to multipath signal effects. Also there is a higher probability

Figure 12. 0.7 METER DISH EQUISENSITIVITY CONTOURS AT 0.806 GHz WITH 40° TILT ANGLE OFF NADIR

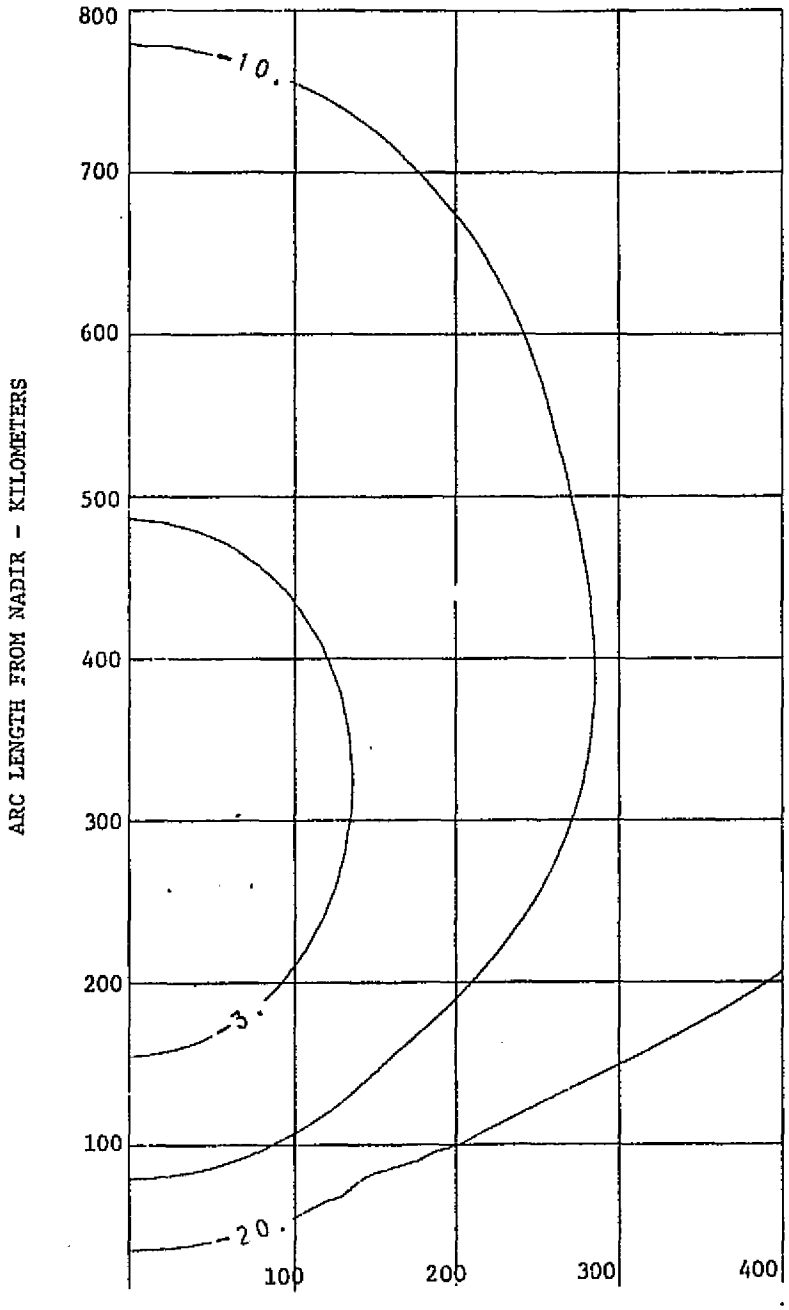

Figure 13. 0.7 METER DISH EQUISENSITIVITY, CONTOURS AT 1.2 GHz WITH 40° TILT ANGLE OFF NADIR

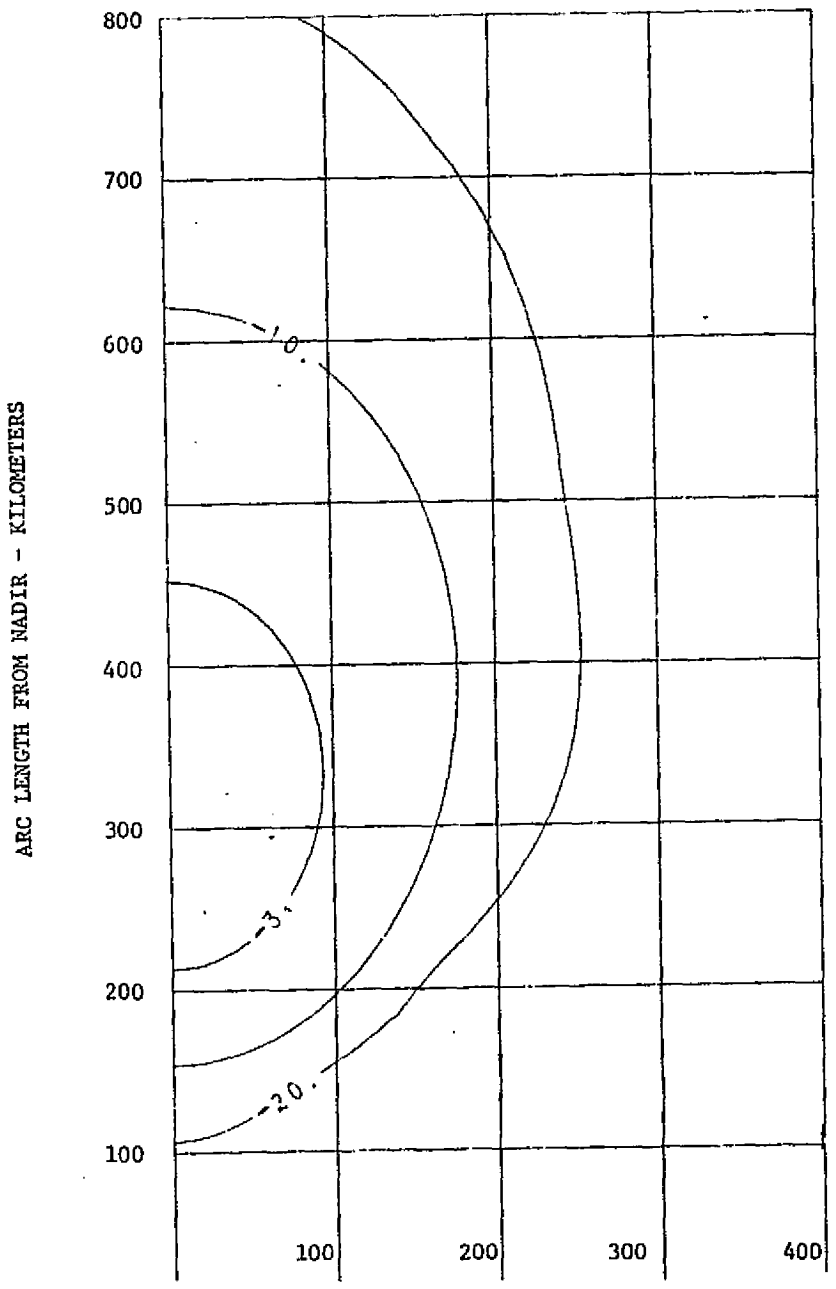

Figure 14. 0.7 METER DISH EQUISENSITIVITY CONTOURS AT 1.3 GHz WITH 40° TILT ANGLE OFF NADIR

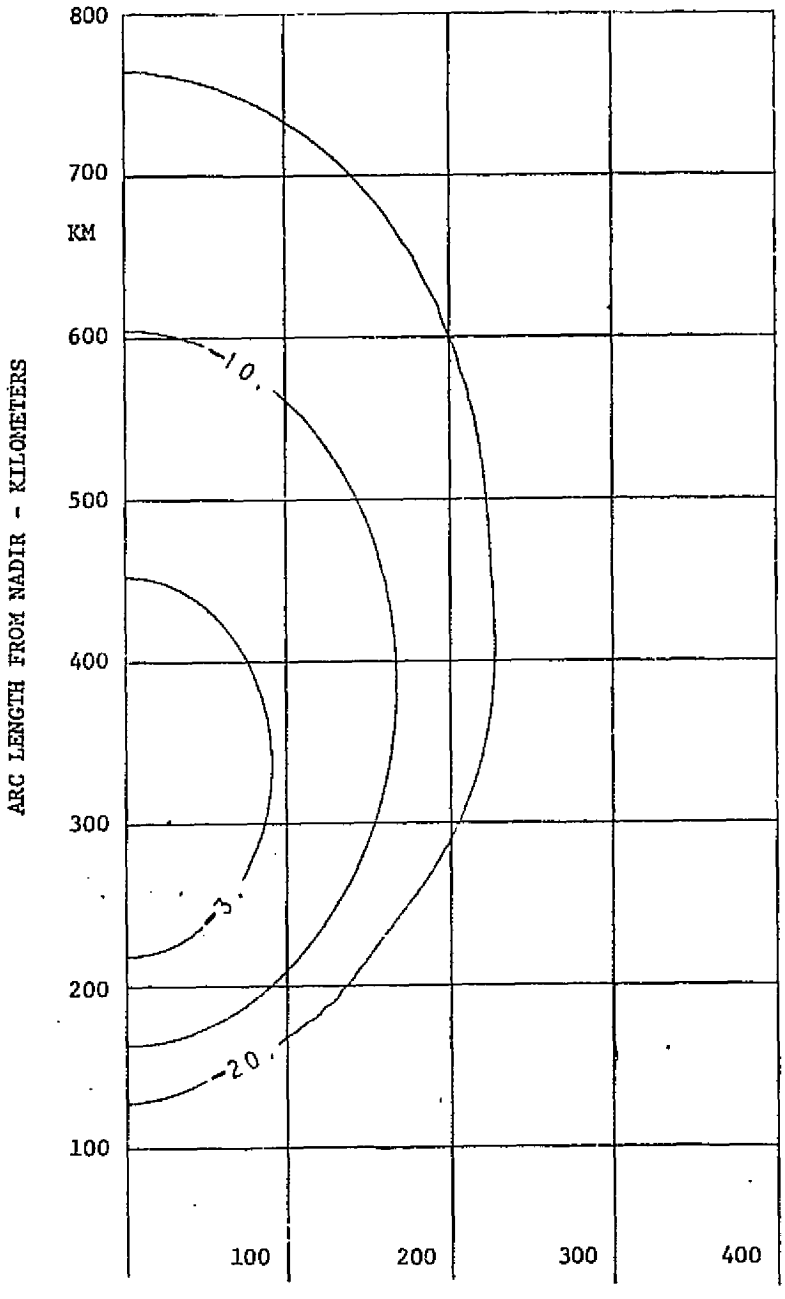

Figure 15. 0.7 METER DISH EQUISENSITIVITY CONTOURS AT 1.7 GHz WITH 40° TILT ANGLE OFF NADIR

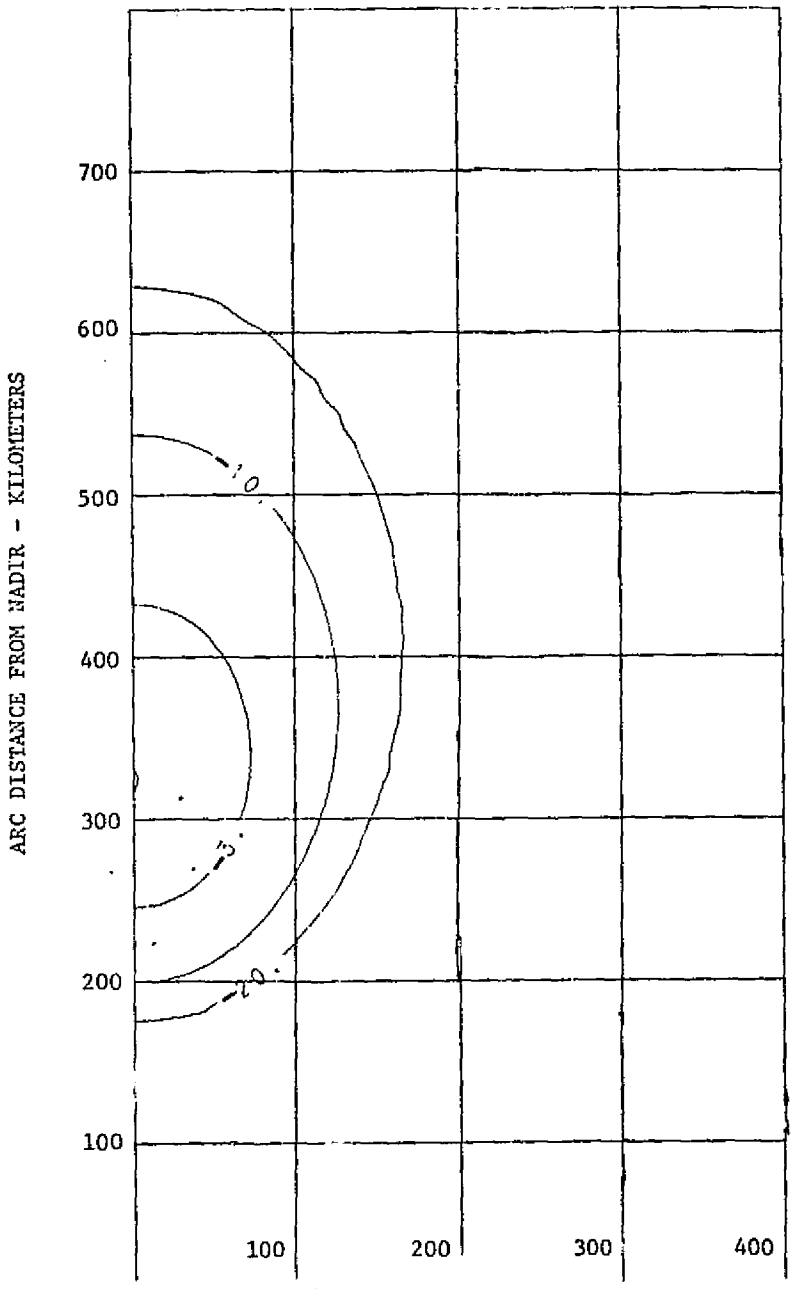

Figure 16. 0.7 METER DISH EQUISENSITIVITY CONTOURS AT 2.4 GHz WITH 40° TILT ANGLE OFF NADIR

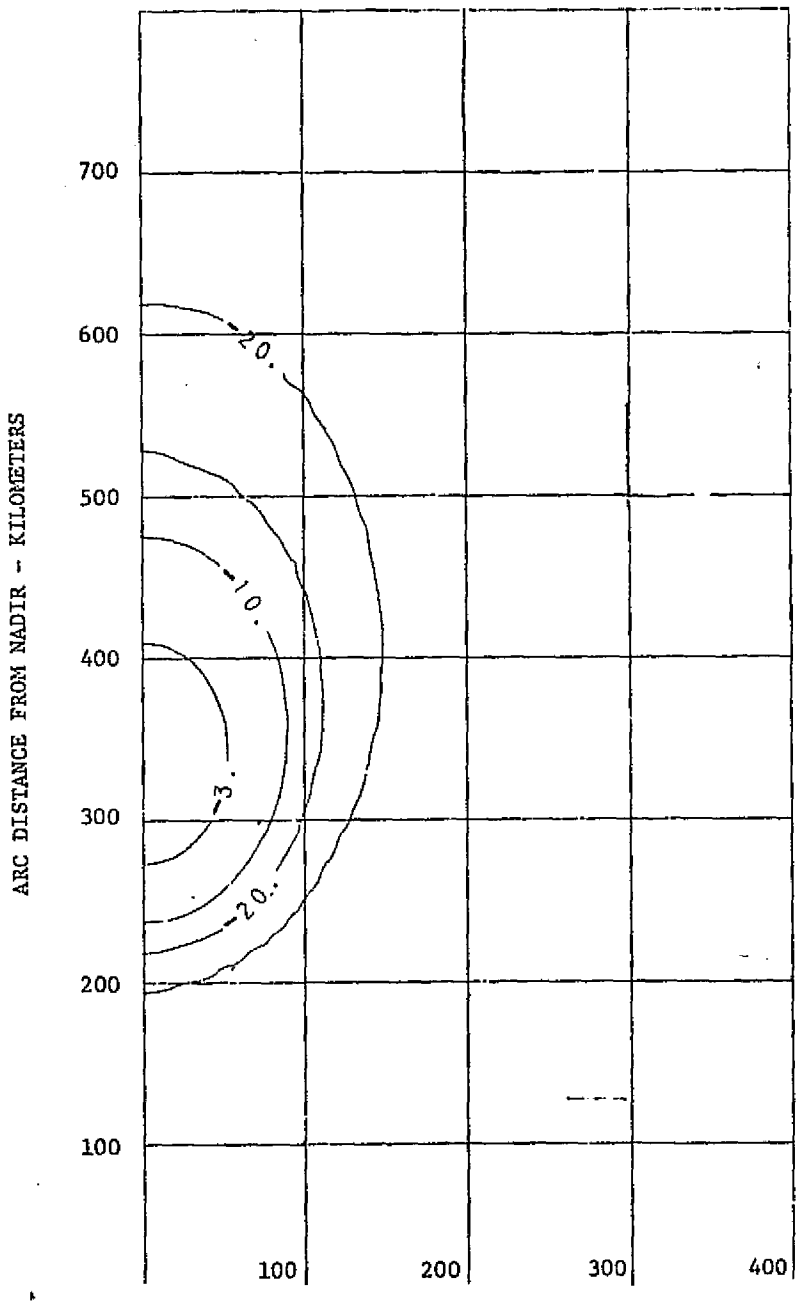

Figure 17. 0.7 METER DISH EQUISENSITIVITY CONTOUR LINES AT 2.7 GHz WITH 40° TILT ANGLE OFF NADIR

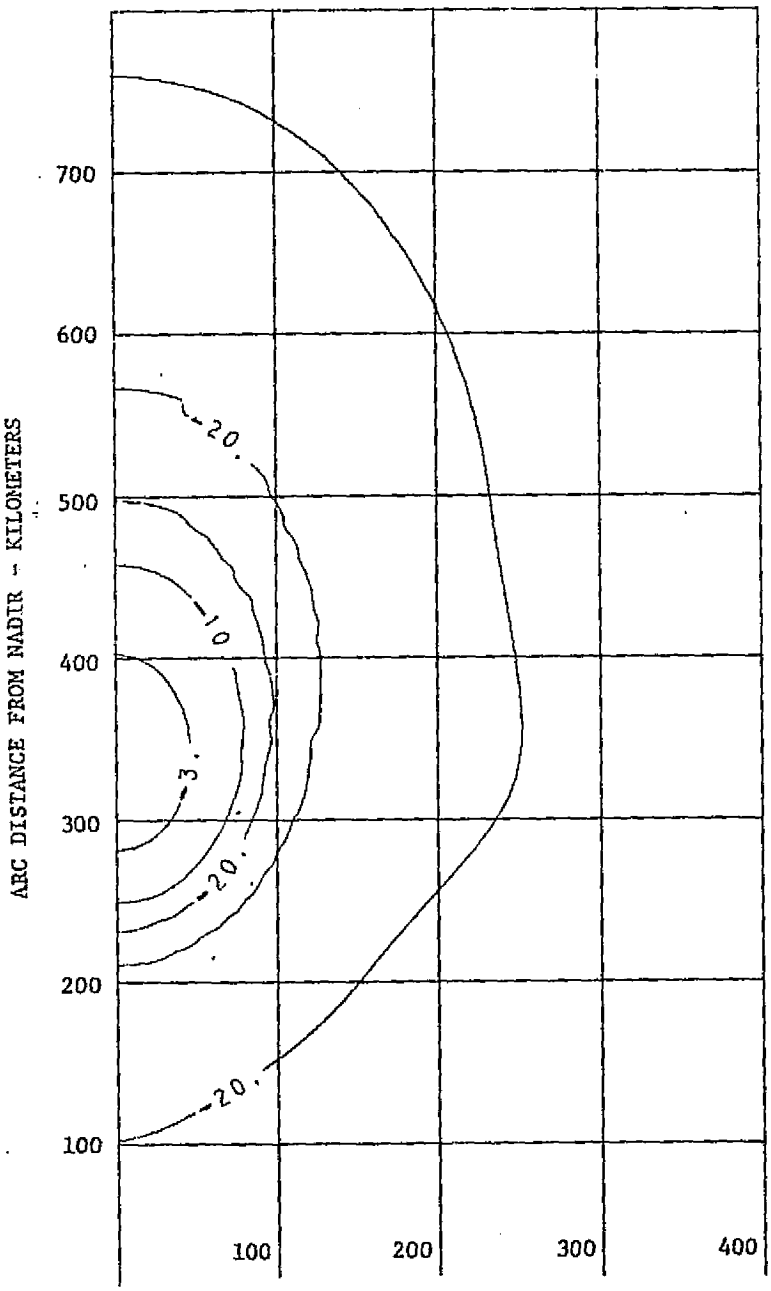

Table 2. EEE-MOD II (2.7 - 43 GHz) Antenna Parameters

ANTENNA TYPE	FREQUENCY RANGE (MHz)	NOMINAL GAIN OVER ISOTROPIC (dB)	NOMINAL 3dB BEAMWIDTH (Degrees)
C-X Bands	2700 - 4000	20.7 - 25.5	13.1^{o} - 9.0^{o}
(2)*- 0.5M Dishes	4000 - 8000	25.5 - 31.5	9.0^{o} - 4.3^{o}
	8000 -12000	31.5 - 34.5	4.3^{o} - 3.1^{o}
K-Q-Bands			
(2)* - 0.25M Dishes	12000 - 18000	28.6 - 32.0	6.4^{o} - 4.2^{o}
	18000 - 26000	32.0 - 35.4	4.2^{o} - 3^{o}
(2)* - 0.25M Dishes	26000 - 43000	35.4 - 39.5	3.0^{o} - 1.8^{o}
(2)* - 0.2M Dishes	43000 - 64000	37.6 - 41.2	2.25^{o} - 1.5^{o}

* Both dishes are identical in design and oriented to directions near the horizon (at approximately 60^{o} off nadir and $\pm$ 45^{o} from the symmetry line of the Shuttle.

of intercepting multiple sources at the same frequency in the larger extended footprints. From Figures 2 and 3 it is determined that look angles near the horizon of approximately 70° off nadir are needed in order to yield footprint sizes similar to those of the sizes of MOD I footprints. The probability of interception of sources, however, may be smaller at the horizon due to very low elevation angles needed for the radiating sources. Therefore a depression angle of a few degrees below the horizon was necessary to increase the source interception probabilities. Table 3 summarizes the link parameters and sensitivity levels of the 0.5 meter and the 0.25 meter dishes of MOD II antennas. The antennas are mounted in two sets of three as shown in Figure 18, to allow for the capability to look at sources at both sides of the Space Shuttle at angles of around $\pm 45^{\circ}$ from the flight path. The redundant antenna systems are mounted on two identical mechanically adjustable supports which allow for pre-flight tilt angle variations in azimuth and in elevation (around a nominal value of 45° in azimuth and a nominal value of 55° in elevation). The location of the antennas on the Shuttle pallet was selected to give as short as possible cable and waveguide runs to the receivers below the pallet platform. It is also necessary to locate these antennas for minimum mutual pattern blockage and interactions with EEE antennas and with other Shuttle experiments or structures.

3.0 SOME HARDWARE CONSIDERATIONS

All of EEE-MOD I (-.12-2.7 GHz) antennas and feed lines are essentially standard catalog items or existing hardware designs with the exception of the 0.7 meter reflector, which should be manufactured using space qualified materials.

MOD II antennas in the 2.7-43 GHz range need special care from the viewpoint of special feed designs in order to perform satisfactorily over the broad bandwidth of frequencies. However, the state of the art is consistent with design of these feeds. The reflectors are not standard items and need similar space-qualified materials design considerations as those of the 0.7 meter dish. The 0.25 meter dish which covers the frequency band of 12-26 GHz uses a rigid WRD 75 waveguide feeding the receivers with associated waveguide switching arrangements, using the same waveguide cross section.

Antenna Type	(GHz) Frequency Range	Feed Line	3 dB Beam Width ("Deg")	Antenna Gain (dB)	Max. Feed Loss (dB)	Sensitivity Gain Factors (dB) Beam Width[1]		F.P. Area[2]		Effective Gain At 3 dB Contour Single Source		Multiple Source	
						Nadir	Tilt	Nadir	Tilt	Nadir	Tilt	Nadir	Tilt
VHF Log Periodic (1.3m x 1.85 AEL APX 1250)	0.1215-0.174 0.2430	Coax Cable	70° (55°x85°)	7	1.0	1.1		0		3		4.1	
UHF Array[3] (1.0m x 1.3m)	0.3999 0.7000	Coax Cable	47°x36° 27°x21°	12.5 12.6	1.0	0.8		0		8.5 8.6		9.3 9.4	
S-Band Conical Helix (0.175 x 0.175 m AEL ALN 509B)	0.700 2.700	Coax Cable	80° 70°-90°	8	1.4	1.2		0		6.6		7.8	
S-Band 0.7m Dish (Feed AEL ASN 113A)	0.700 2.700	Coax Cable	32°-(40°)÷ 10°	13 24	1.4	0.7 0.17	1.8** 0.45**	0 0	9** 10.5**	8.6 19.6	8.6** 19.6**	9.0 19.77	19.4* 30.5
Two 0.5m Dishes	2.7 4.0 8.0 12.0	Coax Cable	13.1° 9.0° 4.3° 3.1°	20.7 25.5 31.5 34.5	1.5 1.5 1.5 1.5	0.2 0.15 0.07 0.04	0.8* 0.42* 0.11* 0.06*	0 0 0 0	13* 13.7* 15.4* 15.6*	16.2 21.0 27.0 30	16.2 21.0 27.0 30	16.4 21.15 27.07 30.04	30.0 35.1 42.5 45.6
Four 0.25m Dishes	12.0 18.0 26.0 43.0	WR75 Ridgid Waveguide WR28	6.4° 4.2° 3.6° 1.8°	28.6 32.0 35.4 39.5	1.7 1.7 2.0 2.0	0.1 0.07 0.04 0.025	0.2* 0.11* 0.06* 0.035*	0 0 0 0	15.1* 15.2* 15.5* 15.7*	23.9 27.3 30.4 34.4	23.9 27.3 30.4 34.4	24.0 27.4 30.4 34.4	39.2 42.6 46.0 50.1

(1) Beam width gain factor = beam integration (weighted by path loss) relative to beam integration (without path loss).
(2) Footprint area factor is referenced to its value at nadir.
(3) Based on a side-lobe level of -25 dB.
* At tilt angle of 65° off nadir.
** At tilt angle of 60° off nadir.
÷ The large beam width would arise from an offset reflector (due to absence of blockage of the wide band cavity backed

FOLDOUT FRAME 2

Table 3. EEE-MOD II Link Parameters and Sensitivity Levels

Effective Gain 3 dB Contour			Free Space Loss (dB)		Atmospheric Attenuation		I. F. Band Width (M Hz)	Rec. N. F. (dB)	Minimum Detectable Signal At Antenna (dBW)	Source Dwell Time Seconds		Detectable EIRP (dBW)			
	Multiple Source			At Tilt	Tilt							Nadir		Tilt Angle	
Tilt	Nadir	Tilt	At Nadir	Angle	Nadir	Angle				Nadir	Tilt	Single	Multiple	Single	Multiple
	4.1		126.1				±0.025	2	-144.0	60		-21.9	-23		
			132.2									-15.8	-16.9		
	9.3		136.5				0.02	2	-148.0	38		-21.0	-21.8		
	9.4		141.4				0.10		-141.0			- 9.2	-10.0		
							1.00		-131.0			0.8	- 0.0		
	7.8		141.4				0.02	2.5	-147.0	66		-13.6	-14.8		
			153.1									- 1.9	- 3.1		
8.6**	9.0	19.4**	141.4	145.9**			0.02	3	-146.6	30	63	-15.2	-15.9	-10.7**	-21.5**
19.6**	19.77	30.55**	153.1	159.6**			0.02		-146.6			-14.5	-14.7	- 8.2**	-18.95**
							1.00		-129.6	7	30**	2.5	2.33	8.0**	- 1.95**
16.2	16.4	30.0*	153.1	160.9*	0.00	0.2*	0.02	3.5	-145.77	13	44*	-10.37	-10.57	-2.57*	-16.4*
21.0	21.15	35.12*	156.5	164.9*	0.00	0.2*	0.02			9	37.3*	-11.5	-11.65	-2.9*	-17.0*
27.0	27.07	42.51*	162.5	171.5*	0.00	0.2*	0.2	4.0	-135.5	4.3	20*	- 1.5	- 1.57	7.7*	- 7.8*
30	30.04	45.66*	166.0	175.1*	0.00	0.2*	0.2	6.0	-133.5	3	14.4*	+1.0	0.96	10.3*	- 5.6*
23.9	24.0	39.2*	166.0	174.8*	0.05	0.2*	0.2	7	-132.3	6.3	28.0*	8.15	8.05	17.1*	-1.8*
27.3	27.4	42.6*	169.5	178.5*	0.2	0.5*	0.2	7	-132.3	4.3	20.0*	8.4	8.33	17.7*	-2.39*
30.4	30.4	46.0*	172.7	181.8*	0.7	1.5*	0.2	12	-127.0	3.0	14.0*	14.0	13.96	23.9*	-8.34*
34.4	34.4	50.1*	177.2	186.3*	1.0	2.2*	0.2	12	-127.0	1.8	8.5*	14.7	14.67	25.0*	-9.4*

thout path loss).

band cavity backed spiral).

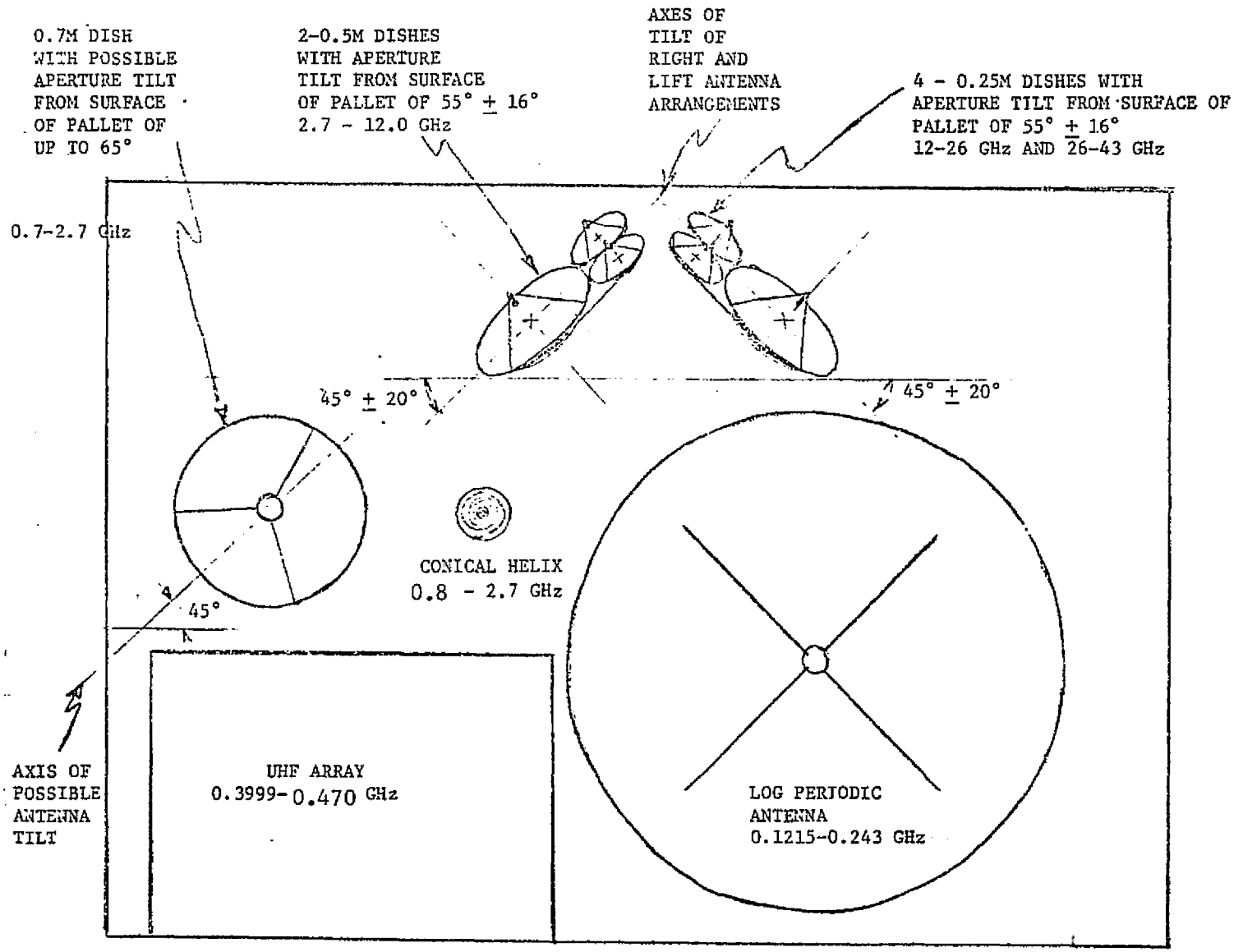

FIGURE 18. PLAN VIEW OF EEE, MOD I AND MOD II ANTENNA ARRANGEMENT

APPENDIX D

ANALYSIS OF EEE SPECTRUM PROCESSOR ACCURACY

1.0 INTRODUCTION

The power spectral density measurement is made by means of a power measurement at the output of a filter, the filter being the device that sets the resolution bandwidth. The power measurement is made by averaging the output of a square law device following the filter.

The relationship between resolution bandwidth, averaging time and the accuracy of the power measurement is derived below. The relationship is derived in two ways: one uses sampling theory and the other uses more conventional, and more general, continuous signal analysis. A simple approximate relationship between the variables is derived and it provides a close approximation to the exact relationship.

It is assumed that the spectral density of the signal to be measured is a white Gaussian process.

Two ways of implementing the Spectral Processor are under consideration. One uses the classical approach of paralleling circuits made up of a cascaded filter, square law device, and an averaging circuit to measure the power density. The other uses a cascaded chirp filter, square law device, averaging circuit and properly timed sampling circuit to measure the power density. Although the filter and averaging circuit parameters are radically different between the two approaches, the effective integration (averaging) time and resolution bandwidth are the same. Therefore the following analyses apply to both implementations.

2.0 SAMPLING THEORY ANALYSIS

It is shown that to measure the power P at the output of a filter of bandwidth B to within a fractional error of v/P requires an integration time after the detector of approximately $T = 1/B(v/P)^2$ seconds.

It is assumed that the process is a zero mean Gaussian. This hypothesis is justified if there is a superposition of several emitters. Under this assumption the analysis of accuracy of power estimate is straightforward.

Assume that the output of the filter is observed long enough to have n independent samples of the Gaussian process. Then the estimate of the power from the samples x_i is:

$$\hat{\sigma}^2 = \frac{x_1^2+x_2^2+\ldots+x_n^2}{n} \qquad (1$$

This "sample variance" will differ from the true power σ^2. The variance of the sample variance can be easily calculated:

$$v^2 = \overline{(\sigma^2-\hat{\sigma}^2)^2} \qquad (2$$

$$= \sigma^4 - \overline{2\hat{\sigma}^2}\,\sigma^2 + \overline{(\hat{\sigma}^2)^2} \quad .$$

since $\overline{x_i^2}=\sigma^2$, σ^2 is an unbiased estimate of $\hat{\sigma}^2$ and equation (2) can be rewritten

$$v^2 = -\sigma^4 + \frac{1}{n^2}\sum_{i=1}^{n}\sum_{j=1}^{n}\overline{x_i^2x_j^2} \qquad (3$$

Since the samples are independent, $\overline{x_i^2x_j^2}=\sigma^4$ for $i\neq j$, and, since the process is zero mean Gaussian, $\overline{x_i^4}=3\sigma^4$. Substituting into equation (3) gives:

$$v^2 = -\sigma^4 + \frac{3}{n}\sigma^4 + \frac{1}{n^2}\sum_{i\neq j}^{n}\sum^{n}\sigma^4 \qquad (4a$$

$$v^2 = \sigma^4 \left(-1 + \frac{3}{n} + \frac{2}{n^2} C_2^n\right) \qquad (4b$$

$$v^2 = \sigma^4 \left(-1 + \frac{3}{n} + \frac{n(n-1)}{n^2}\right) = \frac{2\sigma^4}{n} \qquad (4c$$

The fractional error is

$$\frac{v}{\sigma^2} = \sqrt{\frac{2}{n}} \quad . \qquad (5$$

This is the well known result of root n improvement in estimation. To put this expression in terms of true power, P, bandpass filter bandwidth, B, and integration time, T_a, it is noted that $P = \sigma^2$, $n = 2BT_a$ and v = the standard deviation of the measurement which is taken as the error. Using these relations, equation (5) becomes:

$$v/P = 1 \Big/ \sqrt{BT_a} \qquad (6$$

As an example, consider the measurement of power from a 20 kHz bandwidth filter to an accuracy of 20%. Using equation (5):

$$\sqrt{\frac{2}{n}} = .2 \quad \text{or} \quad n = 50 \quad . \qquad (7$$

In a 20 kHz bandwidth assuming nearly white noise, an independent sample exists every $\frac{1}{2 \times 20 \text{ kHz}}$ seconds or every 25 usec. According to the above arguments, it is necessary to integrate over 50 of these samples or integrate over 1.25 msec to obtain a smoothed estimate.

3.0 CONTINUOUS SIGNAL ANALYSIS

An analysis more precise and general than that of sampling theory is given here. A simplified expression of the analytical result, which provides an upper bound on the fractional error, is the same as that provided by the sampling theory analysis. Consider Figure D-1, which depicts lowpass filtering of a square law operation on a processed signal. This signal serves as the power estimate.

$$P_{est} = \frac{1}{\tau}\int_0^{\tau} y^2(t)dt \ . \qquad (8$$

The expected value is simple:

$$\overline{P}_{est} = \frac{1}{\tau}\int_0^{\tau} \overline{y^2(t)}\, dt = R(o) \ , \qquad (9$$

where R(o) is the autocorrelation function of the y(t) evaluated at zero. Evaluate the variance of this estimate:

$$\begin{aligned} v^2 &= \overline{(P_{est} - \overline{P}_{est})^2} \\ &= \overline{P^2_{est}} - \overline{P}^2_{est} \\ &= \frac{1}{\tau^2}\int_0^{\tau}\int_0^{\tau} \overline{y^2(t)y^2(x)}dtdx - R^2(o) \end{aligned} \qquad (10$$

In general for Gaussian variables there is the familiar formula:

$$\overline{z_1z_2z_3z_4} = \overline{z_1z_2}\ \overline{z_3z_4} + \overline{z_1z_3}\ \overline{z_2z_4} + \overline{z_1z_4}\ \overline{z_2z_3} \qquad (11$$

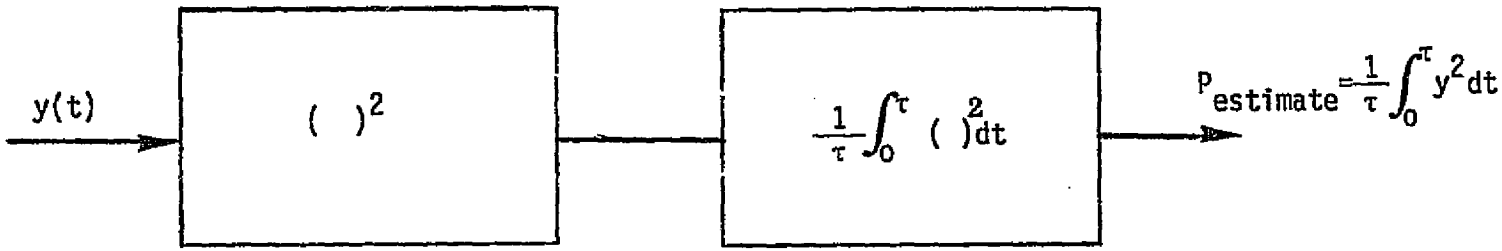

FIGURE D-1

POWER ESTIMATION BY LOWPASS OPERATION ON A SQUARE LAW DETECTOR

This allows Equation (10 to be written:

$$v^2 = \frac{1}{\tau^2}\int_0^\tau \int_0^\tau (2R^2(t-x)+R^2(o))dtdx - R^2(o)$$

or (12

$$v^2 = \frac{2}{\tau^2}\int_0^\tau \int_0^\tau R^2(t-x)dtdx \ .$$

A further simplification is possible by integrating over strips where t-x is constant. The integral in (12 is depicted as shown, letting (t-x)=z

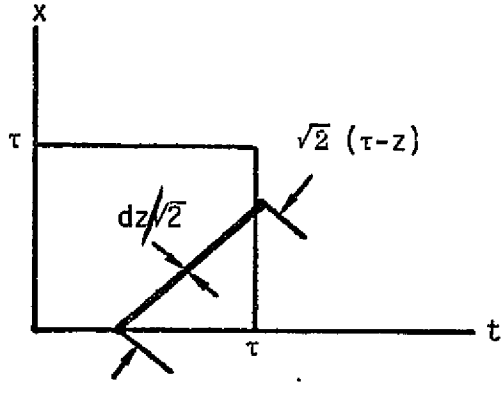

The strip width is $\frac{dz}{\sqrt{2}}$, the strip length is $\sqrt{2}(t-z)$ and the integral can be written

$$v^2 = \frac{4}{\tau}\int_0^\tau R^2(z)(1-\frac{z}{\tau})dz \qquad (13$$

Equation (13 can be used to evaluate the variance of the power estimation for both systems. In order to appreciate the magnitude of the variances, the values for some simple models will be written out. Note that the R^2 term in Equation (13 will produce a lowpass contribution to the integral and a term at $2f_o$. The term at $2f_o$ has negligible contribution to the integral. Consider for example a bandpass process whose R(t) has the form:

$$R(t) = \left(1 - \frac{|t|}{\tau_1}\right) \cos 2\pi f_o t \; ; \; |t| \le \tau_1 = 0 \quad |t| > \tau_1 \tag{14}$$

This process has bandwidth $\frac{1}{t_1} \equiv B$. Substitute into Equation (13 gives:

$$v^2 = \frac{4}{\tau} \int_0^{\tau} \left(1 - \frac{z}{\tau_1}\right)^2 \left(1 - \frac{z}{\tau}\right) \cos^2 2\pi f_o t \, dt \tag{15}$$

$$\approx \frac{2\tau_1}{\tau} \int_0^{\tau} \left(1 - \frac{z}{\tau_1}\right)^2 \frac{\tau_1}{\tau} \left[1 - \frac{z}{\tau_1} + 1 - \frac{\tau_1}{\tau}\right] d\left(\frac{z}{\tau_1}\right)$$

$$\approx \frac{7}{6} \frac{\tau_1}{\tau} - \frac{2}{3} \left(\frac{\tau_1}{\tau}\right)^2$$

For the example worked out in Section 1.0 of this Appendix, $2BT_a = 2B\tau_1 = 50$. This becomes

$$v = \text{RMS variation of estimate} = .22 \; P$$

which is close to the previous estimate.

On the other hand, a "brick wall" bandpass filter yields a variance a little less than predicted sampling theory. R(z) for this case works out to be:

$$R(z) = \cos 2\pi f_o z \, \frac{\sin 2\pi f_1 z}{2\pi f_1 z} \tag{16}$$

Equation (13 becomes:

$$v^2 = \frac{4}{\tau} \int_0^{\tau} \cos^2 2\pi f_o(z) \, \frac{\sin^2 2\pi f_1 z}{(2\pi f_1 z)^2} \left(1 - \frac{z}{\tau}\right) dz$$

$$< \frac{2}{\tau} \int_0^{\infty} \frac{\sin^2 2\pi f_1 z}{(2\pi f_1 z)^2} \, dz = \frac{1}{2\tau f_1} , \tag{17}$$

Noting that $2f_1 = B$ and $\tau = T_a$, this upper bound in the error is the same as the error predicted for sampling theory.

APPENDIX E

EEE SPECTRAL PROCESSOR DESIGN

1.0 INTRODUCTION

Two ways in which the spectrum analyzer portion of the Spectrum Processor (see block diagram, Figure 4-25) can be implemented are discussed in this Appendix E. One employs the "classical" approach of detecting the power from a bandpass filter. The filter bandwidth is the resolution bandwidth of the analyzer. The second approach uses a dispersive (dechirp) filter to perform the integration required to achieve the desired accuracy of the power measurements.

It is proven here that the two approaches can be configured to yield the same accuracy. The choice, then, can be made on the basis of cost, size, weight and power requirements.

In the following analyses the bandwidth over which it is desired to perform the spectral analysis is designated W_A and the time allotted for the analysis is T_A.

2.0 THE CLASSICAL ANALYZER

Figure E-1 is a block diagram of the classical spectrum analyzer. It is assumed that the required resolution bandwidth, B, is small enough in relation to the total bandwidth, W_A, over which the spectral analysis is to be made that it cannot be accomplished by a single filter in the allotted time, T_A. Therefore, a bank of paralleled filters and associated square-law detectors are shown.

In the general case, the total bandwidth, W_A, may be divided into segments, W_i, and different resolution bandwidths and averaging times used in each segment. Relationships between the circuit parameter and constraints on them are derived for the general case. Then an example is worked out for the specific case of a 20 KHz resolution bandwidth used over a 40 GHz input band.

Dividing the input bandwidth into I non-overlapping segments, the sum of the segments must

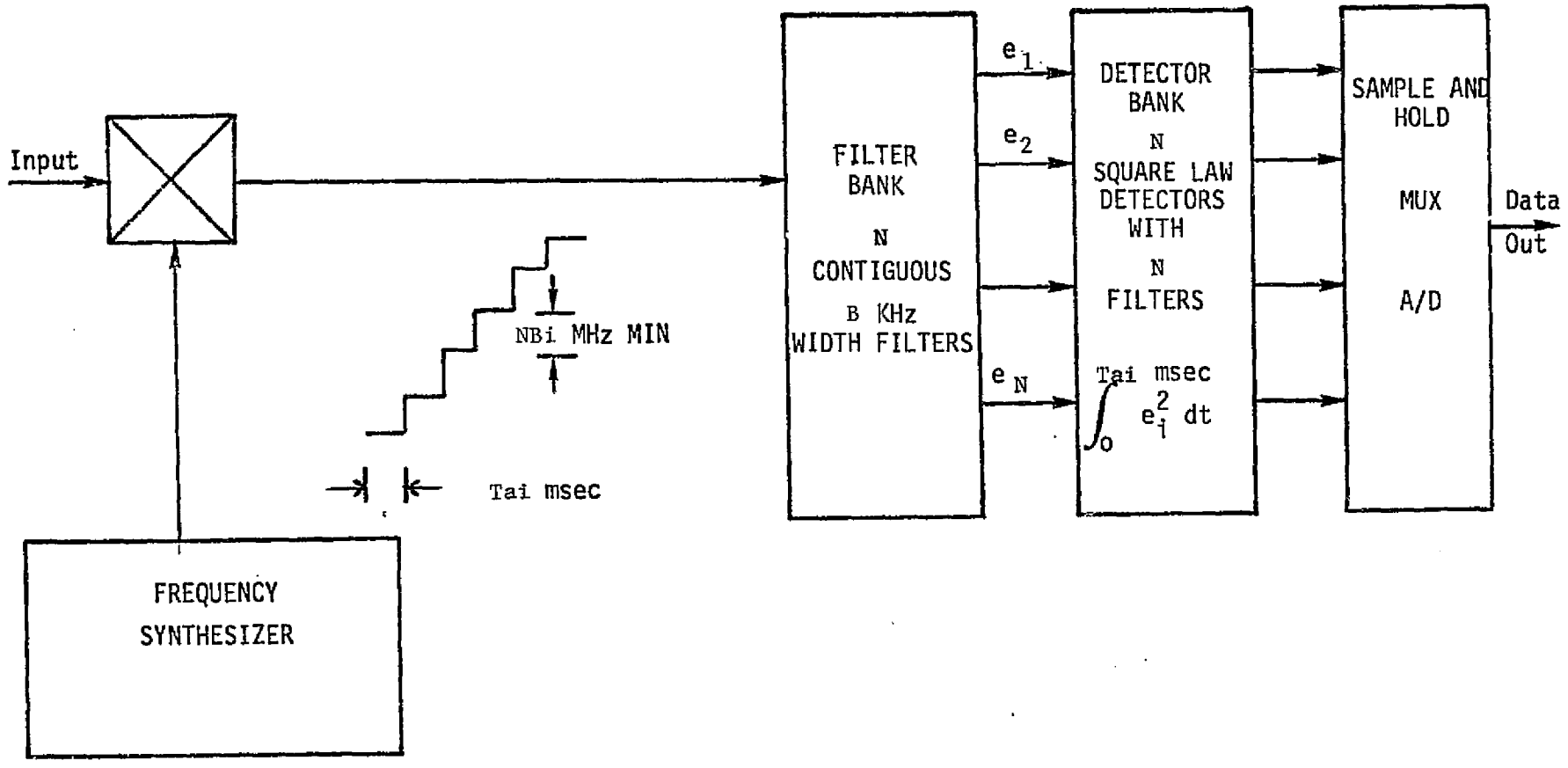

Figure E-1. A Classical Spectral Analysis System

equal the input bandwidth:

$$W_A = \sum_{i=1}^{I} W_i \tag{1}$$

Similarly the sum of times allotted to performing the spectral analysis of each segment must equal the time allowed for the analysis of the complete spectrum:

$$T_A = \sum_{i=1}^{I} T_i \tag{2}$$

If a resolution bandwidth Bi is assigned to the i^{th} segment, there are bi resolution bandwidths in the segment:

$$bi = \frac{Wi}{Bi} \tag{3}$$

The time required to perform the analysis of the i^{th} segment is:

$$Ti = \frac{1}{Ni} \cdot bi \cdot \frac{1}{Bi(v/P)^2} \tag{4}$$

where, from Appendix D, $1/Bi\ (v/P)^2 = Tai$, the averaging time required to achieve a fractional accuracy v/P; Bi is the resolution bandwidth assigned to the i^{th} segment; Ni is the number of parallel circuits.

Using the above relationships and equation (3) in equation (4):

$$Ti = \frac{WiTai}{NiBi} \tag{5}$$

which solved for the number of parallel circuits, Ni, gives:

$$Ni = \frac{Tai}{Ti} \cdot \frac{Wi}{Bi} \tag{6}$$

The local oscillator step-size is:

$$\Delta f_i = NiBi \tag{7}$$

As an example, and not necessarily a realistic one, consider performing a power spectral density analysis under the following conditions:

W_A = 40 GHz = Bandwidth containing signals to be analyzed

T_A = 12.5 seconds

Bi = 20 GHz = the only resolution bandwidth used

$Wi = W_A$
$Ti = T_A$
} Band is not broken into segments

v/P = 0.2 = measurement accuracy desired

Manipulating equation (6), Appendix D, the averaging time is:

$$Ta = 1/B\,(v/P)^2 = 1/20 \times 10^3 \times (0.2)^2$$
$$= 1.25 \text{ msec}$$

From equation (6) the number of parallel channels required in the analyzer is:

$$N = \frac{Ta}{T_A} \cdot \frac{Wa}{B} = \frac{1.25 \times 10^3 \times 40 \times 10^9}{12.5 \times 20 \times 10^3}$$
$$= 200$$

From equation (7) the LO step size is:

$$\Delta f = NB = 200 \times 20 \times 10^3$$
$$= 4 \text{ MHz}$$

3.0 THE DISPERSIVE (DECHIRP) FILTER ANALYZER

It is shown here that an analyzer consisting of a linearly swept local oscillator followed by a single, large bandwidth-time-product dechirp I. F. filter provides an alternative to the classical filter bank system.

The nomenclature used in Section 2.0 for the Classical Analyzer is used here. Although the significance of the parameter in some cases is different, the difference is clear from the context. Preserving the nomenclature makes the equivalence of the two approaches more apparent.

The basic idea is that the local oscillator can be swept rapidly provided the IF impulse response is such that the energy of a single narrowband source input is "coherently" integrated for Ta sec. In this manner independent narrowband spectral analyses are presented in rapid succession. These are square-law detected and averaged over a much shorter time interval to achieve an accurate power estimate. In other words, even though a particular frequency is converted to a rapid sweep, the energy from that frequency is accumulated at the output of the chirp filter. The system is depicted in Figure D-2. In order to cover the entire frequency range W_A, the local oscillator is linearly swept rapidly at a rate of $\Delta f/Ta = NB/Ta$ Hz per second. At any instant the output of the dechirp filter is looking at a discrete frequency for the last Ta sec. The impulse response of the dechirp filter lasts for Ta sec. The B-T product of the dechirp filter is therefore NBT_a. (Dechirp filter B-T products of 5,000 can be implemented with surface-wave devices. See, for example, "The Design and Application of Highly Dispersive Acoustic Surface Wave Filters," By Gerard, et al, IEEE Transactions Microwave Theory Tech., pp. 176-186, April 1973).

At each instant, the strength of a discrete frequency as measured over a Ta sec time is examined. This quadratic content is averaged over a bandwidth, B. This average is accomplished by integrating over only $t_1 = (1/\Delta f)$ (BT) seconds.

In the following paragraphs an attempt is made to justify the fact that this estimate is as accurate as the classical spectrum analyzer which averages over time for Ta sec.

3.1 EFFECTIVE AVERAGING TIME

It is shown here that in order to average the power in a given band B over a time Ta we can average over any set of $2BT_a$ independent coordinates and obtain the same accuracy.

The point here is that in the classical analysis system the power estimate is viewed as taking $2BT_a$ independent time samples sequentially and averaging their quadratic content; while in the swept system the system is viewed as averaging the quadratic content of independent Fourier components. In a white-like noise background any $2BT_a$ orthogonal set of functions can be used. These will be independent random variables.

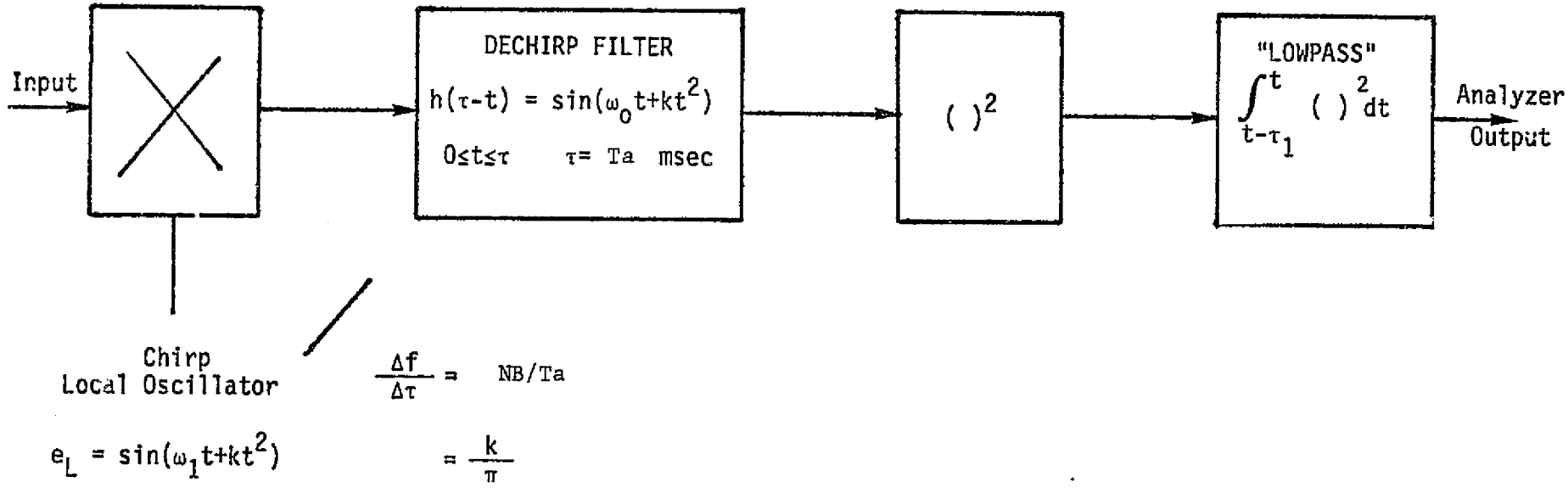

Figure D-2. Chirp Spectrum Analyzer

If the local oscillator can be represented at time t by $e_L = \sin(w_1 t + kt^2)$ and the input by S(t), the output at time Ta and dechirp filter can be written:

$$e_o(Ta) = \int_o^{Ta} S(t) \sin(w_1 t + kt^2) \sin(w_o t + kt^2) dt \quad (8$$

or

$$e_o(Ta) \approx 1/2 \int^{T} S(t) \cos(w_o - w_1)t \, dt \quad (9$$

Neglecting the upconversion components $e_o(Ta)$ analyzes the component of the signal at $w_o - w_1$.

In the next ϵ seconds the output can be written:

$$e_o(Ta+\epsilon) = \int_o^{Ta} S(t+\epsilon)\sin(w_o t + kt^2) \sin\left[(w_1 + 2K\epsilon)t + k(t+\epsilon)^2\right] dt \quad (10$$

$$\approx 1/2 \int_o^{Ta} S(t+\epsilon)\cos\left[(w_o - w_1 - 2k\epsilon)t - k\epsilon^2\right] dt \quad (11$$

Equation (11) says that $e_o(Ta+\epsilon)$ is a new Fourier component at frequency $(w_o - w_1 - 2k\epsilon)$. This will be an independent "orthogonal" harmonic for $2k\epsilon = \frac{\pi}{Ta}$ or in our case $\epsilon = \frac{\pi}{2k\,Ta}$ seconds.

Each of the "coefficients" $e_o(Ta+k\epsilon)$ for integer k will be Gaussian distributed. An average of their squares will then be smoothed estimate of the power in the band. Integration for ϵ sec will cover an average of 2BTa independent Fourier components which are clustered in a B Hz band.

3.2 ADJACENT RESOLUTION CELL INTERFERENCE

It is shown here that there is very little interference spectral overlap in the spectral analysis of contiguous B Hz cells with the swept system. In fact, the output of the dechirp filter can be examined for a single sinusoidal input and its time record observed.

After some frequency conversion:

$$e_o(t) = \frac{2}{Ta} \int_o^{Ta} \sin(w_o x + kx^2) \sin\left[w_o(x+t) + k(x+t)^2\right] dx \qquad (12$$

Neglecting the small contributions of upconversions this can be written:

$$e_o(t) \approx \frac{1}{Ta} \int_o^{Ta} \cos(w_o t + 2kx + kt^2) dx \qquad (13$$

$$e_o(t) \approx \frac{\sin\left[w_o t - ktTa + kt^2\right] - \sin\left[w_o t + kt^2\right]}{2ktTa} \qquad (14$$

$$e_o(t) = \frac{\sin ktTa}{ktTa} \cdot \cos(w_o t + 2ktTa + kt^2) \qquad (15$$

The first side lobe is for $ktTa \approx \frac{3\pi}{2}$.

For an analyzer of resolution bandwidth B = 20 KHz and averaging time Ta = 1.25 msec, t = .375 μ sec. This corresponds to a frequency change of about 1.2 KHz. The integration is over 20 KHz; consequently, the resolution is quite sharply defined. There probably would be more interference in the classical analysis technique if any reasonable filter shape is assumed.

3.3 A/D CONVERTER REQUIREMENTS

The output of the averaging circuit is converted to digital form for transmission. It is shown here that to encode power level over a 60 db dynamic range to 20% accuracy requires an A/D binary word of 7 bits, and for 10% accuracy a word of 8 bits.

First of all, logarithmic companding of the power level is a natural way to represent power level. If the ratio of the largest power level to the smallest power level is 60 db,

then the dynamic range which must be supported is 10^6 in power. Each level is quantized to a 20% accuracy. The number of different levels N, is given by:

$$(1.2)^n = 10^6$$

or

$$n = \frac{6}{\log_{10} 1.2} \approx 75.8$$

The number of bits m required to encode is therefore

$$m \geq \log_2 n$$

or

$$m = 7 \text{ bits}$$

for a 10% accuracy, $n \approx 144$ and $m = 8$ bits (selected as standard).